

**Louisiana Tech University**  
**Louisiana Tech Digital Commons**

---

Doctoral Dissertations

Graduate School

---

Winter 2011

# Sub pixel analysis and processing of sensor data for mobile target intelligence information and verification

Theresa Allen Williams  
*Louisiana Tech University*

Follow this and additional works at: <https://digitalcommons.latech.edu/dissertations>



Part of the [Other Computer Engineering Commons](#)

---

## Recommended Citation

Williams, Theresa Allen, "" (2011). *Dissertation*. 204.  
<https://digitalcommons.latech.edu/dissertations/204>

This Dissertation is brought to you for free and open access by the Graduate School at Louisiana Tech Digital Commons. It has been accepted for inclusion in Doctoral Dissertations by an authorized administrator of Louisiana Tech Digital Commons. For more information, please contact [digitalcommons@latech.edu](mailto:digitalcommons@latech.edu).

**SUB PIXEL ANALYSIS AND PROCESSING OF SENSOR DATA  
FOR MOBILE TARGET INTELLIGENCE INFORMATION  
AND VERIFICATION**

by

Theresa Allen Williams, M.E.

A Dissertation Presented in Partial Fulfillment  
of the Requirements for the Degree  
Doctor of Engineering

COLLEGE OF ENGINEERING AND SCIENCE  
LOUISIANA TECH UNIVERSITY

February 2011

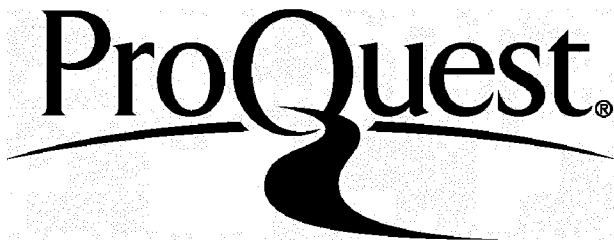
ProQuest Number: 3664381

All rights reserved

INFORMATION TO ALL USERS

The quality of this reproduction is dependent upon the quality of the copy submitted.

In the unlikely event that the author did not send a complete manuscript and there are missing pages, these will be noted. Also, if material had to be removed, a note will indicate the deletion.



ProQuest 3664381

Published by ProQuest LLC(2015). Copyright of the Dissertation is held by the Author.

All rights reserved.

This work is protected against unauthorized copying under Title 17, United States Code.  
Microform Edition © ProQuest LLC.

ProQuest LLC  
789 East Eisenhower Parkway  
P.O. Box 1346  
Ann Arbor, MI 48106-1346

LOUISIANA TECH UNIVERSITY

THE GRADUATE SCHOOL

20 August 2010

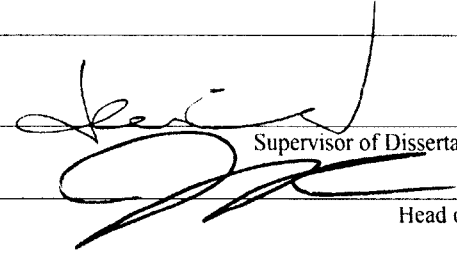
Date

We hereby recommend that the dissertation prepared under our supervision  
by Theresa Allen Williams

entitled

SUB PIXEL ANALYSIS AND PROCESSING OF SENSOR DATA FOR  
MOBILE TARGET INTELLIGENCE INFORMATION AND VERIFICATION

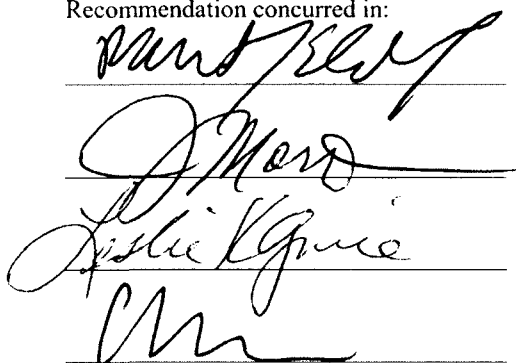
be accepted in partial fulfillment of the requirements for the Degree of  
Doctor of Engineering

  
Supervisor of Dissertation Research

  
Head of Department

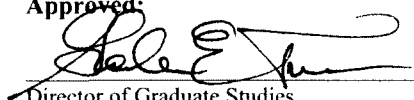
  
Department

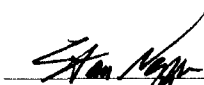
Recommendation concurred in:



Advisory Committee

Approved:

  
Director of Graduate Studies

  
Dean of the College

Approved:

  
Dean of the Graduate School

## **ABSTRACT**

This dissertation introduces a novel process to study and analyze sensor data in order to obtain information pertaining to mobile targets at the sub-pixel level. The process design is modular in nature and utilizes a set of algorithmic tools for change detection, target extraction and analysis, super-pixel processing and target refinement. The scope of this investigation is confined to a staring sensor that records data of sub-pixel vehicles traveling horizontally across the ground. Statistical models of the targets and background are developed with noise and jitter effects. Threshold Change Detection, Duration Change Detection and Fast Adaptive Power Iteration (FAPI) Detection techniques are the three methods used for target detection. The PolyFit and FermiFit are two tools developed and employed for target analysis, which allows for flexible processing. Tunable parameters in the detection methods, along with filters for false alarms, show the adaptability of the procedures. Super-pixel processing tools are designed, and Refinement Through Tracking (RTT) techniques are investigated as post-processing refinement options. The process is tested on simulated datasets, and validated with sensor datasets obtained from RP Flight Systems, Inc.

## APPROVAL FOR SCHOLARLY DISSEMINATION

The author grants to the Prescott Memorial Library of Louisiana Tech University the right to reproduce, by appropriate methods, upon request, any or all portions of this Dissertation. It is understood that "proper request" consists of the agreement, on the part of the requesting party, that said reproduction is for his personal use and that subsequent reproduction will not occur without written approval of the author of this Dissertation. Further, any portions of the Dissertation used in books, papers, and other works must be appropriately referenced to this Dissertation.

Finally, the author of this Dissertation reserves the right to publish freely, in the literature, at any time, any or all portions of this Dissertation.

Author *Theresa Willcox*  
Date *10/21/2010*

## **TABLE OF CONTENTS**

ABSTRACT .....	iii
LIST OF TABLES.....	xi
LIST OF FIGURES .....	xiv
CHAPTER ONE INTRODUCTION.....	1
1.1.    Research Need .....	2
1.1.1.    Meeting the Needs of High Altitude Sensors.....	2
1.1.2.    Applications.....	3
1.1.3.    Overabundance of Data .....	4
1.1.4.    Limited Resources.....	6
1.1.5.    Sensor Validation/Verification via Sub Pixel Process .....	6
1.2.    Dissertation Objectives.....	7
1.3.    Organization of Dissertation.....	7
CHAPTER TWO PROBLEM CONCEPT .....	9
2.1    Problem Statement.....	9
2.2.    Assumptions and Handling.....	10
2.2.1.    Sensors.....	10
2.2.2.    Target.....	10
CHAPTER THREE DATABASE MODELING.....	12
3.1.    Basic Background Model .....	14

3.2.	Basic Target Model.....	14
3.3.	Quantized Fermi Target Model .....	16
3.4.	Incorporating Background and Target.....	17
3.4.1.	Trapezoid Background and Target Model.....	17
3.4.2.	Quantized Fermi Derivative Background and Target Model .....	18
3.4.2.1.	Finding d parameter.....	19
3.4.2.2.	Finding b parameter.....	19
3.4.2.3.	Finding a parameter.....	20
3.4.2.4.	Finding c parameter.....	20
3.5.	Utilizing Realistic Inputs for Modeled Database.....	20
3.6.	Modeling Multiple Pixels .....	23
3.7.	Removing Assumptions.....	26
3.7.1.	Adding Noise .....	26
3.7.2.	Adding Jitter .....	27
3.7.2.1.	Translational Jitter.....	27
3.7.2.2.	Random Jitter.....	29
	CHAPTER FOUR CHANGE DETECTION .....	31
4.1	Threshold Change Detection .....	34
4.1.1.	The Background Model .....	36
4.1.2.	Establishing the Initial Threshold.....	36
4.1.3.	Threshold Detection Binary Matrix.....	37
4.1.4.	Threshold Detection Example .....	38
4.2.	Duration Change Detection .....	39

4.2.1.	Finding the Minimum Required Sample Set.....	39
4.2.2.	Create Histogram and Establish Filter Boundaries .....	41
4.2.3.	Duration Detection Binary Matrix.....	42
4.2.4.	Duration Detection Example .....	42
4.3.	Fast Adaptive Power Iteration (FAPI) Background Estimation.....	44
4.3.1.	FAPI Estimation .....	44
4.3.2.	FAPI Binary Matrix.....	46
4.3.3.	FAPI Background Suppression Example .....	46
4.3.4.	FAPI Change Detection.....	47
4.4.	False Alarm Rate Filter.....	49
4.4.1.	FAR1: Reconnect Disjointed Signals .....	49
4.4.2.	FAR2: Minimum Threshold Requirement .....	50
	CHAPTER FIVE TARGET EXTRACTION AND ANALYSIS .....	52
5.1.	Extract Target .....	54
5.1.1.	Considerations .....	54
5.1.2.	Extraction Example .....	54
5.2.	Target Analysis.....	56
5.2.1.	Assumption Review.....	56
5.2.2.	Calculating Target Velocity and Length .....	56
5.2.3.	FermiFit Analysis .....	57
5.2.3.1.	Finding the Fermi Derivative Parameters.....	57
5.2.3.1.1.	Parameter d .....	58
5.2.3.1.2.	Parameter b .....	58
5.2.3.1.3.	Parameter a .....	58

5.2.3.1.4. Parameter c .....	59
5.2.3.2. Recovering Critical Points.....	60
5.2.3.3. FermiFit Example.....	61
5.2.4. PolyFit Analysis .....	63
5.2.4.1. Least Squares Approximation .....	64
5.2.4.2. Trapezoid Approximation .....	65
5.2.4.3. PolyFit Example .....	67
CHAPTER SIX SUPER PIXEL REFINEMENT .....	69
6.1. Sum Pixel Refinement.....	70
6.2. Enlarge Pixel Refinement.....	72
6.3. Binary Target Matrix .....	73
6.4. Refinement Algorithms and Tools .....	75
6.4.1. Sum Pixel Algorithm.....	75
6.4.2. Enlarge Pixel Algorithm.....	76
6.5. Refined Change Detection.....	78
CHAPTER SEVEN REFINEMENT THROUGH TRACKING (RTT) .....	79
7.1. Historical Binary Target Matrix (HBTM) .....	80
7.2. Considerations .....	81
7.3. Trajectory Scenarios .....	82
7.3.1. X Dominant Travel.....	83
7.3.2. Y Dominant Travel.....	85
7.3.3. Dominant Travel Considerations.....	88
7.3.4. Special Case 1.....	89
7.3.5. Special Case 2.....	90

CHAPTER EIGHT TESTING .....	93
8.1.    Algorithm Verification .....	93
8.2.    Modeled Data Testing.....	94
8.2.1.    Overview .....	94
8.2.2.    Scenarios.....	95
8.2.2.1.    Change Detection Testing .....	95
8.2.2.2.    Target Analysis Testing.....	99
8.3.    Sensor Data Testing.....	103
8.3.1.    Data Information .....	103
8.3.2.    Scenarios.....	104
CHAPTER NINE RESULTS AND DISCUSSION .....	106
9.1.    Sensor Parameter Analysis and Performance.....	106
9.1.1.    Sensor Sample Rate.....	106
9.1.2.    Pixel Size.....	108
9.1.3.    Noise.....	110
9.1.4.    Jitter .....	112
9.2.    Method Analysis and Performance.....	114
9.2.1.    Change Detection .....	114
9.2.2.    Target Analysis.....	115
9.2.3.    Velocity and Length Calculations .....	116
9.3.    Sensor Data Results .....	120
CHAPTER TEN FURTHER WORK.....	133
CHAPTER ELEVEN CONCLUSION.....	135
APPENDIX A ALGORITHM VERIFICATION RESULTS .....	137

APPENDIX B TESTING TABLES .....	140
REFERENCES .....	184

## LIST OF TABLES

Table 3.1 Army Wheeled Vehicles to Test.....	21
Table 4.1 Example Frame Calculation Table for Army Vehicles .....	41
Table 8.1 Example of Excel Output of Modeled Sensor and Target Information for Change Detection Testing.....	95
Table 8.2 Example of Excel Output of Modeled Target Threshold Change Detection with FAR Filters for Change Detection Testing.....	96
Table 8.3 Example of Excel Output of Modeled Target Duration Change Detection with FAR Filters for Change Detection Testing.....	96
Table 8.4 Example of Excel Output of Modeled Target FAPI Change Detection with FAR Filters for Change Detection Testing.....	97
Table 8.5 Batch Run Variations for Sensor Parameters .....	99
Table 8.6 Example of Excel Output of Modeled Sensor and Target Information for Target Analysis Testing.....	100
Table 8.7 Example of Excel Output of Modeled Target Threshold Change Detection with FAR Filters for Target Analysis Testing.....	100
Table 8.8 Example of Excel Output of Modeled Target PolyFit and FermiFit Analysis for Target Analysis Testing .....	101
Table 8.9 Sensor Data Testing Scenario Criteria.....	104
Table 9.1 Sample Rate Effects on Detection and False Alarms .....	107
Table 9.2 Sample Rate Effects on Critical Point Given in Seconds of Error .....	107
Table 9.3 Pixel X Effects on Critical Point Given in Seconds of Error .....	109
Table 9.4 Percent Detection and False Alarm Frames for Noise Variations .....	110
Table 9.5 Percent Detection and False Alarm Frames and Missed Detections in Noisy Sensor with N Variations .....	112
Table 9.6 Percent Detection and False Alarm Frames for Different Jitter Variations.	112

Table 9.7 Percent Detection and False Alarm Frames and Missed Detections for Jittered Pixels with Different N Variations .....	113
Table 9.8 Change Detection Error of Critical Points Enter <sub>1</sub> and Exit <sub>2</sub> .....	114
Table 9.9 Target Analysis Second Error of Critical Points Enter <sub>1</sub> and Exit <sub>2</sub> .....	115
Table 9.10 Velocity and Length Test Results.....	118
Table 9.11 Delta Length and Delta Velocity Calculations .....	119
Table A.1 Algorithm Verification Results .....	138
Table B.1 Detection Comparison: Sensor and Target Information.....	141
Table B.2 Detection Comparison: Threshold Detection Results .....	145
Table B.3 Detection Comparison: Duration Detection Results.....	149
Table B.4 Detection Comparison: FAPI Detection Results .....	153
Table B.5 Analysis Comparison (w/Threshold Detect): Sensor and Target Information .....	157
Table B.6 Analysis Comparison (w/ Threshold Detection): PolyFit and FermiFit Results .....	158
Table B.7 Analysis Comparison (w/ Duration Detect): Sensor and Target Information .....	160
Table B.8 Analysis Comparison (w/ Duration Detect): PolyFit and FermiFit Results .....	161
Table B.9 Analysis Comparison (w/ FAPI Detect): Sensor and Target Information ..	162
Table B.10 Analysis Comparison (w/ FAPI Detect): PolyFit and FermiFit Results .....	162
Table B.11 Sample Rate Analysis Data from Analysis Comparison w/ Duration Detect.....	162
Table B.12 Pixel Size Analysis Data from Analysis comparison w/ Threshold Detect.....	162
Table B.13 Noise Effects Results in Detection Testing .....	163
Table B.14 Noise Effects Analysis.....	171
Table B.15 Jitter Effect Results in Detection Testing .....	172
Table B.16 Jitter Effects Analysis .....	181

Table B.17 Velocity and Length Testing Results.....	181
Table B.18 Sensor Data Threshold Detection .....	183
Table B.19 Sensor Data Duration Detection .....	183
Table B.20 Sensor Data FAPI Detection.....	183
Table B.21 Sensor Data PolyFit and FermiFit Analysis Data.....	183

## LIST OF FIGURES

Figure 1.1	Graphical depiction of the relationship between sensor altitude, instantaneous field of view and the resolution cell .....	2
Figure 1.2	Applying Information to Gain Knowledge .....	5
Figure 2.1	Pictoral Description of Critical Target Points.....	9
Figure 3.1	Trapezoid figure of target within the pixel .....	15
Figure 3.2	(A) Fermi Derivative Model and (B) Quantized Derivative Model Output ..	16
Figure 3.3	Temporal Profile of a Target Moving Through a Pixel .....	17
Figure 3.4	Illustrates the FDM as applied to a sub-pixel environment .....	18
Figure 3.5	Derivation of basic parameters using pixel intensity values.....	21
Figure 3.6	Modeled target moving horizontally in a single row .....	24
Figure 3.7	Single target with horizontal motion split among two rows .....	25
Figure 3.8	Noise added after the target insertion algorithms .....	26
Figure 3.9	(A) Pictorial Description of Translational Jitter (B) Intensity variation due to translational jitter.....	28
Figure 3.10	Multidirectional shifting along a frame caused by jitter .....	29
Figure 4.1	(A) HUMMWV signal before noise and (B) after noise.....	38
Figure 4.2	Standard deviation estimates and Threshold Binary Matrix .....	38
Figure 4.3	(A) M1070 profile with no noise (B) M1070 profile with 0.02 noise .....	42
Figure 4.4	Duration Detection Histogram Plot (Intensity vs. # Frames).....	43
Figure 4.5	(A) Duration Binary Matrix (B) Utilizing the FAR filters to reduce false alarms .....	43
Figure 4.6	(A) Original Background Image (B) FAPI Estimation (C) FAPI Background suppression .....	46

Figure 4.7 (A) M1070 modeled target (B) FAPI suppression results .....	47
Figure 4.8 (A) Threshold Example (B) Threshold Binary Matrix (C) FAPI estimation (D) FAPI Binary Matrix.....	48
Figure 4.9 Results after applying FAR1 filter to FAPI Binary Matrix.....	48
Figure 4.10 (A) Threshold Binary Matrix (B) Application of FAR1 filter to recapture critical target points.....	50
Figure 4.11 (A) Initial target (B) Target with noise (C) Threshold Change Detection (D) Threshold Binary Matrix .....	51
Figure 4.12 (A) FAR1 Results (B) FAR2 Results.....	51
Figure 5.1 M1070 signal with noise profile and critical entry and exit points marked...	55
Figure 5.2 Target Binary Matrix with Extraction Points.....	55
Figure 5.3 (A) HEMTT Target Signal (B) Threshold Binary Matrix .....	61
Figure 5.4 FermiFit approximation superimposed over the HEMTT target signal + noise .....	62
Figure 5.5 Modeled HUMVEE target with critical points marked .....	62
Figure 5.6 A trapezoid approximation using the six intersection points to uncover the four critical points .....	63
Figure 5.7 (A) Modeled target with critical points marked (B) Target profile with noise .....	67
Figure 5.8 PolyFit analysis with original critical points marked.....	68
Figure 6.1 (A) 2x2 pixel array showing temporal profile of same target (B) Sum-pixel result of same target showing trapezoid profile .....	70
Figure 6.2 Multi-pixel target split among two rows.....	71
Figure 6.3 (A) Close up view of Pixel <sub>(2,1)</sub> (B) Result of summing pixels in rows 2 and 3 .....	71
Figure 6.4 (A) Result of summing rows 2 and 3 with columns 1 and 2 (B) Result from summing rows 2 and 3 with columns 1-4.....	72
Figure 6.5 (A) Single-pixel target with 0.25 jitter and 1.25% noise (B) Result from enlarging pixel by a factor of 0.8 .....	73
Figure 6.6 Pictoral description of temporal target binary matrix .....	74

Figure 7.1 Utilizing the HBTM for calculating target trajectory .....	80
Figure 7.2 Target trajectory assessment with Sum-pixel refinement to meet pixel conditions .....	82
Figure 7.3 Temporal elapse of target traveling through a pixel. ....	83
Figure 7.4 (A) Depiction of width parameters (B) Depiction of length parameters .....	84
Figure 7.5 Temporal elapse of target traveling in Y-dominant direction.....	86
Figure 7.6 (A) Depiction of width parameters in Y-dominant travel (B) Depiction of length parameters in Y-dominant travel.....	87
Figure 7.7 Possible Target Shapes for a Given Pixel, Velocity, and Trajectory .....	89
Figure 7.8 (A) Special Case 1 angles of entry (B) Pictorial depiction of Special Case 1 .....	90
Figure 7.9 Pictoral description of Special Case 2 angles of entry into pixel.....	91
Figure 7.10 (A) Target crosses completely in x-direction (B) Target crosses completely in y-direction .....	91
Figure 8.1 Comparative graphic display of change detection algorithms .....	98
Figure 8.2 Example illustration of target analysis plots from PolyFit and FermiFit testing .....	102
Figure 8.3 Image of RP Flight Systems Inc., remote controlled truck with varying background taken from 18 m above ground .....	103
Figure 9.1 (A) $30 \times 30 \text{ m}^2$ Pixel with HEMTT Target (B) $30 \times 5 \text{ m}^2$ Pixel with HEMTT Target.....	108
Figure 9.2 GUI for Sub-pixel Detection and Analysis .....	117
Figure 9.3 Bar Chart Showing the Calculated Target Lengths.....	119
Figure 9.4 Analysis Results of Enlarging a Pixel by 0.5 in X and Y Directions.....	121
Figure 9.5 Analysis Results of Enlarging a Pixel by 1.0 in X and 0.5 in Y .....	122
Figure 9.6 Analysis Results of Mobile Target with Shadowed Background .....	124
Figure 9.7 Analysis Results of Mobile Target in Bright Background.....	125
Figure 9.8 Detection in Bright Background Scenarios.....	126
Figure 9.9 Analysis of Bright Background Scenarios .....	127

Figure 9.10 Analysis of Bright and Shadowed Background with Mobile Target .....	129
Figure 9.11 Analysis of Mobile Target in Changing Background Environment .....	131
Figure 9.12 Detection of Mobile Target in Changing Background Environment.....	132

## **CHAPTER ONE**

### **INTRODUCTION**

With the nation gearing toward a persistent surveillance environment [1], the ability to convert an abundance of raw sensor data into quality information is imperative. One aspiration in this arena is to obtain intelligent information from the data with efficiency and accuracy in order to provide the means to make timely strategic, operational, and tactical decisions concerning targets of interest. This dissertation presents a sub-pixel processing technique that will detect and analyze sensor data and provide moving target information.

Although computational methods currently exist for target detection and analysis, many of these processing and analysis techniques rely on multiple pixels or whole images. Problems with these methods arise when the target is smaller than a pixel. This issue is solved by temporally focusing on single pixels. By capturing the intensity variations of a pixel over time and applying knowledge of a pixel's geometry, it is feasible to detect a mobile target and acquire its characteristics.

The sub-pixel process assumes a staring sensor observing individual targets smaller than a pixel. Using standard detection algorithms, a target is detected and extracted from a frame sequence. Then, the FermiFit and PolyFit methods are utilized to analyze the target's data; yielding the moving target's characteristics of velocity and

length. The process is tested on simulated datasets, using the statistical models, and validated with sensor datasets obtained from RP Flight Systems, Inc.

## 1.1. Research Need

### 1.1.1. Meeting the Needs of High Altitude Sensors

The distance between the sensor and the target plays an important role in determining the level of image detail and the amount of area coverage the sensor can provide. Sensors on high altitude platforms, such as satellites, high altitude aircraft or Remotely Piloted Aircraft (RPAs), typically view large areas, but are limited in detail [2].

The level of image detail depends on the spatial resolution found in the instantaneous field of view. This field of view and the altitude of the sensor determine the size of the resolution cell. In order to detect a homogeneous feature in an image, the object has to be equal to or larger than the resolution cell [2]. Smaller targets are not easily discerned in a single image as the sensor detects the intensity combination of all of the features in the cell (Figure 1.1).

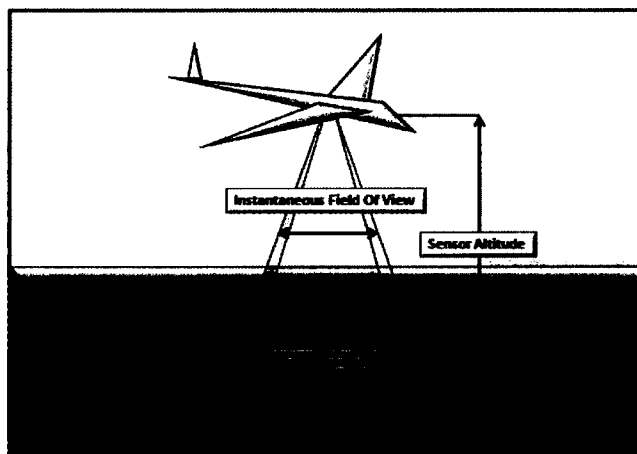


Figure 1.1 Graphical depiction of the relationship between sensor altitude, instantaneous field of view and the resolution cell

Novel methods of detecting these smaller targets to provide target characteristics are useful in military, law enforcement and homeland security applications.

#### 1.1.2. Applications

There are numerous applications for which sub-pixel processing is applicable. Some notable applications are for military Intelligence, Surveillance and Reconnaissance (ISR), border patrol and drug interdiction.

A longer duration staring capability is needed for persistence surveillance, but given ephemeris data, persistent surveillance with high resolution may not be possible. Low Earth Orbiting (LEO) satellites have high resolution but a short dwell-time over the target area, which is dictated by ephemeris data. Obtaining a balance between dwell-time and resolution often means missing target opportunities. Geostationary Earth Orbiting (GEO) satellites, however, provide persistent surveillance, but given the distance from Earth, it has limited resolution. With sub-pixel processing, the low resolutions experienced by geostationary satellites are mitigated, providing new opportunities for the Intelligence, Surveillance, and Reconnaissance (ISR) community.

The U.S. border patrol has a vast amount of area to safeguard, with nearly 6,000 miles of Mexican and Canadian international land borders and over 2,000 miles of coastal waters in its jurisdiction. The Department of Homeland Security does not have the resources or assets to continuously monitor every mile [3]. The sub-pixel process can be useful in detecting the illegal entrance of people or vehicles into the country, especially in remote locations. The algorithm can utilize sensor data from the patrol's existing unmanned aerial vehicles inventory by raising its altitude. This methodology can be applied to the resulting lower resolution of the sensor data to provide analysis of

sub-pixel targets; potentially capturing previously undetected illegal entries or smuggling routes.

The Joint Inter-Agency Task Force South (JIATF-South) performs drug interdiction operations that involve ‘actionable intelligence on the locations of suspect drug trafficking vessels’ [4]. As with the border patrol, JIATF-south has a large area to cover on land and sea. Illegal ‘drugs coming to the United States from South America pass through a 42 million square-mile transit zone, roughly twice the size of the continental U.S.’ [4]. To transport the drug supply, traffickers typically use fishing, high-speed ‘go-fast’, or low-profile semi-submersible vessels [4]. The go-fast and semi-submersible vessels are small and difficult to detect. Stealth is also a consideration as law enforcement officials need to monitor activity without being detected lest they give away their position or opportunity to apprehend the suspect. Small RPAs at high altitudes would provide the opportunity to constantly monitor traffic while in turn, being difficult to detect. This platform is ideal for the sub-pixel process, which has the potential to identify this small, drug trafficking watercraft traveling over a large, relatively static aquatic background.

#### 1.1.3. Overabundance of Data

Data by itself is meaningless. If knowledge is added to this data, it becomes information, which adds value to what is collected. This knowledge can change a previously fruitless search into a productive, efficient, and focused investigation, ultimately providing the end user the capability to make more informed judgments and decisions (Figure 1.2).

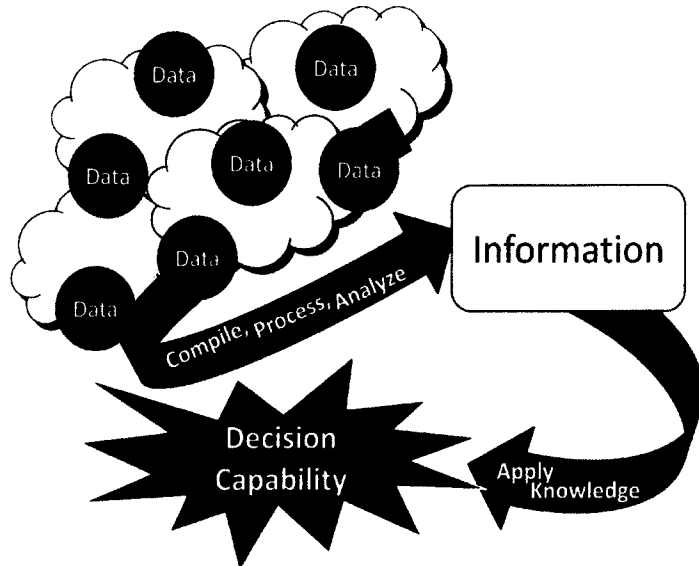


Figure 1.2 Applying Information to Gain Knowledge

A main issue is that the amount of data far outnumbers the trained analysts available to process it into information. Within the intelligence community, the need for applications to help analysts is in the area of image processing used to detect, track and identify targets [5].

There exists a myriad of ways to process images; some of which are discussed in Chapter Four. The desired result is to gain actionable information. There will not always be the proper resolution, the necessary equipment, nor the manpower required to filter through the copious amounts of data. The need to identify novel methods to mitigate these circumstances is paramount.

In low resolution instances, visually analyzing the image to infer information is a daunting task. If a target size is less than a pixel, whole-image and static processing will not be effective. The sub-pixel process described in this dissertation is a concept able to pull actionable information from streams of raw data.

#### 1.1.4. Limited Resources

As former Secretary of Defense Donald Rumsfeld advised, ‘go to war with the army you have, not the army you might want’ [6]. Resources have limitations, such as cost, equipment, and capabilities.

From a sensor based perspective, specifically with satellites, targets of opportunity are limited based on ephemeris data, weather, and target availability. It is not practical or cost effective to go into space and repair a satellite or change out its sensors. It is also not cheap or quick to put up another satellite with a different sensor sweep when the need arises and to have it operational in time.

As discussed earlier, by widening the area of view, thereby decreasing the focus or resolution, one can observe more area at once. The sub-pixel methodology in this dissertation ascribes to this principle. Instead of increasing the number of sensors or platforms in an area, sensors can encompass a larger field of view and still characterize moving targets from the resulting degradation in resolution.

#### 1.1.5. Sensor Validation/Verification via Sub Pixel Process

Sub-pixel processing can also revalidate sensor suites by analyzing the performance capabilities and limits of a given platform and sensor for each of its current applications or by identifying new functions and capabilities of existing sensors.

Current sensors applying the sub-pixel process can re-certify their capability through this analysis. The analysis would provide the new parameters for the sensor altitude and resolution and the subsequent ranges of the detectable target’s size, velocity and percent pixel radiometry.

Used in conjunction with other sensors, the sub-pixel algorithm can compile comparisons to include altitude versus resolution trade-offs as well as sensor and target constraints for detection and characterization capability.

### **1.2. Dissertation Objectives**

The overall objective of this dissertation is to provide an innovative process for imagery data for the purpose of identifying characteristics of sub-pixel mobile target.

The specific objectives for this research involve the development, testing and analysis of the sub-pixel algorithm. The process will study sensor data, identify moving targets within a sensor pixel, and estimate target information.

The follow-on objective after the completion of the dissertation is to incorporate the super-pixel refinement and Refinement Through Tracking (RTT) methods developed in this paper into the sub-pixel process algorithm.

### **1.3. Organization of Dissertation**

The second chapter recaptures the problem and defines the assumptions and their handling, while the third chapter develops the database models for the pixel and target used throughout the dissertation.

The fourth chapter discusses the current techniques in the change detection field, investigates three detection algorithms and develops two false alarm refinement algorithm tools. At the end of each section, examples of each process are provided for illustration purposes.

The fifth chapter provides a brief literature search of target analysis methods, and creates two novel processes for analyzing sub-pixel targets. Illustrative examples are also included in this chapter.

Chapter Six describes the tools produced for super-pixel processing and Chapter Seven does a theoretical investigation on improving target analysis via historical target tracking.

The eighth chapter presents the testing scenarios and Chapter Nine provides the results and discussion portion of the dissertation. Chapter Ten focuses on further work and project exploration. The dissertation concludes with Chapter Eleven.

## CHAPTER TWO

### PROBLEM CONCEPT

#### 2.1 Problem Statement

This dissertation develops a set of tools to process sensor data and analyze sub-pixel mobile targets.

The basic target concept is that an object moving through the pixel will create a trapezoid intensity profile when viewed temporally (Figure 2.1).

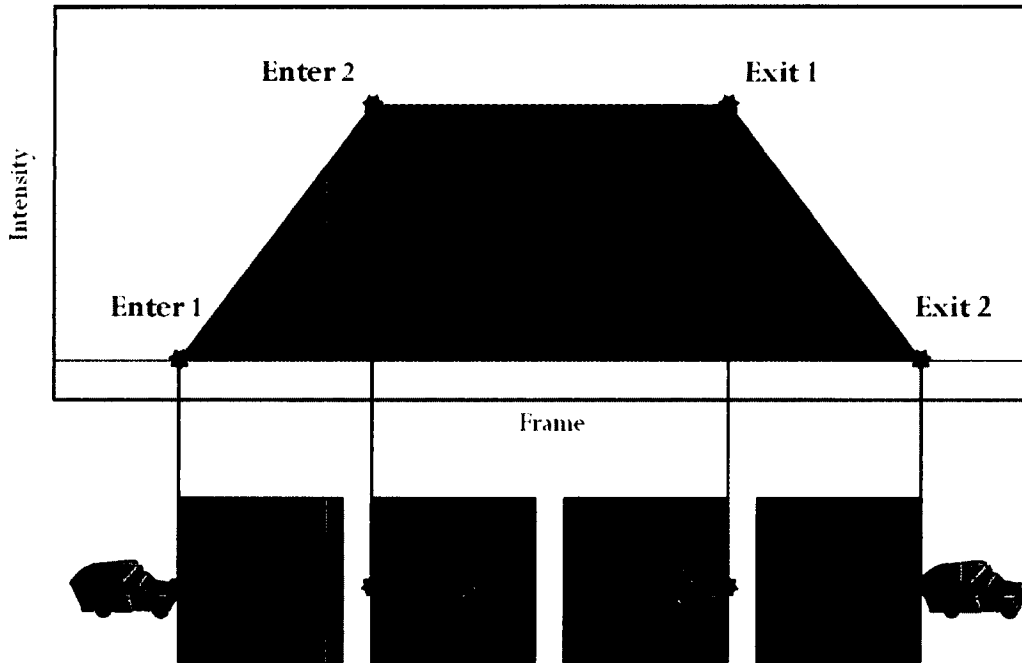


Figure 2.1 Pictoral Description of Critical Target Points

$Enter_1$  is the point where the target first starts to enter the pixel,  $Enter_2$  is the point where the target is fully within the pixel,  $Exit_1$  is the point where the target first starts to exit the pixel, and  $Exit_2$  is the point where the target has fully exited the pixel.

By studying this problem geometrically and temporally, it is feasible to discover target characteristics, such as velocity and length.

## 2.2. Assumptions and Handling

### 2.2.1. Sensors

The sub-pixel algorithm is generic in design such that it will perform for a variety of sensors and platforms. However, some basic assumptions concerning the sensors are necessary for algorithm development. Once completely developed and as these assumptions change, adjustments in the affected areas are possible.

The sensor assumptions include that the data from the sensor is a framing system, which gathers instantaneous measurements at a constant sample rate from the entire scene at once. The pixel geometry is rectangular, with target intensities centered on the pixel and having a point spread function contained within the pixel. The sensor bias is considered constant and the measured noise has a Gaussian profile.

The algorithm processes data as a single intensity value, normalized between zero and one. If other types of data are received, such as RGB data, it is converted to a grayscale dataset and normalized.

### 2.2.2. Target

The sub-pixel algorithm detects and analyzes mobile targets smaller than a pixel. The development of an appropriate target model is imperative for algorithm design and assumptions are made to bound the problem.

The basic target shape is rectangular and emits measurements uniformly across its entire surface area. The target velocity is constant and greater than one frame per pixel and the ground slope is negligible in comparison to the altitude of the sensor.

The initial target trajectories travel in the horizontal plane with respect to the sensor array. Studies later in the dissertation involve relaxing this assumption to refine the algorithm performance during target analysis. However, the assumption remains that the trajectory has a short term linear motion such that within a given pixel sequence; the target will maintain a straight line.

## **CHAPTER THREE**

### **DATABASE MODELING**

Identifying the existence of a moving target is basically a change detection problem. Whether done temporally or spatially, all detection models ‘look’ for a difference between the target and the quasi-static background. When finding objects in the sub-pixel realm, the target rarely presents visually identifying features, such as contours and textures. This limits the ability to detect a target using spatial variations. Temporal processing, therefore, becomes the feasible option for the sub-pixel detection algorithm.

The development and testing of the detection algorithm uses statistical models simulating the background and target profiles. Many researchers, such as Zhang and Barniv, focused primarily on target detection, treat small, moving targets as a point source [7] [8]. Others, [9] [10] [11] [12] [13] [14], rely on background suppression techniques to isolate the target and do not use a target model. Caefer et. al classifies temporal profiles of the static object/sky and a moving target and uses the distinctions between these profiles to segment IR images for target detection via a Triple Temporal Filtering process [15]. Tzannes et. al. furthers this work and performs a series of experimental tests which validates the use of a Fermi derivative equation as a model of IR targets [16]. The purpose of this dissertation is to analyze target characteristics of moving vehicles, so a modeled target is essential for testing an evaluation. Tzannes

Fermi derivative as well as a trapezoid depiction, which is novel to this dissertation, provides the target models for the sub-pixel algorithm development.

A generally accepted background model uses a constant signal with additive Gaussian noise [7] [9] [10] [15] [17] [18] [19] [20] [21]. More complex models use an adaptive approach to accommodate shifts in the background scenario [13] [14] [22] [23]. The sub-pixel algorithm employs both the generic background and an adaptive Fast Approximated Power Iteration background model [13] [14] for a comparative analysis.

For the modeled database, the simplest scenario is created, tested and analyzed. The simplest scenario is a static, uniform background with a single, uniform, well-defined target moving at a constant speed in the horizontal direction from left to right. It assumes no effects from noise, jitter, percent radiometry, and change of target trajectory. The scenario is then complicated by removing these assumptions. Once analysis of the simplest scenario occurs, the scenario complicates itself by removing the assumptions and adds in noise and jitter, varying percent radiometry and different target trajectories.

This analysis uses input datasets with grayscale intensity levels. The single intensity scale values keep the computation complexity minimized and works well for a multitude of environments, such as IR. The input intensity values are stored in  $\text{Pixel}(r, c, f)$  arrays, where  $r$  is the pixel row,  $c$  is the pixel column and  $f$  is the number of frames. For computational purposes and for differing future datasets, all intensity values are converted into normalized values between zero and one.

It is important to note that the sub-pixel algorithm processes data in terms of frame count vs. time. The correlation between the two is expressed by

$$t = \frac{\text{frame}}{\text{SampleRate}}$$

where  $t$  is the passage of time during the dataset,  $frame$  is the total number of frames in the dataset, and  $SampleRate$  is the rate that the data samples are taken in frames per second.

### 3.1. Basic Background Model

Assuming a quasi-static background with all the other assumptions in place, the background can be considered a constant signal.

$$I_{back}(r, c, f) = C,$$

where  $I_{back}$  is the background intensity matrix with indices of row,  $r$ , column,  $c$ , and current frame,  $f$ .  $C$  is the constant background signal.

### 3.2. Basic Target Model

Unless the target has an identical intensity to the background, a uniform target moving across the pixel will experience either a positive intensity change throughout the transit or a negative intensity change. The temporal profile, assuming a constant speed across the pixel, displays a trapezoid geometric configuration. When the target enters the pixel, the intensity increases or decreases linearly until the target is fully within the pixel. With the target fully in the frame, the intensity steadies out. Once the target starts to exit the pixel, the intensity decreases or increases at the same rate, but of opposite slope of the entrance. Once the target fully exits the pixel, the pixel will reflect the background signal (Figure 3.1).

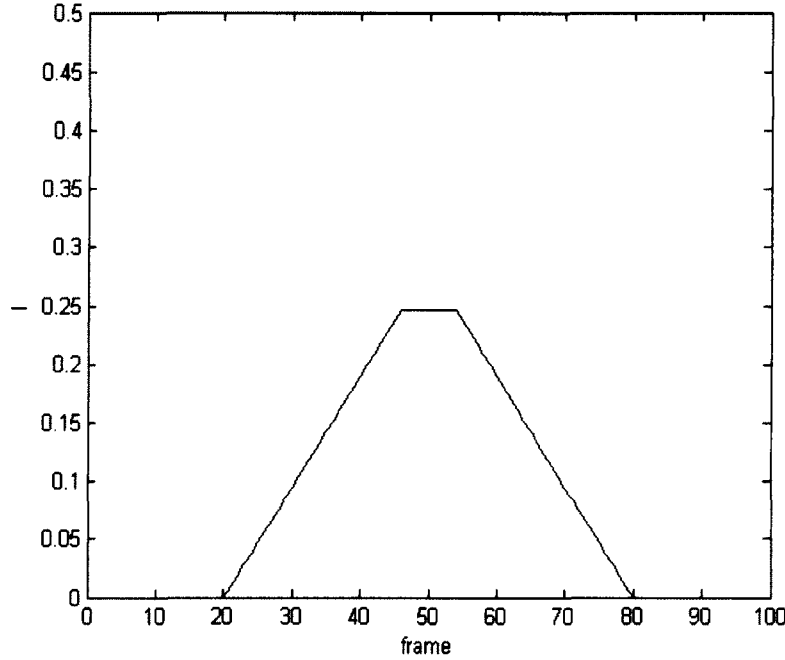


Figure 3.1 Trapezoid figure of target within the pixel

The trapezoidal model equation is given by

$$I_{Target}(r, c, f) = \begin{cases} \frac{(q)}{(Enter_2 - Enter_1)}(f - Enter_1), & \text{if } Enter_1 \leq f \leq Enter_2 \\ q, & \text{if } Enter_2 < f < Exit_1, \\ \frac{(-q)}{(Exit_2 - Exit_1)}(f - Exit_1) + q, & \text{if } Exit_1 \leq f \leq Exit_2 \end{cases}$$

where  $I_{Target}(r, c, f)$  is the temporal target intensity matrix with indices of row,  $r$ , column,  $c$ , and current frame,  $f$ .  $Enter_1$  is the frame at which the target enters the pixel,  $Enter_2$  is the frame at which the target is fully in the pixel,  $Exit_1$  is the frame at which the target starts to leave the pixel,  $Exit_2$  is the frame at which the target has fully exited the pixel, and  $q$  is the uniform intensity of the target. Due to the constant velocity assumption, the target entry and exit frames are equivalent,

$$(Enter_2 - Enter_1 = Exit_2 - Exit_1).$$

### 3.3. Quantized Fermi Target Model

The trapezoidal model is not continuous and an alternative model for comparison purposes is useful. Previous studies by Tzannes use a Fermi derivative to generate the pulse-like shape of IR targets [16] using the equation

$$f_{df}(k; a, b, c, d) = \frac{ae^{\frac{k-b}{c}}}{(e^{\frac{k-b}{c}} + 1)^2} + d, \quad (3.1)$$

where  $k$  is the frame number,  $a$  is proportional to the target intensity,  $b$  is the related to the frame where the target is fully within the pixel,  $c$  controls the width of the function or the velocity parameter, and  $d$  is the background level. This equation uses the normalized intensity vs. the grayscale intensity.

A trapezoid shape is desired because the edges of the max intensities are critical values for target analysis, which is discussed in Chapter Five. Applying a threshold quantization forces the Fermi pulse-like shape into a quasi trapezoidal signal (Figure 3.2).

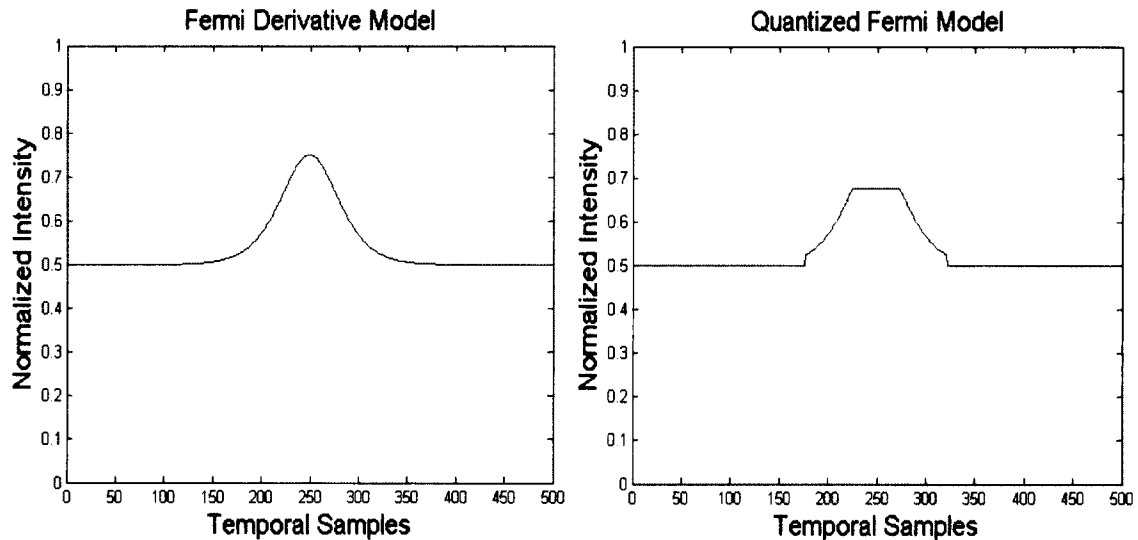


Figure 3.2 (A) Fermi Derivative Model and (B) Quantized Derivative Model Output

### 3.4. Incorporating Background and Target

#### 3.4.1. Trapezoid Background and Target Model

Unlike a multi-pixel target, where the entire pixel is replaced upon passing, when a sub-pixel target moves into the pixel, it replaces only a percentage of the pixel background (Figure 3.3).

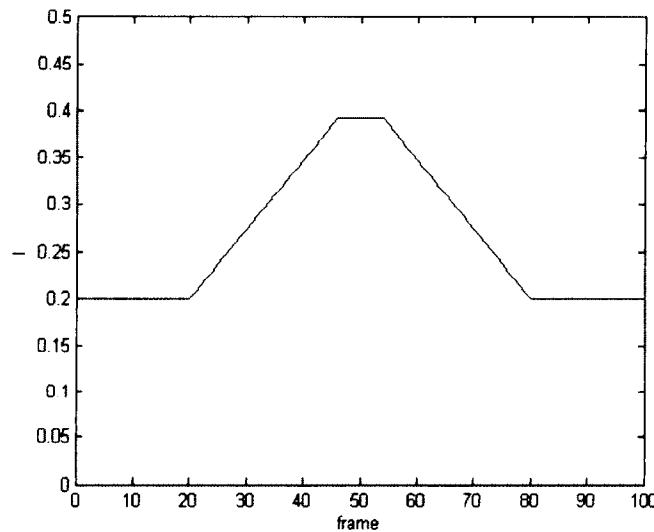


Figure 3.3 Temporal Profile of a Target Moving Through a Pixel

The critical target points from Chapter Two are used to develop the trapezoid model of the mobile target, which is given by

$$I_{Pixel}(r, c, f) = \begin{cases} I_{Back}(r, c, f), & \text{if } f < Enter_1 \\ \frac{q}{(Enter_2 - Enter_1)}(f - Enter_1) + I_{Back}(r, c, f), & \text{if } Enter_1 \leq f \leq Enter_2 \\ (1 - RTP)I_{Back}(r, c, f) + RTP \cdot I_{Target}(r, c, f), & \text{if } Enter_2 < f < Exit_1, \\ \frac{-q}{(Exit_2 - Exit_1)}(t - Exit_1) + q, & \text{if } Exit_1 \leq f \leq Exit_2 \\ I_{Back}(r, c, f), & \text{if } f < Exit_2 \end{cases}$$

where  $I_{Pixel}(r, c, f)$  is the pixel intensity matrix,  $I_{Target}$  is the temporal target intensity matrix, and  $I_{Back}$  is the background intensity matrix. All of the matrices use indices of row,  $r$ , column,  $c$ , and current data frame,  $f$ .  $RTP$  is the ratio of the target size to the pixel size,  $q$  is the uniform target intensity, and  $Enter_1$ ,  $Enter_2$ ,  $Exit_1$ , and  $Exit_2$  are previously defined.

The main issue with incorporating the background is having enough intensity variation between the background and the target to be able to detect the target. The intensity variation is directly proportional to  $RTP$ . As  $RTP$  decreases, the success of the detection algorithm decreases.

### 3.4.2. Quantized Fermi Derivative Background and Target Model

The Fermi Derivative Model (FDM) was not originally designed for sub-pixel targets and the model assumes the target fully covers the pixel ( $RTP \geq 1$ ). However, through analysis, the FDM can work on sub-pixel targets by making a few adaptations, such as correlating the trapezoid model and the FDM to gain knowledge of the target's parameters (Figure 3.4).

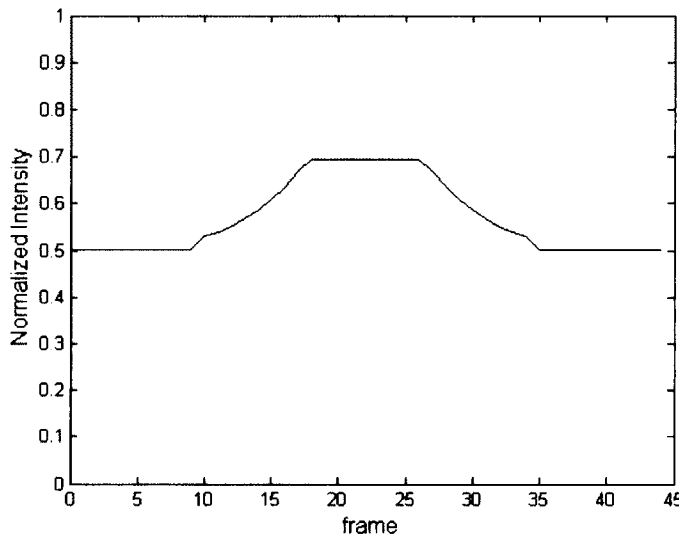


Figure 3.4 Illustrates the FDM as applied to a sub-pixel environment

To relate the FDM into a sub-pixel environment, each parameter within the FDM (Eq. 3.1) defines and correlates the target and sub-pixel environment. The parameters provide the relationship to the trapezoid model needed for ground truth knowledge during testing.

#### 3.4.2.1. Finding d parameter

From Section 3.3,  $k$  is the frame number and  $a$ ,  $b$ ,  $c$ , and  $d$  are constants. As  $k$  approaches infinity,

$$\lim_{k \rightarrow \infty} \frac{ae^{\frac{k-b}{c}}}{(e^{\frac{k-b}{c}} + 1)^2} + d = d, \quad (3.2)$$

and the pixel intensity reduces to  $d$ ,

$$d = I_{Back},$$

which for a staring sensor would be the average background intensity.

#### 3.4.2.2. Finding b parameter

The  $b$  parameter is related to the midpoint of the Fermi derivative, which correlates to the midpoint frame of the target signature. The target transit frames,  $f_{transit}$ , are found by

$$f_{transit} = Exit_2 - Enter_1,$$

where  $Enter_1$  is the first frame of target entry and  $Exit_2$  is the frame where the target exits the pixel. The transit frames are halved and added to the frame of entry to find the target signature midpoint,  $b$ ,

$$b = \frac{f_{transit}}{2} + Enter_1.$$

### 3.4.2.3. Finding a parameter

At the midpoint frame ( $k = b$ ), Eq. 3.2 reduces to:

$$f_{df}(k = b; a, b, c, d) = \frac{a}{2^2} + d,$$

Referencing the trapezoid model in Section 3.4.1., when  $k = b$ , the pixel intensity is the intensity value of the target fully within the pixel frame such that

$$f_{df}(k = b) = (1 - RTP)I_{Back} + RTP \cdot I_{Target},$$

where  $RTP$  is the ratio of the target size to the pixel size,  $I_{Target}$  is the target intensity, and  $I_{Back}$  is the background intensity. These equations are combined to solve for parameter  $a$ ,

$$a = 4([(1 - RTP)I_{Back} + RTP \cdot I_{Target}] - d).$$

### 3.4.2.4. Finding c parameter

The  $c$  parameter relates to the width of the Fermi derivative function and is related to the trapezoid profile via the equation:

$$c = N(Exit_1 - Enter_2),$$

where  $Enter_1$  is the first frame of target entry,  $Exit_2$  is the frame where the target exits the pixel, and  $N$  is an adjustable parameter used to control the width estimation.  $N$  values between one and two effectively model the targets used in this dissertation.

## 3.5. Utilizing Realistic Inputs for Modeled Database

Army vehicle parameters are used for the database modeling because they are known values that can be tested and verified.

Table 3.1 lists the length, width and maximum speed of four common Army vehicles. Throughout the testing scenarios, these Army vehicles will be used as the modeled targets [24].

Table 3.1 Army Wheeled Vehicles to Test

	Length	Width	Max Speed
HUMMWV	4.57 m	2.16 m	29.06 m/s
HEMTT (M977)	10.19 m	2.44 m	25.48 m/s
M1070	24.89 m	3.68 m	20.12 m/s
- Tractor	9.09 m	2.59 m	20.12 m/s
- Trailer	15.80 m	3.68 m	20.12 m/s
- w/ payload			13.41 m/s
PLS			
- Truck	10.95 m	2.44m	25.48 m/s
- Trailer	8.32 m	2.43 m	25.48 m/s
- w/ payload			15.64 m/s

The target's information (length, width and velocity), the pixel size and the sensor sample rate are related to the trapezoid model parameters for programming and signal insertion (Figure 3.5). The equations in this section and throughout the testing scenarios are based on an assumed horizontal trajectory. Alternate target trajectories and their change effects are discussed in Chapter Seven.

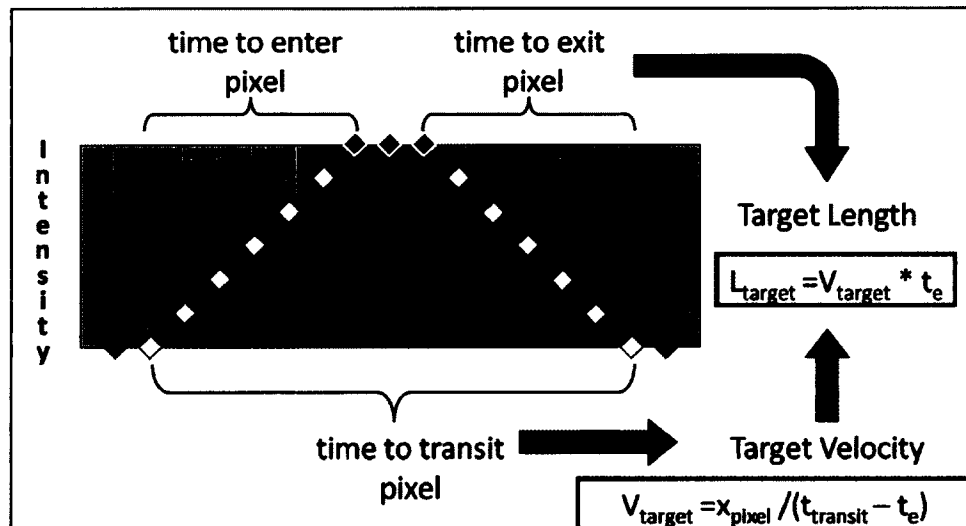


Figure 3.5 Derivation of basic parameters using pixel intensity values

The basic equation for velocity,

$$\text{Velocity} = \frac{\Delta d}{\Delta t} = \frac{x_{pixel}}{Exit_1 - Enter_1} = \frac{x_{pixel}}{Exit_2 - Enter_2},$$

can be related to a vehicle crossing a pixel, where the change in distance,  $\Delta d$ , is the horizontal length of the pixel,  $x_{pixel}$  and the change in time,  $\Delta t$ , is the amount of frames it takes for one point of the target to fully transverse the pixel.  $Enter_1$  is the first frame of target entry,  $Enter_2$  is when the target fully enters the pixel,  $Exit_1$  is when the target starts to exit the pixel, and  $Exit_2$  is the frame where the target exits the pixel.

The front end of the target,  $f_{entry}$ , correlates to

$$f_{entry} = Enter_2 - Enter_1,$$

while the back end of the target,  $f_{exit}$ , correlates to

$$f_{exit} = Exit_2 - Exit_1.$$

Note that at this point, the term frame is interchanged with time, knowing that there is a sample rate conversion factor between frames/s and m/s, shown by

$$t = \frac{\text{frame}}{\text{SampleRate}},$$

where  $t$  is the passage of time during the dataset,  $frame$  is the total number of frames in the dataset, and  $SampleRate$  is the rate that the data samples are taken in frames per second.

The velocity can also be related to the length of the target,  $L_{target}$  by

$$V_{target} = \frac{L_{target}}{f_{entry/exit}},$$

where  $f_{entry/exit}$  is the number of frames it takes the target to either enter or exit the pixel.

The target transit time can be calculated by

$$f_{transit} = \frac{x_{pixel}}{V_{target}} + f_{entry},$$

where  $f_{transit}$  is the number of frames it takes the target to completely transverse the pixel.

From these equations, and knowing the frame number where the target starts to enter the pixel, the critical target points can be found by:

$$Enter_2 = f_{entry} + Enter_1,$$

$$Exit_1 = Exit_2 - f_{entry},$$

and

$$Exit_2 = Enter_1 + f_{transit}.$$

From the vehicle and the pixel area, the ratio of target to pixel,  $RTP$  can be found via

$$RTP = \frac{L_{target} W_{target}}{x_{pixel} y_{pixel}},$$

where  $L_{target}$  is the length of the target,  $W_{target}$  is the width of the target,  $x_{pixel}$  is the pixel size in the x-direction, and  $y_{pixel}$  is the pixel size in the y-direction.

### 3.6. Modeling Multiple Pixels

The sub-pixel algorithm is designed to find target characteristics for a single pixel. However, recording and comparing the target's information across multiple arrays allows for jitter effects, target refinement and target tracking.

To model the target across multiple pixels, an  $n \times m$  array of background pixels is created, such as in Figure 3.6, although the figure shows more than just the background. The background is initially uniform across all pixels, but later testing will allow for background pixel variation to further test jitter effects.

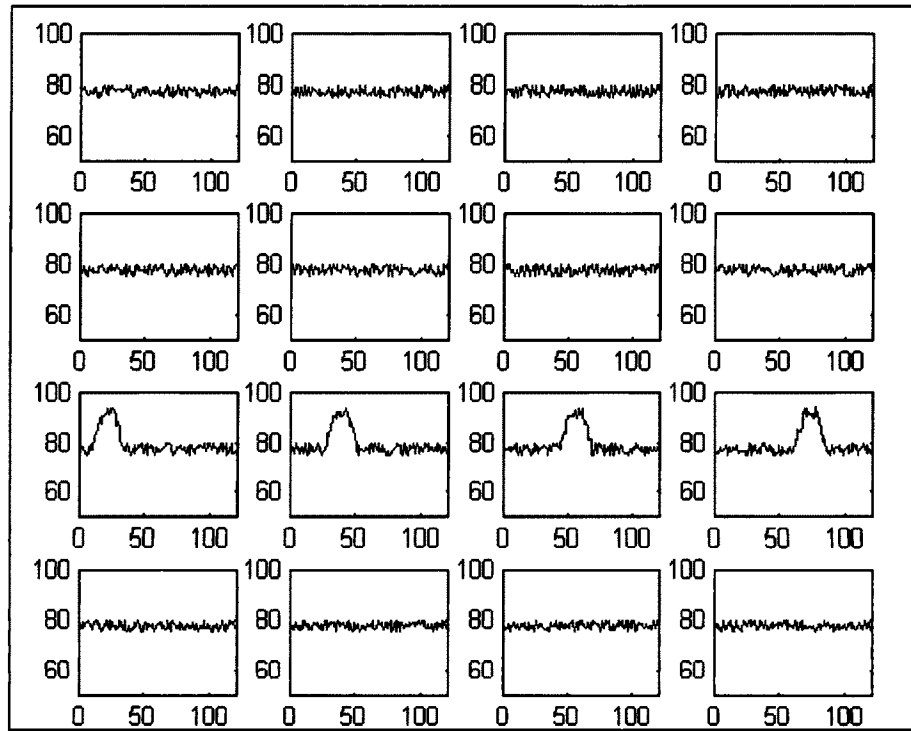


Figure 3.6 Modeled target moving horizontally in a single row

The first multiple-pixel dataset uses a target model that moves in the horizontal direction from left to right and only traverses in a single row. The development of the database is created in the same manner of the single pixel, with the exception of the time of entry in each pixel,

$$Entry_{1(i+1)} = Exit_{1i},$$

where the frame of target entry in the next pixel,  $Entry_{1(i+1)}$ , is equivalent to the frame the target starts to exit the previous pixel,  $Exit_{1i}$ , and  $i$  is the next column in the row.

The second multiple-pixel database uses the same target model with the exception that the single target traverses in two rows, splitting the pixel, so that half the target is in one row and the other half is in the row immediately below it. To model this scenario, the target's width was reduced by a factor of two (Figure 3.7).

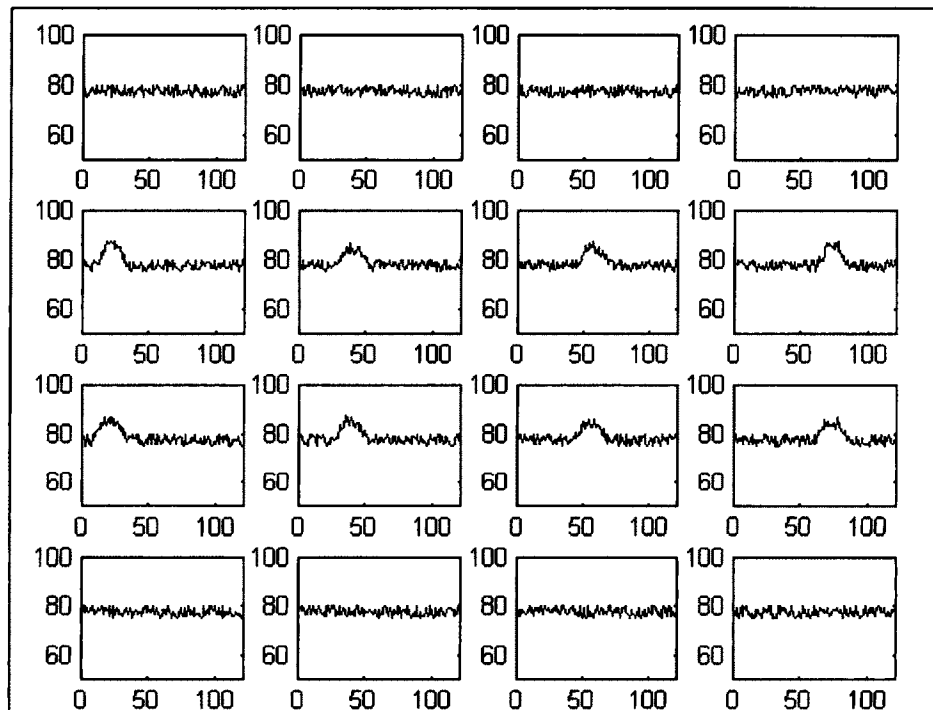


Figure 3.7 Single target with horizontal motion split among two rows

Variations in the datasets have differing background intensities between pixels and the ability to choose the split ratio of the target's width. Due to the sub-pixel nature of the targets and the horizontal direction of travel, the split will only happen between two rows. Changes in this assumption create a much more complex insertion method, which will be discussed theoretically in Chapter Seven.

### 3.7. Removing Assumptions

Noise and jitter is sensor specific. After the target and the background model are complete, noise is added to model the sensor's surroundings and jitter is added over the noise to ensure frame uniformity, i.e. to make sure the target, background and noise all jitter together. This method and order of removing assumptions better models reality.

#### 3.7.1. Adding Noise

Noise is assumed to be a random process, modeling an independent Gaussian function,

$$I_{Total}(t) = I_{Pixel}(t) + N(t),$$

with zero mean and standard deviation,  $\sigma$ , found via

$$N(t) \sim N(0, \sigma),$$

where  $I_{Total}$  is the total pixel value,  $I_{Pixel}$  is the original pixel, and  $N$  is the noise. A commonly accepted noise profile, with widely accepted parameters, used with detection algorithms is the independent Gaussian function [7]. The modeled noise is shown in Figure 3.8.

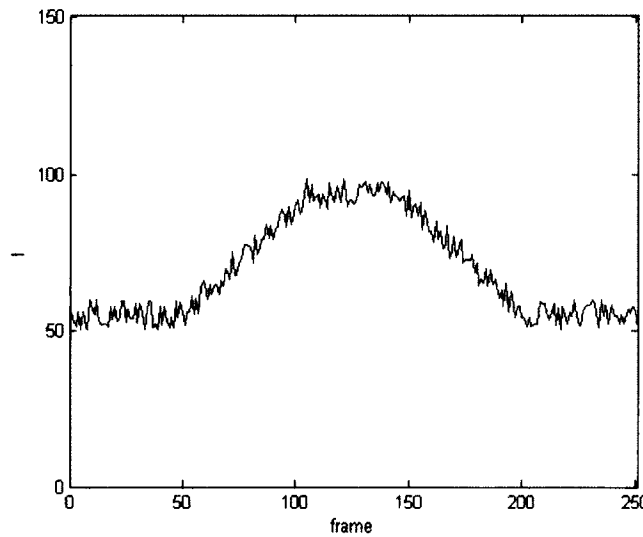


Figure 3.8 Noise added after the target insertion algorithms

### 3.7.2. Adding Jitter

Sensor jitter is a major concern in digital imaging [25]. If the jitter between pixels is significant, the background intensity no longer remains quasi-static. Jitter is specific to each individual sensor and its environment. Over time, jitter can be predicted and removed. However, the techniques employed for jitter removal could smooth out or completely erase the sub-pixel target. For this dissertation, an analysis of jitter effects will be performed in order to find the sub-pixel target algorithm's performance and limitations. This dissertation investigates two types of jitter, translational jitter and random jitter.

#### 3.7.2.1. Translational Jitter

As a generalization, translational jitter assumes a horizontal linear motion, with the sensor behaving as a simple harmonic oscillator [26] such that

$$\text{Shift}(t) = A \sin\left(\frac{2\pi}{T}t + \varphi\right),$$

where  $\text{Shift}(t)$ , is the current sensor shift position,  $A$  is the total jitter percent shift,  $T$  is the period of the jitter cycle, and  $\varphi$ , is the phase, which is set to zero for this model. Figure 3.10.A shows the jitter from the hardware perspective and Figure 3.10.B shows the jitter from the signal perspective.

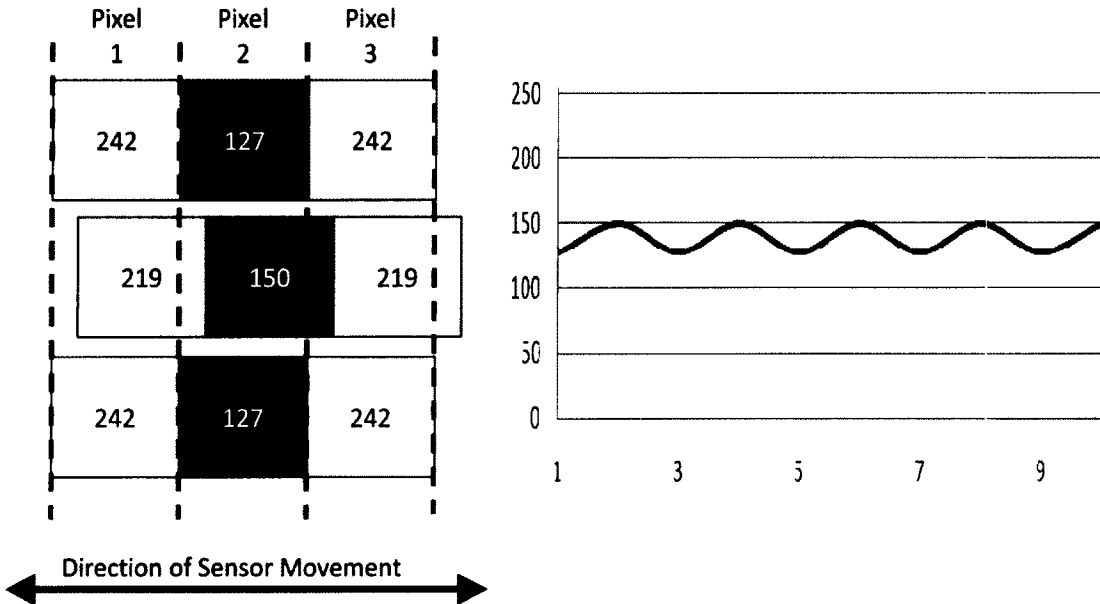


Figure 3.9 (A) Pictorial Description of Translational Jitter (B) Intensity variation due to translational jitter

The pixel intensity variations due to sensor jitter can be expressed as a linear combination of the pixels related to the percent jitter shift by

$$Pixel_{2_{new}}(t) = \begin{cases} (1 + Shift(t))Pixel_2 - Shift(t)Pixel_1, & \text{for } Shift(t) < 0 \\ Pixel_2, & \text{for } Shift(t) = 0, \\ (1 - Shift(t))Pixel_2 + Shift(t)Pixel_3, & \text{for } Shift(t) > 0 \end{cases}$$

where  $Pixel_{2_{new}}$  is the jittered pixel and  $Pixel_1$ ,  $Pixel_2$ , and  $Pixel_3$  are the original pixels as shown in Figure 3.9.A.

The pixels on the frame edges will substitute the  $Pixel_2$  value for the missing parameter. Jitter will be modeled at different percents in order to analyze its effect on the algorithm's ability to detect and characterize targets.

### 3.7.2.2. Random Jitter

Random jitter allows for the entire pixel array to vary with a uniform distribution for a specified jitter parameter,  $J$ . The jitter parameter can be as large as a multiple pixel shift or restricted within a pixel fraction. The jitter equations are calculated via:

$$J_{row} = J(1 - 2[1]),$$

and

$$J_{col} = J(1 - 2[1]),$$

where  $J_{row}$  is the random row shift and  $J_{col}$  is the random column shift. Both shift factors are randomly updated per frame with a uniform distribution on the interval  $[-J, J]$ . The two shift factors allow for multidirectional shifting along the frame (Figure 3.10).

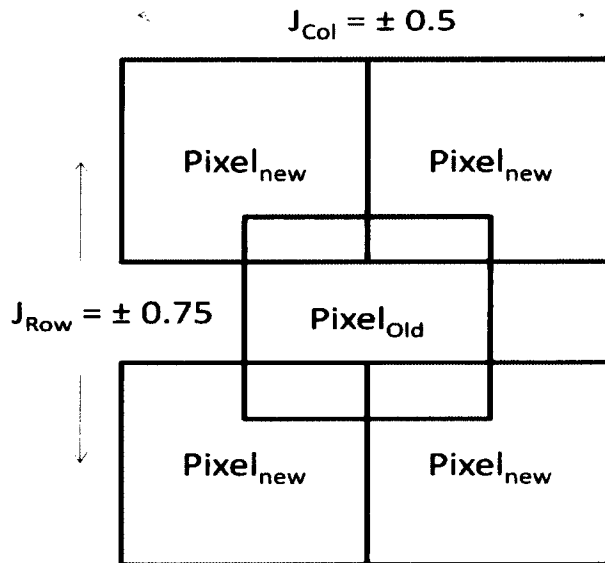


Figure 3.10 Multidirectional shifting along a frame caused by jitter

The pixel intensity variations due to sensor jitter can be expressed as a linear combination of the pixels related to the percent of jitter shift using

$$\begin{aligned}
 I_{PixelJitter}(r, c, f) = & \\
 I_{Pixel}(r + \lfloor J_{row}(f) \rfloor, c + \lfloor J_{col}(f) \rfloor, f) \cdot (1 - J_{row}(f))(1 - J_{col}(f)) & \\
 + I_{Pixel}(r + \lfloor J_{row}(f) \rfloor, c + \lceil J_{col}(f) \rceil, f) \cdot (1 - J_{row}(f))J_{col}(f) & \\
 + I_{Pixel}(r + \lceil J_{row}(f) \rceil, c + \lfloor J_{col}(f) \rfloor, f) \cdot J_{row}(f)(1 - J_{col}(f)) & \\
 + I_{Pixel}(r + \lceil J_{row}(f) \rceil, c + \lceil J_{col}(f) \rceil, f) \cdot J_{row}(f)J_{col}(f),
 \end{aligned}$$

where  $I_{PixelJitter}$  is the resulting jittered pixel matrix,  $I_{Pixel}$  is the original pixel matrix, and the indices of the matrices are row,  $r$ , column,  $c$ , and current frame,  $f$ .  $J_{row}$  is the random row shift and  $J_{col}$  is the random column shift. If the row or column indices are exceeded during the calculation, in which case the jitter shift is past the pixel array frame, the last row or column index is used as a substitution.

## CHAPTER FOUR

### CHANGE DETECTION

Target detection is essentially a change detection problem and can be done in the spatial, temporal or spatio-temporal domain. Spatial-image processing analyzes the intensity feature variation in a single frame and works well for multi-pixel or high-contrast targets. Some of these processing techniques include Matched Filtering (MF) [27], Dynamic Programming Algorithm (DPA) [28], and Multistage Hypothesis Testing (MAHT) [9]. Temporal-image processing capitalizes on the intensity changes over a sequence of frame data and works well for small, dim, point-like moving targets. Spatio-temporal processing does a combination of both.

The main goal is to differentiate the target from the background signal. As the target moves through the pixel, a pulse-like signal is generated, interrupting the background signal. This scenario is perfect for temporal analysis.

A straightforward change detection method uses a simple differencing method,

$$D(f) = I_2(f) - I_1(f),$$

where  $I$  represents two images,  $D$  is the differences between the images, and  $f$  is the frame sequence. For this method, the decision factor on detection is determined by an empirical threshold [29]. Rosin did an extensive survey on different methods to choose the proper threshold [30] [31]. Instead of automating the threshold process, Simonson allows for flexibility by keeping the threshold variable a tunable parameter [13]. This

simple differencing threshold change detection method is computationally inexpensive and provides a quick check method for target detection. However, this method is sensitive to noise and variations in background intensity changes [29]. To mitigate these problems, adaptive background models and thresholds are effective [32].

Extensive research in background modeling and suppression has been done and is especially useful for temporal problems with either historical data or multiple frame sequences, where changes happen over a short span of time [13]. Some background segmentation techniques involve neural network with edge constraints [33], fuzzy threshold and edge detection [34], contrast boxes, double gated filter, spoke filter [35], morphological techniques: top hat transform [36], and Gabor filtering functions [36]. One form of background suppression involves wavelet transformations [11] [21] [23]. An advantage of wavelet transforms is that in target detection techniques they can operate as matching filter, multi-resolution image analyzer, a multi-dimensional image analyzer, a singularity detector, and an orthogonal extractor [37]. Problems with this method are its intrinsic complexity [14]. Fast subspace tracking methods utilize a power iteration technique, which can also be computationally expensive [38] [39] [40]. Badeau et al. uses a low complexity update to the background estimation called a Fast Approximated Power Iteration (FAPI) subspace tracking [14]. Simonson shows success with this method in noisy and highly jittered environments [13].

This summary of change detection methods just scratches the surface of the abundant information found in the academic communities. The target detection is a necessity in order to proceed to the target analysis and is part of the overall sub-pixel process. However, a particular detection mechanism is not a necessity as the modularity of the design allows for interchangeability. For initial algorithm design, two generic and

computationally inexpensive methods, and one more robust, adaptive background estimation method comprise the change detection methodology. The temporal change detection methods described in this section are the Threshold Change Detection, the Duration Change Detection, and the Fast Adaptive Power Iteration (FAPI) Detection methods.

The Threshold and Duration methods are straightforward comparison methods, are computationally efficient and work well in low noise and jitter environments. These methods are good tools for quick and easy target detection which is especially useful in the initial testing of the sub-pixel target analysis. When noise and jitter effects are introduced into the testing scenarios, a more robust detection scheme, like FAPI, is a necessary tool to have in the analysis arsenal.

When working with the detection algorithms, it is important to keep as much of the signal as possible, especially in a low Signal-to-Noise Ratio (SNR) environment. For this reason, pre-processing smoothing techniques are not considered due to the high probability that the target signal will be lost or corrupted. In all the algorithms described in this section, the original pixel sequence is preserved globally so that it can be utilized in its original state during the analysis section.

A major product of the change detection algorithms is the Binary Target Matrix. This matrix stores the target detection results as either a one for a target or a zero for no target. This matrix helps differentiate between actual targets and false alarms and helps discover the target's entry and exit frames for a particular pixel.

For this dissertation, the sensor platform is assumed to be a constant staring camera, where the background is quasi-static. Although over time, it may be possible to characterize the background, noise and jitter, for this algorithm, it is assumed that this *a priori* knowledge does not exist.

#### 4.1 Threshold Change Detection

The image sequences of the sensor,  $I_{Pixel}$ , are stored in 3D arrays,

$$I_{Pixel}(NRow, NCol, NFrames),$$

where  $NRow$  is the total number of rows in the sensor frame,  $NCol$  is the total number of columns in the sensor frame, and  $NFrames$  is the total number of frames in the data sequence.

The total number of pixels per frame,  $NPixels$ , is found by

$$NPixels = NRow \cdot NCol,$$

and a single pixel is referenced as

$$I_{Pixel}(r, c, f),$$

where  $r$  is the current row,  $c$  is the current column, and  $f$  is the current frame.

At each discrete time frame, a new image is stored into the  $I_{Pixel}$  array. The objective at each frame is to determine whether the intensity of the pixel of the new frame is consistent with the current temporal background model of the pixel. A target is detected in those pixels with observed intensities that vary from the model.

Since time is a factor, a general method for comparison is simple normalized differences [25]:

$$\Delta_{Pixel}(r, c, f) = \frac{I_{Pixel}(r, c, f) - I_{Back}(r, c, f)}{\zeta_{Pixel}(r, c, f - 1)},$$

where  $\Delta_{Pixel}$  is the normalized difference,  $I_{Back}$  is the current background model and  $\zeta_{Pixel}$  is the previous standard deviation estimate. The standard deviation estimate can be initialized with the first few background frames,  $B$ , such that

$$\zeta_{Pixel}(r, c, 0) = \sqrt{\frac{\sum_{f=1}^B (I_{Pixel}(r, c, f) - I_{Back}(r, c, f))^2}{B}}. \quad (4.1)$$

Recursive standard deviation estimates are updated with

$$\zeta_{Pixel}(r, c, f) = \sqrt{\gamma \zeta_{Pixel}^2(r, c, f-1) + (1-\gamma)(I_{Pixel}(r, c, f) - I_{Back}(r, c, f))^2},$$

where  $\gamma \in [0,1]$  is the forgetting factor which applies a weight to the old and new frames. The forgetting factor allows for the ability to apply importance to new information. In essence it is a weighting factor, preserving the opportunity to tailor the standard deviation function later [25].

The assessment of compliance can be determined via thresholding, where

$$\Delta_{Pixel}(r, c, f) > T$$

is the condition required for target detection. The threshold value,  $T$ , is user defined and sensor specific. An effective threshold value compares the target detection rate vs. the false alarm rate, discussed in Section 4.4., where the false alarm rate is much lower than the target detection rate [25]. A generic method, which allows for algorithm adaptability, uses a threshold value as  $N$  standard deviations from the modeled background [41] [42] [43]. Target pixels are those frames that satisfy

$$\Delta_{Pixel}(r, c, f) > N\sigma,$$

where  $\sigma$  is the standard deviation and  $N$  is the tunable integer factor.

#### 4.1.1. The Background Model

Due to the relatively small timeframe of the pixel sequence, it can reasonably be assumed that the background will not change significantly in temporal intensity throughout the sequence capture. The initial standard deviation estimate found using Eq. 4.1 and the first few data frames serves as a simplistic background model, with the stipulation that no targets are located in these frames such that the background intensity,  $I_{Back}$ , is given by

$$I_{Back} = \zeta_{Pixel}(r, c, 0),$$

where  $\zeta_{Pixel}$  is found using Eqn. 4.1.

This method of background estimation eases the burden of requiring *a priori* knowledge of the scene and allows for utilization in real or near-real-time processing. After establishing a historical database, it would be possible to cross check new background models to ensure accuracy or determine long term background changes.

#### 4.1.2. Establishing the Initial Threshold

The threshold value determination varies with each sensor. The effectiveness of the threshold value is measured via the target detection rate vs. the false alarm rate.

One method of detection assumes the first few frames are background data and Gaussian noise. The intensity values in these frames are used to find the background value and the noise threshold. The standard deviation,  $\sigma$  is given by

$$\sigma = \sqrt{\frac{\sum(I_{Pixel}(r, c, f) - I_{Back})^2}{n}},$$

where  $I_{Pixel}$  is the pixel intensity values,  $I_{Back}$  is the mean value of the first few frames, and  $n$  is the number of frames used for the background calculation. The threshold value is calculated as

$$\text{Threshold} = \pm N\sigma,$$

with  $N$  being the number of standard deviations. For example, an  $N$  value of two captures approximately 95% of the noise deviation, assuming a Gaussian profile [44]. The variability of  $N$  is important because if the SNR is very low, a large  $N$  value will completely ignore the target. Too low of a  $N$  value will cause a higher false alarm rate, which can be mitigated with the False Alarm Rate filters (FAR filter), which is explained in Section 4.4. The range of  $N$  values varies based on sensor. Testing refines the  $N$  value to achieve the ideal number.

#### 4.1.3. Threshold Detection Binary Matrix

The detection binary matrix,  $\text{Pixel}_{\text{Binary}}(r, c, f)$ , stores the pixel target detections using

$$\text{Pixel}_{\text{Binary}}(r, c, f) = \begin{cases} 1, & \text{if } \Delta_{\text{Pixel}}(r, c, f) > T \\ 0, & \text{if } \Delta_{\text{Pixel}}(r, c, f) \leq T' \end{cases}$$

where the row,  $r$ , column,  $c$ , and frame,  $f$ , represent the matrix indices,  $\Delta_{\text{Pixel}}$ , is the normalized difference, and  $T$  is the threshold. A value of one indicates a detected target. The temporal profile of the matrix gives a good visual indication of actual targets versus the false alarms and can be used as a tool in the FAR filter algorithm to reduce the number of false alarms.

A potential problem with threshold detection is that the target may enter in the first few frames, skewing the noise threshold which would allow the target to go undetected. This is mitigated using Duration Detection (Section 4.2).

#### 4.1.4. Threshold Detection Example

A HUMMWV traveling at 23.5 m/s is inserted into a 30x30 m<sup>2</sup> pixel sampled at a rate of 120 frames/s (Figure 4.1.A). Noise is added to the signal (Figure 4.1.B) and then the array is sent to the Threshold Detection algorithm.

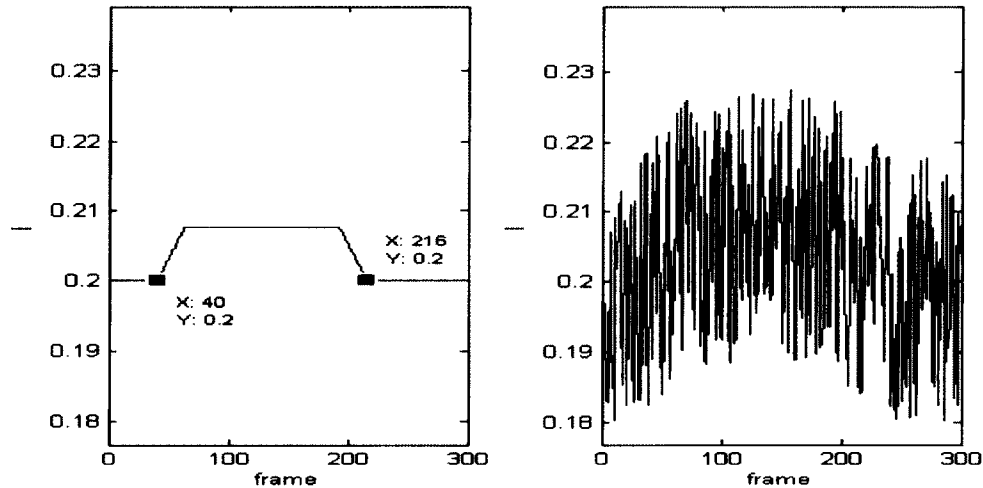


Figure 4.1 (A) HUMMWV signal before noise and (B) after noise

The standard deviation estimates are compared to the background model threshold. The frames that exceed the threshold are shown in Figure 4.2.

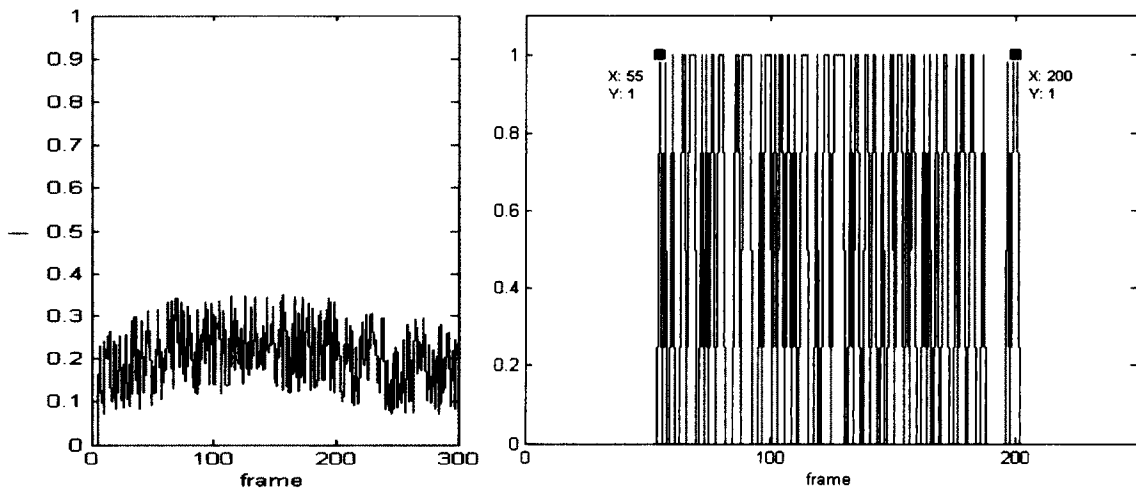


Figure 4.2 Standard deviation estimates and Threshold Binary Matrix

In depth analysis and discussion of the target transit points' accuracy, the detection vs. false alarm rates, noise, jitter and threshold selection can be found in Chapter Nine.

## 4.2. Duration Change Detection

Duration Change Detection finds the most frequent data points and uses this intensity as a critical point for filtering. The philosophy behind this method is that for the majority of the time, the pixel will be comprised solely of background information, with targets sporadically interrupting the constancy. As a result, the critical filter point is considered the background model. The critical filter point is found at the highest frequency bin of a frame sequence histogram.

### 4.2.1. Finding the Minimum Required Sample Set

Duration Detection capitalizes on the stationary background characteristic of a staring sensor. Assuming a single target profile, a minimum number of sample frames need to be recorded ensuring the background data points are the majority in the set. In this scenario, a duration filter segments out the background signal and leaves only the target profile. Whole and partial targets can be detected during any portion of the dataset, providing this condition is met:

$$\#frames_{background} > (f_{transit} - 2f_{entry}) + \epsilon,$$

where  $\#frames_{background}$  is the minimum number of background data frames required,  $f_{transit}$  is the target transit time, and  $f_{entry}$  it the number of frames it takes for the target to fully enter the pixel. The error term,  $\epsilon$ , accounts for rounding error due to an integer requirement for the frame number.

If the sensor pixel size and sample rate,  $\text{SampleRate}$ , are known, the total minimum frame number required in the dataset to filter out the background signal for specific targets can be found. The number of frames the target will be in the pixel,  $f_{\text{transit}}$ , is found via

$$f_{\text{transit}} = \frac{(x_{\text{pixel}} + L_{\text{target}})\text{SampleRate}}{V_{\text{target}}},$$

where  $x_{\text{pixel}}$  is the size of the pixel in the x-direction,  $L_{\text{target}}$  is the length of the target, and  $V_{\text{target}}$  is the target velocity. In order for the duration process to work, the number of background frames,  $\#\text{frames}_{\text{background}}$ , must be larger than  $f_{\text{transit}}$  such that

$$\#\text{frames}_{\text{background}} > \frac{(x_{\text{pixel}} - L_{\text{target}})\text{SampleRate}}{V_{\text{target}}} + \epsilon.$$

The total number of frames required is given by

$$\#\text{frames}_{\text{total}} > \#\text{frames}_{\text{target}} + \#\text{frames}_{\text{background}}$$

and

$$\#\text{frames}_{\text{total}} > \frac{2x_{\text{pixel}}\text{SampleRate}}{V_{\text{target}}} + \epsilon.$$

For example, for each of the four Army vehicles defined earlier, the expected targets, the minimum number of frames needed to detect each vehicle was calculated and presented in Table 4.1.

Table 4.1 Example Frame Calculation Table for Army Vehicles

Vehicle	Max Speed (m/s)	Pixel Size(m)	Sample Rate (frame/sec)	Min Frame #
HUMMWV	29.06	10	30	21
HEMTT (M977)	25.48	10	30	24
M1070	20.12	10	30	30
- Tractor	20.12	10	30	30
- Trailer	20.12	10	30	30
- w/ payload	13.41	10	30	45
PLS				
- Truck	25.48	10	30	24
- Trailer	25.48	10	30	24
- w/ payload	15.64	10	30	39

#### 4.2.2. Create Histogram and Establish Filter Boundaries

The histogram computes the frequency distribution of the intensity elements in a pixel dataset and sorts them into a number of discrete bins,  $b$ . The bins have equal width of

$$w = \frac{B_u - B_l}{b},$$

where  $B_u$  is the upper limit of the histogram and  $B_l$  is the lower limit of the histogram. The pixel dataset used for the histogram is a normalized dataset, with intensity values between zero and one, which are  $B_l$  and  $B_u$  respectively. The centers of the bins are found by the equation:

$$\text{center} = B_l + \left( k + \frac{1}{2} \right) w \quad k = 0, 1, \dots, b - 1.$$

The input values that fall on the border between two bins are placed into the lower valued bin, and each bin includes its upper boundary [45]. The array of bin frequencies,  $\text{Hist}_{pixel}$ , comprises the temporal frequency histogram.

The bin with the maximum frequency establishes the background baseline. The bins within  $N$  sigma of the baseline establish the temporal frequency filter boundaries, *Filter*, such that

$$\text{Filter} = \pm N\sigma_{\text{Baseline}},$$

where  $N$  is a tunable parameter that can be adjusted by the user, and  $\sigma$  is the standard deviation.

#### 4.2.3. Duration Detection Binary Matrix

The detection binary matrix,  $\text{Pixel}_{\text{Binary}}(r, c, f)$ , stores pixel target detections.

$$\text{Pixel}_{\text{Binary}}(r, c, f) = \begin{cases} 1, & \text{if } I_{\text{Pixel}}(r, c, f) > \text{Filter} \\ 0, & \text{if } I_{\text{Pixel}}(r, c, f) \leq \text{Filter} \end{cases}$$

where the row,  $r$ , column,  $c$ , and frame,  $f$ , represent the matrix indices,  $I_{\text{Pixel}}$  is the pixel intensity, and a value of one indicates a detected target.

#### 4.2.4. Duration Detection Example

A M1070 traveling at 20 m/s is inserted into a 30x30 m<sup>2</sup> pixel sampled at a rate of 120 frames/s (Figure 4.3.A). Noise is added to the signal (Figure 4.3.B) and then the array is sent to the Duration Detection algorithm.

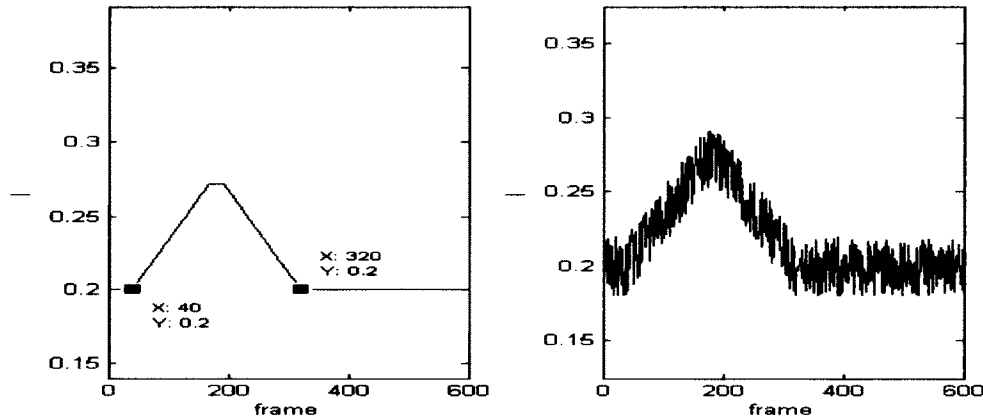


Figure 4.3 (A) M1070 profile with no noise (B) M1070 profile with 0.02 noise

The histogram plot is shown in Figure 4.4.

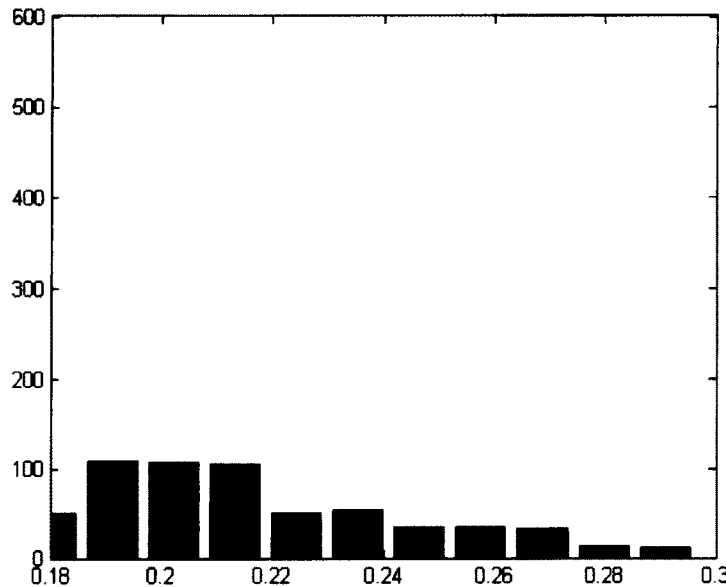


Figure 4.4 Duration Detection Histogram Plot (Intensity vs. # Frames)

The resulting Duration Binary Matrix has quite a few detections, as seen in Figure 4.5. The addition of the false alarm rate filters (Section 4.4) reduce the false alarms to zero in Figure 4.5, increasing the critical point accuracy times.

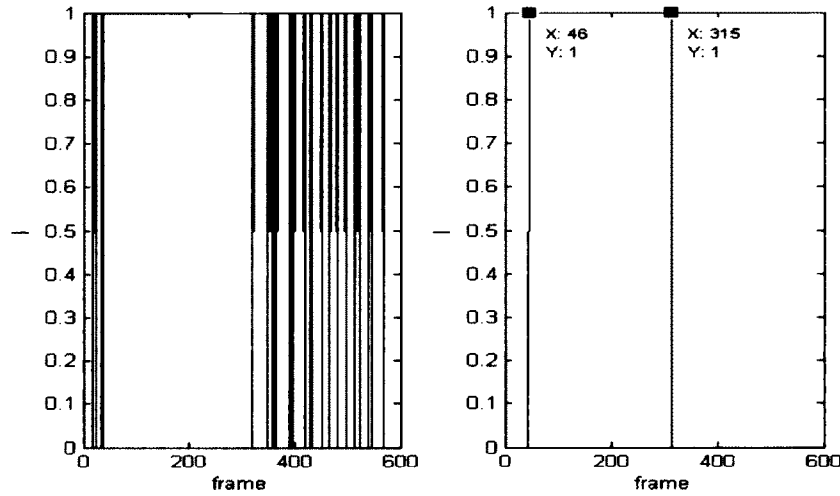


Figure 4.5 (A) Duration Binary Matrix (B) Utilizing the FAR filters to reduce false alarms

### 4.3. Fast Adaptive Power Iteration (FAPI) Background Estimation

The previously mentioned methods of change detection are extremely sensitive to jitter. The Fast Adaptive Power Iteration (FAPI) method mitigates problems in finding targets in high jitter environments, by providing robust adaptive updates to the background model [46].

Although computationally more expensive than the background averaging method or duration filtering, the increase in detection magnitude is worth the extra processing time [46]. Examining the FAPI background estimation method is required now versus earlier because the previous concepts and corresponding equations are used.

The FAPI algorithm provides estimates for the orthonormal basis vector at each iteration step. This vector is used for the adaptive background modeling. The estimates are such that the dominant subspace is spanned by the covariance matrix,

$$C_{XX}(f) = \sum_{u=-\infty}^{f_0} \beta C_{XX}(f-1) + I_{Pixel_v}(f) I_{Pixel_v}^T(f),$$

where the weighting parameter,  $\beta$ , is contained within [0,1] and determines the importance of each update in the estimation. It is imperative to note that the intensity pixel matrix  $I_{Pixel}$  must be vectorized in an Nx1 matrix for the FAPI method. The notation  $I_{Pixel_v}$  is used to identify the vectorized matrix [46] and  $f$ , represents the pixel frame.

#### 4.3.1. FAPI Estimation

Instead of continually computing and decomposing  $C_{XX}(f)$ , the current basis vectors are stored in a weighting matrix,  $W(f)$ , which are updated at every frame. Badeau et al. developed a comprehensive method for the  $W(f)$  update and the algorithm and mathematic specifics are found in the referenced publication [46].

Badeau utilizes an  $R$  dimensional identity matrix for the initialization of an auxiliary matrix,  $Z$ , where the value of  $R$  is user defined. He initializes  $W$ , an RxN orthonormal matrix, with an identity block sized RxR and zeros everywhere else. Simonson refined the initialization and achieves rapid and repeatable convergence using a Gram-Schmidt process given by

$$V_1 = \sum_{f=1}^8 I_{Pixel}(f),$$

$$V_r = I_{Pixel}(r+7) - \sum_{s=1}^{r-1} \frac{I_{Pixel}(r+7)^T V_s}{V_s^T V_s} V_s, \quad r = 2, \dots, R,$$

and

$$W_r(r+7) = \frac{V_r}{\|V_r\|}, \quad r = 1, \dots, R.$$

where  $V_l$  and  $V_r$  are the basis vectors, and  $W_r$  is the initial weighting matrix.  $V_l$  utilizes the first  $R+7$  frames for the initialization. Simonson found  $R = 3$  to give the most advantage vs. computational cost [25].

The background model,  $I_{Back}$ , can be found with

$$I_{Back}(f) = W(f-1)W^T(f-1)I_{Pixel}(f),$$

where  $f$  is the frame.

This value is used in the Threshold Change Detection formulas to check for consistency using

$$\Delta_{Pixel}(r, c, f) > T,$$

where  $\Delta_{Pixel}$  is the normalized difference,  $r$  is the row,  $c$  is the column,  $f$  is the frame, and  $T$  is the threshold.

#### 4.3.2. FAPI Binary Matrix

The FAPI Binary Matrix uses the same decision tools as the Threshold Detection algorithm and the Duration Detection algorithm. The detection binary matrix,  $\text{Pixel}_{\text{Binary}}(r, c, f)$ , stores the pixel target detections by

$$\text{Pixel}_{\text{Binary}}(r, c, f) = \begin{cases} 1, & \text{if } \Delta_{\text{Pixel}}(r, c, f) > T \\ 0, & \text{if } \Delta_{\text{Pixel}}(r, c, f) \leq T' \end{cases}$$

where the row,  $r$ , column,  $c$ , and frame,  $f$ , represent the matrix indices,  $\Delta_{\text{Pixel}}$  is the pixel intensity,  $T$  is the threshold, and a value of one indicates a detected target.

#### 4.3.3. FAPI Background Suppression Example

A 50x50 pixel array of a grayscale camouflage background represents a jitter sensitive complex background with high spatial gradients. Random jitter with a three pixel maximum shift is introduced throughout a 50 frame data sequence (Figure 4.6.A). The first 10 frames are used to initialize the FAPI basis vectors using  $R = 3$  and  $\beta = 0.95$ . After cycling through 40 additional frames, a FAPI background estimation is done on the 51<sup>st</sup> frame which is shown in Figure 4.6.B. The background estimation is subtracted from the original frame in Figure 4.6 to show the effectiveness of FAPI for background suppression (Figure 4.6.C).

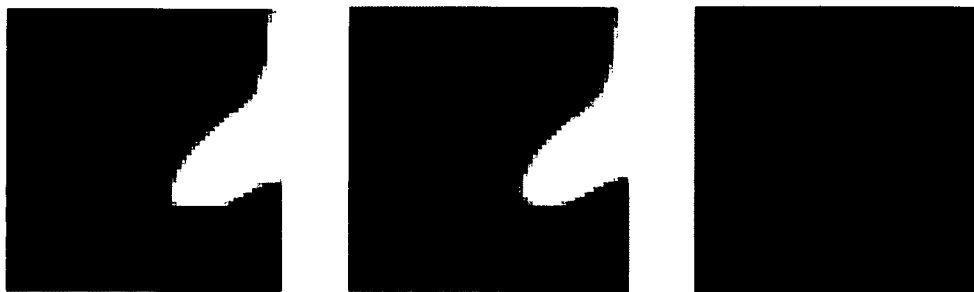


Figure 4.6 (A) Original Background Image (B) FAPI Estimation (C) FAPI Background suppression

#### 4.3.4. FAPI Change Detection

Using over 300 frames of the camo background, an M1070 (target) is introduced in a region with high spatial gradient, pixel(23,19) through pixel(23,21), and subjected to random jitter with a 0.25 pixel maximum shift. (Figure 4.7.A).

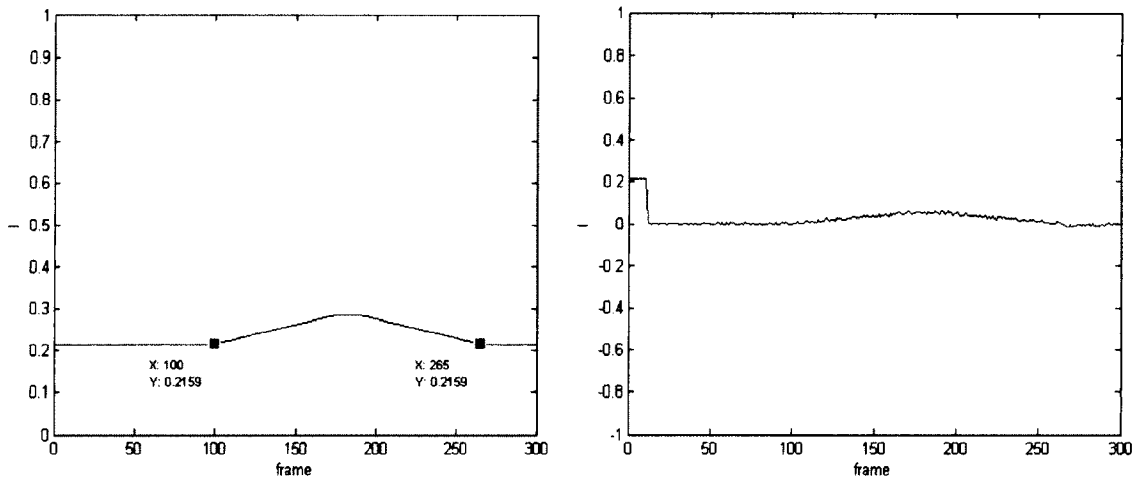


Figure 4.7 (A) M1070 modeled target (B) FAPI suppression results

The pixel array is sent to the FAPI Detection algorithm with  $R = 3$  and  $\beta = 0.95$ . The background suppression residuals are shown in Figure 4.7. The background model is sent to the Threshold Change Detection algorithm for processing. The background model in Section 4.1.1. was used for comparison purposes (Figure 4.8.A and 4.8.B.). The FAPI background estimation method increased the normalized standard deviation estimates by more than a factor of 10 (Figure 4.8.C and 4.8.D) and significantly reduced the number of false alarms.

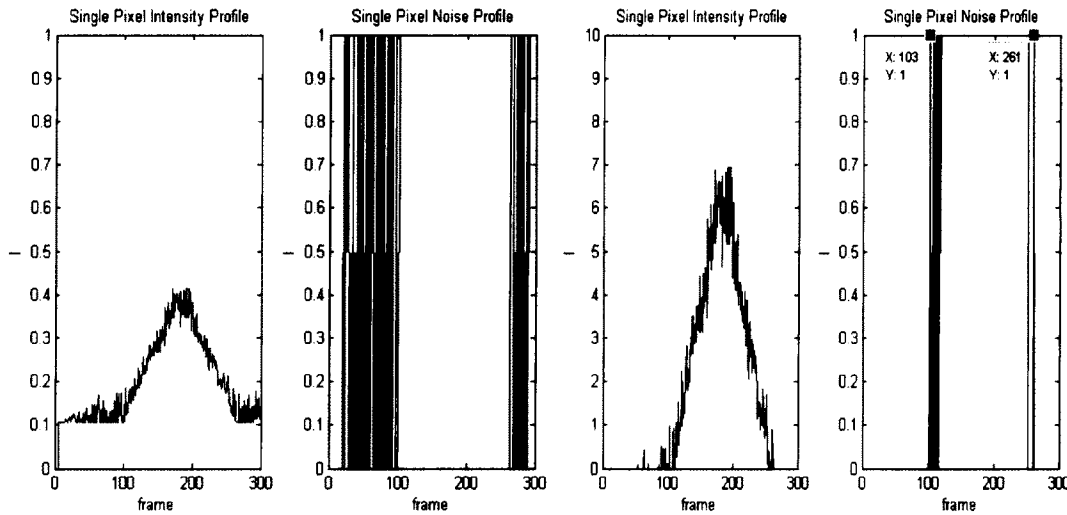


Figure 4.8 (A) Threshold Example (B) Threshold Binary Matrix (C) FAPI estimation (D) FAPI Binary Matrix

The FAR1 filter application (Section 4.4) eliminates the false alarms completely and comes within three frames accuracy for the target  $Enter_1$  and  $Exit_2$  points (Figure 4.9). In Figure 4.8.D, point  $Enter_1$  had a value of  $x = 100$  and point  $Exit_2$  had a value of  $x = 265$ . That same binary matrix, with FAR1 applied, shows  $Enter_1$  with a value of  $x = 103$  and  $Exit_2$  with a value of  $x = 261$  (Figure 4.9). The significance and locations of points  $Enter_1$  and  $Exit_2$  will be explained later in the analysis section in Chapter Five.

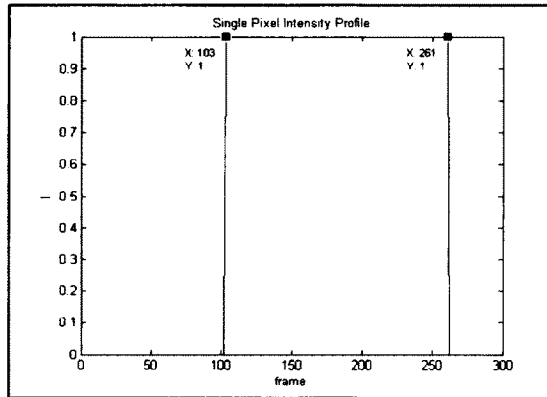


Figure 4.9 Results after applying FAR1 filter to FAPI Binary Matrix

#### 4.4. False Alarm Rate Filter

A detected change in a signal does not always constitute an actual target, but may be a false alarm. False alarms can arise from bad pixels, jitter and noise that are not eliminated via proper boundaries, or a partial target signal loss in the threshold or filtering process. There is a negotiable balance between the probability of detecting the target and an acceptable False-Alarm Rate (FAR). With dim targets, a low threshold or filter is required or the target will not be detected. However, this allows a high number of false alarms to arise, which would lead to a high computational or manpower expense if all these events were processed.

When looking for targets at the sub-pixel level, it is possible to temporally differentiate between actual target detections and false alarms. As an example, it is assumed that a target transverses a single pixel over multiple frames. Therefore, any signal that lasts under a set temporal threshold can be considered a false alarm. By capitalizing on the target temporal transversal boundaries, the FAR can be significantly reduced.

Two types of FAR filter tools are used to reduce the False-Alarm Rate. The first tool responds to the situation where a single target appears as several targets and reconnects the signal. The second tool eliminates false alarms that do not meet the minimum target duration timeframe. For scenarios with both types of false alarms, it is necessary to first reconnect the split target before applying the duration threshold.

##### 4.4.1. FAR1: Reconnect Disjointed Signals

Due to noise and jitter, part of the target signal is lost during the detection algorithm. As a result, a single signal might be detected as a multiple signal (Figure 4.10.A). To correct this problem, a temporal filter can be applied to the detection signal.

If spacing between each frame shows values less than the minimum number of frames between detected targets,  $T_{FAR1}$ , then the binary matrix value is set to 1, thereby reconstituting the original signal (Figure 4.10.B).  $T_{FAR1}$  is user defined based on the sensor and detection algorithm chosen.

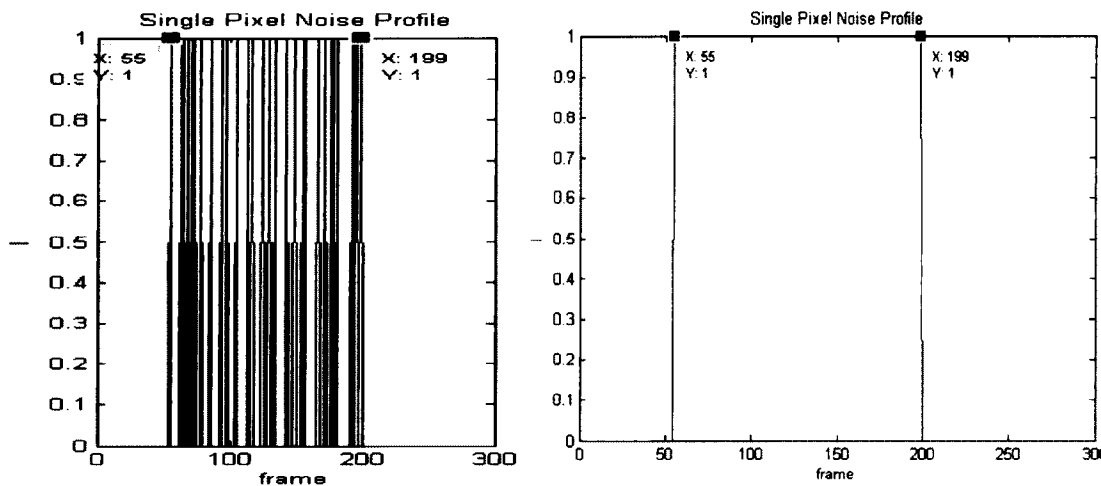


Figure 4.10 (A) Threshold Binary Matrix (B) Application of FAR1 filter to recapture critical target points

#### 4.4.2. FAR2: Minimum Threshold Requirement

If the detection threshold or filters are too low or if bad pixels exist, the algorithm will classify non-target frames as targets. However, these false alarms are detected over a minimum number of consecutive frames. FAR2 establishes that a detection is only considered an actual target if the number of consecutive frame detections meet the minimum threshold requirement,  $T_{FAR2}$ . Therefore, if the number of frames of the detected target is less than  $T_{FAR2}$ , it is a false alarm.

Figure 4.11 is target profile of a M1070 travelling at 20 m/s through a 30x30 m<sup>2</sup> pixel frame. Figure 4.11 are the noise and standard deviation plots, respectively. Figure 4.11 is the result from the Threshold Change Detection algorithm.

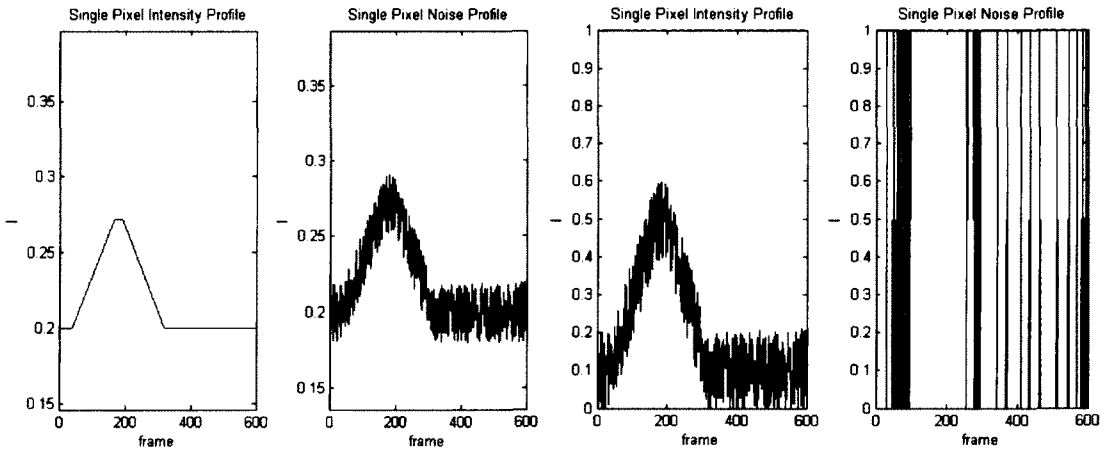


Figure 4.11 (A) Initial target (B) Target with noise (C) Threshold Change Detection (D) Threshold Binary Matrix

The FAR1 filter is used first, followed by the FAR2 filter, resulting in a complete reduction of the false alarms (Figure 4.12).  $T_{FAR2}$  is user defined and based on background knowledge of the target.

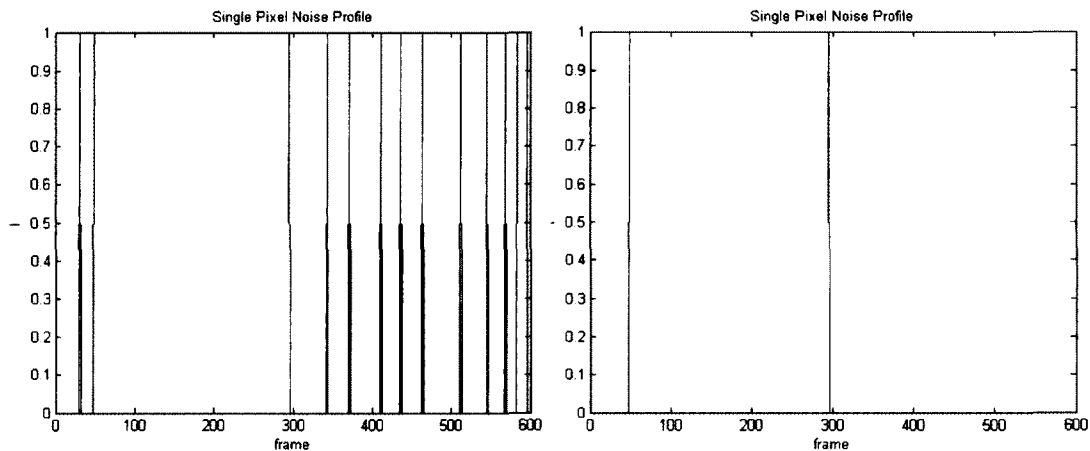


Figure 4.12 (A) FAR1 Results (B) FAR2 Results

## **CHAPTER FIVE**

### **TARGET EXTRACTION AND ANALYSIS**

Current target extraction and analysis methods are geared toward multi-pixel targets. Analysis techniques are spatial in nature and use feature and texture criterion to train the algorithms and create extensive databases for target comparison and classification.

Choi and Mei use a method of whole template matching to find feature similarities between the detected target and an existing database. Choi uses scale-invariant features transform (SIFT) algorithm to recognize a target and extract rotation-invariant features from the image [47]. The features are matched with a database for target classification. Prior training and sample tests are needed to create an indexed database. Mei first finds a target bounding box via image Euclidean distance and image weighted distance, then does a template matching comparison against a stored database [12].

Instead of whole template matching, Nair uses a classification of the target by parts and creates a very complex hierarchical modular level Bayesian object recognition system. The recognition is based on the whole static image and is spatially processed [48]. Vehicles are classified into 3 types; tanks, trucks and armored personnel carriers. The levels of recognition are tiered into low-level, which does basic edge detection and image segmentation, mid-level, which represents and describes the pattern shape and

extraction features, and the higher level, which provides visible pattern category assignment.

Manikandan does an evaluation of edge detection spatial processing for automatic target recognition, which goes on the basis that the edge of an object will have a higher intensity gradient than the object itself and the background [49]. The different edge techniques evaluated were Prewitt, Sobel, Roberts, Canny (with and without thresholding) and LoG (with and without thresholding). The simulation results showed a 95-97% detection rate for IR images. Clarkson's target recognition is very complex and requires the storage of a model database which he indexed as a single hierarchically constructed model tree using a neural network. The edge detected target is compared to the list of available target databases for recognition. [50]

Gupte uses a novel method which implements a GUI spatial process to calculate vehicle parameters [51]. The vehicles' dimensions are used to categorize vehicles into two categories, cars and non cars. This process requires graphical manipulation by the end user and the calculations are based on the user's ability to correctly surround the region of interest.

These methods use groups of pixels to identify the target. As the target decreases in size, these methods lose their effectiveness. The sub-pixel algorithm in this dissertation focuses on each individual pixel and processes them independently for target detection. This independent focus allows for sub-pixel level discovery. In addition, the temporal method of target analysis does not require an extensive database or target training to extract target dimension characteristics.

## 5.1. Extract Target

As briefly discussed earlier, each change detection algorithm produces a Target Binary Matrix, which captures all detected targets held within a frame sequence. For each target detected, the beginning frame,  $Enter_1$ , and the last frame,  $Exit_2$ , of the target sequence are recorded as target counters. The counters are critical points as they are integral in finding the target characteristics. The counters and the original frame sequence are forwarded to the target analysis algorithm for processing.

### 5.1.1. Considerations

The FAR filters are designed to temporally separate detections and false alarms in order to reduce the false alarm rate. However, in certain scenarios, false alarms are not completely eliminated, or split targets are not rejoined. Since the extraction algorithm does not discriminate between an actual target and a false alarm, the entire frame sequence, not just the target, is available for further differentiation in the analysis section.

One major issue in target extraction is the complete capture of the detected signal. Based upon the amount of noise and jitter, partial loss of the target frame length is expected when building the Target Binary Matrix. The methods used in the target analysis section address this issue.

### 5.1.2. Extraction Example

This modeled example has the considerations and assumptions stated in previous sections, where a M1070 traveling at 20 m/s is the target with a noise value of  $\sigma = 0.02$  applied to the signal. The signal undergoes all the filtering mechanisms also stated in the previous sections to yield values for points  $Enter_1$  and  $Exit_2$  of 60 and 270, respectively (Figure 5.1).

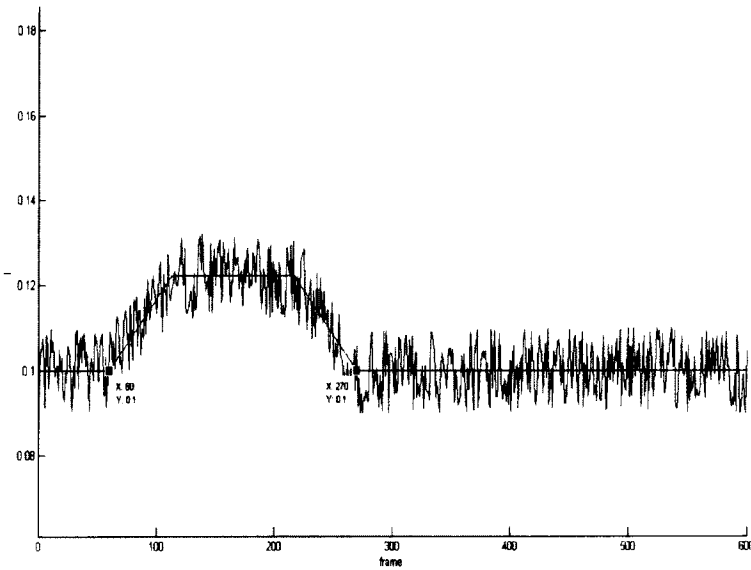


Figure 5.1 M1070 signal with noise profile and critical entry and exit points marked

The extraction algorithm records  $Enter_1 = 66$  and  $Exit_2 = 255$ , which have % errors of 10% and 5.6% respectively, with a transit time % error of 11.1% (Figure 5.2). These critical points along with the original signal are forwarded to the target analysis algorithm for processing.

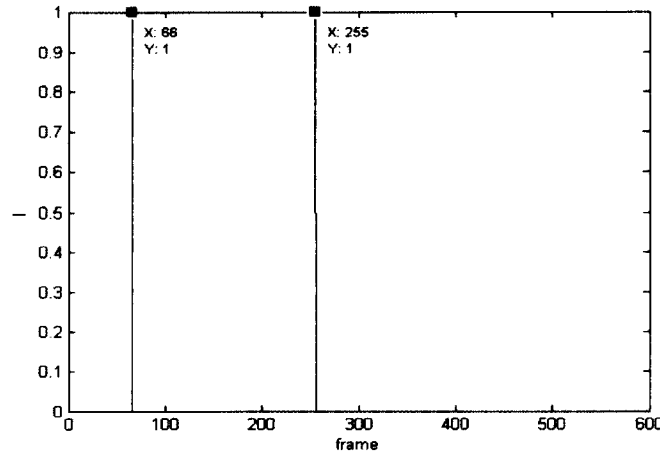


Figure 5.2 Target Binary Matrix with Extraction Points

## 5.2. Target Analysis

Once detection occurs, the target is extracted from the frame sequence and analyzed. The target analysis is temporal in nature and based on the expected target model profile, resulting in the approximated sub-pixel target characteristics of velocity and length.

### 5.2.1. Assumption Review

The target is going in a horizontal linear direction with a constant velocity during the frame sequence. The ground terrain slope is negligible and there is a single target in transit. Additional assumptions are that the pixels sizes are known, are uniform in size and have a rectangular shape.

### 5.2.2. Calculating Target Velocity and Length

When the target is smaller than a pixel and the pixel size is known, target information, such as velocity and object length can be found using the linear temporal signal and the pixel's geometric configuration.

Given the critical target points,  $Enter_1$ ,  $Enter_2$ ,  $Exit_1$ , and  $Exit_2$ ,

$$f_{entry} = Enter_2 - Enter_1 = Exit_2 - Exit_1,$$

where  $f_{entry}$  is the number of frames it takes for the target to fully enter the pixel. In an ideal situation,  $f_{entry}$  and  $f_{exit}$  should be the same value. However, differences do arise due to noise, jitter, and other effects. To accommodate these differences,  $f_{entry}$  is calculated by averaging the entry and exit frames, using

$$f_{entry} = \frac{(Enter_2 - Enter_1) + (Exit_2 - Exit_1)}{2},$$

The number of frames it takes for the target to transit the pixel is found by

$$f_{transit} = Exit_2 - Enter_1,$$

and the velocity of the target is found by

$$V_{target} = \frac{x_{pixel}}{(f_{transit} - f_{entry})},$$

where  $V_{target}$  is the target velocity in m/frames.

Due to the horizontal motion constraint  $L_{target} = V_{target} f_{entry}$ , the length can be found by

$$L_{target} = V_{target} f_{entry},$$

where the length of the target,  $L_{target}$ , is in meters. If the trajectory constraint is removed, information concerning the target's width and area may be found. This concept is discussed in detail in Chapter Seven.

### 5.2.3. FermiFit Analysis

The relationship between the trapezoid model and the Fermi derivative is explained in Chapter Three for the purpose of target modeling. Capitalizing on this relationship, if the Fermi derivative can be fitted to a target's signal data, the critical points can be recovered.

#### 5.2.3.1. Finding the Fermi Derivative Parameters

From Eq. 3.1, the Fermi derivative is found with the equation:

$$f_{df}(k; a, b, c, d) = \frac{ae^{\frac{k-b}{c}}}{(e^{\frac{k-b}{c}} + 1)^2} + d,$$

where  $k$  is the frame number and  $a$ ,  $b$ ,  $c$ , and  $d$  are constants.

### 5.2.3.1.1. Parameter d

As  $k$  approaches infinity, the pixel intensity reduces to  $d$ ,

$$\lim_{k \rightarrow \infty} \frac{ae^{\frac{k-b}{c}}}{(e^{\frac{k-b}{c}} + 1)^2} + d = d = I_{Back},$$

which is the background intensity model found by the change detection algorithms.

### 5.2.3.1.2. Parameter b

The detection algorithm discovers the frame range where the temporal profile deviates from the background, where the first frame in this range is the frame of target entry into the pixel,  $Enter_1$ , and the last frame in the range is the frame of target exit from the pixel,  $Exit_2$ . These two values comprise the target transit frames given by

$$f_{transit} = Exit_2 - Enter_1.$$

The  $b$  constant correlates to the midpoint frame of the target signature using

$$b = \frac{f_{transit}}{2} + Enter_1.$$

### 5.2.3.1.3. Parameter a

At the midpoint frame ( $k = b$ ), the equation reduces to:

$$f_{df}(k = b; a, b, c, d) = \frac{a}{2^2} + d.$$

When  $k = b$ , the pixel intensity is the intensity value of the target fully within the pixel frame as shown in the trapezoidal model in Section 3.4.1. It is now possible to estimate the value of  $a$  given by

$$a = 4(f_{df}(k = b) - d).$$

#### 5.2.3.1.4. Parameter c

To find parameter  $c$ , an additional data point is required where  $k \neq b$ . Since  $c$  represents the width of the Fermi derivative function, the data point is chosen from the target entry or exit slope ( $k_{slope}, f_{dfslope}$ ). Using this data point in the Fermi derivative model results in

$$f_{dfslope} = \frac{ae^{\frac{k_{slope}-b}{c}}}{(e^{\frac{k_{slope}-b}{c}} + 1)^2} + d.$$

Let

$$z = e^{\frac{(k_{slope}-b)}{c}}.$$

Substitute  $z$  into the Fermi derivative model,

$$f_{dfslope} = \frac{az}{(z+1)^2} + d,$$

rearrange into quadratic form,

$$z^2 + \left(2 - \frac{a}{(f_{dfslope} - d)}\right)z + 1 = 0,$$

and solve for  $z$ ,

$$z = -1 + \frac{1 \pm \sqrt{1 - 4 \frac{(f_{dfslope} - d)}{a}}}{2(f_{dfslope} - d)}.$$

Combining the  $z$  equations results in

$$e^{\frac{(k_{slope}-b)}{c}} = -1 + \frac{1 \pm \sqrt{1 - 4 \frac{(f_{dfslope} - d)}{a}}}{2(f_{dfslope} - d)},$$

and

$$\frac{(k_{slope} - b)}{c} = \ln \left( -1 + \frac{1 \pm \sqrt{1 - 4 \frac{(f_{dfslope} - d)}{a}}}{\frac{2(f_{dfslope} - d)}{a}} \right).$$

Finally, solve for  $c$  using

$$c = \frac{(k_{slope} - b)}{\ln \left( -1 + \frac{1 \pm \sqrt{1 - 4 \frac{(f_{dfslope} - d)}{a}}}{\frac{2(f_{dfslope} - d)}{a}} \right)},$$

and substitute in the parameters  $a$ ,  $b$ ,  $c$  and  $d$  to complete the Fermi derivative model.

The  $c$  parameter has two solutions, such that

$$c_+ = -c_-,$$

where  $c_+$  is the solution using the positive sign and  $c_-$  is the solution using the negative sign in the  $c$  parameter equation. If  $k_{slope}$  is chosen on the target's exit slope and  $b$  is the midpoint,  $k_{slope} - b$  is positive and  $c_+$  is used. If  $k_{slope}$  is chosen on the target's entry slope,  $k_{slope} - b$  is negative and  $c_-$  is used.

#### 5.2.3.2. Recovering Critical Points

In Chapter Four, the critical points,  $Enter_1$  and  $Exit_2$  were shown to be found via the change detection algorithm. The other critical points,  $Enter_2$  and  $Exit_1$  are found using the parameters  $b$  and  $c$ . Using  $b$  as the midpoint of the trapezoid and  $Nc$  as the time the target is fully in the pixel,  $Enter_2$  is the smallest value given by

$$Enter_2 = b - \frac{Nc}{2},$$

and  $Exit_1$  is the largest value given by

$$Exit_1 = b + \frac{Nc}{2},$$

where  $N$  is a tunable parameter between one and two.

### 5.2.3.3. FermiFit Example

A HEMTT target model is inserted into a single pixel, travelling at 20 m/s and sampled at 120 frames/s (Figure 5.3.A). A noise value of  $\sigma = 0.01$  is added to the pixel signal before sending the data to the Threshold Detection algorithm and the FAR filters (Figure 5.3.B).

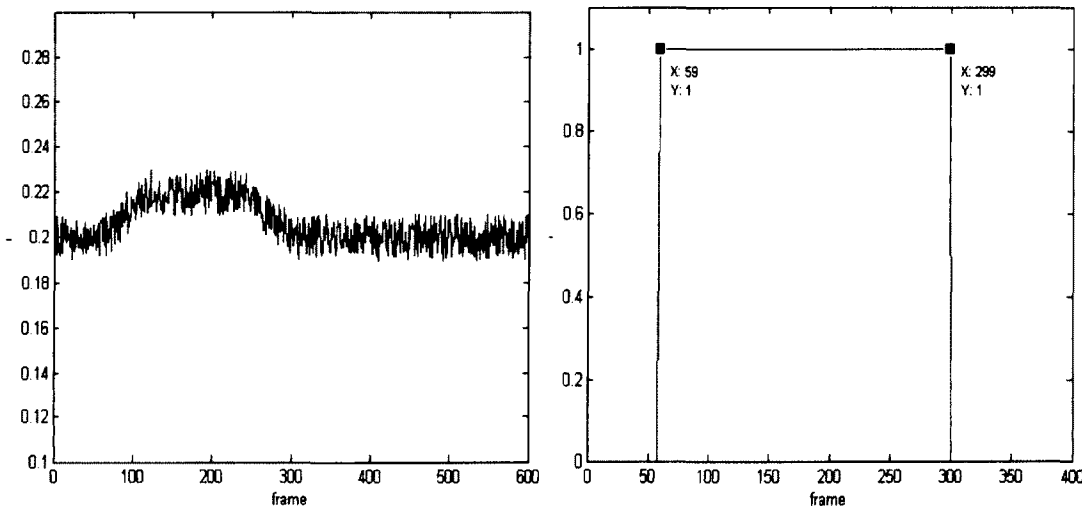


Figure 5.3 (A) HEMTT Target Signal (B) Threshold Binary Matrix

From the detection portion, two critical points are found where  $Enter_1 = 59$  and  $Exit_2 = 299$ . From the FermiFit analysis (Figure 5.4), the calculated Fermi derivative parameters were found to be  $a = 0.6789$ ,  $b = 179.5$ ,  $c = 35.2447$  and  $d = 0.1104$ . The tunable parameter  $N$ , was set to 1.7.

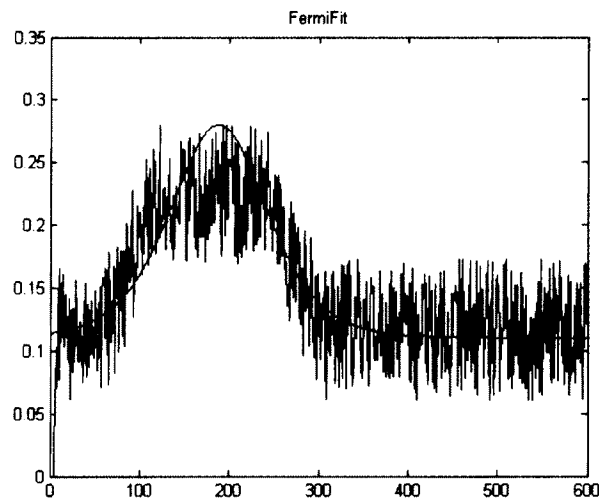


Figure 5.4 FermiFit approximation superimposed over the HEMTT target signal + noise

The two remaining critical points were then calculated as  $Enter_2 = 120$  and  $Exit_1 = 239$ . The target velocity and length are calculated to be 19.95 m/s ( $\% \text{ error} = 0.25$ ) and 10.07 m ( $\% \text{ error} = 1.18$ ), respectively. The original signal is found in Figure 5.5 and has the critical points marked for comparison purposes.

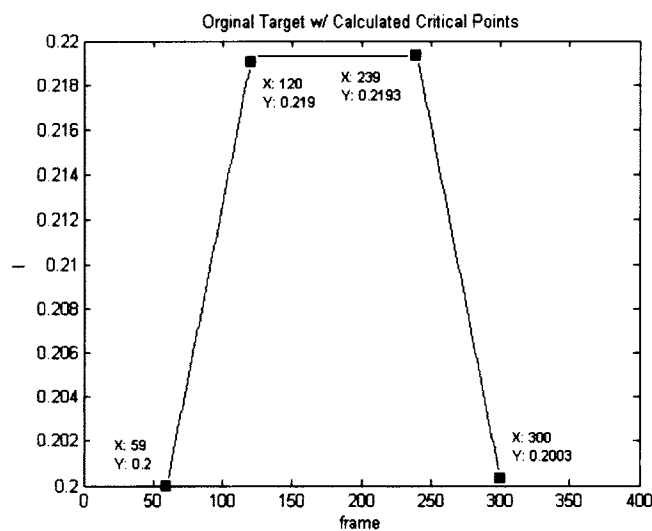


Figure 5.5 Modeled HUMVEE target with critical points marked

#### 5.2.4. PolyFit Analysis

The purpose of this method is to find an approximation of the trapezoid profile. The critical points are located at the extreme points of trapezoid's intersections. While a single approximation function may get the general shape, the function will not recover the intersections with any accuracy. The next section explains how using the least squares approximation models the original signal in the form of a polynomial. Utilizing two approximating polynomials, a sixth and fourth degree, the six different intersections from these functions can be used to estimate the original target. This is done by using the six intersections to create the three lines forming the trapezoid as in Figure 5.6. The trapezoid approximation uncovers the four critical points,  $Enter_1$ ,  $Enter_2$ ,  $Exit_1$  and  $Exit_2$ .

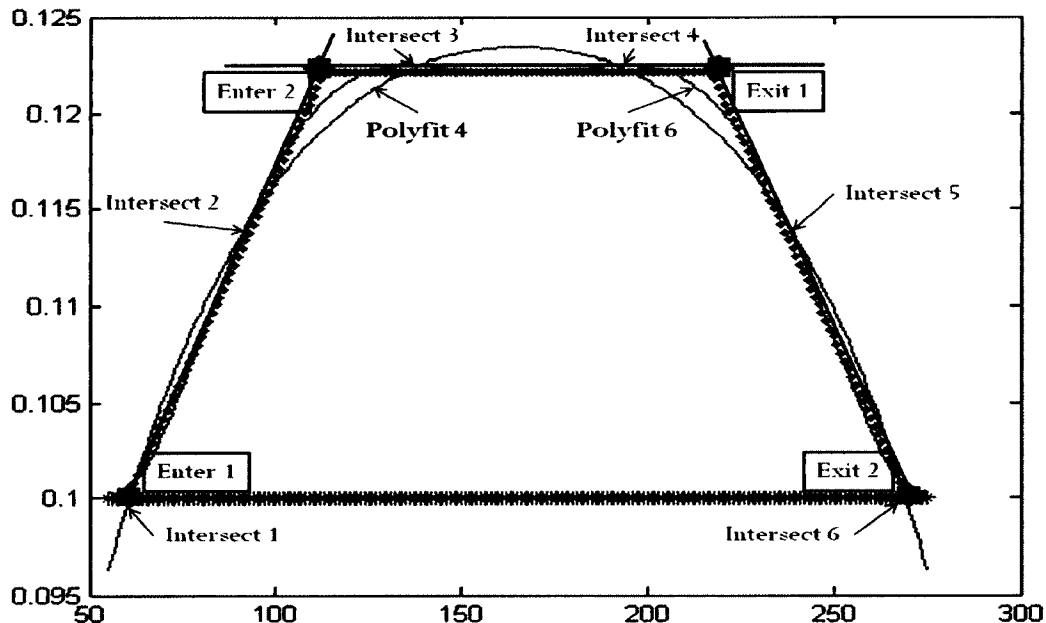


Figure 5.6 A trapezoid approximation using the 6 intersection points to uncover the 4 critical points

#### 5.2.4.1. Least Squares Approximation

A signal is a sequence of discrete data points measured by the sensor. The Least Squares Approximation finds an estimated fit of the signal data via an approximating function that passes through the set of points in the best possible manner without requiring the function to pass through each point.

Given  $N$  data points,  $(x_i, y_i)$ , the goal is to find the best fit to the  $n^{\text{th}}$  degree polynomial approximating function,

$$P_n(x) = a_1x^n + a_2x^{n-1} + \cdots + a_nx + a_{n+1},$$

where  $a_1, \dots, a_n$  are coefficients.

The sum of the squares of the deviations,  $S$ , are found by

$$S(a_1, a_2, \dots, a_{n+1}) = \sum_{i=1}^N (y_i - a_{n+1} - a_n - \cdots - a_1x_i^n)^2$$

and  $S$  is at a minimum when the partial derivatives are equal to zero as shown by

$$\frac{\partial S}{\partial a_0} = \sum_{i=1}^N 2(y_i - a_{n+1} - a_n - \cdots - a_1x_i^n)(-1) = 0,$$

.

.

$$\frac{\partial S}{\partial a_n} = \sum_{i=1}^N 2(y_i - a_{n+1} - a_n - \cdots - a_1x_i^n)(-x_i^n) = 0,$$

and

$$\frac{\partial S}{\partial a_{n+1}} = \sum_{i=1}^N 2(y_i - a_{n+1} - a_n - \cdots - a_1x_i^n)(-x_i^n) = 0.$$

Dividing the partial derivatives by two yields the normal equations,

$$\sum_{i=1}^N y_i = a_1 \sum_{i=1}^N x_i^n + \cdots + a_n \sum_{i=1}^N x_i + a_{n+1} N,$$

.

.

.

and

$$\sum_{i=1}^N x_i^n y_i = a_1 \sum_{i=1}^N x_i^{2n} + \cdots + a_n \sum_{i=1}^N x_i^{n+1} + a_{n+1} \sum_{i=1}^N x_i^n,$$

that can be solved for the coefficients  $a_1, \dots, a_n$  by Gaussian elimination [52].

The resulting solutions for the  $n^{\text{th}}$  degree polynomials,  $\text{Poly}_n$ , are stored in the matrix form

$$\text{Poly}_n(r, c, :) = [a_1 \quad \dots \quad a_n \quad a_{n+1}],$$

where the  $r$  is the row index and  $c$  is the column index.

This method can encounter problems for higher  $N$  values because the coefficients can vary over a range of several orders of magnitude. Normalizing each equation and using double precision variables help prevent the ill-conditioned system problem. However, it is not recommended to have  $N$  values over six [52].

#### 5.2.4.2. Trapezoid Approximation

The target's critical points can be found by the linear geometry relationships between  $\text{PolyValue}_6$ ,  $\text{PolyValue}_4$  and the estimated background.

The first step is to approximate the trapezoid. First, set

$$\text{Poly}_6 = \text{Poly}_4,$$

and find the zeros

$$\text{PolyZeros}_6(r, c, :) = [z_{x1} \quad z_{x2} \quad z_{x3} \quad z_{x4} \quad z_{x5} \quad z_{x6}],$$

where  $z_1, z_2, \dots, z_6$  are the  $x$  or frame values where  $Poly_6$  and  $Poly_4$  intersect.

Next, solve for the corresponding  $y$  or intensity values for each  $x$  to gather the trapezoid's six intersection points given by

$$P_6(z_{x1}) = z_{y1},$$

.

.

.

and

$$P_6(z_{x6}) = z_{y6}.$$

From these points, three lines are created such that

$$\text{Line 1}(x) = z_{y1} + \frac{(z_{y2} - z_{y1})}{(z_{x2} - z_{x1})}(x - z_{x1}),$$

$$\text{Line 2}(x) = z_{y3} + \frac{(z_{y4} - z_{y3})}{(z_{x4} - z_{x3})}(x - z_{x3}),$$

and

$$\text{Line 3}(x) = z_{y5} + \frac{(z_{y6} - z_{y5})}{(z_{x6} - z_{x5})}(x - z_{x5}).$$

The fourth line is created from the background model,

$$\text{Line 4}(x) = I_{\text{Back}}.$$

The intersections of the lines create the four critical points,

$$Enter_1 = \text{zeros}(\text{Line1} - \text{Line4}),$$

$$Enter_2 = \text{zeros}(\text{Line2} - \text{Line1}),$$

$$Exit_1 = \text{zeros}(\text{Line3} - \text{Line2}),$$

and

$$Exit_2 = \text{zeros}(\text{Line4} - \text{Line3}),$$

where zeros is a MATLAB function that finds the x-intercept.

#### 5.2.4.3. PolyFit Example

A HEMTT target ( $L = 10.19$  m) traveling at 23 m/s is inserted into a  $30 \times 30$  m<sup>2</sup> single-pixel with noise ( $\sigma = 0.02$ ) added (Figure 5.7.A., 5.7.B). After running the change threshold detection algorithm, the binary matrix is sent to the PolyFit subroutine.

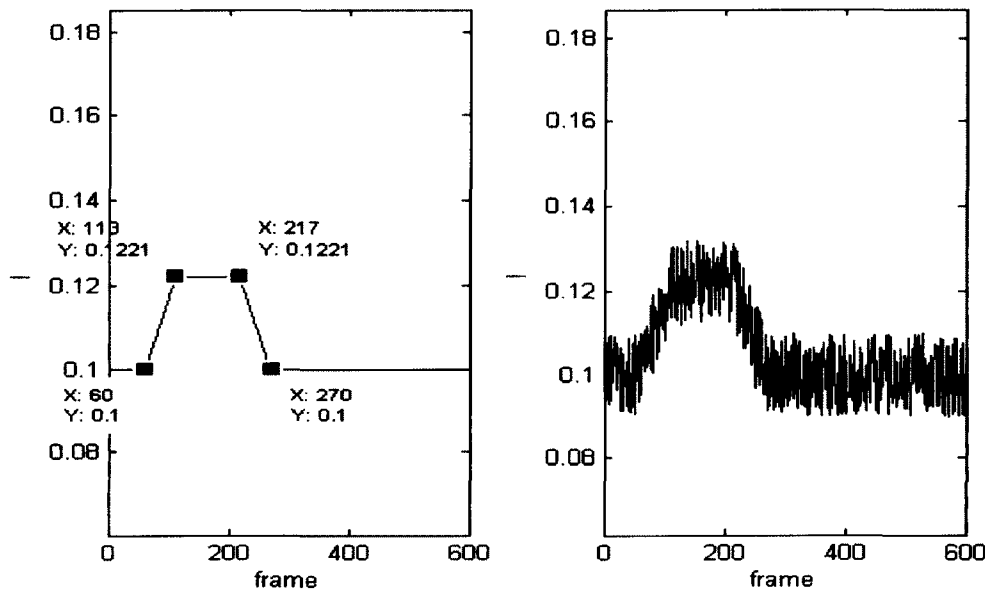


Figure 5.7 (A) Modeled target with critical points marked (B) Target profile with noise

The PolyFit algorithm finds the fourth and sixth degree polynomial fits and calculates the critical points. Figure 5.8 shows the original signal,  $Poly_6$ , and  $Poly_4$ . Lines are drawn to show the critical point intersections.

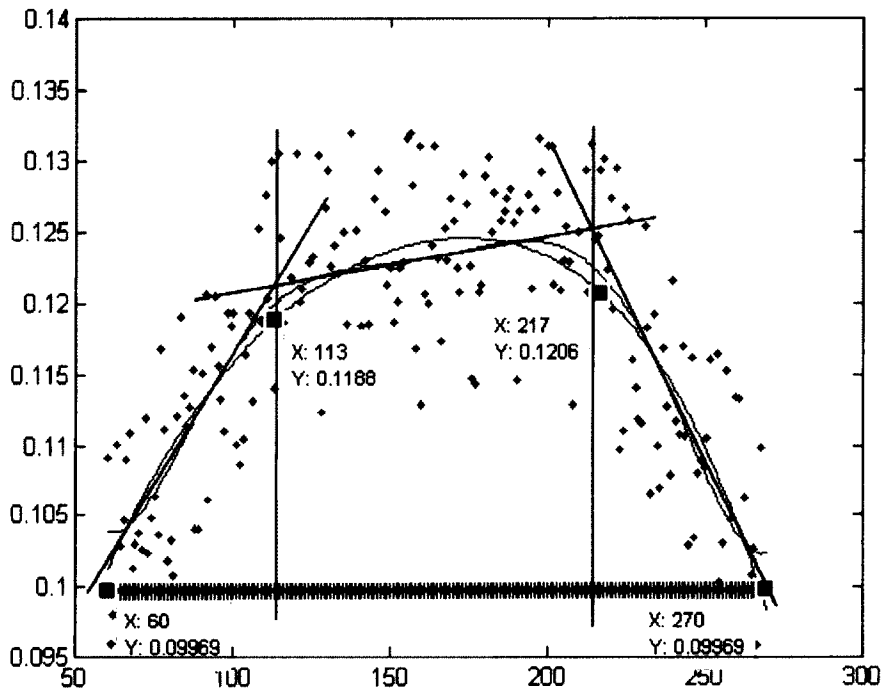


Figure 5.8 PolyFit analysis with original critical points marked

The calculated critical points are  $Enter_1 = 55$ ,  $Enter_2 = 113$ ,  $Exit_1 = 216$ , and  $Exit_2 = 270$ . The calculated velocity and target length are 22.93 m/s and 10.13 m, respectively. Comparing the calculated values with true values,  $Enter_2$  and  $Exit_2$  were exact.  $Enter_1$  and  $Exit_1$  had a five or less frame difference. From Chapter Three, a HEMTT vehicle is 10.19 m long, showing differences of only 0.06 m (error of 0.5%) and a velocity delta of 0.07 m/s (error of 0.3%).

## **CHAPTER SIX**

### **SUPER PIXEL REFINEMENT**

During target extraction significant information can be missed during single-pixel analysis when a target is split amongst several pixels, with consequential inaccuracies in the target characteristics. By reconnecting the split pixels, the entire target profile is captured. When using actual sensor data, two more tools become necessary to refine the signal enough to derive critical information. At certain times, the target does not travel completely through a single pixel horizontally. Instead the target may travel through part of two different pixels. At other times, the target travels at such a speed to give an insufficient temporal profile. Yet another potential problem exists when the target may be just a bit bigger than a pixel, but not big enough to distinguish its characteristics by using conventional spatial methods.

Therefore, instead of super-resolution, this section investigates super-pixel refinement. The two tools to accomplish this refinement are the Sum-pixel and Enlarge-pixel methods. The balance is to ensure the signal is not lost in this process.

The figures in Figure 6.1 represents sensor data taken from a video clip of a remote control vehicle moving horizontally through the screen on a grass and sand background. In the first figure (set of four graphs), the target is split amongst the four pixels [53]. The second figure (larger single graph) uses the sum pixel process to

capture the entire target. The critical target entry and exit points are now well defined (Figure 6.1).

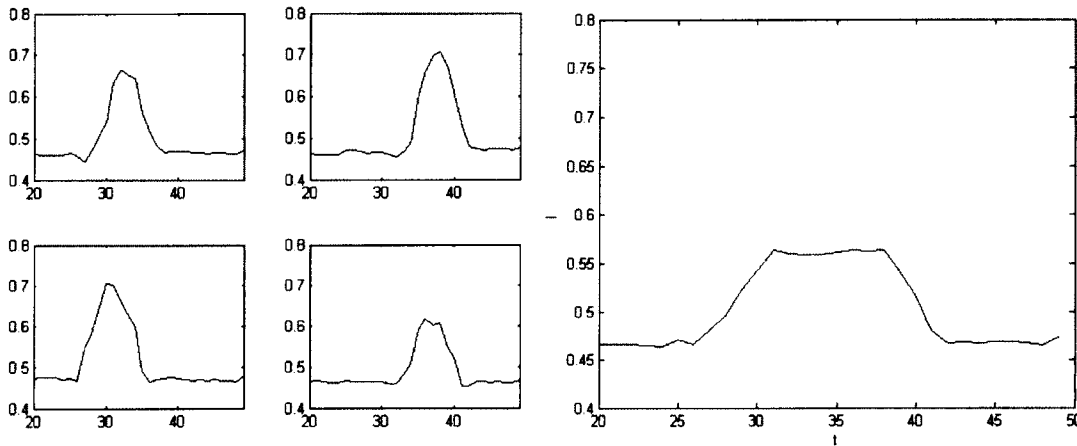


Figure 6.1 (A) 2x2 pixel array showing temporal profile of same target (B) Sum-pixel result of same target showing trapezoid profile

### 6.1. Sum Pixel Refinement

Sum-pixel refinement creates a better understanding of the detected target by merging neighboring pixels in order to gather more temporal target data within a pixel. The benefits of this process are longer target profiles and some reduction in noise and jitter. This method generally exacts a price of a reduced target to pixel ratio and lower target to background intensities, so care must be taken not to lose the target signal.

Figure 6.2 shows a 4x4 array with a modeled target signal inserted into a non uniform background with a jitter value of 0.25 pixel and a noise value of 1.5%. The signal is split between the second and third rows of the array simulating a non centered target.

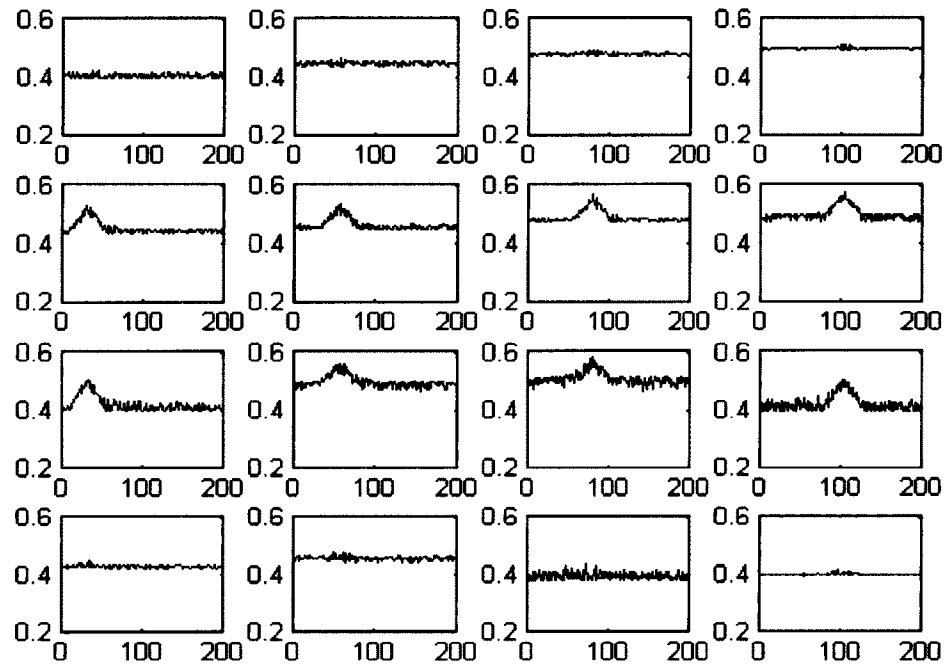


Figure 6.2 Multi-pixel target split among two rows

Figure 6.3.A is a close up view of  $\text{Pixel}_{(2,1)}$  from Figure 6.2. Notice that the target signal has a very short time peak where the target is fully within the frame, making it harder to get the correct velocity. Figure 6.3.B is the summed pixel,  $\text{Pixel}_{(2:3,1)}$ , which is the result of summing rows two and three from the array in Figure 6.2.

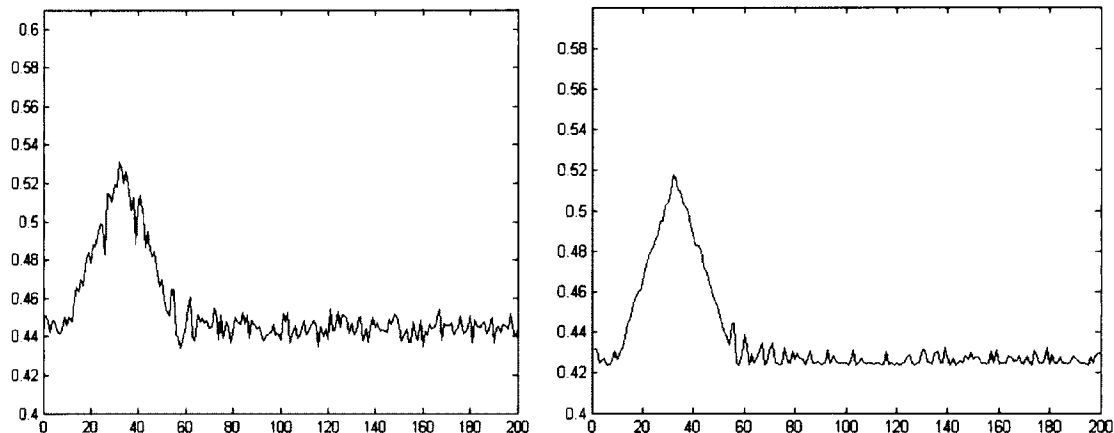


Figure 6.3 (A) Close up view of  $\text{Pixel}_{(2,1)}$  (B) Result of summing pixels in rows 2 and 3

Figure 6.4.A and 6.4.B are the summed pixel,  $\text{Pixel}_{(2:3,1:2)}$ , and the summed pixel,  $\text{Pixel}_{(2:3,1:4)}$ , respectively.

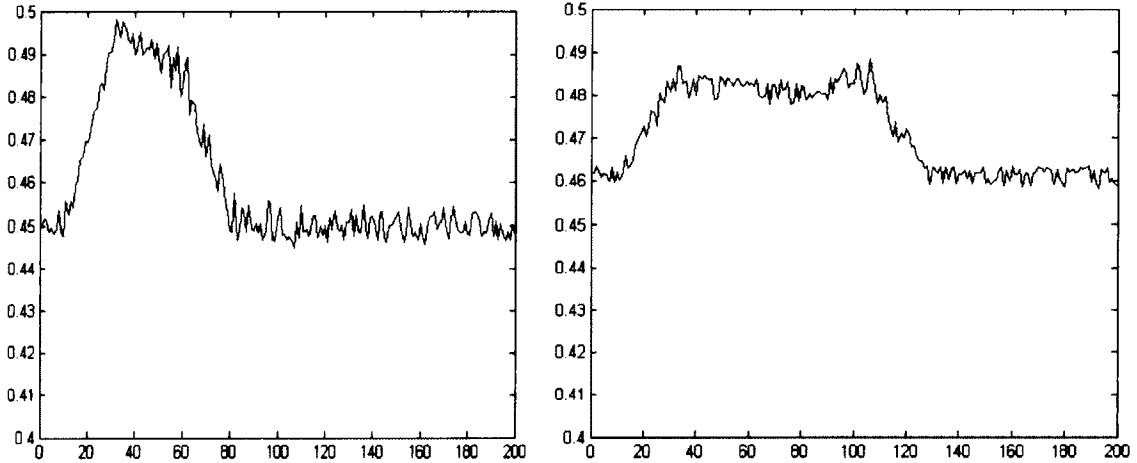


Figure 6.4 (A) Result of summing rows 2 and 3 with columns 1 and 2 (B) Result from summing rows 2 and 3 with columns 1-4

As the pixels are summed in the direction of travel, i.e. the columns, there are more quality frames for target analysis. In addition, summing the two rows of the split targets reduced the amount of noise and jitter present.

## 6.2. Enlarge Pixel Refinement

Enlarging the pixel is especially useful for targets with a high ratio of target to pixel (RTP), in which case the target area encompasses the majority of the pixel. These targets have high detection probabilities, but cause problems within the target characterization algorithms. In these scenarios, the duration of the target remaining completely within the pixel is minimal, creating a single point peak, instead of the desired trapezoid profile. By enlarging the pixel along the target trajectory, the temporal profile is expanded, recovering the trapezoid. This tool has an advantage over the Sum

Pixel process in that it can expand partial pixels and can focus on narrower regions of interest (Figure 6.5.A and 6.5.B).

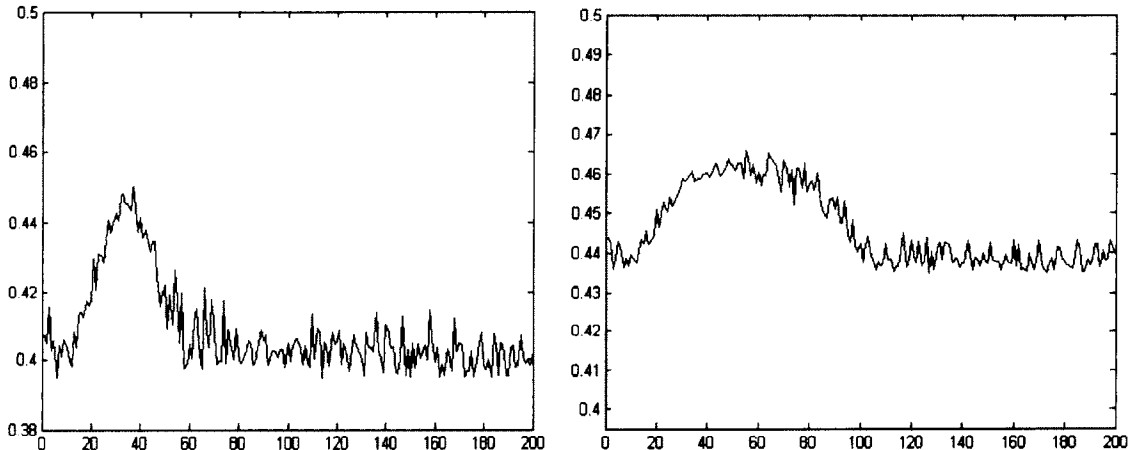


Figure 6.5 (A) Single-pixel target with 0.25 jitter and 1.25% noise (B) Result from enlarging pixel by a factor of 0.8

### 6.3. Binary Target Matrix

The Sum Pixel process is considered a refinement step because prior target detection knowledge is integral in selecting regions of interest to sum or enlarge. The task of choosing the appropriate pixel increase factor is made easier via the Binary Target Matrix produced in the change detection algorithms. The Binary Target Matrix shows the temporal target neighbors and serves as the Sum Pixel refinement starting point (Figure 6.6).

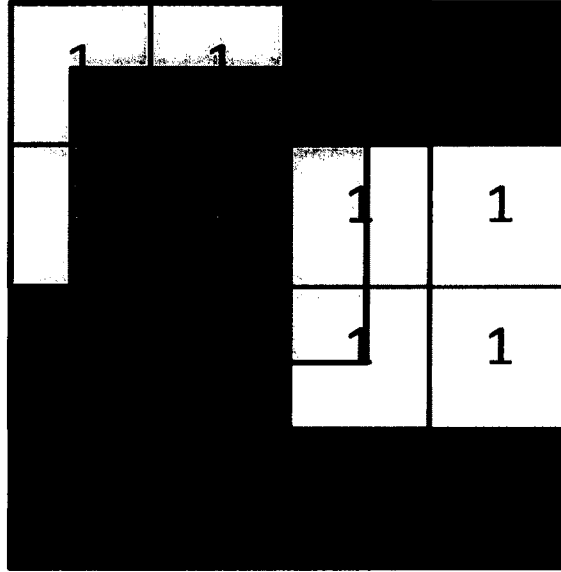


Figure 6.6 Pictoral description of temporal target binary matrix

Using the binary matrix in Figure 6.6, a good input for the Sum-pixel algorithm would be the highlighted sub matrix,  $\text{Pixel}_{(1:2,1:2)}$  and a good input for the Enlarge-pixel algorithm would be the highlighted partial pixel box,  $\text{Pixel}_{(0.5:2.5,0.5:2.5)}$ , using the expansion factors of  $N_{row} = 0.5$  and  $N_{col} = 0.5$ .

Super-pixels do not have to be equal in the row and column direction. Different options for choosing the best increase factor include resizing the entire matrix or a sub-matrix by an integer multiple, or expanding a single pixel to include a target's temporal neighbors. The best choices involve using a minimum number of pixels with a zero value. Currently, the summation and enlargement factors are chosen manually as a post-processing step, but future work would include automating this process.

## 6.4. Refinement Algorithms and Tools

The two tools for super-pixel processing are the Sum-pixel algorithm, which can resize the frame array into a smaller number of pixels and the Enlarge-pixel algorithm, which enlarges a single pixel to focus onto a region of interest and give a larger viewpoint.

### 6.4.1. Sum Pixel Algorithm

In this algorithm, the frames are resized to accommodate the new pixel size and the intensities of the old pixels are averaged to create the new pixel intensity.

The Sum-pixel algorithm resizes the  $m \times n \times f$  array to a  $p \times q \times f$  array:

- 1) Calculate the combination factor for the rows and columns given by

$$F_{row} = \frac{m}{p},$$

and

$$F_{col} = \frac{n}{q},$$

where  $F_{row}$  and  $F_{col}$  are the number of old rows and old columns that will make up a new pixel size. As of this time,  $F_{row}$  and  $F_{col}$  need to be an integer value.

- 2) Calculate the new pixels for each frame of the new matrix given by

$$\sum_{f=1}^{NumFrames} \sum_{c_n=1}^q \sum_{r_n=1}^p Pixel_{new}(r_n, c_n, f) = \sum_{c_o=col_{start}}^{col_{stop}} \sum_{r_o=row_{start}}^{row_{stop}} \frac{Pixel_{old}(r_o, c_o, f)}{F_{row} F_{col}},$$

where

$$row_{start} = (F_{row}(r_n - 1)) + 1,$$

$$row_{stop} = F_{row}r_n,$$

$$col_{start} = (F_{col}(c_n - 1)) + 1,$$

and

$$col_{stop} = F_{col} \cdot c_n.$$

The new pixel,  $Pixel_{new}$ , uses  $r_n$ ,  $c_n$ , and  $f$  for the row, column and frame indices, while the old pixel,  $Pixel_{old}$ , uses  $r_o$ ,  $c_o$ , and  $f$  for the row, column and frame indices.

For example, given a pixel frame,

$$Pixel_{old}(:,:,1) = \begin{bmatrix} 118 & 123 & 125 & 80 \\ 122 & 121 & 86 & 85 \\ 120 & 119 & 91 & 96 \\ 121 & 120 & 124 & 117 \end{bmatrix},$$

and given new row and column values of two, the new pixel frame would be,

$$\sum_{f=1}^1 \sum_{c_n=1}^2 \sum_{r_n=1}^2 Pixel_{new}(r_n, c_n, 1) = \begin{bmatrix} 121 & 94 \\ 120 & 107 \end{bmatrix}.$$

It is important to note that the dimensions of the pixel will change during this process such that the size of the new pixel in the x-direction is given by

$$x_{pixel_{new}} = x_{pixel_{old}} F_{col},$$

and the size of the new pixel in the y-direction is given by

$$y_{pixel_{new}} = y_{pixel_{old}} F_{row}.$$

#### 6.4.2. Enlarge Pixel Algorithm

To enlarge a single pixel,  $Pixel_{old}(Row, Col, f)$  by a factor of  $N_{row}$  and  $N_{col}$  to create a new pixel,  $Pixel_{new}(I, J, f)$ , use the Enlarge-pixel algorithm:

- 1) Calculate start and stop values for the row and column summations using

$$row_{start} = Row - [N_{row}],$$

$$row_{stop} = Row + [N_{row}],$$

$$col_{start} = Col - [N_{row}],$$

and

$$col_{stop} = Col - \lfloor N_{row} \rfloor,$$

where *Row* and *Col* are row and column index of the chosen pixel to enlarge,  $Pixel_{old}$ , and the *f* index represents all of the frames in the data sequence.

2) Calculate  $Pixel_{new}$  using

$$\sum_{f=1}^{NumFrames} Pixel_{new}(1,1,f) = \frac{\sum_{c_o=col_{start}}^{col_{stop}} \sum_{r_o=row_{start}}^{row_{stop}} F_r F_c Pixel_{old}(r_o, c_o, f)}{\sum_{c_o=col_{start}}^{col_{stop}} \sum_{r_o=row_{start}}^{row_{stop}} F_r F_c},$$

where the partial pixel row factor is  $F_r$ , and the partial pixel column factor is,  $F_c$ .  $F_r$  is equal to one unless *r* is at the start and stop value of the row summation. At these points,

$$F_r = N_{row} - \lfloor N_{row} \rfloor.$$

$F_c$  is equal to one unless *c* is at the start and stop values of the column summation. At these two points,

$$F_c = N_{col} - \lfloor N_{col} \rfloor.$$

For example, given a pixel frame of

$$Pixel_{old}(:,:,1) = \begin{bmatrix} 118 & 123 & 125 & 80 \\ 122 & 121 & 86 & 85 \\ 120 & 119 & 91 & 96 \\ 121 & 120 & 124 & 117 \end{bmatrix},$$

and the task of finding  $Pixel_{new}(1,1,1)$  using  $Pixel_{old}(2,2,1)$ ,  $N_{row} = 0.5$ , and  $N_{col} = 0.7$ , the new pixel value would be

$$Pixel_{new}(1,1,1) = [114].$$

As with the Sum-pixel algorithm, the dimensions of the pixel will change such that the size of the new pixel in the *x-direction* is given by

$$x_{pixel_{new}} = x_{pixel_{old}}(1 + 2N_{col}),$$

and the size of the new pixel in the *y-direction* is given by

$$y_{pixel_{new}} = y_{pixel_{old}}(1 + 2N_{row}).$$

### 6.5. Refined Change Detection

Once the Sum-pixel algorithm is complete,  $\text{Pixel}_{new}$  is sent to the change detection algorithms as a new source of data. Several refinements can be compared or averaged together to increase the accuracy of the target assessments. The main concern in using this algorithm is not to lose the target signal.

## CHAPTER SEVEN

### REFINEMENT THROUGH TRACKING (RTT)

In a staged environment, one can create scenarios with only horizontal target movement. Outside of this environment, these cases are not readily available. This is an issue as the target length characteristic calculated in Chapter Five is actually the dimension of the target in the x-direction,  $d_x$ . If the target moves in the horizontal direction, this accurately corresponds to the target length, but any other direction of travel would produce a length calculation error. The actual length of the target would be bounded by the horizontal length calculation and movement at a  $45^\circ$  angle. The error is found by,

$$\varepsilon_{length} \leq \sqrt{2}d_x,$$

where  $\varepsilon_{length}$  is the length error and  $d_x$  is the calculated length found in Chapter Five. It is possible to minimize this error by using a Refinement Through Tracking technique. For the purposes of this discussion, it is assumed that the target trajectory is known or historical data exists where the trajectory can be calculated. Further work will investigate different tracking methods for algorithm implementation.

If you know the trajectory angle of the target, it is possible to find out more information than just the target velocity and length. The spatial target radiometry describes a target's area. By combining the temporal profile of the sub-pixel target with the spatial trajectory, it is geometrically possible to refine the target's parameters of

length and width. With the given information of the target's entry time, transit time and trajectory angle, the target length and width are not singular. This problem can be resolved by calculating an additional trajectory and from another temporal profile. Some suggestions for gaining the additional trajectory include finding a pixel where the target changes directions or rotating the static sensor. Another solution consists of applying the expected target width to length ratios to test the target profile potential categories.

### 7.1. Historical Binary Target Matrix (HBTM)

The Historical Binary Target Matrix (HBTM) is a useful tool in calculating the target trajectory angle. The HBTM historically captures the spatio-temporal progress of the target in zeros and ones, where a value of one indicates target detection occurred during the frame sequence (Figure 7.1).

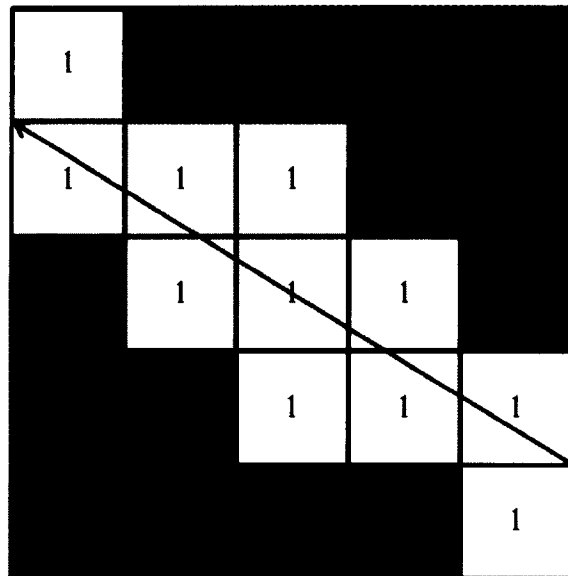


Figure 7.1 Utilizing the HBTM for calculating target trajectory

An estimated target trajectory can be found via the slope of the target pixels in the HBTM. Using the row and column range values from the HBTM, and the pixel's dimensions, the slope of the target trajectory is found by

$$Slope = \frac{(row_B - row_A)Pixel_y}{(col_B - col_A)Pixel_x},$$

where  $row_B - row_A$  and  $col_B - col_A$  are the rows and columns the target traverses,  $Pixel_x$  is the x-dimension of the pixel, and  $Pixel_y$  is the y-dimension of the pixel.

The target trajectory,  $\theta$ , is the inverse tangent of the slope,

$$\theta = \tan^{-1}(Slope).$$

## 7.2. Considerations

The target must traverse the entire pixel in the x- or y-direction. Several techniques mitigate this requirement. The Historical Binary Target Matrix is one such technique. If  $I_{Pixel}(r, c, :)$  is the pixel of interest over a period of frames, one of these conditions must be true:

$$HBTM(r - 1, c) = 1 = HBTM(r + 1, c)$$

or

$$HBTM(r, c - 1) = 1 = HBTM(r, c + 1).$$

If the pixel of interest does not meet these conditions, then the user can choose a valid pixel from the HBTM or use one of the Super-pixel algorithm tools to ensure compliance. In Figure 7.2 the arrow marks the trajectory and the bold pixel is the Pixel of Interest (POI), in which the target does not traverse the entire pixel. By using the Sum-pixel algorithm to average the shaded pixels, the new POI is now in compliance because the target passes the entire pixel from right to left.

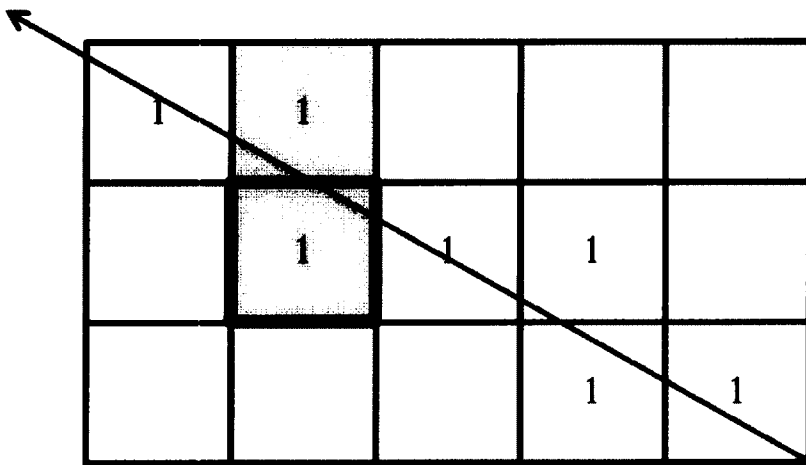


Figure 7.2 Target trajectory assessment with Sum-pixel refinement to meet pixel conditions

The Refinement Through Tracking process considers all the same assumptions as the work in the previous sections, with the exception that horizontal movement restriction is no longer required.

### 7.3. Trajectory Scenarios

Depending on the direction of travel, different dimensions of the target are found using methods described in the Target Analysis chapter, but require different calculations for each scenario. The two most interesting cases are the X-dominant and Y-dominant travel. The term dominant describes the aspect that the target will cross the entire pixel in a particular dimension (x or y). In these cases, it is still possible to calculate the target's length and width.

There are two special cases, where the target travels in a completely horizontal or vertical direction and where the target travels in a diagonal nature. In both of these cases, it is possible to find dimension for the target's length. The target's width, however, is non-singular.

### 7.3.1. X Dominant Travel

X-dominant travel describes the scenario where the target travels across the complete pixel in the x- direction (Figure 7.3).  $\theta$  indicates the target's trajectory angle in the direction of travel and  $d_x$  is the x component of the target's dimension.



Figure 7.3 Temporal elapse of target traveling through a pixel.

The target analysis algorithm calculates the velocity in the horizontal, or x-direction. Knowing this velocity,

$$V_x = \frac{Pixel_x}{(f_{transit} - f_{entry})}$$

calculating the x component of the target's dimension,  $d_x$ , is possible using

$$d_x = V_x f_{entry},$$

where  $Pixel_x$  is the length of the pixel in the x-direction,  $f_{entry}$  is the number of frames it takes the target to completely enter the pixel and  $f_{transit}$  is the number of frames it takes the target to completely cross the pixel. The Target Analysis Section describes the calculations for both  $f_{entry}$  and  $f_{transit}$ .

A boundary box surrounds the target and  $d_x$  describes the x-dimension of the target (Figure 7.4.A). Let  $\alpha$  describe the partial segment of  $d_x$  where the target intersects the boundary box (Figure 7.4.A).

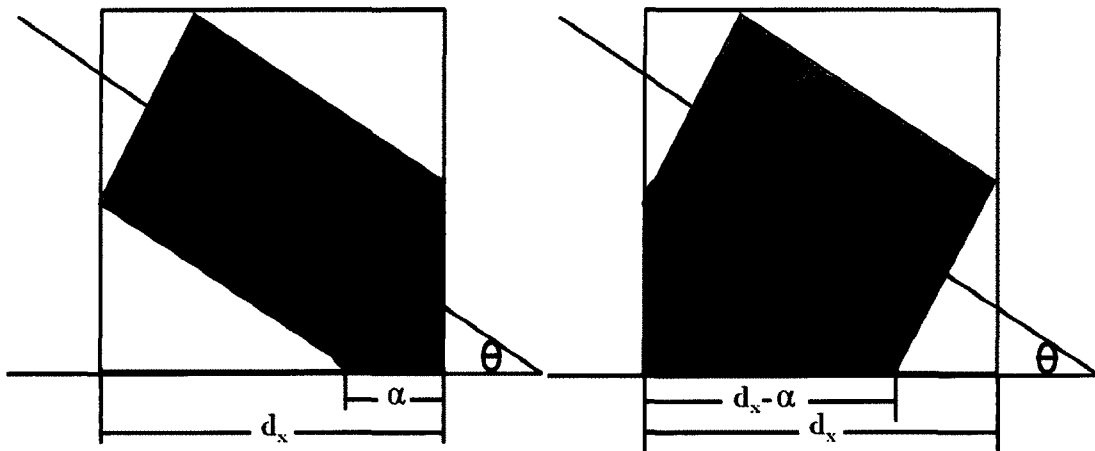


Figure 7.4 (A) Depiction of width parameters (B) Depiction of length parameters

Using the laws of sines and cosines of a right triangle, these geometrical relationships are true:

$$\sin \theta = \frac{\alpha}{d_w},$$

and

$$\cos \theta = \frac{d_{x_\theta} - \alpha}{d_l},$$

where  $\theta$  is the target trajectory angle,  $d_{x_\theta}$  is the x-dimension of the target found by  $\theta$ ,  $d_w$  is the width of the target and  $d_l$  is the length of the target. If  $\theta > 90^\circ$ , the supplementary angle must be used.

To solve for  $d_{x\theta}$ , set the equations equal to  $\alpha$  to get

$$d_{x\theta} = d_w \sin \theta + d_l \cos \theta.$$

Now, there is one equation and two unknowns,  $d_w$  and  $d_l$ , which is a non-singular solution. If the target changes direction or the sensor is rotated, then another trajectory angle,  $\gamma$ , exists for the equation,

$$d_{x\gamma} = d_w \sin \gamma + d_l \cos \gamma,$$

and combined with  $d_{x\theta}$ , can be solved for the target's width and length,

$$d_w = \frac{d_{x\gamma} - \frac{d_{x\theta} \cos \gamma}{\cos \theta}}{\sin \gamma - \tan \theta \cos \gamma},$$

and

$$d_l = \frac{d_{x\theta}}{\cos \theta} - d_w \tan \theta.$$

Note that this process assumes both equations have X-dominant travel. If there is one trajectory with Y-dominant travel, the equation in the next section must be substituted for trajectory angle  $\gamma$ .

### 7.3.2. Y Dominant Travel

Y-dominant travel describes the scenario where the target travels across the complete pixel in the y-direction (Figure 7.5).  $\theta$  indicates the target's trajectory angle in the direction of travel and  $d_y$  is the y component of the target's dimension.

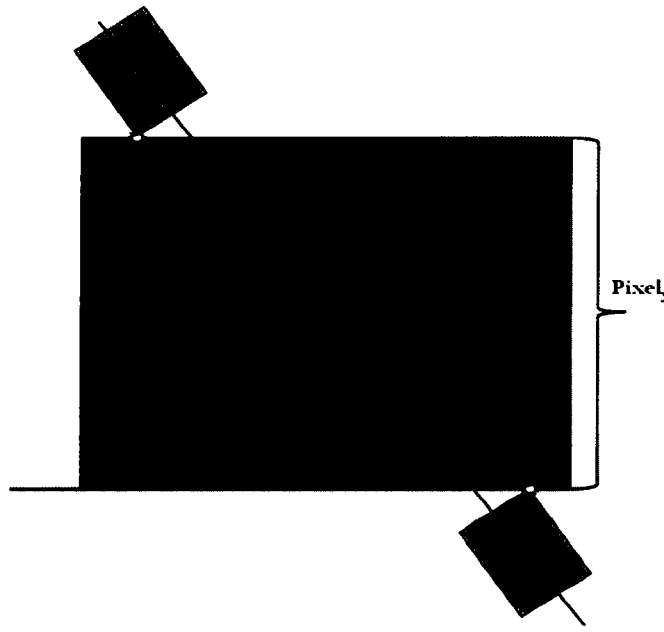


Figure 7.5 Temporal elapse of target traveling in Y-dominant direction

Due to the dominant y-direction, using the  $Pixel_y$  values becomes critical in the velocity calculation. Knowing the velocity in the y-direction,

$$V_y = \frac{Pixel_y}{(f_{transit} - f_{entry})},$$

calculating the y component of the target's dimension,  $d_y$ , is possible using

$$d_y = V_y f_{entry},$$

where  $Pixel_y$  is the length of the pixel in the y-direction,  $f_{entry}$ , is the number of frames it takes the target to completely enter the pixel and  $f_{transit}$  is the number of frames it takes the target to completely cross the pixel. The Target Analysis Section describes the calculations for both  $f_{entry}$  and  $f_{transit}$ .

A boundary box surrounds the target and  $d_y$  describes the y-dimension of the target (Figure 7.6.A). Let  $\beta$  describe as the partial segment of  $d_y$  where the target intersects the boundary box (Figure 7.6.B).

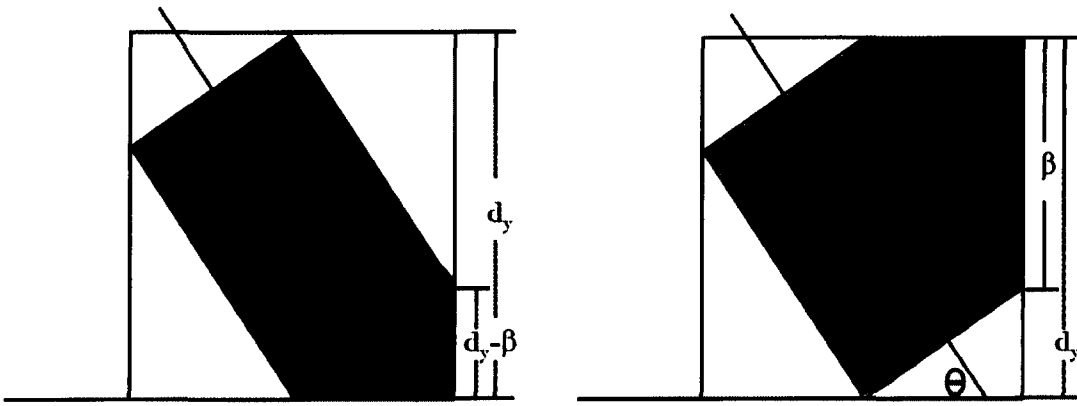


Figure 7.6 (A) Depiction of width parameters in Y-dominant travel (B) Depiction of length parameters in Y-dominant travel

Using the laws of sines and cosines of a right triangle, these geometrical relationships are true:

$$\sin \theta = \frac{\beta}{d_l},$$

and

$$\cos \theta = \frac{d_{y\theta} - \beta}{d_w},$$

where  $\theta$  is the target trajectory angle,  $d_{y\theta}$  is the y-dimension of the target found by  $\theta$ ,  $d_w$  is the width of the target and  $d_l$  is the length of the target. If  $\theta > 90^\circ$ , the supplementary angle must be used.

Set the equations equal to  $\beta$ ,

$$d_l \sin \theta = \beta = d_{y\theta} - d_w \cos \theta,$$

and solve for  $d_{y\theta}$  using

$$d_{y\theta} = d_l \sin \theta + d_w \cos \theta.$$

Just as in the X-dominant travel calculations, there is one equation and two unknowns,  $d_w$  and  $d_l$ , which is a non-singular solution. If the target changes direction or the sensor is rotated, then another trajectory angle,  $\gamma$ , can be used for the equation

$$d_{y\gamma} = d_l \sin \gamma + d_w \cos \gamma,$$

and combined with  $d_{y\theta}$  and solved for the target's width and length,

$$d_l = \frac{d_{y\gamma} - \frac{d_{y\theta} \cos \gamma}{\cos \theta}}{\sin \gamma - \tan \theta \cos \gamma},$$

and

$$d_w = \frac{d_{y\theta}}{\cos \theta} - d_w \tan \theta.$$

Note that this process assumes that both equations have Y-dominant travel. If there is one trajectory with X-dominant travel, the equation from Section 7.3.1. must be substituted for trajectory angle  $\gamma$ .

### 7.3.3. Dominant Travel Considerations

In both the X- and Y- dominant travel calculations, if the target fails to change directions and the sensor cannot rotate, then comparative analysis may uncover the target's parameters. This concept involves bounding the target with the non-singular solution equations found earlier for  $d_{x\theta}$  and  $d_{y\theta}$ .

Given these mathematical equations, there are, by definition, a number of values for length and width that will make this equation valid. Furthermore, for every value of length that falls within the equation boundaries, there is a specific and unique value for width that will fit and vice versa (Figure 7.7).

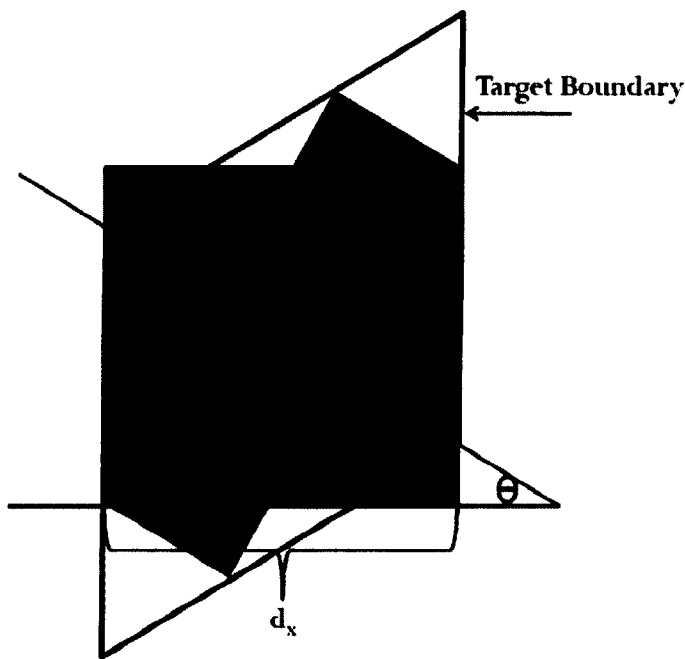


Figure 7.7 Possible Target Shapes for a Given Pixel, Velocity, and Trajectory

Therefore, the target in question is said to be described by the non-singular solution equation. Using deductive reasoning and a database of known length and width values for similar targets, inserting the values into the equation will determine if the database target matches the unidentified target's parameters.

#### 7.3.4. Special Case 1

For targets that transverse the pixel horizontally, at  $0^\circ$  and  $180^\circ$ , or vertically, at  $90^\circ$  and  $270^\circ$  (Figure 7.8.A and 7.8.B) the length can be calculated geometrically while the target width remains an unknown parameter.

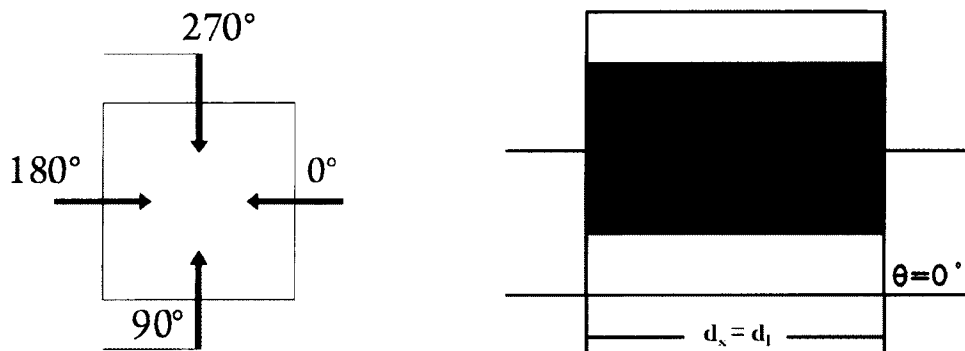


Figure 7.8 (A) Special Case 1 angles of entry (B) Pictorial depiction of Special Case 1

For cases with 0° and 180° target trajectory, the target velocity is given by

$$V_x = \frac{Pixel_x}{(f_{transit} - f_{entry})},$$

and the target length is given by

$$d_x = d_l = V_x f_{entry}.$$

For targets travelling in the vertical direction, the 90° and 270° cases,  $Pixel_y$ , would be substituted for  $Pixel_x$ , resulting in a target velocity of

$$V_y = \frac{Pixel_y}{(f_{transit} - f_{entry})},$$

and a target length of

$$d_y = d_l = V_y f_{entry}.$$

### 7.3.5. Special Case 2

For targets that enter a pixel from the corner at  $\theta = 45^\circ, 135^\circ, 225^\circ$ , or  $315^\circ$  (Figure 7.9), the length can be calculated geometrically while the target width will remain an unknown parameter.

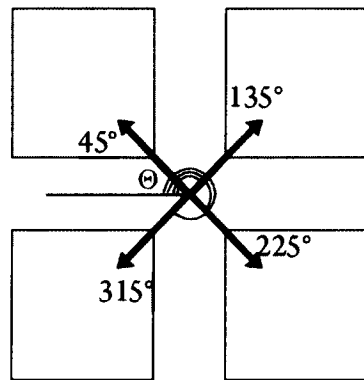


Figure 7.9 Pictoral description of Special Case 2 angles of entry into pixel

The difference between this case and Special Case 1 is that the pixel size must be converted by a  $\sqrt{2}$  factor. The dominant direction of travel, shown in Figure 7.10, determines the proper equation set to use.

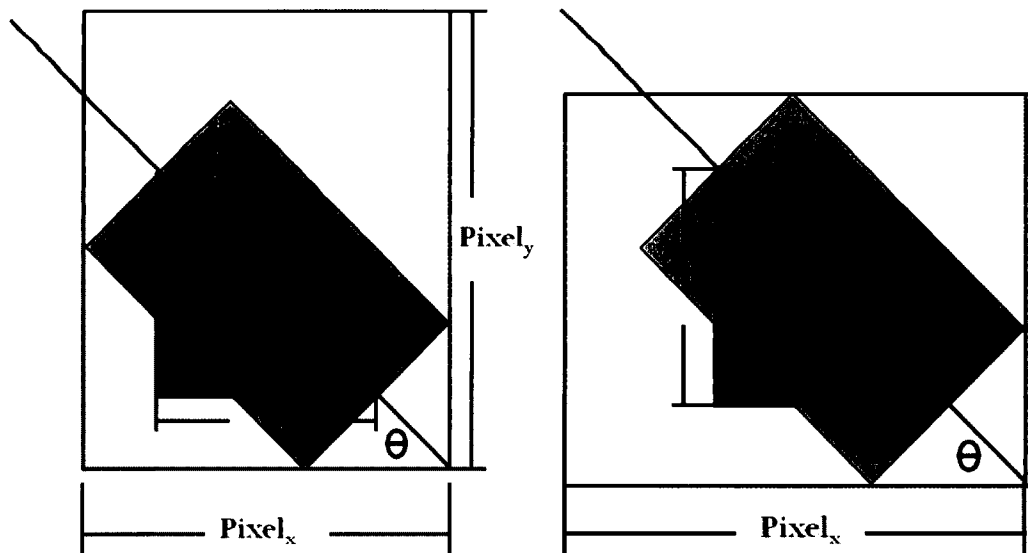


Figure 7.10 (A) Target crosses completely in x-direction (B) Target crosses completely in y-direction

For Special Case 2 scenarios with  $\text{Pixel}_x < \text{Pixel}_y$ , the target will completely cross the pixel in the x-direction and these equations are valid:

$$V_x = \frac{\text{Pixel}_x}{(f_{transit} - f_{entry})}$$

$$d_x = V_x \cdot f_{entry},$$

and the length of the target is found via

$$L_{target} = \sqrt{2} \cdot d_x.$$

For Special Case 2 scenarios with  $\text{Pixel}_y < \text{Pixel}_x$ , the target will completely cross the pixel in the y-direction and  $\text{Pixel}_y$  is substituted for  $\text{Pixel}_x$  in the velocity and length calculations.

## **CHAPTER EIGHT**

## **TESTING**

The sub-pixel algorithm can be used for a variety of situations and targets. For this dissertation, the model base uses ground based vehicles for detection and analysis. Therefore, the test scenarios were designed to analyze the algorithm performance for this specific situation.

There are three different sections for testing. The first is algorithm verification, which tests the computer algorithms against a compliance method, such as hand calculations, to ensure they work properly. The second test section uses the modeled data to find the boundaries of the sub-pixel algorithm. The final test section uses sensor data sequences for authentication of algorithm work and sub-pixel processing theories.

### **8.1. Algorithm Verification**

MATLAB was used for algorithm development and testing. The basic data structure in MATLAB is the array, which is naturally suited to the representation of real-valued images annotated as ordered sets of intensity data. MATLAB stores the images as matrices, allowing for efficient computation of multifaceted data.

Upon coding completion, individual function testing verifies run time accuracy for each algorithm or function tool. The tables containing the different computer modules, expected results, verification method and the algorithm compliance assessment are located in Appendix A.

## **8.2. Modeled Data Testing**

### **8.2.1. Overview**

Each modeled simulation set starts with a staring sensor having set characteristics for sample rate, pixel size, noise and jitter. Different ground vehicles, listed in Chapter Two, are randomly chosen for insertion into single or multiple pixels (Note: Single-pixel tests will have a value of zero for jitter). The vehicle's speed is randomly selected with values ranging from half of its maximum velocity to full maximum velocity. The intensity of the vehicle is randomly chosen as well. The background intensities for the single-pixel tests are constant values. The multiple-pixel scenarios have a low gradient intensity variation across the background array.

Tests are run in batches to emulate near-real-time processing. The data outputs to an Excel Spreadsheet for further analysis and processing. The results of each test determine the parameters to refine in the change detection and analysis algorithms for optimum sensor performance. Performance metrics are Detection Rate vs. False Alarm Rate and % error evaluation of the calculated target characteristics of velocity and length to the expected values.

## 8.2.2. Scenarios

### 8.2.2.1. Change Detection Testing

The goal of these scenarios is the comparison of the different detection methods performance on sub-pixel moving targets. The testing algorithm processes a batch of pixel frame sequences containing a modeled target through all of the change detection methods (Threshold, Duration, FAPI and the FAR filters). The Excel output files records the modeled sensor information (*Sample Rate, Pixel X, Pixel Y, Noise and Jitter*), the modeled target information (*Target ID, Target Length, Target Width, Target Velocity, and Target Intensity*), the expected critical points (*Enter<sub>1</sub>, Enter<sub>2</sub>, Exit<sub>1</sub> and Exit<sub>2</sub>*), each change detection's calculated critical points from the binary matrices (*Enter<sub>1</sub>, and Exit<sub>2</sub>*), and the number of targets detected from each change detection method (Table 8.1 – Table 8.4).

Table 8.1 Example of Excel Output of Modeled Sensor and Target Information for Change Detection Testing

Run	S Info	S Rate	Pixel X	Pixel Y	Noise	Jitter	T Info	#	Length	Width	Speed	blk	blk	No Noise	En1	En2	Ex1	Ex2
1		120	30	30	0	0		6	8.32	2.43	24.06	0.2	0.9		60	101	210	251
2		120	30	30	0	0		2	10.19	2.44	19.022	0.2	0.9		60	124	249	313
3		120	30	30	0	0		2	10.19	2.44	21.784	0.2	0.9		60	116	225	281
4		120	30	30	0	0		5	19.27	2.44	15.491	0.2	0.9		60	209	292	441
5		120	30	30	0	0		2	10.19	2.44	23.079	0.2	0.9		60	113	216	269
6		120	30	30	0	0		1	4.57	2.16	18.843	0.2	0.9		60	89	251	280
7		120	30	30	0	0		2	10.19	2.44	20.828	0.2	0.9		60	119	233	292
8		120	30	30	0	0		2	10.19	2.44	21.293	0.2	0.9		60	117	229	286
9		120	30	30	0	0		4	9.08	2.59	16.892	0.2	0.9		60	125	273	338
10		120	30	30	0	0		5	19.27	2.44	18.755	0.2	0.9		60	183	252	375
11		120	30	30	0	0		5	19.27	2.44	17.892	0.2	0.9		60	189	261	390
12		120	30	30	0	0		6	8.32	2.43	17.802	0.2	0.9		60	116	262	318
13		120	30	30	0	0		4	9.08	2.59	12.968	0.2	0.9		60	144	338	422
14		120	30	30	0	0		3	24.89	3.68	12.673	0.2	0.9		60	296	344	580

Table 8.2 Example of Excel Output of Modeled Target Threshold Change Detection with FAR Filters for Change Detection Testing

Run	Threshold	N	Y	#T	En1	Ex2	FAR1	#T	En1	Ex2	FAR2	#T	En1	Ex2
1		1	1	1	61	251	15	1	61	251	30	1	61	251
2		1	1	1	61	313	15	1	61	313	30	1	61	313
3		1	1	1	61	281	15	1	61	281	30	1	61	281
4		1	1	1	61	441	15	1	61	441	30	1	61	441
5		1	1	1	61	269	15	1	61	269	30	1	61	269
6		1	1	1	61	280	15	1	61	280	30	1	61	280
7		1	1	1	61	292	15	1	61	292	30	1	61	292
8		1	1	1	61	286	15	1	61	286	30	1	61	286
9		1	1	1	61	338	15	1	61	338	30	1	61	338
10		1	1	1	61	375	15	1	61	375	30	1	61	375
11		1	1	1	61	390	15	1	61	390	30	1	61	390
12		1	1	1	61	318	15	1	61	318	30	1	61	318
13		1	1	1	61	422	15	1	61	422	30	1	61	422
14		1	1	1	61	580	15	1	61	580	30	1	61	580

Table 8.3 Example of Excel Output of Modeled Target Duration Change Detection with FAR Filters for Change Detection Testing

Run	Duration	N	#T	En1	Ex2	FAR1	#T	En1	Ex2	FAR2	#T	En1	Ex2
1		1	1	73	239	15	1	73	239	30	1	73	239
2		1	1	71	303	15	1	71	303	30	1	71	303
3		1	1	70	272	15	1	70	272	30	1	70	272
4		1	1	92	410	15	1	92	410	30	1	92	410
5		1	1	69	261	15	1	69	261	30	1	69	261
6		1	1	68	273	15	1	68	273	30	1	68	273
7		1	1	70	283	15	1	70	283	30	1	70	283
8		1	1	70	277	15	1	70	277	30	1	70	277
9		1	1	69	330	15	1	69	330	30	1	69	330
10		1	1	86	350	15	1	86	350	30	1	86	350
11		1	1	88	363	15	1	88	363	30	1	88	363
12		1	1	77	302	15	1	77	302	30	1	77	302
13		1	1	72	411	15	1	72	411	30	1	72	411
14		1	1	82	559	15	1	82	559	30	1	82	559

**Table 8.4 Example of Excel Output of Modeled Target FAPI Change Detection with FAR Filters for Change Detection Testing**

Run	FAPI	N	Y	#T	En1	Ex2	FAR1	#T	En1	Ex2	FAR2	#T	En1	Ex2
1		1	1	1	63	290	15	1	63	290	50	1	63	290
2		1	1	1	64	349	15	1	64	349	50	1	64	349
3		1	1	1	63	319	15	1	63	319	50	1	63	319
4		1	1	1	64	475	15	1	64	475	50	1	64	475
5		1	1	1	63	307	15	1	63	307	50	1	63	307
6		1	1	1	64	314	15	1	64	314	50	1	64	314
7		1	1	1	63	329	15	1	63	329	50	1	63	329
8		1	1	1	63	324	15	1	63	324	50	1	63	324
9		1	1	1	64	374	15	1	64	374	50	1	64	374
10		1	1	1	64	411	15	1	64	411	50	1	64	411
11		1	1	1	64	426	15	1	64	426	50	1	64	426
12		1	1	1	64	354	15	1	64	354	50	1	64	354
13		1	1	1	64	455	15	1	64	455	50	1	64	455
14		1	1	2	78	581	15	2	78	581	50	1	78	581

For visual comparison, a comparative graphic displays the modeled target signal and the change detection information (Figure 8.1). The change detection testing results are located in Appendix B.

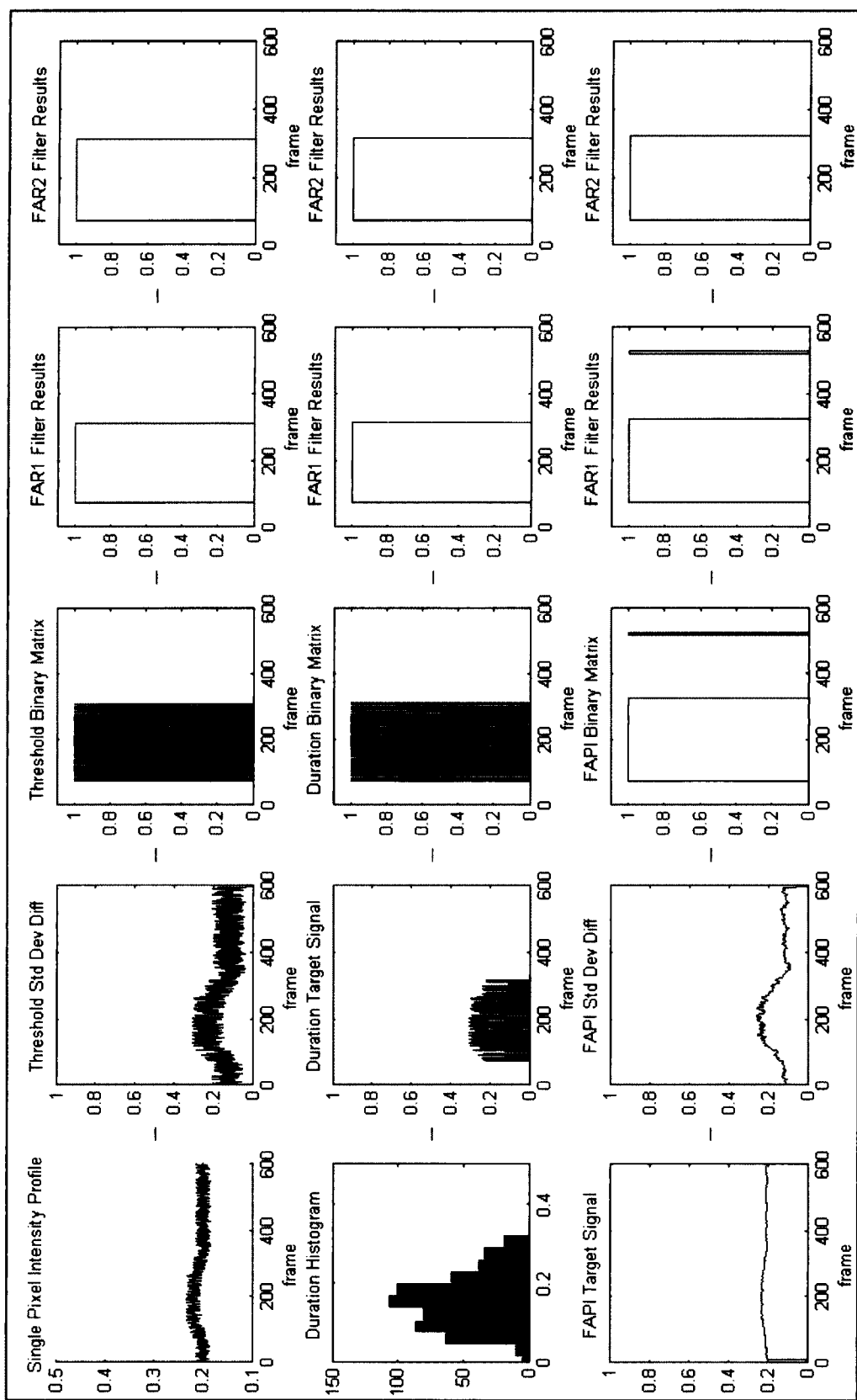


Figure 8.1 Comparative graphic display of change detection algorithms

The target model parameters for the first batch run has a constant sample rate (120 frames/s), pixel size ( $30 \times 30 \text{ m}^2$ ), zero noise and zero jitter with random variations, as described in the previous section. Consecutive batches vary the sensor parameters as shown in Table 8.5. To ensure sub-pixel targets, values for Pixel X and Y must be larger than the respective modeled target vehicle parameters in Chapter Two.

Table 8.5 Batch Run Variations for Sensor Parameters

	Variations
Sample Rate (frames/sec)	30, 60, 90, 120
Pixel X (m)	30 – 60
Pixel Y (m)	5 - 60
Noise	0 - 0.05
Jitter	0 - 0.5

#### 8.2.2.2. Target Analysis Testing

The target analysis testing utilizes the same sensor and target inputs as the change detection testing scenarios with the same variations as seen in Table 8.5. Every test batch includes three runs for each sensor and target model. The first run uses the Threshold Change Detection and feeds the results into a simultaneously run Polyfit and Fermifit algorithm. MATLAB exports the outcome to an Excel file.

Table 8.6 Example of Excel Output of Modeled Sensor and Target Information for Target Analysis Testing

Run	S Info	S Rate	Pixel X	Pixel Y	Noise	Jitter	T Info	#	Length	Width	Speed	Ibk	ITgt	No Noise	En1	En2	Ex1	Ex2
1		120	30	30	0.01	0.1		4	9.08	2.59	16.36	0.2	0.9		60	127	280	347
2		120	30	30	0.01	0.1		5	19.27	2.44	16.52	0.2	0.9		60	200	278	418
3		120	30	30	0.01	0.1		5	19.27	2.44	20.5	0.2	0.9		60	173	236	349
4		120	30	30	0.01	0.1		6	8.32	2.43	22.02	0.2	0.9		60	105	224	269
5		120	30	30	0.01	0.1		3	24.89	3.68	19.27	0.2	0.9		60	215	247	402
6		120	30	30	0.01	0.1		3	24.89	3.68	14.99	0.2	0.9		60	259	300	499
7		120	30	30	0.01	0.1		1	4.57	2.16	18.59	0.2	0.9		60	89	254	283
8		120	30	30	0.01	0.1		4	9.08	2.59	18.16	0.2	0.9		60	120	258	318
9		120	30	30	0.01	0.1		5	19.27	2.44	17.03	0.2	0.9		60	196	271	407
10		120	30	30	0.01	0.1		1	4.57	2.16	17.35	0.2	0.9		60	92	268	300

Table 8.7 Example of Excel Output of Modeled Target Threshold Change Detection with FAR Filters for Target Analysis Testing

Run	Threshold	N	Y	#T	En1	Ex2	FAR1	#T	En1	Ex2	FAR2	#T	En1	Ex2
1		3	1	51	272	283	15	1	87	328	30	1	87	328
2		3	1	25	154	313	15	1	101	378	30	1	101	378
3		3	1	24	126	279	15	1	73	336	30	1	73	336
4		3	1	23	103	106	15	1	84	240	30	1	84	240
5		3	1	38	153	303	15	2	69	383	30	1	69	383
6		3	1	47	176	391	15	5	81	465	30	1	81	465
7		3	1	27	236	239	15	8	115	256	30	1	115	256
8		3	1	74	136	144	15	10	67	298	30	2	67	298
9		3	1	42	186	191	15	4	167	305	30	1	167	305
10		3	1	20	236	238	15	9	236	270	30	2	236	270

**Table 8.8 Example of Excel Output of Modeled Target PolyFit and FermiFit Analysis for Target Analysis Testing**

Run	Poly	En1	En2	Ex1	Ex2	Fermi	En1	En2	Ex1	Ex2
1		63	131	289	345.3		63	131	289	345.3076
2		59	196	276	419.4		59	196	276	419.3685
3		50	172	239	352.4		50	172	239	352.3753
4		20	86	223	259.2		20	75	204	259
5		51	218	241	406.1		51	160	297	406
6		56	256	308	503.8		56	197	363	504
7		100	126	238	270.6		100	135	236	271
8		64	99	245	307.8		64	127	245	308
9		130	189	292	330.1		130	185	275	330
10		233	238	284	320.4		233	260	293	320

The second and third runs exchange the Threshold Change Detection algorithm for the Duration Change Detection and FAPI Change Detection, respectively. As with the change detection testing, a visual comparison graph displays for the user (Figure 8.2).

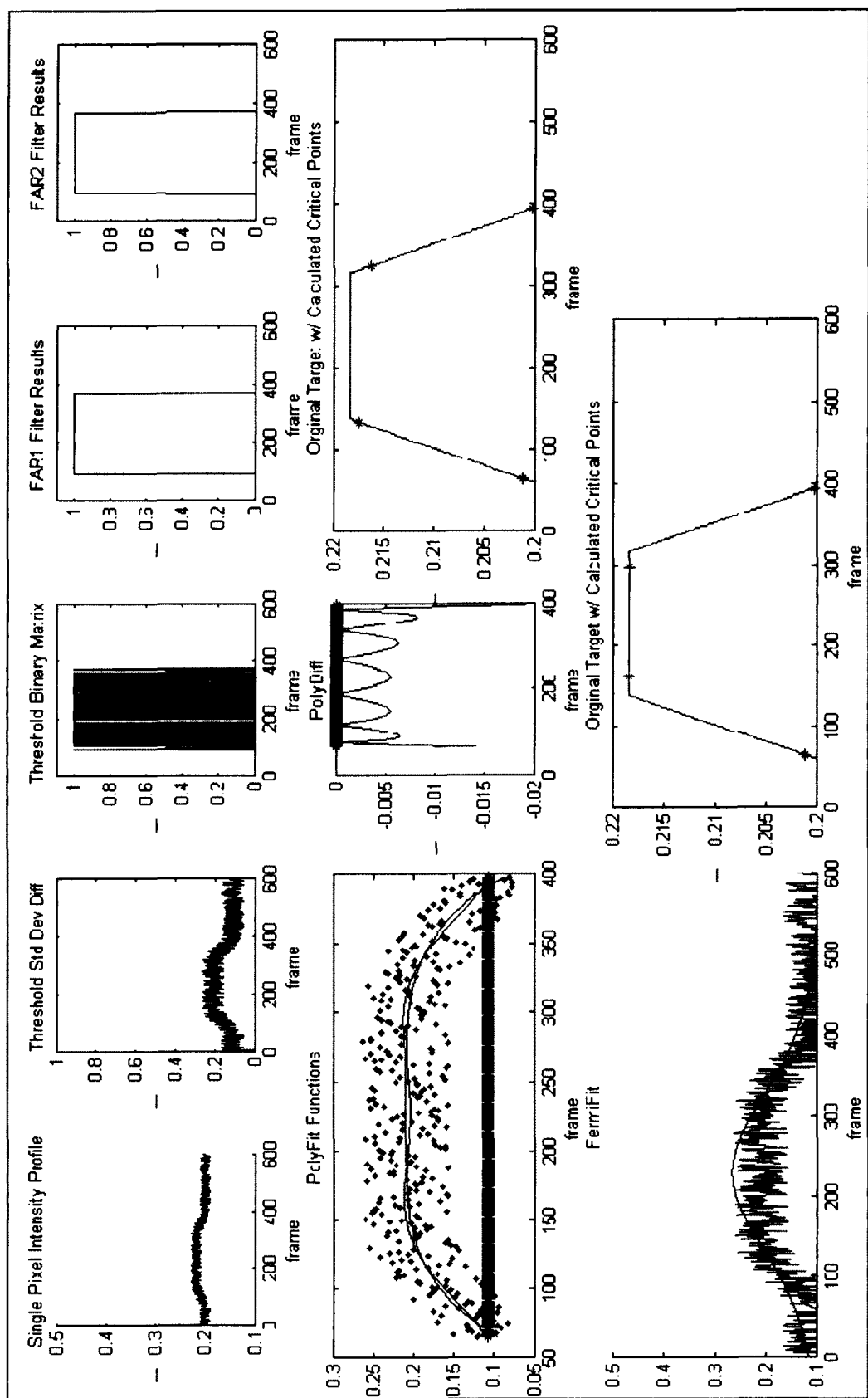


Figure 8.2 Example illustration of target analysis plots from PolyFit and FermiFit

### 8.3. Sensor Data Testing

#### 8.3.1. Data Information

RP Flight Systems Inc., who specializes in aerial data collection systems, provided a series of sensor data for testing. A stationary Panasonic Lumix LX2 secured to a tower 18 m above ground level shot sequences of continuous video of a remote controlled truck crossing a bumpy, grassy terrain. The target has a body color that, starting from the front, changes from orange to yellow to white to silver to black. The windshield and windows are solid black. The dimensions of the truck body are 0.406 m long by 0.165 m wide [53].

The data sequences have both horizontal and diagonal target travel, which provides information to test both the main and the refinement through tracking algorithms. The target travels through portions of heavily shadowed background as well as extremely bright areas (Figure 8.3).



Figure 8.3 Image of RP Flight Systems Inc., remote controlled truck with varying background taken from 18 m above ground

The target in the datasets is not sub-pixel. To ensure conformity with the nature of this dissertation, the Super-pixel algorithms enlarge or sum the pixels so they are larger than the target.

### 8.3.2. Scenarios

The data scenarios test the change detection, target analysis, super-pixel and Refinement Through Tracking (RTT) algorithms. In order to keep computational time to a minimum, specific pixel sequences of the original dataset pertinent to testing the algorithm robustness are chosen and saved in smaller data files. The criteria for choosing pixel sections are background intensity, target motion and pixel shape (Table 8.9).

Table 8.9 Sensor Data Testing Scenario Criteria

<b>Algorithm Focus</b>	<b>Pixel Shape</b>	<b>Background</b>	<b>Target Motion</b>
Change Detection Target Analysis Sum Pixel Enlarge Pixel	Multipixel	Uniform bright	Horizontal
	Large Square	Uniform bright	Horizontal
	Small Square	Uniform bright	Horizontal
	Short Rectangle	Uniform bright	Horizontal
	Long Rectangle	Uniform bright	Horizontal
	Multipixel	Uniform shadow	Horizontal
	Large Square	Uniform shadow	Horizontal
	Small Square	Uniform shadow	Horizontal
	Short Rectangle	Uniform shadow	Horizontal
	Long Rectangle	Uniform shadow	Horizontal
	Multipixel	Split bright/shadow	Horizontal
	Large Square	Split bright/shadow	Horizontal
	Small Square	Split bright/shadow	Horizontal
	Short Rectangle	Split bright/shadow	Horizontal
	Long Rectangle	Split bright/shadow	Horizontal

The testing algorithm imports the saved file, formats the sequences into a single intensity  $I_{Pixel}(r, c, f)$  array, and runs the appropriate sub-pixel algorithm. MATLAB exports the testing results to an Excel file, similar to the ones created in the modeled data testing, for post-run analysis.

## **CHAPTER NINE**

### **RESULTS AND DISCUSSION**

This section encompasses a summary and discussion of the modeled and sensor data test results. Appendix B contains the unabridged tabular data outputs.

#### **9.1. Sensor Parameter Analysis and Performance**

As expected, the sensor characteristics of sample rate, pixel size, noise and jitter varied throughout the modeled testing portion, and affected the algorithm's performance. The analysis in this section examines these effects in detail.

##### **9.1.1. Sensor Sample Rate**

As sensor sample rate increases, there are more data points during a specified time interval. In the change detection algorithms, this translates to a higher false alarm rate as a higher number of noisy or jittered points exceed the thresholds or duration filters.

Table 9.1 shows the results of the Duration Change Detection algorithm for a  $30 \times 30 \text{ m}^2$  pixel frame, with a noise and jitter value of 0.01 and 0.05 respectively. The false alarms were calculated from an average of 10 runs per sample rate (Appendix B).

Table 9.1 Sample Rate Effects on Detection and False Alarms

<b>Sample Rate (frames/s)</b>	<b>Correct Detections</b>	<b>False Alarms</b>
10	1	2.3
30	1	8.7
60	1	14.7
90	1	20.8
120	1	22

An advantage to the longer temporal profile of the higher sampled sequences is reduction in the target characteristic percent error calculations. Table 9.2 shows the results of the PolyFit algorithm for a 30x30 m<sup>2</sup> pixel frame, with a noise and jitter value of 0.01 and 0.05 respectively. The error was calculated from an average of 10 runs per sample rate and normalized to seconds instead of frames to provide a consistent comparison (Appendix B).

Table 9.2 Sample Rate Effects on Critical Point Given in Seconds of Error

<b>Sample Rate</b>	<b>Enter<sub>1</sub> (s)</b>	<b>Enter<sub>2</sub> (s)</b>	<b>Exit<sub>1</sub> (s)</b>	<b>Exit<sub>2</sub> (s)</b>	<b>Total Error (s)</b>
10	0.316	2.353	3.464	5.141	2.818
30	0.163	0.208	0.258	0.246	0.219
60	0.128	0.206	0.362	0.145	0.210
90	0.109	0.170	0.195	0.111	0.146
120	0.103	0.151	0.165	0.046	0.116

The initial assumption that a target must travel through more than one frame in the sequence limits the sample rates minimum value because the target may not be recorded at all during sensor data gathering. In addition to this consideration, the sample rate is independent of the algorithms ability to detect the target.

The parameters that influence the success of the change detection algorithm are the ones that determine the differences in intensity values between the background and the target. The pixel size, noise and jitter directly affect this difference.

#### 9.1.2. Pixel Size

The pixel size is inversely proportional to the intensity delta. However, smaller pixels provide a shorter target travel time resulting in larger critical point % error as determined with the sample rates. A rectangular shape that minimizes the background with a shorter width and a longer horizontal length provides the best target to pixel ratio and largest intensity variation. Figure 9.1 shows the increase in intensity variation between the background and a target (HEMTT traveling at 23m/s with 0.02 noise and sampled at 120 frames/s) by changing from a  $30 \times 30 \text{ m}^2$  to a  $30 \times 5 \text{ m}^2$  pixel.

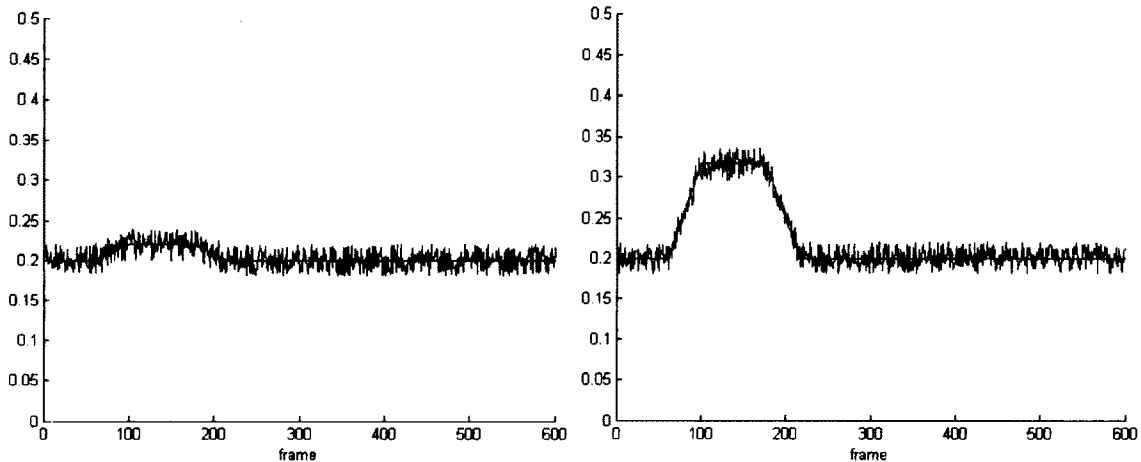


Figure 9.1 (A)  $30 \times 30 \text{ m}^2$  Pixel with HEMTT Target (B)  $30 \times 5 \text{ m}^2$  Pixel with HEMTT Target

Utilizing this concept might not be feasible in the original processing of the sensor data due to a fixed pixel size, but when employing the Super-pixel algorithms, summing or enlarging pixels to a rectangular shape in the motion of target trajectory is beneficial.

The longer target profile has a more accurate target approximation with the PolyFit and FermiFit functions. Table 9.3 shows the results of the PolyFit algorithm for modeled targets, with a noise value of 0.01 and a Sample Rate of 120. The *Pixel X* value was 30 m and the *Pixel Y* varied from 5 to 10 to 30 m. The % error was calculated from an average of 10 runs per sample rate and normalized to seconds instead of frames (Appendix B). As expected, the narrow rectangular pixel with 30x5 m<sup>2</sup> dimensions had better approximations of the critical target point.

Table 9.3 Pixel X Effects on Critical Point Given in Seconds of Error

<b>Pixel Y</b>	<b>Enter<sub>1</sub> (s)</b>	<b>Enter<sub>2</sub> (s)</b>	<b>Exit<sub>1</sub> (s)</b>	<b>Exit<sub>2</sub> (s)</b>	<b>Total Error (s)</b>
5	0.762	0.905	0.701	3.049	1.354
10	0.902	1.027	0.784	3.417	1.532
30	1.217	0.968	0.977	3.319	1.620

### 9.1.3. Noise

As anticipated, the higher the noise, the harder the target is to detect. Table 9.4 shows the change detection performance for different values of noise.

Table 9.4 Percent Detection and False Alarm Frames for Noise Variations

<b>N=2</b>	<b>Threshold</b>		<b>After FAR Filters</b>	
	<b>Noise</b>	<b>Detect</b>	<b>False Alarms</b>	<b>Detect</b>
0	69.48%	0.00%	69.48%	0.00%
0.01	52.11%	0.11%	77.98%	0.48%
0.02	41.17%	2.34%	81.32%	13.13%
0.03	31.58%	4.46%	83.40%	24.96%
0.04	26.96%	2.87%	76.18%	14.85%
0.05	19.30%	3.36%	66.94%	23.45%

The testing scenario used for the table had a threshold  $N$  value of 2.0, jitter equal to zero, a  $30 \times 30 \text{ m}^2$  pixel frame, a 120 frame/s sample rate, and modeled targets that varied in target type and velocity. The noise ranged from 0.0 to 0.5, with 50 runs per noise value (300 total runs) used for the data analysis (Appendix B). The detection percentages, *Detect %*, reflect the number of frames detected that were actual target frames, divided by the total number of target frames, which is given by,

$$\text{Detect \%} = \frac{\text{Detected Target Frames}}{\text{Total Target Frames}}. \quad (9.1)$$

The False-Alarm percentages reflect the number of frames that were improperly categorized as having a target, given by

$$\text{False Alarm \%} = \frac{\text{Detected Non - Target Frames}}{\text{Total Non - Target Frames}}. \quad (9.2)$$

On a positive note, the False-Alarm Rate (FAR) filters do reduce the number of false alarms by connecting the disjointed signals and by filtering out targets that do not meet the minimum temporal frame requirement. The FAR filters are successful at increasing the number of target frames detected, but this is at the expense of extra computation requirements for processing the false alarms. However, the FAR filter variables are tunable and the filter algorithm showed success when ran more than once. The testing used the same values for the FAR variables for all noise situations to provide a robust comparison. In practice, a sensor with a known noise value would have the FAR filters fine tuned for particular situations to reduce the FAR percentages.

Other tunable parameters are the  $N$  values in the detection algorithms, which determine the number of standard deviations it uses as the threshold values or the number of bins to use for the duration method. A low value of  $N$  ensures maximum detection, but this is at the expense of a large amount of false alarms. In many instances, with a low  $N$  value, every frame is a detection, which renders the change detection algorithm useless. In addition, in these cases, the FAR filters offer little value as there is no way to temporally distinguish what is a target and what is not. If the  $N$  value is too high, although there are no false alarms, the target will not be detected at all. Depending on the sensor, an analysis should be done to find the best  $N$  value for target detection.

Table 9.5 shows an example analysis for a noisy sensor with zero jitter, a 120 frame/s Sample Rate, a  $30 \times 30 \text{ m}^2$  pixel size and a variety of targets travelling at different speeds.

Table 9.5 Percent Detection and False Alarm Frames and Missed Detections in Noisy Sensor with N Variations

Noise=0.05		Threshold		After FAR Filters		Missed Detects
N	Detect	False Alarms	Detect	False Alarms		
1.0	46.66%	26.10%	99.98%	91.00%	0/50	
1.5	35.20%	13.89%	96.97%	67.10%	0/50	
2.0	19.30%	3.36%	69.36%	23.45%	2/50	
2.5	14.78%	0.02%	46.00%	0.24%	12/50	
3.0	7.58%	0.00%	27.64%	0.00%	24/50	
3.5	2.28%	0.00%	7.58%	0.00%	38/50	
4.0	1.39%	0.00%	5.84%	0.00%	41/50	

For each value varying from 1.0 to 4.0, the threshold detection algorithm tested 50 modeled targets. The number of frames detected and the number of false alarm frames were calculated using Eqns. (9.1) and (9.2). The detection algorithm kept track of the number of missed detections for additional comparison. For this example, the best  $N$  value is 2.0, which detected 96% of the targets.

#### 9.1.4. Jitter

Jitter affects the capabilities of the detection algorithms much like the noise parameter. Table 9.6 shows the analysis of varying the jitter values of a pixel from 0 to 0.5.

Table 9.6 Percent Detection and False Alarm Frames for Different Jitter Variations

N=2.5		Threshold		After FAR Filters	
Jitter	Detect	False Alarms	Detect	False Alarms	
0	28.32%	0.00%	28.32%	0.00%	
0.1	20.39%	0.00%	21.71%	0.00%	
0.2	19.03%	0.00%	24.94%	0.00%	
0.3	14.50%	0.12%	25.77%	1.13%	
0.4	18.86%	0.93%	35.82%	5.31%	
0.5	12.89%	1.34%	38.24%	7.39%	

Fifty modeled targets varying in type and velocity traveled through an area imaged by a sensor that had zero noise, a 120 frame/s sample rate and recorded a 4x4 image array with varying background and 30x30 m<sup>2</sup> pixel sizes. The table values are calculated using Eqs. (9.1) and (9.2). A threshold detection  $N$  value of 2.5 showed a decreased performance over the noise table, but the trend was still the same.

The same scenario was used to analyze the threshold  $N$  parameter in jitter situations, with the exception that jitter was held constant and the  $N$  value varied from 1.0 to 4.0 (Table 9.7).

**Table 9.7 Percent Detection and False Alarm Frames and Missed Detections for Jittered Pixels with Different N Variations**

<b>Jitter=0.25</b>		<b>Threshold</b>		<b>After FAR Filters</b>		<b>Missed Detects</b>
<b>N</b>	<b>Detect</b>	<b>False Alarms</b>	<b>Detect</b>	<b>False Alarms</b>		
1.0	78.61%	19.58%	99.54%	85.68%	0/50	
1.5	54.00%	5.12%	90.09%	31.09%	0/50	
2.0	40.65%	0.35%	65.23%	1.51%	2/50	
2.5	18.80%	0.05%	28.90%	0.25%	28/50	
3.0	17.20%	0.01%	23.45%	0.00%	33/50	
3.5	10.55%	0.00%	12.75%	0.00%	36/50	
4.0	8.91%	0.00%	11.77%	0.00%	39/50	

The results mirror those from the noise analysis, with an  $N$  value of 2.0 providing the best overall value for the change detection algorithm. This value remains tunable, but as a consequence of these tests, the detection algorithms were set to a default value of 2.0 in the MATLAB coding.

As shown previously, changes in sensor characteristics produce significant differences in the performance of sub-pixel detection and analysis. For this reason, the tunable variables in the threshold, duration, FAPI, and FAR filters are imperative to the algorithms success for a variety of sensors and target situations.

## 9.2. Method Analysis and Performance

### 9.2.1. Change Detection

The best measures of the change detection algorithms for the sub-pixel algorithm are the ability to detect the target and the accuracy of the critical  $Enter_1$  and  $Exit_2$  points. These measures are vital as detection is necessary to proceed to the target analysis algorithm and the accuracy of the critical points determines the effectiveness of the PolyFit and FermiFit methods. Table 9.8 compares the different change detection algorithms. The testing scenario ran 250 tests varying target vehicle and target speed. The Sample Rates ranged from 30 to 120 frames per second, the noise values were between 0 and 0.05, and the pixel size ranged from a  $30 \times 30 \text{ m}^2$  to a  $60 \times 60 \text{ m}^2$  pixel, with rectangular pixels included.

Table 9.8 Change Detection Error of Critical Points  $Enter_1$  and  $Exit_2$

	<b>Error in Seconds</b>	
	<b>Enter<sub>1</sub></b>	<b>Exit<sub>2</sub></b>
<b>Threshold</b>	0.821	1.087
<b>Duration</b>	0.870	1.142
<b>FAPI</b>	0.513	2.560

The Table 9.8 only includes runs where the FAPI algorithm received no run time errors. For the majority of the runs, the FAPI algorithm did not work, leaving the Threshold and Duration algorithms as the most effective. The FAPI had convergence

issues due to the weighting matrix initialization and is not very reliable. Only the tests that worked for FAPI are included in the previous table. Further work will include an investigation on how to mitigate the convergence problems.

The modular process provides an additional positive outcome. Since the already existing change detection algorithms were slightly modified using the Binary Matrix technique, newer or improved change detection algorithms can be similarly modified and used within this process.

#### 9.2.2. Target Analysis

Both the PolyFit and the FermiFit methods served well in obtaining the target's critical points  $\text{Enter}_2$  and  $\text{Exit}_1$ . Table 9.9 shows the error, in seconds, for the critical point calculation via the PolyFit and FermiFit methods (Table B.11).

Table 9.9 Target Analysis Second Error of Critical Points  $\text{Enter}_1$  and  $\text{Exit}_2$

	<b>Error in Seconds</b>			
	<b>Enter<sub>1</sub></b>	<b>Enter<sub>2</sub></b>	<b>Exit<sub>1</sub></b>	<b>Exit<sub>2</sub></b>
<b>PolyFit</b>	0.163	0.617	0.879	1.135
<b>FermiFit</b>	0.046	0.502	0.838	1.015

The FermiFit  $\text{Enter}_1$  and  $\text{Exit}_2$  points are independent of the FermiFit analysis and are dependent completely on the change detection method chosen in the sub-pixel process.

The challenge encountered with the PolyFit function was how to handle circumstances with less than six intersection points. If the PolyFit analysis does not find six intersection points between  $\text{Poly}_6$  and  $\text{Poly}_4$ , the algorithm stops working. The source of this problem traces back to the  $\text{Enter}_1$  and  $\text{Exit}_2$  critical points retrieved from the Target Binary Matrix. When target frames are lost during the detection algorithm,

there are not enough data points to accurately recapture the trapezoid shape. The successful solution to this issue was to create a patch program that performs a quick error check during the intersect point calculation. If there are less than six intersection points found, frames are added to the target sequence until the requirement is met. If all sequence frames are accounted for, then the target does not exist and the analyzed sequence categorizes as a false alarm.

The FermiFit analysis is very sensitive to the critical points  $Enter_1$  and  $Exit_2$  and is highly dependent on the detection algorithm for these values. While PolyFit can adjust for a truncated Target Binary Matrix by adding frames until it meets the six intersection point criteria, FermiFit does not have this error check. As a result, critical points  $Enter_1$  and  $Exit_2$  do not undergo any refinement in this process and is therefore less adaptable.

Overall, the best choice for analyzing the target is the PolyFit method due to the ability of the algorithm to refine the critical  $Enter_1$  and  $Exit_2$  data points. For this method, the main requirement is to detect the target and to get a general estimation of the target length.

#### 9.2.3. Velocity and Length Calculations

A graphical user interface (GUI) ran a series of post processing tests, which allowed the user to tune the  $N$  and  $FAR$  values for each scenario (Figure 9.2). The actual target velocity and lengths were entered into the upper left hand corner of the GUI and the resulting calculations were displayed adjacently for comparison purposes.

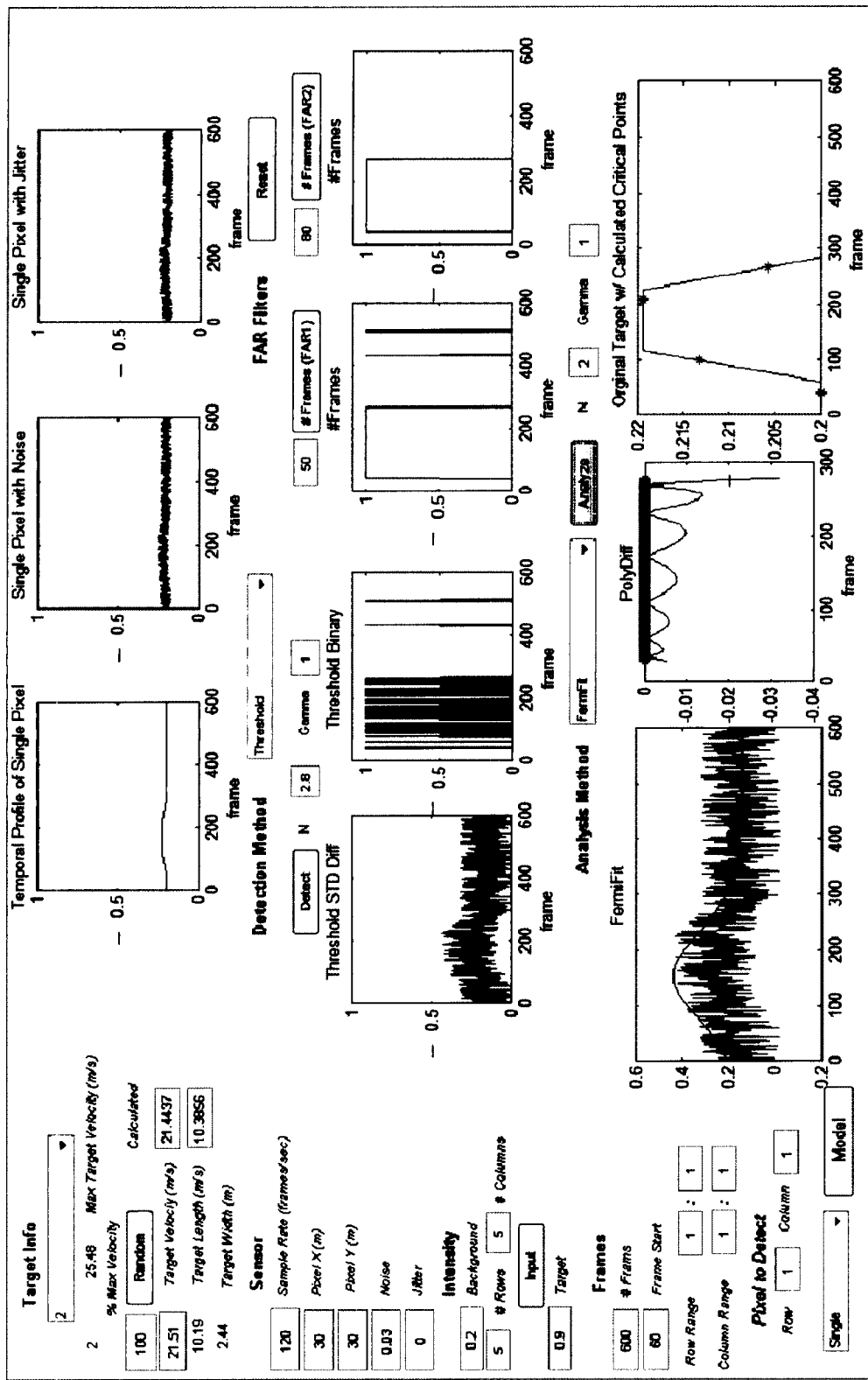


Figure 9.2 GUI for Sub-pixel Detection and Analysis

The scenarios evaluated three types of vehicles, the HUMMWV (4.57 m length), the HEMTT (10.19 m length), and the M1070 (24.89 m length). The noise values varied from 0.01 to 0.03 with 30 tests run on each scenario. The velocity values were randomly selected from 50% to maximum velocity. The detection and analysis methods varied for each run to show the modularity of the process. With tuning, the sub-pixel process detected the target, found the critical target points, and calculated the length and velocity. Table 9.10 shows the averaging of the length and the percent errors for each target and noise value; the actual test runs are located in Table B.17.

Table 9.10 Velocity and Length Test Results

		<b>Actual</b>	<b>Calculated</b>		
<b>Target</b>	<b>Noise</b>	<b>Length</b>	<b>Length</b>	<b>Length % Error</b>	<b>Velocity % Error</b>
<b>HUMMWV</b>	0.01	4.57m	4.69 m	2.54	7.99
	0.02		4.40 m	3.69	7.61
	0.03		4.95 m	8.22	14.38
<b>HEMTT</b>	0.01	10.19 m	10.02 m	1.69	5.27
	0.02		10.45 m	1.40	6.22
	0.03		10.62 m	4.31	3.52
<b>M1070</b>	0.01	24.89 m	23.10 m	7.18	6.51
	0.02		23.46 m	5.73	11.33
	0.03		21.24 m	14.64	3.21

The velocity and length calculations are very sensitive to the tunable parameters. The accuracy of the algorithm decreases when the noise increases in value, as expected. Table 9.11 put the results into perspective.

Table 9.11 Delta Length and Delta Velocity Calculations

	<b>Pixel X</b>	<b>Δ Length</b>	<b>Delta Velocity</b>	
<b>HUMMWV</b>	30 m	0.12 m	1.22 m/s	2.73 miles/hr
<b>HEMTT</b>	30 m	0.10 m	0.19 m/s	0.42 miles/hr
<b>M1070</b>	45 m	1.98m	1.02 m/s	2.28 miles/hr

As a post processing tool, the sub-pixel algorithm increases the user's knowledge of sub-pixel moving targets. Figure 9.3 shows the bar chart of the calculated lengths. The targets naturally fall into three categories, which correspond to the specific vehicle lengths in the test.

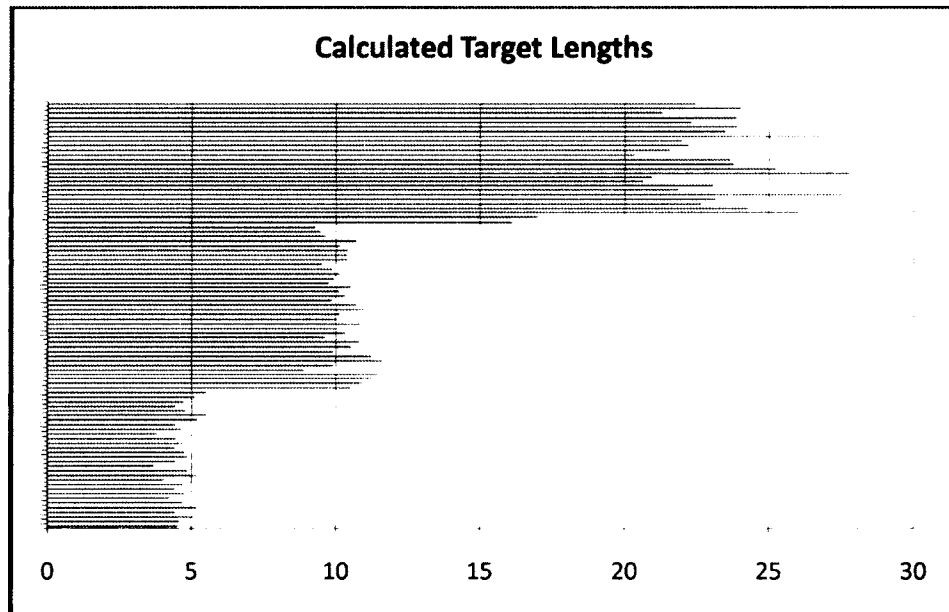


Figure 9.3 Bar Chart Showing the Calculated Target Lengths

However, the sub-pixel process is not accurate enough to distinguish between similar sized vehicles, such as the HEMTT, the M1070 tractor and the PLS truck, which range from 9.09 to 10.95 m in length. Further work in this area would focus on real-time processing techniques to automate the *N* and *FAR* parameter tuning.

### 9.3. Sensor Data Results

The scenarios chosen from the sensor datasets to analyze emulate different sensor and environmental effects to challenge the robustness of the sub-pixel algorithm. In the majority of the data sequences, the sensor image was shaky with unregistered frames, and the terrain was grassy and bumpy. Some scenes were shot with higher wind, causing the grass to sway, which added clutter noise to the pixel intensity. One data scene had a relatively stable sequence with minimal jitter. This scene provided the control dataset.

Using all of the sensor data scenarios, the algorithms were still able to detect and analyze the target. The results show the detection and the target analysis for selected scenarios with a brief description of the test case. Appendix B contains additional testing results.

The first set of scenarios evaluated the ability of the sub-pixel algorithm to detect a target within a variety of rectangular and square pixel shapes. The pixel shapes directly affect the target time in the frame. For horizontal travel, the size of the pixel in the y-direction was not as important factor as the size in the x-direction. A longer Pixel Y did reduce the overall delta intensity, but the detection and analysis methods continued to perform satisfactorily. Figure 9.4 and Figure 9.5 show the test results of changing the pixel size.

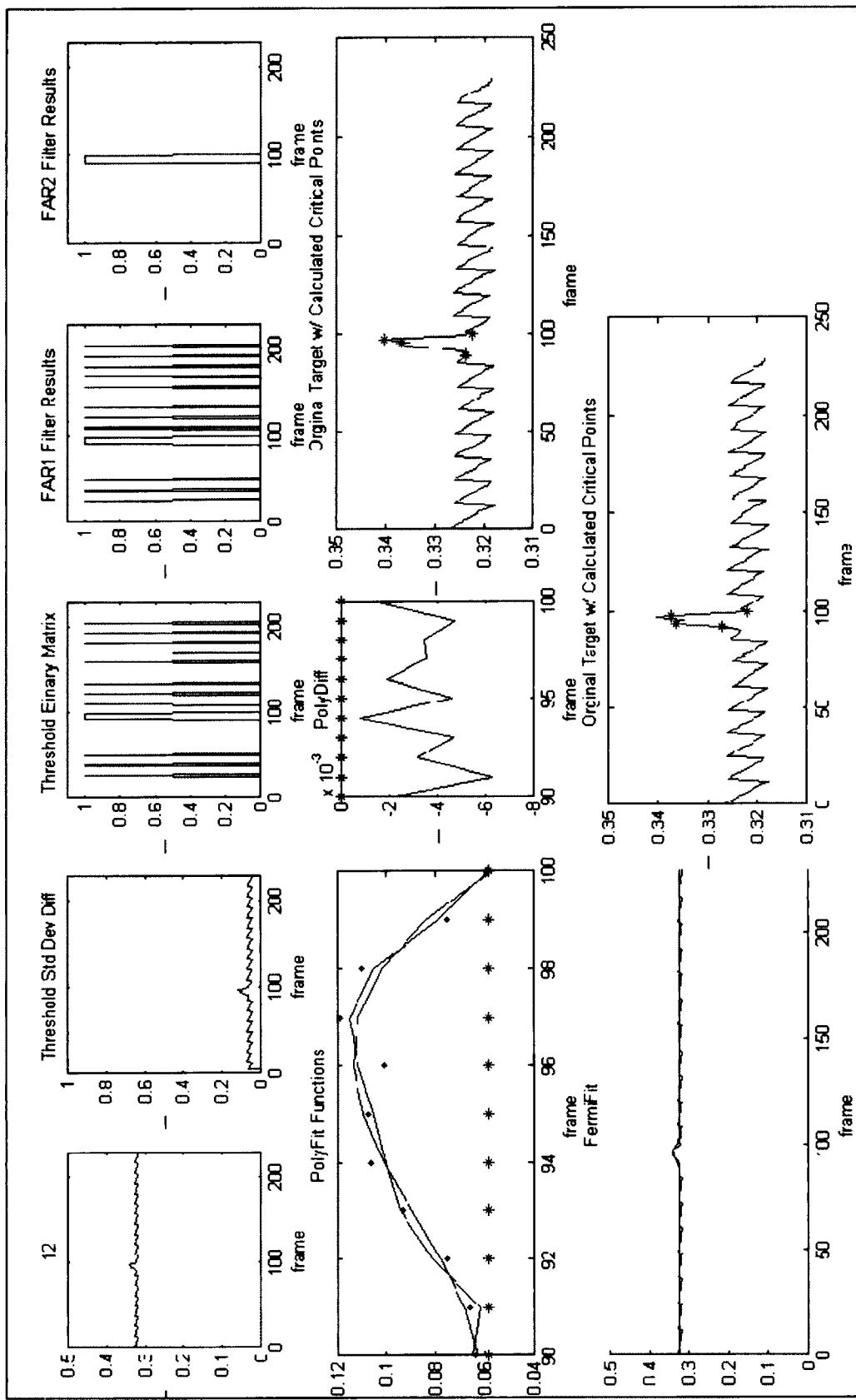


Figure 9.4 Analysis Results of Enlarging a Pixel by 0.5 in X and Y Directions

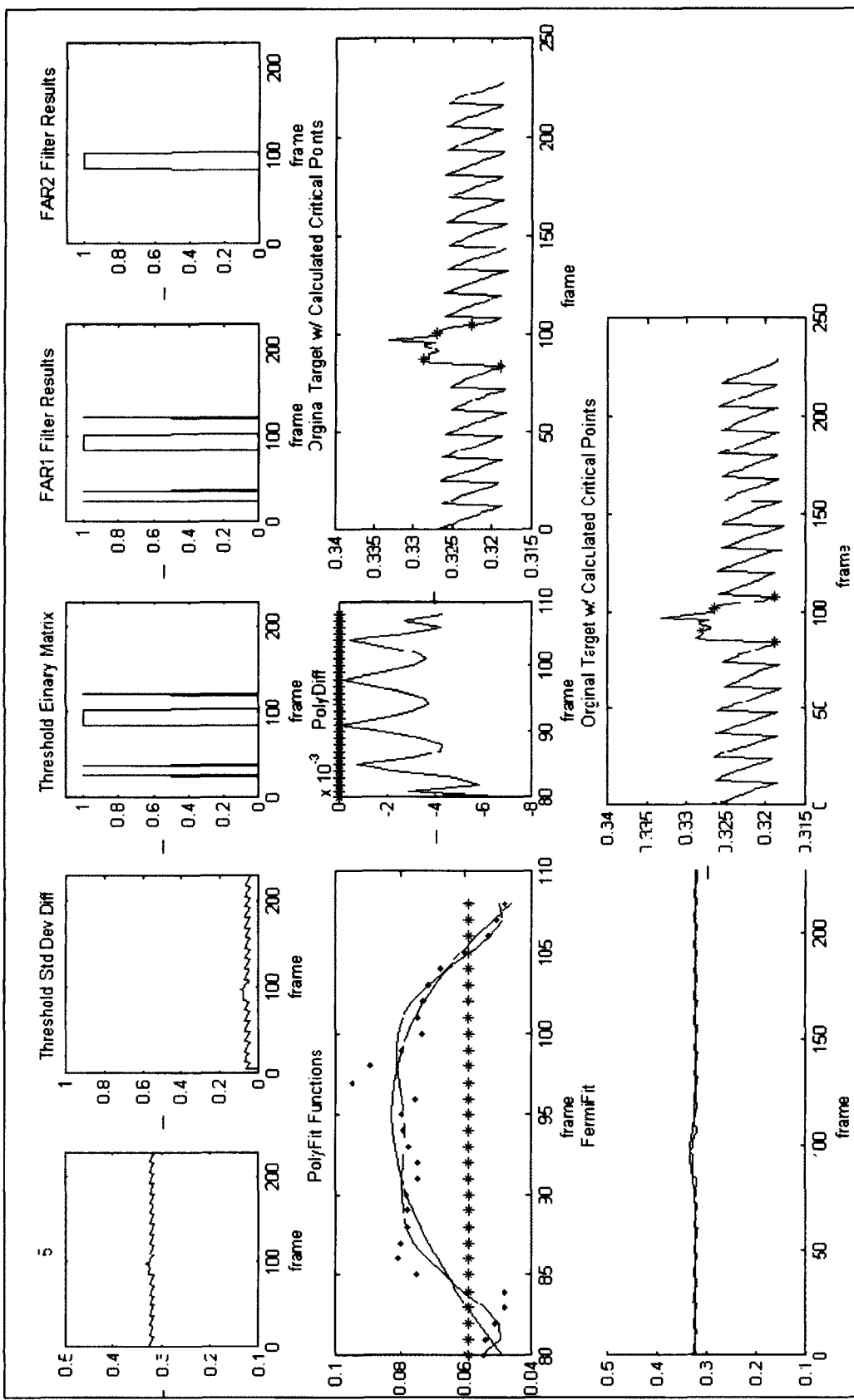


Figure 9.5 Analysis Results of Enlarging a Pixel by 1.0 in X and 0.5 in Y

The testing scenario enlarged the pixels in both the x- and y-direction as the original signal did not obtain valid results (Appendix B). Figure 9.4 enlarged the pixel by a half of a pixel in both directions, while Figure 9.5 enlarged the pixel only half a pixel in the y-direction and by a full pixel in the x-direction, providing a longer target profile. Consequently, the results in Figure 9.5 only detected 3 false alarms while the results in Figure 9.4, detected 11 false alarms. Figure 9.5 showed an improvement in the critical point calculation.

The algorithms were originally designed for darker background and lighter targets, i.e. infrared imagery. However, with visible images, this was not always the case. The pixels with a darker background, which were chosen in the tower's shadow, easily detected the lighter target (Figure 9.6). When testing a brightly lit background, detection was still possible by using the inverse binary matrix of the duration filter (Figure 9.7).

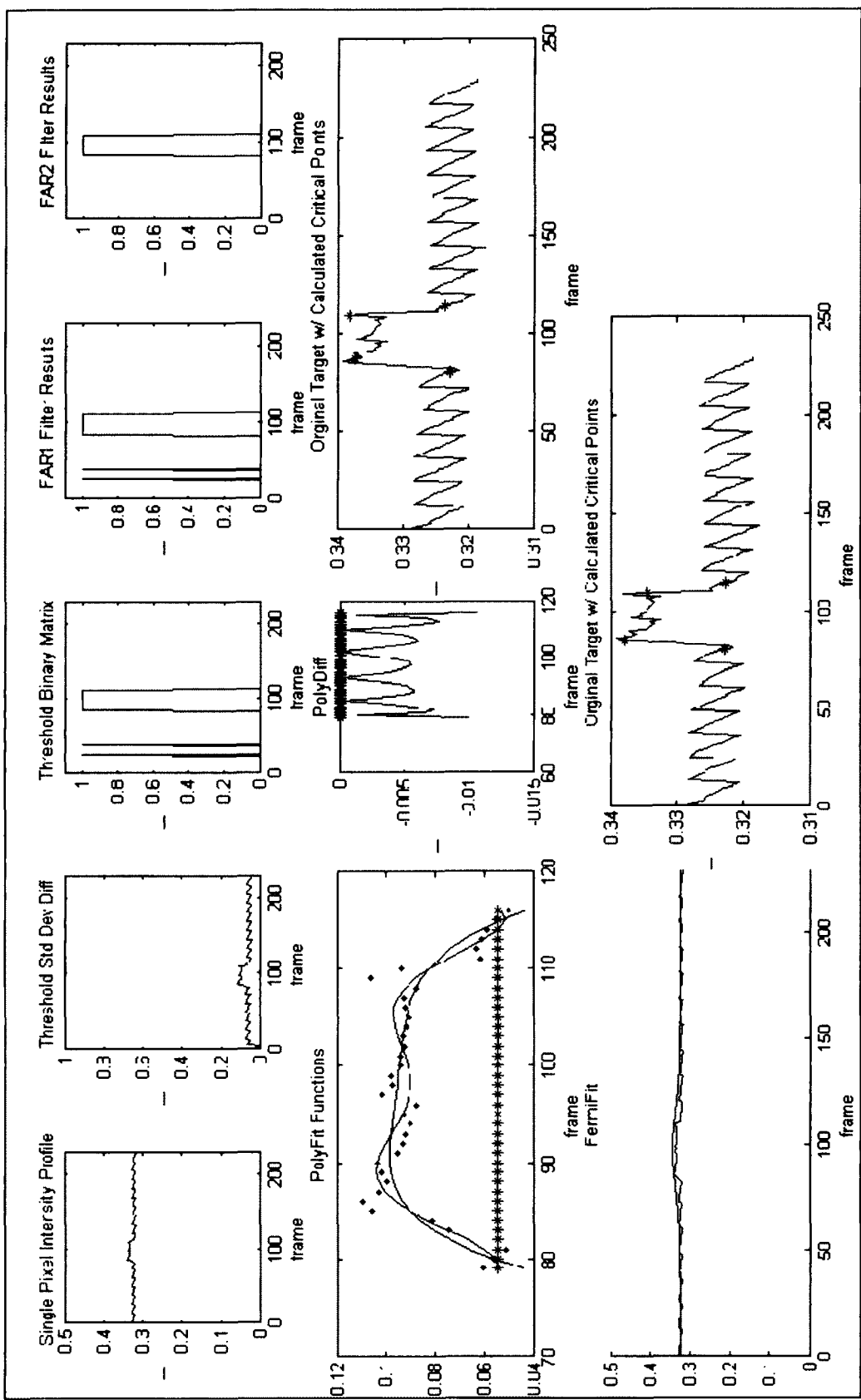


Figure 9.6 Analysis Results of Mobile Target with Shadowed Background

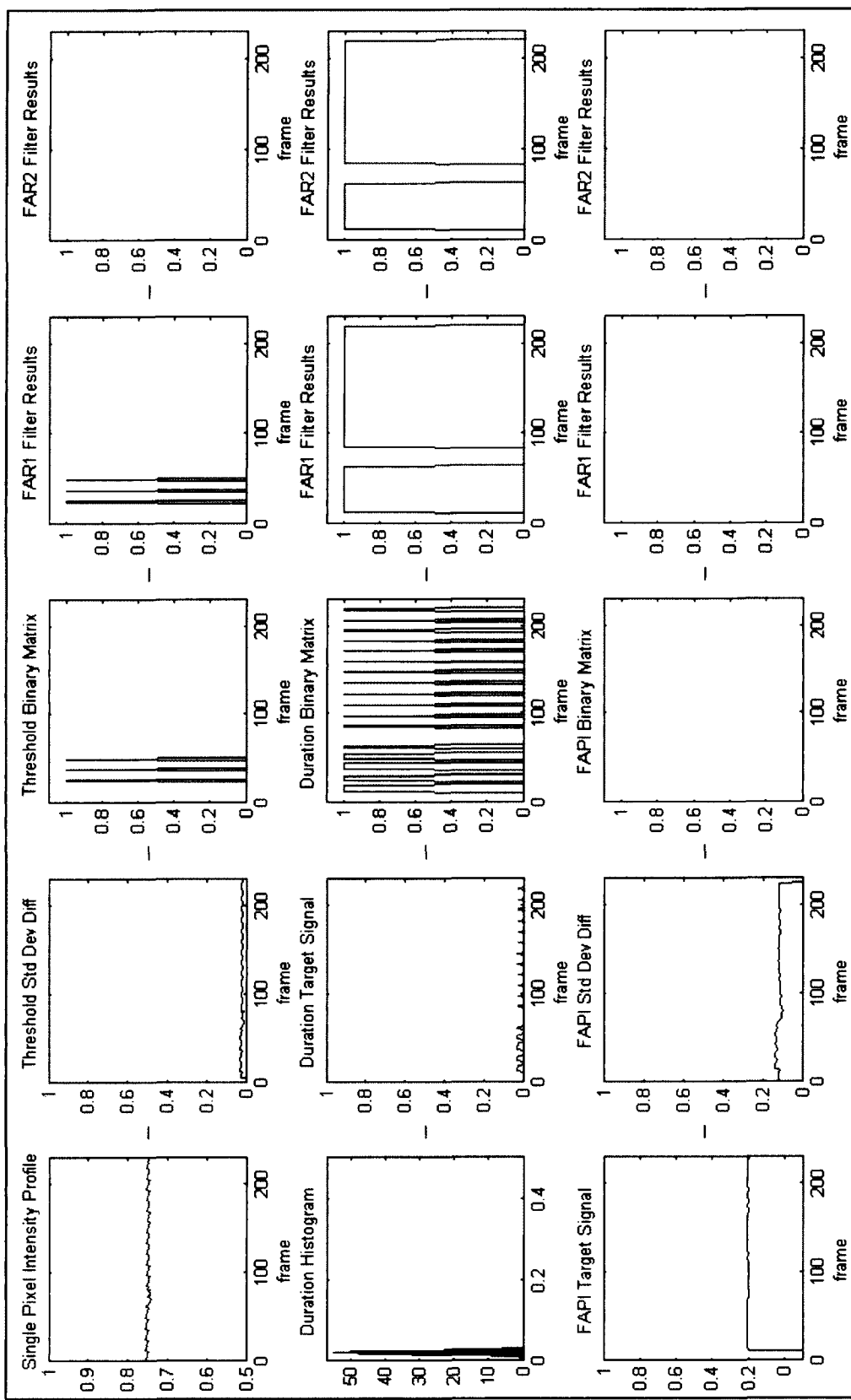


Figure 9.7 Analysis Results of Mobile Target in Bright Background

These results prompted a coding patch to incorporate the negative threshold and duration values. The desired results show effective detection in the threshold and duration algorithms in Figure 9.8.

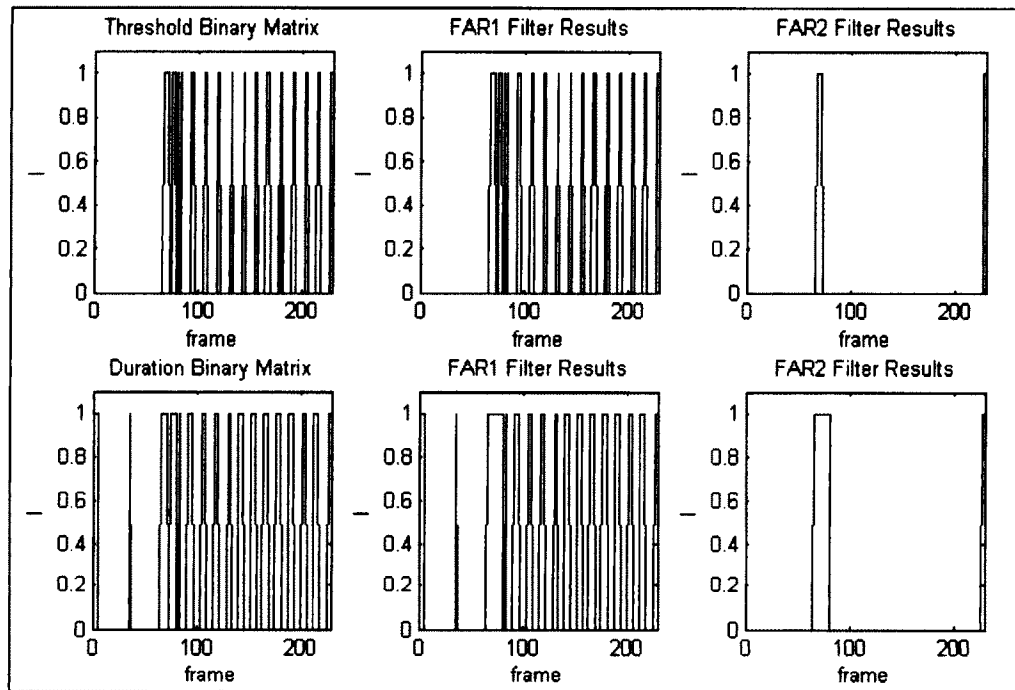


Figure 9.8 Detection in Bright Background Scenarios

The target analysis results for the bright background scenario are shown in Figure 9.9. Even though the FermiFit plot is the inverse of the actual signal, the critical points are still captured.

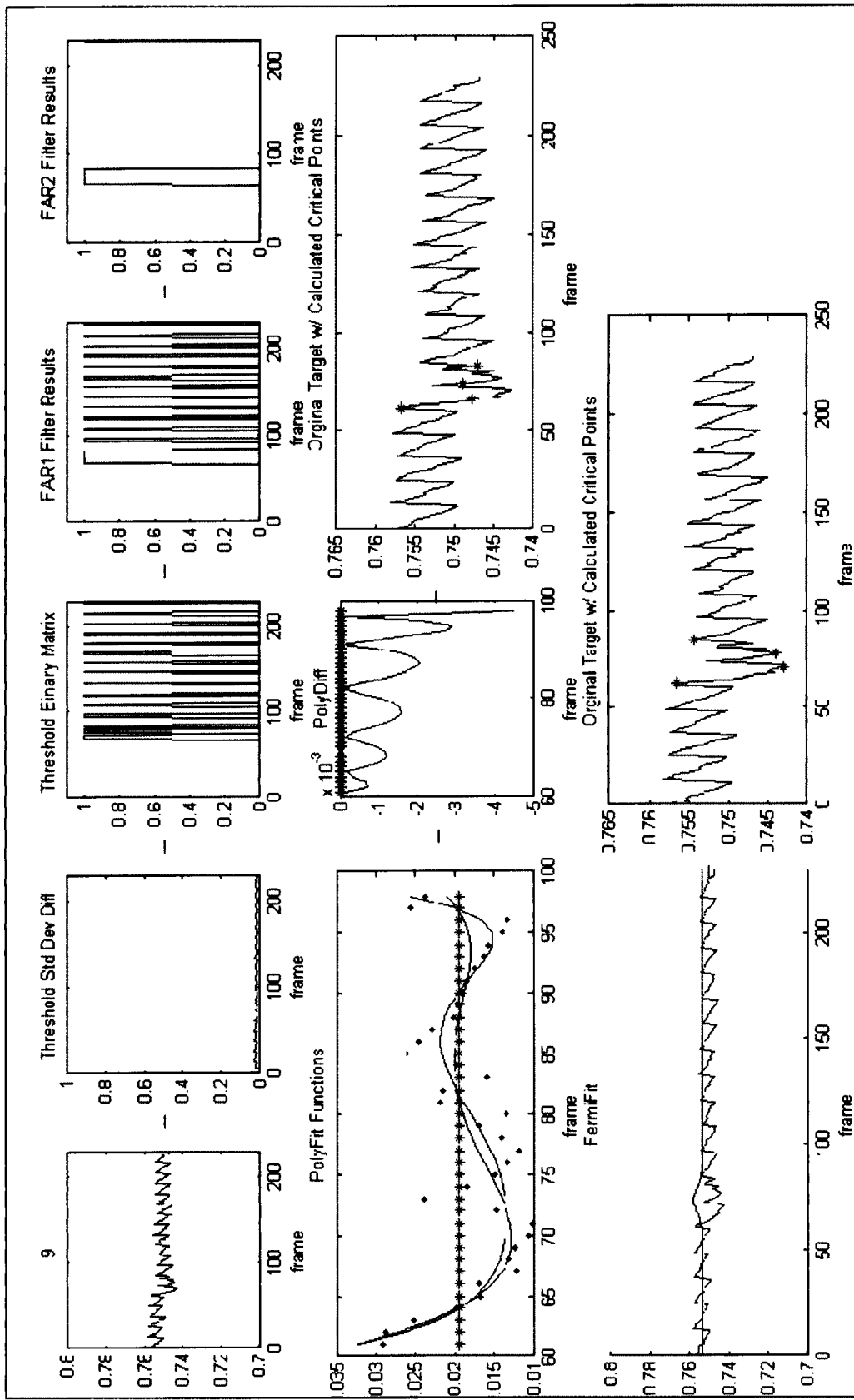


Figure 9.9 Analysis of Bright Background Scenarios

In the case of a pixel with both a light and dark background, the detection algorithm only detects a lighter target. However, the PolyFit algorithm was able to recover the whole target. It did require parameter modification to allow for a wider input range than the detected enter and exit points. In this case, the PolyFit analysis created an inversion instead of a trapezoid model, which is expected if it crosses a background intensity variation within a frame (Figure 9.10).

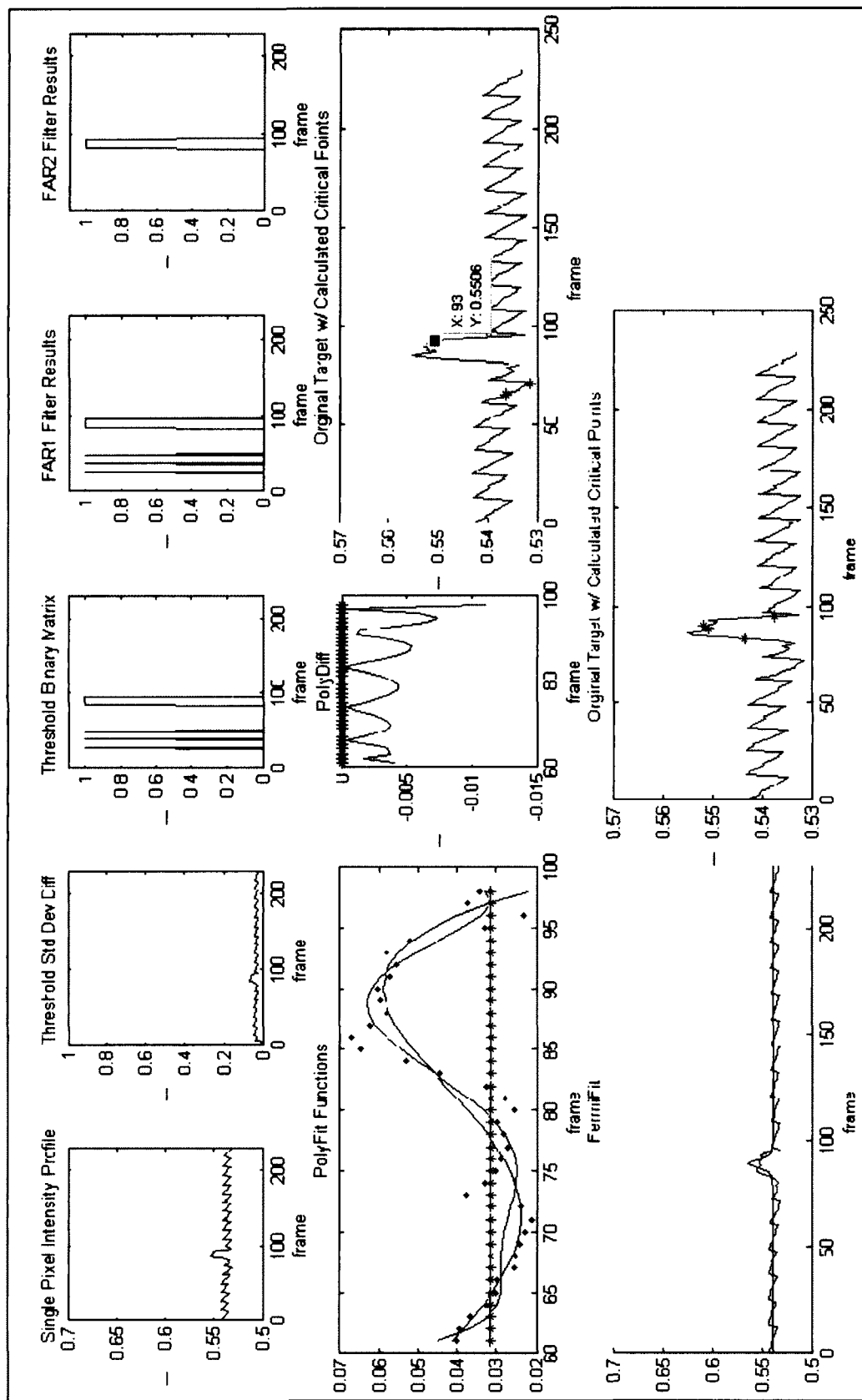


Figure 9.10 Analysis of Bright and Shadowed Background with Mobile Target

Initially a jittery or changing background during the frame sequence was not expected to produce results. However, the threshold and the duration methods did detect a target. The FAPI method had trouble detecting the target in these conditions. Conversely, the PolyFit and FermiFit were able to approximate the critical points fairly well. This situation is encountered in the next scenario that has a background intensity that significantly changes during the frame sequence. Figure 9.11 shows the Threshold Change Detection, the PolyFit analysis and the FermiFit analysis of this scenario.

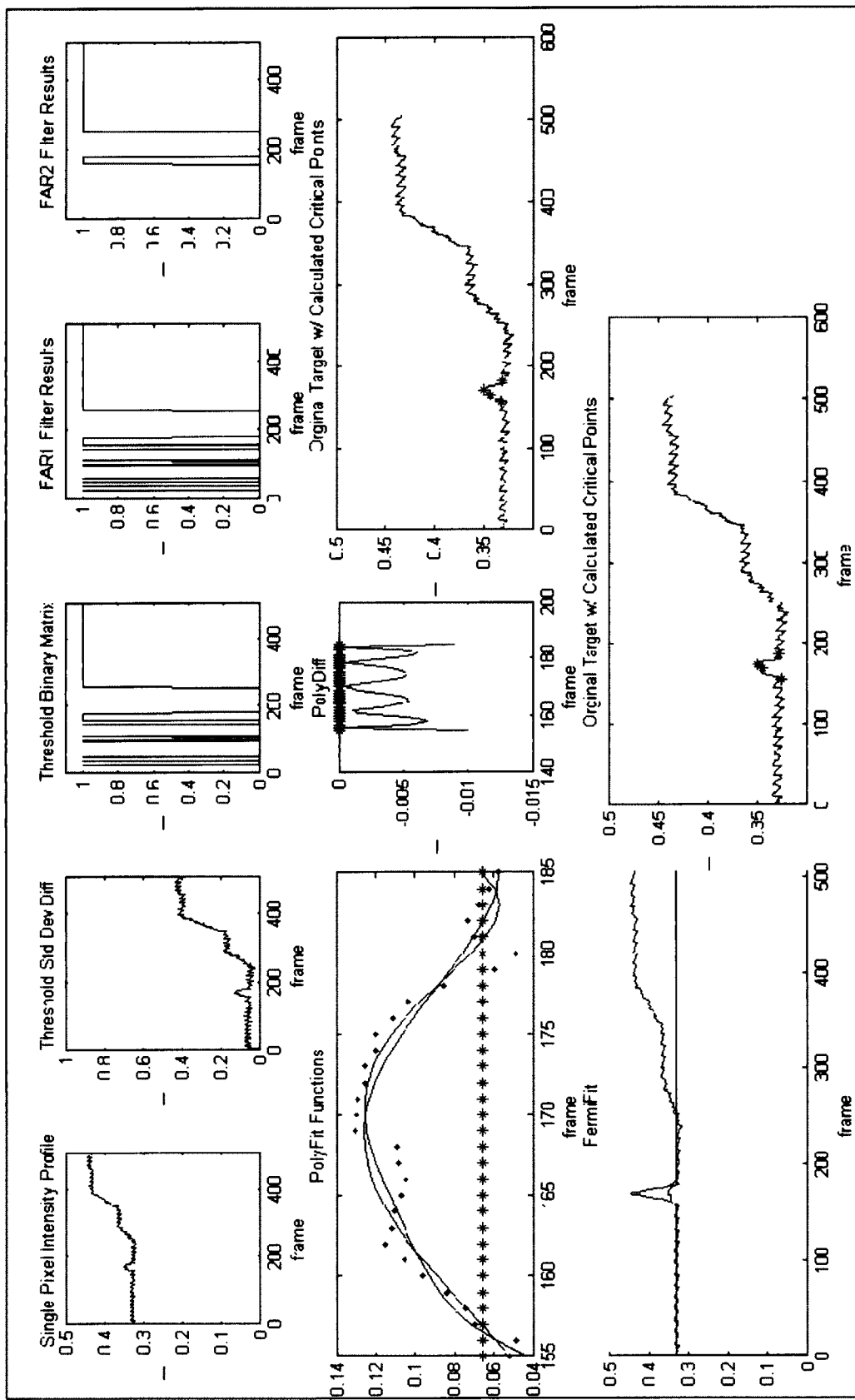


Figure 9.11 Analysis of Mobile Target in Changing Background Environment

Both the PolyFit and FermiFit algorithms performed very well in this challenging environment. Because there were enough initial background frames to establish the background model in the Threshold Change Detection, it was able to gather the target information, with only one false alarm due to the abrupt shift in the background intensity. There were enough low level background frames for the duration algorithm to work. The FAPI did not detect this target due to a convergence error (Figure 9.12).

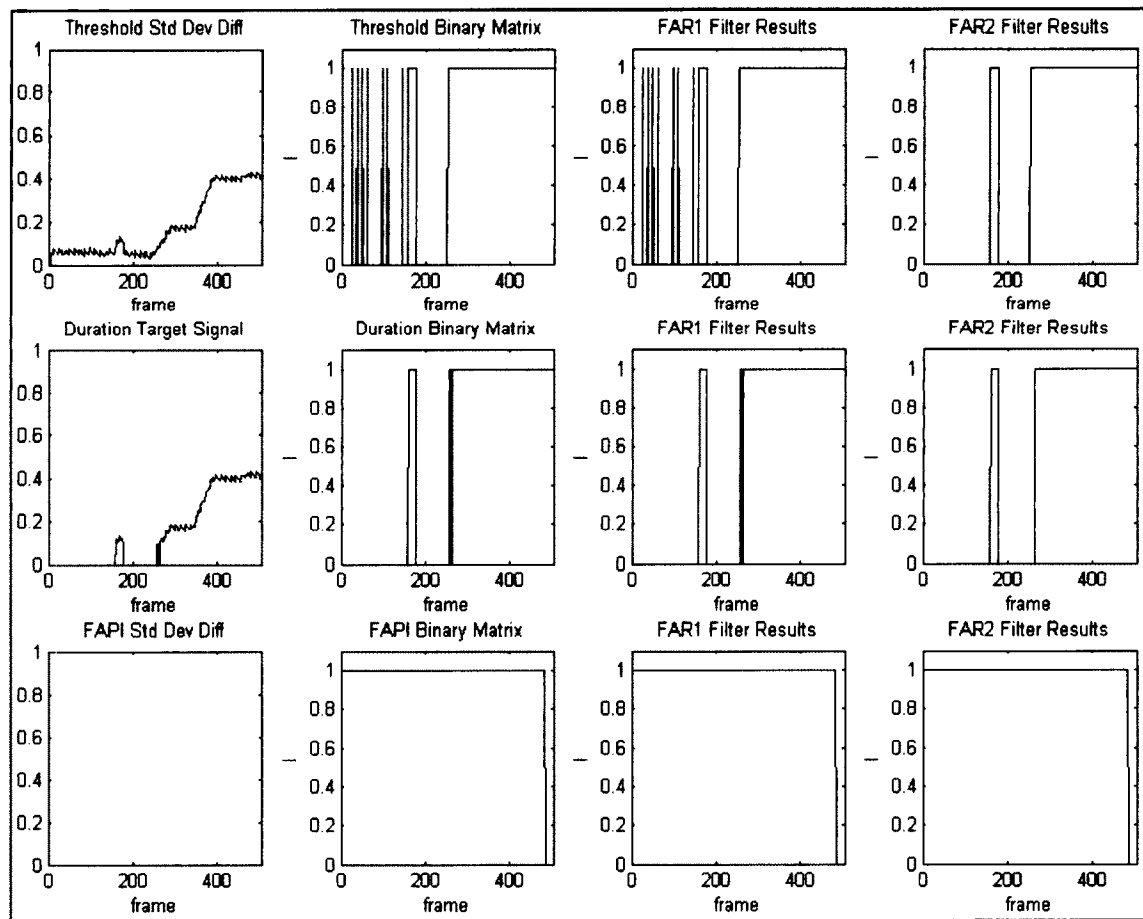


Figure 9.12 Detection of Mobile Target in Changing Background Environment

## **CHAPTER TEN**

### **FURTHER WORK**

Method analysis and testing results showed the feasibility of the sub-pixel algorithm for modeled and experimental situations. As with any research project, endless areas of exploration exist and all of them cannot be confined to a single dissertation.

The Refinement Through Tracking (RTT) methodology contained in this dissertation was theoretical in nature, but it is an imperative process needed to encompass the variety of target trajectories. Automating the target tracking, implementing the RTT algorithm into the sub-pixel algorithm, and testing the product is a project currently on the books.

Another area of research is to make the change detection algorithm more robust by investigating different initialization weighting matrices for the FAPI algorithm that provide more convergence reliability and to perform more comparisons of other change detection methods.

As the PolyFit and FermiFit analysis methods provide an estimation of target velocity, a refinement algorithm incorporating a Velocity Matched Filter technique might prove a feasible way to significantly improve target signal intensities [54]. Also, this analysis used a rectangular pixel as a basis for the calculations. Further work will investigate other pixel geometries, multiple targets and the algorithm adaptation.

A major objective of research is to end up with a marketable product. Two Graphical User Interfaces (GUIs) incorporating the sub-pixel algorithms were designed as basic prototypes for end user application testing. The next step involves field testing these designs with a variety of classified datasets containing known targets and parameters. Future works in application implementation are exploring parallel processing capabilities and near-real-time execution.

## **CHAPTER ELEVEN**

### **CONCLUSION**

Overall, the process, techniques, and methods presented in this dissertation are viable. Independent algorithm verification tested the quality and repeatability of the coding design.

The model data proved the concept works, through the various series of tests. The tests also indicated how flexible the process is. With slight adjustments, the parameters of the environment can be adjusted to fine tune the detection algorithms, thus lowering the false alarm rate. These adjustments can be done real-time, as needed.

The experimental tests validated the process. Because of the limited data availability, the datasets were taken in a controlled setting from a sensor positioned 18 meters in altitude. The sensor took videos of a single target, which was a remotely controlled car. However, since the process has proven to be so adaptable, the parameters can be adjustable and a user with knowledge of their sensor can apply this process and techniques to yield spectacular results. Due to the modularity of the sub-pixel detection and characterization process, as sensors change and detection algorithms evolve, the parameters and new algorithms can be incorporated easily. In essence, this methodology is an open and adaptable system.

Applying this technique correctly, should allow the intelligence community to process copious amounts of data more efficiently and leverage more capability from existing legacy systems with lower resolution. As an out-of-the-box solution, agencies can take existing higher resolution systems and elevate them, thus expanding the imagery capture area and lowering their resolution intentionally to detect moving targets that otherwise would be outside of their narrower field of view.

**APPENDIX A**

**ALGORITHM VERIFICATION RESULTS**

Table A.1 Algorithm Verification Results

<b>Algorithm File</b>	<b>Tests</b>	<b>Results</b>	<b>Method</b>
<b>Target Modeling</b>			
InfoSensor	- Get sensor information	Verified	Test code
InfoTarget	- Get target information	Verified	Test code
DBTargetTrapP	<ul style="list-style-type: none"> <li>- Plot trapezoid</li> <li>- Incorporate background</li> <li>- Different noise values</li> <li>- Different jitter values</li> <li>- Different target intensities</li> <li>- Different background intensities</li> <li>- Different frame total values</li> <li>- Different frame start times</li> </ul>	Verified	Test code, plots, hand calcs
DBTargetTrapMultiP	<ul style="list-style-type: none"> <li>- Plot trapezoid</li> <li>- Incorporate background</li> <li>- Insert signal in multiple-pixels</li> <li>- Plot multiple-pixels</li> <li>- Different background intensities</li> <li>- Different frame total values</li> <li>- Different frame start times</li> <li>- Check target travel in pixels</li> </ul>	Verified	Test code, plots
ExtractNoNoise	<ul style="list-style-type: none"> <li>- Check Enter<sub>1</sub> calculation</li> <li>- Check Exit<sub>2</sub> calculation</li> <li>- Plot results</li> </ul>	Verified	Test code, plots, hand calcs
AddNoise	<ul style="list-style-type: none"> <li>- Add noise to single-pixel</li> <li>- Add noise to multiple-pixel</li> <li>- Add noise to target signal</li> <li>- Test Gaussian profile</li> <li>- Test random functions</li> <li>- Plot results</li> </ul>	Verified	Test code, plots, hand calcs
AddJitter	<ul style="list-style-type: none"> <li>- Jitter complex background</li> <li>- Test with inserted signal</li> <li>- Jitter less than 1 pixel</li> <li>- Jitter more than 1 pixel</li> <li>- Plot results</li> </ul>	Verified	Test code, plots, hand calcs
<b>Target Detection</b>			
DetectDuration	<ul style="list-style-type: none"> <li>- Vary N values</li> <li>- Test histogram function</li> <li>- Test filter calculation</li> <li>- Test IDuration</li> <li>- Test TargetBinary</li> <li>- Test repeatability</li> <li>- Plot results</li> </ul>	Verified	Test code, plots

DetectThreshold	<ul style="list-style-type: none"> <li>- Vary N values</li> <li>- Vary gamma values</li> <li>- Test threshold calculation</li> <li>- Test ZetaPixel calculation</li> <li>- Test PixelDelta</li> <li>- Test TargetBinary</li> <li>- Plot Results</li> </ul>	Verified	Test code, plots
DetectFAPI	<ul style="list-style-type: none"> <li>- Test Vectorization</li> <li>- Test Badeau's initialization matrix</li> <li>- Test Simonson's initialization matrix</li> <li>- Test with complex background</li> <li>- Test FAPIPixel</li> <li>- Test XBack</li> <li>- Plot Results</li> </ul>	Verified	Test code, plots
DetectFAR1	<ul style="list-style-type: none"> <li>- Test different F1 values</li> <li>- Plot BinaryMatrixNew</li> </ul>	Verified	Test code, plots
DetectFAR2	<ul style="list-style-type: none"> <li>- Test different F2 values</li> <li>- Plot BinaryMatrixNew</li> </ul>	Verified	Test code, plots
NumberTargets	<ul style="list-style-type: none"> <li>- Test Enter<sub>1</sub> calculation</li> <li>- Test Exit<sub>2</sub> calculation</li> <li>- Test # targets calculated</li> <li>- Print results</li> </ul>	Verified	Test code
<b>Target Analysis</b>			
AnalyzeFermiFit	<ul style="list-style-type: none"> <li>- Test parameter calculations</li> <li>- Test method to choose c</li> <li>- Test Enter<sub>1</sub> calculation</li> <li>- Test Enter<sub>2</sub> calculation</li> <li>- Test Exit<sub>1</sub> calculation</li> <li>- Test Exit<sub>2</sub> calculation</li> <li>- Test repeatability</li> <li>- Plot results</li> </ul>	Verified	Test code, plots
AnalyzePolyFit	<ul style="list-style-type: none"> <li>- Test PolyFit functions</li> <li>- Test findpeaks functions</li> <li>- Test intersection calculations</li> <li>- Test Enter<sub>1</sub> calculation</li> <li>- Test Enter<sub>2</sub> calculation</li> <li>- Test Exit<sub>1</sub> calculation</li> <li>- Test Exit<sub>2</sub> calculation</li> <li>- Plot results</li> </ul>	Verified	Test code, plots

**APPENDIX B**

**TESTING TABLES**

Table B.1 Detection Comparison: Sensor and Target Information

S Info	S Rate	Pixel X	Pixel Y	Noise	Jitter	T Info #	Length	Width	Speed	Ibk	ITgt	No Noise	En1	En2	Ex1	Ex2
30	30	30	0	0	0	2	10.19	2.44	21.936	0.2	0.9	60	74	101	115	
30	30	30	0	0	0	4	9.08	2.59	12.655	0.2	0.9	60	82	131	153	
30	30	30	0	0	0	5	19.27	2.44	18.929	0.2	0.9	60	91	108	139	
30	30	30	0	0	0	1	4.57	2.16	22.001	0.2	0.9	60	66	101	107	
30	30	30	0	0	0	6	8.32	2.43	13.812	0.2	0.9	60	78	125	143	
30	30	30	0	0	0	4	9.08	2.59	12.626	0.2	0.9	60	82	131	153	
30	30	30	0	0	0	4	9.08	2.59	14.665	0.2	0.9	60	79	121	140	
30	30	30	0	0	0	4	9.08	2.59	17.616	0.2	0.9	60	75	111	126	
30	30	30	0	0	0	2	10.19	2.44	22.541	0.2	0.9	60	74	100	114	
30	30	30	0	0	0	4	9.08	2.59	13.325	0.2	0.9	60	80	128	148	
30	30	30	0	0	0	4	9.08	2.59	15.975	0.2	0.9	60	77	116	133	
30	30	30	0	0	0	3	24.89	3.68	18.333	0.2	0.9	60	101	109	150	
30	30	30	0	0	0	3	24.89	3.68	14.423	0.2	0.9	60	112	122	174	
30	30	30	0	0	0	2	10.19	2.44	19.008	0.2	0.9	60	76	107	123	
30	30	30	0	0	0	4	9.08	2.59	10.872	0.2	0.9	60	85	143	168	
30	30	30	0	0	0	5	19.27	2.44	16.318	0.2	0.9	60	95	115	150	
30	30	30	0	0	0	6	8.32	2.43	22.125	0.2	0.9	60	71	101	112	
30	30	30	0	0	0	4	9.08	2.59	13.464	0.2	0.9	60	80	127	147	
30	30	30	0	0	0	2	10.19	2.44	21.411	0.2	0.9	60	74	102	116	
30	30	30	0	0	0	4	9.08	2.59	12.339	0.2	0.9	60	82	133	155	
30	60	60	0	0	0	3	24.89	3.68	13.117	0.2	0.9	60	117	197	254	
30	60	60	0	0	0	6	8.32	2.43	25.477	0.2	0.9	60	70	131	141	
30	60	60	0	0	0	6	8.32	2.43	23.354	0.2	0.9	60	71	137	148	
30	60	60	0	0	0	1	4.57	2.16	20.849	0.2	0.9	60	67	146	153	
30	60	60	0	0	0	5	19.27	2.44	18.638	0.2	0.9	60	91	157	188	
30	60	60	0	0	0	4	9.08	2.59	11.133	0.2	0.9	60	84	222	246	
30	60	60	0	0	0	5	19.27	2.44	22.227	0.2	0.9	60	86	141	167	
30	60	60	0	0	0	4	9.08	2.59	17.759	0.2	0.9	60	75	161	176	
30	60	60	0	0	0	4	9.08	2.59	14.366	0.2	0.9	60	79	185	204	
30	60	60	0	0	0	6	8.32	2.43	15.607	0.2	0.9	60	76	175	191	
30	60	60	0	0	0	3	24.89	3.68	19.421	0.2	0.9	60	98	153	191	
30	60	60	0	0	0	1	4.57	2.16	17.418	0.2	0.9	60	68	163	171	
30	60	60	0	0	0	2	10.19	2.44	12.83	0.2	0.9	60	84	200	224	
30	60	60	0	0	0	4	9.08	2.59	18.001	0.2	0.9	60	75	160	175	
30	60	60	0	0	0	5	19.27	2.44	23.077	0.2	0.9	60	85	138	163	
30	60	60	0	0	0	4	9.08	2.59	15.397	0.2	0.9	60	78	177	195	
30	60	60	0	0	0	6	8.32	2.43	16.373	0.2	0.9	60	75	170	185	
30	60	60	0	0	0	3	24.89	3.68	19.856	0.2	0.9	60	98	151	189	
30	60	60	0	0	0	4	9.08	2.59	17.064	0.2	0.9	60	76	165	181	
30	60	60	0	0	0	4	9.08	2.59	14.865	0.2	0.9	60	78	181	199	
10	30	30	0	0	0	3	24.89	3.68	14.37	0.2	0.9	60	77	81	98	
10	30	30	0	0	0	6	8.32	2.43	19.283	0.2	0.9	60	64	76	80	
10	30	30	0	0	0	3	24.89	3.68	15.055	0.2	0.9	60	77	80	97	
10	30	30	0	0	0	2	10.19	2.44	16.853	0.2	0.9	60	66	78	84	
10	30	30	0	0	0	2	10.19	2.44	16.803	0.2	0.9	60	66	78	84	
10	30	30	0	0	0	1	4.57	2.16	22.084	0.2	0.9	60	62	74	76	
10	30	30	0	0	0	4	9.08	2.59	16.392	0.2	0.9	60	66	78	84	
10	30	30	0	0	0	5	19.27	2.44	13.993	0.2	0.9	60	74	81	95	
10	30	30	0	0	0	6	8.32	2.43	24.51	0.2	0.9	60	63	72	75	
10	30	30	0	0	0	4	9.08	2.59	14.308	0.2	0.9	60	66	81	87	
10	30	30	0	0	0	3	24.89	3.68	16.569	0.2	0.9	60	75	78	93	
10	30	30	0	0	0	5	19.27	2.44	20.33	0.2	0.9	60	69	75	84	
10	30	30	0	0	0	2	10.19	2.44	14.605	0.2	0.9	60	67	81	88	
10	30	30	0	0	0	4	9.08	2.59	16.342	0.2	0.9	60	66	78	84	
10	30	30	0	0	0	1	4.57	2.16	23.762	0.2	0.9	60	62	73	75	
10	30	30	0	0	0	1	4.57	2.16	20.448	0.2	0.9	60	62	75	77	
10	30	30	0	0	0	3	24.89	3.68	18.717	0.2	0.9	60	73	76	89	
10	30	30	0	0	0	2	10.19	2.44	17.69	0.2	0.9	60	66	77	83	
10	30	30	0	0	0	1	4.57	2.16	27.799	0.2	0.9	60	62	71	73	
10	30	30	0	0	0	6	8.32	2.43	22.424	0.2	0.9	60	64	73	77	
30	30	30	0.05	0	0	6	8.32	2.43	20.131	0.2	0.9	60	72	105	117	
30	30	30	0.05	0	0	3	24.89	3.68	16.712	0.2	0.9	60	105	114	159	
30	30	30	0.05	0	0	5	19.27	2.44	12.954	0.2	0.9	60	105	129	174	
30	30	30	0.05	0	0	5	19.27	2.44	15.809	0.2	0.9	60	97	117	154	
30	30	30	0.05	0	0	6	8.32	2.43	20.999	0.2	0.9	60	72	103	115	
30	30	30	0.05	0	0	2	10.19	2.44	13.408	0.2	0.9	60	83	127	150	
30	30	30	0.05	0	0	6	8.32	2.43	16.728	0.2	0.9	60	75	114	129	
30	30	30	0.05	0	0	2	10.19	2.44	17.452	0.2	0.9	60	78	112	130	
30	30	30	0.05	0	0	5	19.27	2.44	17.285	0.2	0.9	60	93	112	145	
30	30	30	0.05	0	0	1	4.57	2.16	18.628	0.2	0.9	60	67	108	115	
30	30	30	0.05	0	0	3	24.89	3.68	12.769	0.2	0.9	60	118	130	188	
30	30	30	0.05	0	0	2	10.19	2.44	19.735	0.2	0.9	60	75	106	121	
30	30	30	0.05	0	0	4	9.08	2.59	12.369	0.2	0.9	60	82	133	155	

30	30	30	0.05	0	3	24.89	3.68	11.633	0.2	0.9	60	124	137	201
30	30	30	0.05	0	5	19.27	2.44	19.513	0.2	0.9	60	90	106	136
30	30	30	0.05	0	3	24.89	3.68	12.449	0.2	0.9	60	120	132	192
30	30	30	0.05	0	5	19.27	2.44	17.056	0.2	0.9	60	94	113	147
30	30	30	0.05	0	2	10.19	2.44	15.276	0.2	0.9	60	80	119	139
30	30	30	0.05	0	3	24.89	3.68	15.422	0.2	0.9	60	108	118	166
60	30	30	0.05	0	1	4.57	2.16	22.394	0.2	0.9	60	72	140	152
60	30	30	0.05	0	5	19.27	2.44	12.759	0.2	0.9	60	151	201	292
60	30	30	0.05	0	1	4.57	2.16	14.935	0.2	0.9	60	78	181	199
60	30	30	0.05	0	3	24.89	3.68	15.999	0.2	0.9	60	153	173	266
60	30	30	0.05	0	3	24.89	3.68	12.477	0.2	0.9	60	180	204	324
60	30	30	0.05	0	5	19.27	2.44	22.264	0.2	0.9	60	112	141	193
60	30	30	0.05	0	4	9.08	2.59	13.372	0.2	0.9	60	101	195	236
60	30	30	0.05	0	1	4.57	2.16	26.649	0.2	0.9	60	70	128	138
60	30	30	0.05	0	1	4.57	2.16	21.553	0.2	0.9	60	73	144	157
60	30	30	0.05	0	2	10.19	2.44	21.196	0.2	0.9	60	89	145	174
60	30	30	0.05	0	1	4.57	2.16	26.606	0.2	0.9	60	70	128	138
60	30	30	0.05	0	6	8.32	2.43	25.257	0.2	0.9	60	80	131	151
60	30	30	0.05	0	6	8.32	2.43	23.748	0.2	0.9	60	81	136	157
60	30	30	0.05	0	6	8.32	2.43	22.864	0.2	0.9	60	82	139	161
60	30	30	0.05	0	2	10.19	2.44	16.822	0.2	0.9	60	96	167	203
60	30	30	0.05	0	4	9.08	2.59	16.231	0.2	0.9	60	94	171	205
60	30	30	0.05	0	2	10.19	2.44	22.864	0.2	0.9	60	87	139	166
60	30	30	0.05	0	1	4.57	2.16	19.418	0.2	0.9	60	74	153	167
60	30	30	0.05	0	1	4.57	2.16	22.81	0.2	0.9	60	72	139	151
60	30	30	0.05	0	5	19.27	2.44	13.223	0.2	0.9	60	147	196	283
120	30	30	0.05	0	5	19.27	2.44	24.435	0.2	0.9	60	155	207	302
120	30	30	0.05	0	2	10.19	2.44	24.663	0.2	0.9	60	110	206	256
120	30	30	0.05	0	4	9.08	2.59	12.376	0.2	0.9	60	148	351	439
120	30	30	0.05	0	6	8.32	2.43	18.902	0.2	0.9	60	113	250	303
120	30	30	0.05	0	2	10.19	2.44	14.94	0.2	0.9	60	142	301	383
120	30	30	0.05	0	6	8.32	2.43	17.309	0.2	0.9	60	118	268	326
120	30	30	0.05	0	2	10.19	2.44	15.263	0.2	0.9	60	140	296	376
120	30	30	0.05	0	2	10.19	2.44	16.996	0.2	0.9	60	132	272	344
120	30	30	0.05	0	1	4.57	2.16	25.769	0.2	0.9	60	81	200	221
120	30	30	0.05	0	3	24.89	3.68	16.751	0.2	0.9	60	238	275	453
120	30	30	0.05	0	3	24.89	3.68	11.261	0.2	0.9	60	325	380	0
120	30	30	0.05	0	6	8.32	2.43	15.66	0.2	0.9	60	124	290	354
120	30	30	0.05	0	3	24.89	3.68	16.278	0.2	0.9	60	243	281	464
120	30	30	0.05	0	3	24.89	3.68	16.205	0.2	0.9	60	244	282	466
120	30	30	0.05	0	3	24.89	3.68	13.861	0.2	0.9	60	275	320	535
120	30	30	0.05	0	3	24.89	3.68	17.327	0.2	0.9	60	232	268	440
120	30	30	0.05	0	6	8.32	2.43	20.934	0.2	0.9	60	108	232	280
120	30	30	0.05	0	5	19.27	2.44	14.693	0.2	0.9	60	217	305	462
120	30	30	0.05	0	1	4.57	2.16	22.832	0.2	0.9	60	84	218	242
120	30	30	0.05	0	4	9.08	2.59	18.208	0.2	0.9	60	120	258	318
120	30	30	0.05	0	3	24.89	3.68	19.308	0.2	0.9	60	215	246	401
120	30	30	0.05	0	1	4.57	2.16	24.417	0.2	0.9	60	82	207	229
120	30	30	0.05	0	2	10.19	2.44	13.256	0.2	0.9	60	152	332	424
120	30	30	0.05	0	6	8.32	2.43	25.447	0.2	0.9	60	99	201	240
120	30	30	0.05	0	6	8.32	2.43	23.108	0.2	0.9	60	103	216	259
120	30	30	0.04	0	4	9.08	2.59	12.229	0.2	0.9	60	149	354	443
120	30	30	0.04	0	6	8.32	2.43	15.647	0.2	0.9	60	124	290	354
120	30	30	0.04	0	2	10.19	2.44	17.62	0.2	0.9	60	129	264	333
120	30	30	0.04	0	2	10.19	2.44	15.45	0.2	0.9	60	139	293	372
120	30	30	0.04	0	3	24.89	3.68	15.014	0.2	0.9	60	259	300	499
120	30	30	0.04	0	3	24.89	3.68	14.135	0.2	0.9	60	271	315	526
120	30	30	0.04	0	3	24.89	3.68	15.081	0.2	0.9	60	258	299	497
120	30	30	0.04	0	4	9.08	2.59	10.196	0.2	0.9	60	167	413	520
120	30	30	0.04	0	2	10.19	2.44	22.05	0.2	0.9	60	115	223	278
120	30	30	0.04	0	1	4.57	2.16	27.472	0.2	0.9	60	80	191	211
120	30	30	0.04	0	3	24.89	3.68	14.54	0.2	0.9	60	265	308	513
120	30	30	0.04	0	3	24.89	3.68	12.338	0.2	0.9	60	302	352	594
120	30	30	0.04	0	5	19.27	2.44	23.078	0.2	0.9	60	160	216	316
120	30	30	0.04	0	4	9.08	2.59	13.44	0.2	0.9	60	141	328	409
120	30	30	0.04	0	6	8.32	2.43	13.741	0.2	0.9	60	133	322	395
120	30	30	0.02	0	3	24.89	3.68	12.51	0.2	0.9	60	299	348	587
120	30	30	0.02	0	2	10.19	2.44	19.876	0.2	0.9	60	122	241	303
120	30	30	0.02	0	3	24.89	3.68	12.933	0.2	0.9	60	291	338	569
120	30	30	0.02	0	4	9.08	2.59	19.527	0.2	0.9	60	116	244	300
120	30	30	0.02	0	1	4.57	2.16	17.538	0.2	0.9	60	91	265	296
120	30	30	0.02	0	6	8.32	2.43	23.205	0.2	0.9	60	103	215	258
120	30	30	0.02	0	1	4.57	2.16	22.136	0.2	0.9	60	85	223	248
120	30	30	0.02	0	1	4.57	2.16	19.548	0.2	0.9	60	88	244	272
120	30	30	0.02	0	2	10.19	2.44	21.813	0.2	0.9	60	116	225	281
120	30	30	0.02	0	6	8.32	2.43	19.645	0.2	0.9	60	111	243	294
120	30	30	0.02	0	5	19.27	2.44	18.785	0.2	0.9	60	183	252	375
120	30	30	0.02	0	3	24.89	3.68	14.038	0.2	0.9	60	273	316	529

120	30	30	0.02	0	3	24.89	3.68	19.181	0.2	0.9	60	216	248	404
120	30	30	0.02	0	6	8.32	2.43	25.328	0.2	0.9	60	99	202	241
120	30	30	0.02	0	6	8.32	2.43	19.839	0.2	0.9	60	110	241	291
120	30	30	0.02	0	4	9.08	2.59	10.418	0.2	0.9	60	165	406	511
120	30	30	0.02	0	2	10.19	2.44	21.111	0.2	0.9	60	118	231	289
120	30	30	0.02	0	6	8.32	2.43	14.592	0.2	0.9	60	128	307	375
120	30	30	0.02	0	2	10.19	2.44	14.042	0.2	0.9	60	147	316	403
120	30	30	0.02	0	1	4.57	2.16	26.903	0.2	0.9	60	80	194	214
120	30	30	0.02	0.5	4	9.08	2.59	15.251	0.2	0.9	60	131	296	367
120	30	30	0.02	0.5	6	8.32	2.43	18.751	0.2	0.9	60	113	252	305
120	30	30	0.02	0.5	5	19.27	2.44	23.297	0.2	0.9	60	159	215	314
120	30	30	0.02	0.5	2	10.19	2.44	14.92	0.2	0.9	60	142	301	383
120	30	30	0.02	0.5	5	19.27	2.44	24.22	0.2	0.9	60	155	209	304
120	30	30	0.02	0.5	1	4.57	2.16	21.315	0.2	0.9	60	86	229	255
120	30	30	0.02	0.5	2	10.19	2.44	18.196	0.2	0.9	60	127	258	325
120	30	30	0.02	0.5	3	24.89	3.68	13.951	0.2	0.9	60	274	318	532
120	30	30	0.02	0.5	1	4.57	2.16	15.979	0.2	0.9	60	94	285	319
120	30	30	0.02	0.5	2	10.19	2.44	14.194	0.2	0.9	60	146	314	400
120	30	30	0.02	0.5	1	4.57	2.16	28.248	0.2	0.9	60	79	187	206
120	30	30	0.02	0.5	1	4.57	2.16	15.053	0.2	0.9	60	96	299	335
120	30	30	0.02	0.5	3	24.89	3.68	16.392	0.2	0.9	60	242	280	462
120	30	30	0.02	0.5	3	24.89	3.68	20.085	0.2	0.9	60	209	239	388
120	30	30	0.02	0.5	2	10.19	2.44	17.05	0.2	0.9	60	132	271	343
120	30	30	0.02	0.5	3	24.89	3.68	16.986	0.2	0.9	60	236	272	448
120	30	30	0.02	0.5	4	9.08	2.59	17.275	0.2	0.9	60	123	268	331
120	30	30	0.02	0.5	2	10.19	2.44	14.374	0.2	0.9	60	145	310	395
120	30	30	0.02	0.5	6	8.32	2.43	13.464	0.2	0.9	60	134	327	401
120	30	30	0.02	0.5	5	19.27	2.44	16.414	0.2	0.9	60	201	279	420
120	30	30	0.02	0.25	6	8.32	2.43	14.34	0.2	0.9	60	130	311	381
120	30	30	0.02	0.25	2	10.19	2.44	24.056	0.2	0.9	60	111	210	261
120	30	30	0.02	0.25	4	9.08	2.59	10.492	0.2	0.9	60	164	403	507
120	30	30	0.02	0.25	5	19.27	2.44	12.951	0.2	0.9	60	239	338	517
120	30	30	0.02	0.25	2	10.19	2.44	22.251	0.2	0.9	60	115	222	277
120	30	30	0.02	0.25	1	4.57	2.16	20.022	0.2	0.9	60	87	240	267
120	30	30	0.02	0.25	1	4.57	2.16	17.152	0.2	0.9	60	92	270	302
120	30	30	0.02	0.25	3	24.89	3.68	18.613	0.2	0.9	60	220	253	413
120	30	30	0.02	0.25	1	4.57	2.16	27.735	0.2	0.9	60	80	190	210
120	30	30	0.02	0.25	5	19.27	2.44	24.52	0.2	0.9	60	154	207	301
120	30	30	0.02	0.25	2	10.19	2.44	16.486	0.2	0.9	60	134	278	352
120	30	30	0.02	0.25	4	9.08	2.59	15.606	0.2	0.9	60	130	291	361
120	30	30	0.02	0.25	1	4.57	2.16	18.642	0.2	0.9	60	89	253	282
120	30	30	0.02	0.25	4	9.08	2.59	16.919	0.2	0.9	60	124	273	337
120	30	30	0.02	0.25	1	4.57	2.16	18.844	0.2	0.9	60	89	251	280
120	30	30	0.02	0.25	2	10.19	2.44	18.695	0.2	0.9	60	125	253	318
120	30	30	0.02	0.25	3	24.89	3.68	14.653	0.2	0.9	60	264	306	510
120	30	30	0.02	0.25	2	10.19	2.44	25.219	0.2	0.9	60	108	203	251
120	30	30	0.02	0.25	4	9.08	2.59	18.434	0.2	0.9	60	119	255	314
120	30	30	0.02	0.25	4	9.08	2.59	17.635	0.2	0.9	60	122	264	326
120	30	5	0.01	0.25	3	24.89	3.68	18.2	0.2	0.9	60	224	258	422
120	30	5	0.01	0.25	5	19.27	2.44	16.728	0.2	0.9	60	198	275	413
120	30	5	0.01	0.25	4	9.08	2.59	16.648	0.2	0.9	60	125	276	341
120	30	5	0.01	0.25	4	9.08	2.59	11.198	0.2	0.9	60	157	381	478
120	30	5	0.01	0.25	6	8.32	2.43	13.711	0.2	0.9	60	133	323	396
120	30	5	0.01	0.25	5	19.27	2.44	21.519	0.2	0.9	60	167	227	334
120	30	5	0.01	0.25	5	19.27	2.44	18.999	0.2	0.9	60	182	249	371
120	30	5	0.01	0.25	3	24.89	3.68	16.733	0.2	0.9	60	239	275	454
120	30	5	0.01	0.25	4	9.08	2.59	10.532	0.2	0.9	60	163	402	505
120	30	5	0.01	0.25	4	9.08	2.59	16.849	0.2	0.9	60	125	274	339
120	30	5	0.01	0.25	5	19.27	2.44	17.355	0.2	0.9	60	193	267	400
120	30	5	0.01	0.25	5	19.27	2.44	19.401	0.2	0.9	60	179	246	365
120	30	5	0.01	0.25	1	4.57	2.16	28.547	0.2	0.9	60	79	186	205
120	30	5	0.01	0.25	1	4.57	2.16	26.62	0.2	0.9	60	81	195	216
120	30	5	0.01	0.25	3	24.89	3.68	16.655	0.2	0.9	60	239	276	455
120	30	5	0.01	0.25	5	19.27	2.44	13.744	0.2	0.9	60	228	322	490
120	30	5	0.01	0.25	4	9.08	2.59	16.84	0.2	0.9	60	125	274	339
120	30	5	0.01	0.25	4	9.08	2.59	18.459	0.2	0.9	60	119	255	314
120	30	5	0.01	0.25	2	10.19	2.44	24.201	0.2	0.9	60	111	209	260
120	30	5	0.01	0.25	6	8.32	2.43	23.454	0.2	0.9	60	103	213	256
120	30	30	0.01	0.25	5	19.27	2.44	19.959	0.2	0.9	60	176	240	356
120	30	30	0.01	0.25	5	19.27	2.44	17.796	0.2	0.9	60	190	262	392
120	30	30	0.01	0.25	4	9.08	2.59	13.9	0.2	0.9	60	138	319	397
120	30	30	0.01	0.25	6	8.32	2.43	16.341	0.2	0.9	60	121	280	341
120	30	30	0.01	0.25	3	24.89	3.68	16.47	0.2	0.9	60	241	279	460
120	30	30	0.01	0.25	4	9.08	2.59	13.217	0.2	0.9	60	142	332	414
120	30	30	0.01	0.25	2	10.19	2.44	16.705	0.2	0.9	60	133	276	349
120	30	30	0.01	0.25	2	10.19	2.44	18.648	0.2	0.9	60	126	253	319
120	30	30	0.01	0.25	5	19.27	2.44	13.588	0.2	0.9	60	230	325	495
120	30	30	0.01	0.25	4	9.08	2.59	13.75	0.2	0.9	60	139	322	401

120	30	30	0.01	0.25	3	24.89	3.68	16.829	0.2	0.9	60	237	274	451
120	30	30	0.01	0.25	4	9.08	2.59	13.107	0.2	0.9	60	143	335	418
120	30	30	0.01	0.25	6	8.32	2.43	16.8	0.2	0.9	60	119	274	333
120	30	30	0.01	0.25	5	19.27	2.44	17.302	0.2	0.9	60	194	268	402
120	30	30	0.01	0.25	4	9.08	2.59	17.915	0.2	0.9	60	121	261	322
120	30	30	0.01	0.25	4	9.08	2.59	20.081	0.2	0.9	60	114	239	293
120	30	30	0.01	0.25	3	24.89	3.68	14.001	0.2	0.9	60	273	317	530
120	30	30	0.01	0.25	3	24.89	3.68	13.677	0.2	0.9	60	278	323	541
120	30	30	0.01	0.25	4	9.08	2.59	14.131	0.2	0.9	60	137	315	392
120	30	30	0.01	0.25	3	24.89	3.68	12.323	0.2	0.9	60	302	352	594

Table B.2 Detection Comparison: Threshold Detection Results

Threshold	N	$\gamma$	#T	En1	Ex2	FARI	#T	En1	Ex2	FAR2	#T	En1	Ex2	Threshold		
														DiffTEn1	DiffTEx2	DiffTE
2	1	1	61	115	15	1	61	115	30	1	61	115	0.0333	0.0000		
2	1	1	61	153	15	1	61	153	30	1	61	153	0.0333	0.0000		
2	1	1	61	139	15	1	61	139	30	1	61	139	0.0333	0.0000		
2	1	1	61	107	15	1	61	107	30	1	61	107	0.0333	0.0000		
1	1	1	61	143	15	1	61	143	30	1	61	143	0.0333	0.0000		
1	1	1	61	153	15	1	61	153	30	1	61	153	0.0333	0.0000		
1	1	1	61	140	15	1	61	140	30	1	61	140	0.0333	0.0000		
1	1	1	61	126	15	1	61	126	30	1	61	126	0.0333	0.0000		
1	1	1	61	114	15	1	61	114	30	1	61	114	0.0333	0.0000		
1	1	1	61	148	15	1	61	148	30	1	61	148	0.0333	0.0000		
1	1	1	61	133	15	1	61	133	30	1	61	133	0.0333	0.0000		
1	1	1	61	150	15	1	61	150	30	1	61	150	0.0333	0.0000		
1	1	1	61	174	15	1	61	174	30	1	61	174	0.0333	0.0000		
1	1	1	61	123	15	1	61	123	30	1	61	123	0.0333	0.0000		
1	1	1	61	168	15	1	61	168	30	1	61	168	0.0333	0.0000		
1	1	1	61	150	15	1	61	150	30	1	61	150	0.0333	0.0000		
1	1	1	61	112	15	1	61	112	30	1	61	112	0.0333	0.0000		
1	1	1	61	147	15	1	61	147	30	1	61	147	0.0333	0.0000		
1	1	1	61	116	15	1	61	116	30	1	61	116	0.0333	0.0000		
1	1	1	61	155	15	1	61	155	30	1	61	155	0.0333	0.0000		
1	1	1	61	254	15	1	61	254	30	1	61	254	0.0333	0.0000		
1	1	1	61	141	15	1	61	141	30	1	61	141	0.0333	0.0000		
1	1	1	61	148	15	1	61	148	30	1	61	148	0.0333	0.0000		
1	1	1	61	153	15	1	61	153	30	1	61	153	0.0333	0.0000		
1	1	1	61	188	15	1	61	188	30	1	61	188	0.0333	0.0000		
1	1	1	61	246	15	1	61	246	30	1	61	246	0.0333	0.0000		
1	1	1	61	167	15	1	61	167	30	1	61	167	0.0333	0.0000		
1	1	1	61	176	15	1	61	176	30	1	61	176	0.0333	0.0000		
1	1	1	61	204	15	1	61	204	30	1	61	204	0.0333	0.0000		
1	1	1	61	191	15	1	61	191	30	1	61	191	0.0333	0.0000		
1	1	1	61	191	15	1	61	191	30	1	61	191	0.0333	0.0000		
1	1	1	61	171	15	1	61	171	30	1	61	171	0.0333	0.0000		
1	1	1	61	224	15	1	61	224	30	1	61	224	0.0333	0.0000		
1	1	1	61	175	15	1	61	175	30	1	61	175	0.0333	0.0000		
1	1	1	61	163	15	1	61	163	30	1	61	163	0.0333	0.0000		
1	1	1	61	195	15	1	61	195	30	1	61	195	0.0333	0.0000		
1	1	1	61	185	15	1	61	185	30	1	61	185	0.0333	0.0000		
1	1	1	61	189	15	1	61	189	30	1	61	189	0.0333	0.0000		
1	1	1	61	181	15	1	61	181	30	1	61	181	0.0333	0.0000		
1	1	1	61	199	15	1	61	199	30	1	61	199	0.0333	0.0000		
1	1	1	61	98	15	1	61	98	30	1	61	98	0.1000	0.0000		
1	1	1	61	80	15	1	61	80	30	0	0	0	0.1000	0.0000		
1	1	1	61	97	15	1	61	97	30	1	61	97	0.1000	0.0000		
1	1	1	61	84	15	1	61	84	30	0	0	0	0.1000	0.0000		
1	1	1	61	84	15	1	61	84	30	0	0	0	0.1000	0.0000		
1	1	1	61	76	15	1	61	76	30	0	0	0	0.1000	0.0000		
1	1	1	61	84	15	1	61	84	30	0	0	0	0.1000	0.0000		
1	1	1	61	95	15	1	61	95	30	1	61	95	0.1000	0.0000		
1	1	1	61	75	15	1	61	75	30	0	0	0	0.1000	0.0000		
1	1	1	61	87	15	1	61	87	30	0	0	0	0.1000	0.0000		
1	1	1	61	93	15	1	61	93	30	1	61	93	0.1000	0.0000		
1	1	1	61	84	15	1	61	84	30	0	0	0	0.1000	0.0000		
1	1	1	61	88	15	1	61	88	30	0	0	0	0.1000	0.0000		
1	1	1	61	84	15	1	61	84	30	0	0	0	0.1000	0.0000		
1	1	1	61	75	15	1	61	75	30	0	0	0	0.1000	0.0000		
1	1	1	61	77	15	1	61	77	30	0	0	0	0.1000	0.0000		
1	1	1	61	89	15	1	61	89	30	0	0	0	0.1000	0.0000		
1	1	1	61	83	15	1	61	83	30	0	0	0	0.1000	0.0000		
1	1	1	61	73	15	1	61	73	30	0	0	0	0.1000	0.0000		
1	1	1	61	77	15	1	61	77	30	0	0	0	0.1000	0.0000		
1	1	82	8	10	15	7	41	259	30	3	41	259	1.7333	3.5667		
1	1	123	98	117	15	2	2	515	30	2	2	515	1.2667	1.4000		
1	1	32	114	121	15	12	78	165	30	2	78	165	1.8000	1.7667		
1	1	77	#	394	15	10	461	571	30	4	461	571	11.0000	8.0000		
2	1	0	0	0	15	0	0	0	30	0	0	0	2.0000	3.8333		
2	1	8	85	88	15	1	75	116	30	1	75	116	0.8333	2.0667		
2	1	1	75	76	15	1	75	76	30	0	0	0	0.5000	1.7667		
2	1	2	80	81	15	2	80	81	30	0	0	0	0.6667	1.6333		
2	1	31	84	87	50	3	291	467	30	2	291	467	0.8000	1.9333		
2	1	36	88	90	50	3	180	461	30	2	180	461	0.9333	0.8333		
2	1	16	127	131	50	1	81	164	30	1	81	164	2.2333	1.9000		
2	1	2	75	76	50	1	75	94	30	0	0	0	0.5000	1.5000		
2	1	10	89	92	50	1	68	145	30	1	68	145	0.9667	2.1000		

2	1	15	138	141	25	1	91	172	30	1	91	172	2.6000	2.0000
2	1	15	102	105	25	4	76	114	30	1	76	114	1.4000	1.0333
2	1	20	140	144	25	1	89	161	30	1	89	161	2.6667	1.6000
2	1	12	91	94	25	1	79	138	30	1	79	138	1.0333	1.7667
2	1	9	117	119	25	1	80	126	30	1	80	126	1.9000	0.6667
2	1	7	107	109	25	1	92	123	30	1	92	123	1.5667	1.9000
2	1	1	78	79	25	1	78	79	30	0	0	0	0.3000	1.2167
2	1	19	163	167	25	1	113	240	30	1	113	240	1.7167	2.0833
2	1	50	2	4	25	7	136	353	30	4	136	353	0.9667	3.2500
2	1	87	142	165	25	3	3	505	30	1	3	505	1.3667	1.6833
2	1	32	182	188	25	1	115	271	30	1	115	271	2.0333	2.2667
2	1	24	107	109	25	1	70	179	30	1	70	179	0.7833	1.4000
2	1	109	129	133	25	1	4	566	30	1	4	566	1.1500	1.7167
2	1	0	0	0	25	0	0	0	30	0	0	0	1.0000	2.3000
2	1	86	15	18	25	2	237	580	30	2	237	580	0.7500	2.3167
2	1	1	140	141	25	1	140	141	30	0	0	0	1.3333	0.5500
2	1	63	#	292	25	3	339	567	30	3	339	567	3.8167	2.5667
2	1	7	98	99	25	1	98	132	30	1	98	132	0.6333	0.8667
2	1	130	8	15	25	1	2	576	30	1	2	576	0.8667	2.3667
2	1	4	93	94	25	2	129	138	30	0	0	0	0.5500	1.1167
2	1	7	157	159	25	1	97	162	30	1	97	162	1.6167	0.7333
2	1	0	0	0	25	0	0	0	30	0	0	0	1.0000	3.4167
2	1	9	93	94	25	1	93	149	30	1	93	149	0.5500	1.2000
2	1	23	9	11	25	7	148	219	30	4	148	219	0.8500	2.6000
2	1	63	6	8	25	2	298	568	30	2	298	568	0.9000	2.3833
2	1	11	131	132	25	1	131	217	30	1	131	217	1.1833	2.5167
2	1	47	140	146	25	1	82	281	30	1	82	281	0.6667	1.3000
2	1	0	0	0	25	0	0	0	30	0	0	0	0.5000	2.1333
2	1	21	132	134	25	3	275	367	30	2	275	367	0.6000	2.5417
2	1	9	146	149	25	4	180	220	30	1	180	220	0.7167	1.2833
2	1	15	147	149	25	2	147	295	30	1	147	295	0.7250	1.9500
2	1	3	126	127	25	3	126	127	30	0	0	0	0.5500	1.6583
2	1	4	183	184	25	2	183	206	30	0	0	0	1.0250	1.6000
2	1	18	108	109	25	2	174	297	30	2	174	297	0.4000	1.9583
2	1	85	140	144	25	1	6	581	30	1	6	581	0.6667	0.6417
2	1	51	#	230	25	2	165	393	30	1	165	393	1.3583	1.8583
2	1	79	321	326	25	1	154	519	30	1	154	519	2.1750	2.7167
2	1	37	195	198	25	2	123	323	30	1	123	323	1.1250	1.3000
2	1	57	#	334	25	1	146	395	30	1	146	395	2.2333	1.0833
2	1	67	#	253	25	1	103	421	30	1	103	421	1.5667	1.7750
2	1	101	#	259	25	3	82	500	30	3	82	500	1.5583	2.3000
2	1	111	221	247	25	1	2	580	30	1	2	580	1.3417	1.6083
2	1	11	100	102	25	3	156	213	30	1	156	213	0.3333	1.4833
2	1	16	#	300	25	1	182	341	30	1	182	341	1.9833	1.3500
2	1	0	0	0	25	0	0	0	30	0	0	0	0.5000	2.0167
2	1	43	135	139	25	3	63	369	30	1	63	369	0.6250	1.4917
2	1	86	211	218	25	4	6	453	30	1	6	453	1.2583	1.5250
2	1	0	0	0	25	0	0	0	30	0	0	0	0.5000	1.9083
2	1	0	0	0	25	0	0	0	30	0	0	0	0.5000	3.5333
2	1	8	96	97	25	3	142	183	30	1	142	183	0.3000	1.1917
2	1	0	0	0	25	0	0	0	30	0	0	0	0.5000	2.1583
2	1	25	121	122	25	3	260	377	30	2	260	377	0.5083	2.6750
2	1	13	#	207	25	2	196	286	30	2	196	286	1.2083	1.2250
2	1	2	#	206	25	1	205	217	30	0	0	0	1.2083	1.0583
2	1	38	128	130	25	2	192	325	30	2	192	325	0.5667	2.0167
2	1	94	#	312	25	3	9	508	30	1	9	508	1.6583	1.5583
2	1	86	#	352	25	2	9	460	30	2	9	460	1.4667	1.4500
2	1	80	#	291	25	1	107	459	30	1	107	459	1.8250	1.7167
2	1	107	111	117	25	1	4	561	30	1	4	561	0.4250	3.3583
2	1	29	115	118	25	1	84	256	30	1	84	256	0.4583	1.3333
2	1	1	104	105	25	1	104	105	30	0	0	0	0.3667	0.8833
2	1	52	#	292	25	2	190	426	30	1	190	426	1.8333	1.8417
2	1	77	#	346	25	3	108	577	30	1	108	577	1.8667	2.0667
2	1	39	#	226	25	1	91	296	30	1	91	296	1.3500	0.7500
2	1	72	91	95	25	3	72	430	30	1	72	430	0.2583	2.6167
2	1	110	155	159	25	1	9	581	30	1	9	581	0.7917	1.9667
2	1	49	217	430	25	1	104	553	30	1	104	553	1.3083	1.3083
2	1	74	154	168	25	4	71	309	30	4	71	309	0.7833	1.1250
2	1	48	180	443	25	1	76	537	30	1	76	537	1.0000	1.0500
2	1	36	178	181	25	1	77	272	30	1	77	272	0.9833	0.9917
2	1	19	103	105	25	2	149	266	30	1	149	266	0.3583	1.5917
2	1	26	189	195	25	1	91	234	30	1	91	234	1.0750	0.5250
2	1	10	96	97	25	3	96	144	30	1	96	144	0.3000	1.2583
2	1	51	95	99	25	4	63	209	30	3	63	209	0.2917	1.4417
2	1	45	161	166	25	1	67	263	30	1	67	263	0.8417	0.9583
2	1	29	117	119	25	2	93	210	30	1	93	210	0.4750	1.4583
2	1	42	#	225	25	1	75	354	30	1	75	354	1.2167	1.2500
2	1	44	#	390	25	1	102	492	30	1	102	492	1.1917	1.1583

2	1	31	156	310	25	1	84	373	30	1	84	373	0.8000	0.7833
2	1	32	115	118	25	1	84	220	30	1	84	220	0.4583	1.0250
2	1	93	187	192	25	1	8	581	30	1	8	581	1.0583	0.8250
2	1	89	312	317	25	1	76	468	30	1	76	468	2.1000	1.6167
2	1	34	106	108	25	1	98	259	30	1	98	259	0.3833	1.5083
2	1	6	185	186	25	2	185	227	30	1	185	227	1.0417	1.5750
2	1	63	#	310	25	1	94	387	30	1	94	387	2.0000	0.7750
2	1	19	138	140	25	1	76	200	30	1	76	200	0.6500	0.6167
2	1	1	570	571	25	1	570	571	30	0	0	0	4.2500	1.7000
2	1	55	112	114	25	5	91	309	30	3	91	309	0.4333	1.5917
2	1	50	#	248	25	2	29	423	30	1	29	423	1.5250	0.5500
2	1	23	144	146	25	9	332	398	30	2	332	398	0.7000	1.9750
2	1	53	183	187	25	5	85	264	30	3	85	264	1.0250	0.9750
2	1	2	129	130	25	2	129	130	30	0	0	0	0.5750	1.0417
2	1	13	#	255	25	5	217	278	30	2	217	278	1.6083	0.5833
2	1	14	#	272	25	3	244	348	30	1	244	348	1.7500	2.1667
2	1	57	#	244	25	3	50	369	30	3	50	369	1.5167	0.6250
2	1	90	121	124	25	1	5	574	30	1	5	574	0.5083	2.3000
2	1	33	#	287	25	9	407	498	30	5	407	498	1.8750	0.6750
2	1	46	117	119	25	8	25	119	30	5	25	119	0.4750	1.8000
2	1	83	#	250	25	3	101	532	30	1	101	532	1.5000	1.7667
2	1	39	#	232	25	4	183	328	30	1	183	328	1.3750	1.3000
2	1	2	291	292	25	2	291	292	30	0	0	0	1.9250	0.4250
2	1	82	#	245	25	3	86	491	30	1	86	491	1.4417	1.6917
2	1	64	558	562	25	6	104	291	30	3	104	291	4.1500	1.9250
2	1	12	#	411	25	7	149	185	30	1	149	185	2.9083	0.1333
2	1	18	#	372	25	5	269	403	30	1	269	403	2.5750	0.2417
2	1	81	#	256	25	4	84	446	30	2	84	446	1.6000	1.3667
2	1	69	#	228	25	4	29	371	30	2	29	371	1.3750	1.2750
2	1	8	183	185	25	3	171	207	30	1	171	207	1.0250	0.6333
2	1	27	#	282	25	5	126	241	30	3	126	241	1.8250	1.8750
2	1	1	#	279	25	1	278	279	30	0	0	0	1.8167	1.9833
2	1	16	116	118	25	3	88	250	30	1	88	250	0.4667	1.3250
2	1	41	106	108	25	8	381	490	30	4	381	490	0.3833	1.3250
2	1	15	31	32	25	7	148	206	30	2	148	206	0.2417	2.2500
2	1	64	173	190	25	3	84	461	30	1	84	461	0.9417	1.8583
2	1	33	33	36	25	10	15	89	30	3	15	89	0.2250	1.4500
2	1	31	145	148	25	1	114	266	30	1	114	266	0.7083	1.2750
2	1	69	121	125	25	7	64	332	30	1	64	332	0.5083	1.8917
2	1	9	#	222	25	6	287	304	30	0	0	0	1.3333	1.1583
2	1	129	164	169	25	1	2	581	30	1	2	581	0.8667	0.9417
2	1	7	100	101	25	4	212	223	30	0	0	0	0.3333	1.9667
2	1	53	69	71	25	6	21	269	30	3	21	269	0.0750	1.7417
2	1	22	137	139	25	4	98	270	30	1	98	270	0.6417	1.4917
2	1	52	251	257	25	4	169	392	30	1	169	392	1.5917	2.1083
2	1	6	159	161	25	2	103	161	30	1	103	161	0.8250	0.7500
2	1	54	#	245	25	5	35	309	30	3	35	309	1.5000	0.5750
2	1	72	145	148	25	4	63	393	30	2	63	393	0.7083	1.4833
2	1	25	80	401	25	1	77	559	30	1	77	559	0.1667	0.1750
2	1	46	80	387	25	2	48	578	30	1	48	578	0.1667	0.2167
2	1	38	85	321	25	2	67	501	30	1	67	501	0.2083	0.1667
2	1	19	111	437	25	2	88	480	30	1	88	480	0.4250	0.3417
2	1	14	112	345	25	2	88	378	30	1	88	378	0.4333	0.4250
2	1	27	75	317	25	2	60	447	30	1	60	447	0.1250	0.1417
2	1	57	73	361	25	2	29	581	30	1	29	581	0.1083	0.0833
2	1	28	101	420	25	2	88	533	30	1	88	533	0.3417	0.2833
2	1	14	132	444	25	1	106	481	30	1	106	481	0.6000	0.5083
2	1	32	79	313	25	5	61	327	30	3	61	327	0.1583	0.2167
2	1	44	81	377	25	2	50	577	30	1	50	577	0.1750	0.1917
2	1	33	77	349	25	2	48	455	30	2	48	455	0.1417	0.1333
2	1	45	69	193	25	5	65	330	30	2	65	330	0.0750	0.1000
2	1	56	73	204	25	5	2	383	30	2	2	383	0.1083	0.1000
2	1	32	84	429	25	1	75	572	30	1	75	572	0.2000	0.2167
2	1	18	128	415	25	2	113	474	30	1	113	474	0.5667	0.6250
2	1	44	77	318	25	2	67	540	30	1	67	540	0.1417	0.1750
2	1	27	78	299	25	2	71	487	30	1	71	487	0.1500	0.1250
2	1	22	78	245	25	1	72	394	30	1	72	394	0.1500	0.1250
2	1	38	76	250	25	4	60	404	30	2	60	404	0.1333	0.0500
2	1	67	#	227	25	5	77	344	30	3	77	344	1.2333	1.0750
2	1	73	151	318	25	1	2	578	30	1	2	578	0.7583	0.6167
2	1	19	#	242	25	3	119	300	30	1	119	300	1.4917	1.2917
2	1	44	192	195	25	6	108	311	30	1	108	311	1.1000	1.2167
2	1	55	155	360	25	2	52	547	30	1	52	547	0.7917	0.8333
2	1	26	157	160	25	5	191	260	30	2	191	260	0.8083	2.1167
2	1	90	146	154	25	4	76	341	30	4	76	341	0.7167	1.6250
2	1	26	145	147	25	2	99	292	30	2	99	292	0.7083	1.4333
2	1	69	#	250	25	5	92	449	30	2	92	449	1.4417	2.0417
2	1	13	126	127	25	6	126	176	30	1	126	176	0.5500	2.2833

2	1	54	135	373	25	1	24	575	30	1	24	575	0.6250	0.6500
2	1	76	#	238	25	4	66	393	30	2	66	393	1.4417	1.5000
2	1	103	123	131	25	1	9	581	30	1	9	581	0.5250	1.6833
2	1	65	#	275	25	3	41	420	30	2	41	420	1.4667	1.0583
2	1	6	112	113	25	3	206	228	30	0	0	0	0.4333	1.7417
2	1	77	196	202	25	5	80	331	30	4	80	331	1.1333	0.7583
2	1	45	180	391	25	2	80	503	30	1	80	503	1.0000	1.1583
2	1	44	192	402	25	2	85	502	30	1	85	502	1.1000	1.1583
2	1	3	152	153	25	3	152	153	30	0	0	0	0.7667	1.9917
2	1	48	#	436	25	2	119	580	30	1	119	580	1.4500	1.3167

Table B.3 Detection Comparison: Duration Detection Results

Duration	N	#T	Duration											
			En1	Ex2	FAR1	#T	En1	Ex2	FAR2	#T	En1	Ex2	DifffDEn1	DifffDEx2
2	1	66	110	15	1	66	110	30	1	66	110	0.2000	0.1667	
2	1	68	146	15	1	68	146	30	1	68	146	0.2667	0.2333	
2	1	72	128	15	1	72	128	30	1	72	128	0.4000	0.3667	
2	1	64	104	15	1	64	104	30	1	64	104	0.1333	0.1000	
1	1	66	138	15	1	66	138	30	1	66	138	0.2000	0.1667	
1	1	64	150	15	1	64	150	30	1	64	150	0.1333	0.1000	
1	1	63	138	15	1	63	138	30	1	63	138	0.1000	0.0667	
1	1	63	124	15	1	63	124	30	1	63	124	0.1000	0.0667	
1	1	63	112	15	1	63	112	30	1	63	112	0.1000	0.0667	
1	1	63	146	15	1	63	146	30	1	63	146	0.1000	0.0667	
1	1	63	131	15	1	63	131	30	1	63	131	0.1000	0.0667	
1	1	64	147	15	1	64	147	30	1	64	147	0.1333	0.1000	
1	1	65	170	15	1	65	170	30	1	65	170	0.1667	0.1333	
1	1	63	121	15	1	63	121	30	1	63	121	0.1000	0.0667	
1	1	64	165	15	1	64	165	30	1	64	165	0.1333	0.1000	
1	1	68	143	15	1	68	143	30	1	68	143	0.2667	0.2333	
1	1	64	109	15	1	64	109	30	1	64	109	0.1333	0.1000	
1	1	63	145	15	1	63	145	30	1	63	145	0.1000	0.0667	
1	1	63	114	15	1	63	114	30	1	63	114	0.1000	0.0667	
1	1	64	152	15	1	64	152	30	1	64	152	0.1333	0.1000	
1	1	68	247	15	1	68	247	30	1	68	247	0.2667	0.2333	
1	1	64	138	15	1	64	138	30	1	64	138	0.1333	0.1000	
1	1	64	145	15	1	64	145	30	1	64	145	0.1333	0.1000	
1	1	67	147	15	1	67	147	30	1	67	147	0.2333	0.2000	
1	1	71	178	15	1	71	178	30	1	71	178	0.3667	0.3333	
1	1	71	236	15	1	71	236	30	1	71	236	0.3667	0.3333	
1	1	69	159	15	1	69	159	30	1	69	159	0.3000	0.2667	
1	1	67	170	15	1	67	170	30	1	67	170	0.2333	0.2000	
1	1	69	196	15	1	69	196	30	1	69	196	0.3000	0.2667	
1	1	66	186	15	1	66	186	30	1	66	186	0.2000	0.1667	
1	1	65	187	15	1	65	187	30	1	65	187	0.1667	0.1333	
1	1	68	164	15	1	68	164	30	1	68	164	0.2667	0.2333	
1	1	72	213	15	1	72	213	30	1	72	213	0.4000	0.3667	
1	1	67	169	15	1	67	169	30	1	67	169	0.2333	0.2000	
1	1	69	155	15	1	69	155	30	1	69	155	0.3000	0.2667	
1	1	68	188	15	1	68	188	30	1	68	188	0.2667	0.2333	
1	1	66	180	15	1	66	180	30	1	66	180	0.2000	0.1667	
1	1	65	185	15	1	65	185	30	1	65	185	0.1667	0.1333	
1	1	68	174	15	1	68	174	30	1	68	174	0.2667	0.2333	
1	1	68	192	15	1	68	192	30	1	68	192	0.2667	0.2333	
1	1	62	97	15	1	62	97	30	1	62	97	0.2000	0.1000	
1	1	62	79	15	1	62	79	30	0	0	0	0.2000	0.1000	
1	1	62	96	15	1	62	96	30	1	62	96	0.2000	0.1000	
1	1	61	84	15	1	61	84	30	0	0	0	0.1000	0.0000	
1	1	61	84	15	1	61	84	30	0	0	0	0.1000	0.0000	
1	1	61	76	15	1	61	76	30	0	0	0	0.1000	0.0000	
1	1	61	84	15	1	61	84	30	0	0	0	0.1000	0.0000	
1	1	63	93	15	1	63	93	30	1	63	93	0.3000	0.2000	
1	1	61	75	15	1	61	75	30	0	0	0	0.1000	0.0000	
1	1	61	87	15	1	61	87	30	0	0	0	0.1000	0.0000	
1	1	62	92	15	1	62	92	30	1	62	92	0.2000	0.1000	
1	1	62	83	15	1	62	83	30	0	0	0	0.2000	0.1000	
1	1	62	87	15	1	62	87	30	0	0	0	0.2000	0.1000	
1	1	61	84	15	1	61	84	30	0	0	0	0.1000	0.0000	
1	1	61	75	15	1	61	75	30	0	0	0	0.1000	0.0000	
1	1	61	77	15	1	61	77	30	0	0	0	0.1000	0.0000	
1	1	62	88	15	1	62	88	30	0	0	0	0.2000	0.1000	
1	1	61	83	15	1	61	83	30	0	0	0	0.1000	0.0000	
1	1	61	73	15	1	61	73	30	0	0	0	0.1000	0.0000	
1	1	62	76	15	1	62	76	30	0	0	0	0.2000	0.1000	
1	7	69	70	15	1	69	101	30	1	69	101	0.3000	1.5667	
1	121	57	146	15	1	2	596	30	1	2	596	0.1000	0.4333	
1	137	93	135	15	1	2	595	30	1	2	595	1.1000	1.3000	
1	15	81	83	15	2	81	142	30	1	81	142	0.7000	2.3667	
2	##	97	105	15	1	2	595	30	1	2	595	1.2333	0.3333	
2	##	428	442	15	1	2	596	30	1	2	596	12.2667	9.7333	
2	94	81	85	15	8	##	413	30	3	##	413	0.7000	1.4667	
2	##	105	111	15	3	2	460	30	2	2	460	1.5000	0.6333	
3	18	101	103	15	1	68	137	30	1	68	137	1.3667	1.4000	
3	##	77	86	15	1	2	596	30	1	2	596	0.5667	0.9667	
3	55	105	112	15	12	69	189	30	2	69	189	1.5000	2.5333	
3	112	77	82	15	1	2	595	30	1	2	595	0.5667	1.3000	
3	107	81	86	15	6	53	381	30	4	53	381	0.7000	2.3000	

3	16	138	141	15	3	106	147	30	1	106	147	2.6000	2.0000
3	8	98	100	15	1	79	114	30	1	79	114	1.2667	1.2000
3	72	135	144	15	11	76	183	30	4	76	183	2.5000	1.6000
3	#	88	96	15	1	6	586	30	1	6	586	0.9333	1.7000
3	75	116	119	15	11	#	544	30	4	#	544	1.8667	0.6667
3	12	117	120	15	1	92	137	30	1	92	137	1.9000	1.5333
3	4	78	79	15	2	125	140	30	0	0	0	0.3000	1.2167
3	117	157	167	15	2	2	541	30	2	2	541	1.6167	2.0833
3	152	136	146	15	1	2	596	30	1	2	596	1.2667	0.8833
3	65	144	165	15	11	57	249	30	1	57	249	1.4000	1.6833
3	38	182	188	15	1	115	279	30	1	115	279	2.0333	2.2667
3	92	107	112	15	9	8	229	30	4	8	229	0.7833	1.3500
3	#	161	173	15	1	4	594	30	1	4	594	1.6833	1.0500
3	#	539	548	15	1	8	591	30	1	8	591	7.9833	6.8333
3	8	109	111	15	3	72	111	30	1	72	111	0.8167	0.7667
3	11	71	73	15	3	71	113	30	1	71	113	0.1833	1.6833
3	127	308	313	15	3	#	594	30	3	#	594	4.1333	2.9167
3	17	81	83	15	9	65	83	30	0	0	0	0.3500	1.1333
3	#	8	15	15	2	2	576	30	1	2	576	0.8667	2.3667
3	154	76	86	15	1	2	596	30	1	2	596	0.2667	1.2500
3	6	97	98	15	3	142	162	30	0	0	0	0.6167	1.7500
3	6	107	109	15	1	84	117	30	1	84	117	0.7833	1.6000
3	119	38	42	15	3	2	363	30	3	2	363	0.3667	2.0667
3	99	94	99	15	5	195	432	30	5	195	432	0.5667	1.1333
3	#	27	34	15	2	2	532	30	2	2	532	0.5500	1.9500
3	5	145	146	15	3	145	166	30	0	0	0	1.4167	2.2833
3	79	140	146	15	12	81	289	30	1	81	289	0.6667	1.3000
3	#	105	112	15	1	2	596	30	1	2	596	0.3750	1.2000
3	#	327	331	15	8	56	308	30	5	56	308	2.2250	0.9000
3	0	0	0	15	0	0	0	30	0	0	0	0.5000	2.5250
3	77	171	176	15	8	24	370	30	2	24	370	0.9250	1.7250
3	91	107	110	15	7	65	343	30	3	65	343	0.3917	1.8000
3	0	0	0	15	0	0	0	30	0	0	0	0.5000	3.1333
3	125	191	199	15	1	2	592	30	1	2	592	1.0917	1.2083
3	#	104	109	15	1	4	594	30	1	4	594	0.3667	0.9333
3	40	238	244	15	1	165	355	30	1	165	355	1.4833	1.7417
3	66	321	326	15	3	#	507	30	1	#	507	2.1750	2.7167
3	50	123	126	15	6	123	323	30	1	123	323	0.5250	1.9000
3	44	290	295	15	1	146	373	30	1	146	373	1.9167	1.4083
3	45	261	264	15	4	174	333	30	1	174	333	1.6750	1.6833
3	56	358	363	15	2	#	434	30	2	#	434	2.4833	1.4333
3	45	263	268	15	1	140	354	30	1	140	354	1.6917	1.4333
3	#	137	143	15	1	2	592	30	1	2	592	0.6417	1.1417
3	#	325	332	15	6	67	466	30	2	67	466	2.2083	1.0833
3	110	114	117	15	4	5	309	30	3	5	309	0.4500	1.0417
3	#	142	148	15	1	8	596	30	1	8	596	0.6833	1.4167
3	45	138	142	15	2	138	344	30	1	138	344	0.6500	2.1583
3	54	35	37	15	17	#	411	30	3	#	411	0.2083	1.6000
3	16	228	230	15	5	#	284	30	1	#	284	1.4000	1.6167
3	37	80	82	15	13	125	183	30	1	125	183	0.1667	1.3167
3	#	104	111	15	2	#	595	30	2	#	595	0.3667	1.2333
3	113	372	377	15	2	3	445	30	2	3	445	2.6000	0.5500
3	#	144	152	15	1	5	596	30	1	5	596	0.7000	1.6833
3	84	161	165	15	8	124	255	30	5	124	255	0.8417	1.4000
3	12	124	125	15	4	#	295	30	1	#	295	0.5333	2.0583
3	44	242	247	15	3	187	375	30	1	187	375	1.5167	2.1000
3	69	253	259	15	1	140	439	30	1	140	439	1.6083	2.2250
3	42	279	284	15	2	185	376	30	1	185	376	1.8250	1.7750
3	0	0	0	15	0	0	0	30	0	0	0	0.5000	4.3333
3	59	97	100	15	12	84	269	30	2	84	269	0.3083	1.4833
3	87	154	159	15	7	78	315	30	5	78	315	0.7833	0.4333
3	39	280	292	15	2	190	392	30	1	190	392	1.8333	1.8417
3	77	297	303	15	3	166	462	30	1	166	462	1.9750	2.4250
3	69	151	156	15	9	78	307	30	2	78	307	0.7583	1.3333
3	44	138	141	15	2	126	379	30	1	126	379	0.6500	2.2333
3	41	281	284	15	3	96	262	30	2	96	262	1.8417	0.9250
3	9	328	330	15	2	#	330	30	1	#	330	2.2333	2.1417
3	43	157	165	15	2	94	269	30	1	94	269	0.8083	1.1500
3	41	259	359	15	1	176	464	30	1	176	464	1.6583	1.7500
3	39	137	141	15	1	77	272	30	1	77	272	0.6417	1.3250
3	10	241	243	15	4	189	204	30	0	0	0	1.5083	0.4417
3	20	189	195	15	1	98	229	30	1	98	229	1.0750	0.5250
3	84	139	144	15	9	#	595	30	5	#	595	0.6583	0.8667
3	31	116	120	15	3	68	154	30	2	68	154	0.4667	1.2667
3	38	161	166	15	1	83	257	30	1	83	257	0.8417	0.9583
3	7	186	188	15	6	#	210	30	0	0	0	1.0500	0.8833
3	39	196	205	15	1	121	294	30	1	121	294	1.1333	1.4167
3	41	222	354	15	1	131	454	30	1	131	454	1.3500	1.4583

3	36	193	290	15	1	111	346	30	1	111	346	1.1083	0.9500
3	30	115	118	15	1	84	206	30	1	84	206	0.4583	1.0250
3	45	98	102	15	2	70	263	30	1	70	263	0.3167	1.5750
3	64	163	166	15	1	131	447	30	1	131	447	0.8583	2.8750
3	26	106	108	15	3	157	240	30	2	157	240	0.3833	1.5083
3	35	226	230	15	5	111	246	30	1	111	246	1.3833	1.2083
3	44	134	137	15	1	116	353	30	1	116	353	0.6167	2.2167
3	7	95	96	15	2	95	153	30	1	95	153	0.2917	0.9833
3	54	104	106	15	13	173	271	30	3	173	271	0.3667	2.1750
3	47	112	114	15	12	181	258	30	3	181	258	0.4333	1.5917
3	59	243	248	15	9	82	252	30	2	82	252	1.5250	0.5500
3	56	89	91	15	12	##	313	30	3	##	313	0.2417	2.4333
3	39	183	187	15	8	98	233	30	2	98	233	1.0250	0.9750
3	31	8	9	15	13	98	133	30	1	98	133	0.4333	2.0500
3	42	253	256	15	13	##	278	30	2	##	278	1.6083	0.5750
3	50	283	290	15	7	197	411	30	1	197	411	1.8583	2.0167
3	65	239	244	15	8	114	269	30	5	114	269	1.4917	0.6250
3	101	205	210	15	8	101	368	30	3	101	368	1.2083	1.5833
3	50	92	94	15	15	321	382	30	2	321	382	0.2667	0.9333
3	51	117	119	15	14	51	119	30	3	51	119	0.4750	1.8000
3	46	244	248	15	8	199	354	30	2	199	354	1.5333	1.7833
3	40	225	232	15	5	183	263	30	2	183	263	1.3750	1.3000
3	64	134	136	15	14	##	535	30	5	##	535	0.6167	1.7250
3	48	271	276	15	9	219	332	30	1	219	332	1.7583	1.4333
3	48	104	106	15	11	##	475	30	3	##	475	0.3667	1.8750
3	32	259	261	15	15	111	153	30	2	111	153	1.6583	1.1167
3	19	369	372	15	12	127	154	30	0	0	0	2.5750	0.2417
3	58	178	180	15	11	171	282	30	3	171	282	0.9833	2.0000
3	77	225	230	15	7	29	186	30	3	29	186	1.3750	1.2583
3	40	133	137	15	11	90	213	30	1	90	213	0.6083	1.0333
3	24	279	282	15	13	318	363	30	1	318	363	1.8250	1.8750
3	47	281	284	15	6	189	407	30	1	189	407	1.8417	1.9417
3	107	116	122	15	5	78	254	30	5	78	254	0.4667	1.2917
3	##	69	72	15	5	149	467	30	4	149	467	0.0750	1.6250
3	117	203	208	15	2	##	596	30	2	##	596	1.1917	0.7833
3	51	228	235	15	3	122	334	30	1	122	334	1.4000	1.4833
3	36	33	36	15	14	54	95	30	1	54	95	0.2250	1.4500
3	33	145	148	15	3	114	233	30	1	114	233	0.7083	1.2750
3	##	184	192	15	5	52	444	30	2	52	444	1.0333	1.3333
3	##	97	101	15	5	5	347	30	3	5	347	0.3083	2.1667
3	97	254	258	15	5	2	329	30	4	2	329	1.6167	0.2000
3	##	220	226	15	1	2	591	30	1	2	591	1.3333	0.9250
3	75	120	126	15	12	93	269	30	2	93	269	0.5000	1.2833
3	43	136	139	15	10	98	270	30	1	98	270	0.6333	1.4917
3	45	251	257	15	1	198	385	30	1	198	385	1.5917	2.1083
3	50	102	106	15	9	26	257	30	1	26	257	0.3500	1.2083
3	52	240	245	15	12	89	265	30	1	89	265	1.5000	0.5750
3	25	190	193	15	7	181	268	30	2	181	268	1.0833	1.1083
3	14	127	359	15	1	112	390	30	1	112	390	0.5583	0.5250
3	11	115	363	15	2	101	380	30	1	101	380	0.4583	0.4167
3	8	89	311	15	3	87	323	30	1	87	323	0.2417	0.2500
3	0	0	0	15	0	0	0	30	0	0	0	0.5000	3.9833
3	20	102	359	15	7	85	387	30	1	85	387	0.3500	0.3083
3	11	105	290	15	1	98	330	30	1	98	330	0.3750	0.3667
3	13	113	339	15	2	100	372	30	1	100	372	0.4417	0.2667
3	9	140	386	15	1	118	414	30	1	118	414	0.6667	0.5667
3	0	0	0	15	0	0	0	30	0	0	0	0.5000	4.2083
3	14	86	306	15	5	80	327	30	1	80	327	0.2167	0.2750
3	14	112	350	15	2	98	388	30	1	98	388	0.4333	0.4167
3	15	108	319	15	2	95	364	30	1	95	364	0.4000	0.3833
3	17	133	193	15	8	67	199	30	1	67	199	0.6083	0.1000
3	69	73	205	15	7	34	383	30	2	34	383	0.1083	0.0917
3	9	137	381	15	1	124	396	30	1	124	396	0.6417	0.6167
3	17	136	415	15	3	113	456	30	1	113	456	0.6333	0.6250
3	18	90	306	15	5	81	320	30	1	81	320	0.2500	0.2750
3	11	93	287	15	6	79	296	30	1	79	296	0.2750	0.2250
3	5	85	237	15	2	79	244	30	1	79	244	0.2083	0.1917
3	15	81	233	15	5	76	249	30	1	76	249	0.1750	0.1917
3	50	245	253	15	5	116	320	30	1	116	320	1.5417	0.8583
3	52	218	229	15	6	147	340	30	1	147	340	1.3167	1.3583
3	23	239	242	15	10	##	276	30	2	##	276	1.4917	1.2917
3	23	192	195	15	8	##	283	30	1	##	283	1.1000	1.2167
3	47	170	330	15	5	105	438	30	1	105	438	0.9167	1.0833
3	71	157	160	15	7	103	382	30	1	103	382	0.8083	2.1167
3	60	155	159	15	8	105	319	30	2	105	319	0.7917	1.5833
3	88	153	160	15	10	88	340	30	1	88	340	0.7750	1.3250
3	64	233	250	15	6	154	425	30	1	154	425	1.4417	2.0417
3	68	231	235	15	5	97	363	30	2	97	363	1.4250	1.3833

3	46	176	349	15	5	101	441	30	1	101	441	0.9667	0.8500
3	47	148	151	15	8	131	351	30	1	131	351	0.7333	2.2250
3	63	123	128	15	10	94	381	30	1	94	381	0.5250	1.7083
3	43	185	191	15	3	154	344	30	1	154	344	1.0417	1.7583
3	21	205	207	15	6	191	228	30	2	191	228	1.2083	0.9583
3	44	197	201	15	9	98	240	30	1	98	240	1.1417	0.7667
3	47	205	381	15	3	111	501	30	1	111	501	1.2083	1.2417
3	6	323	325	15	3	#	325	30	0	0	0	2.1917	1.8000
3	19	136	138	15	7	#	309	30	2	#	309	0.6333	2.1167
3	48	241	382	15	4	147	515	30	1	147	515	1.5083	1.7667

**Table B.4 Detection Comparison: FAPI Detection Results**

FAPI	N	Y	#T	En1	Ex2	FAR1	#T	En1	Ex2	FAR2	#T	En1	Ex2	FAPI	
														DiffFE1	DiffFE2
1	2	1	1	62	164	15	1	62	164	50	1	62	164	0.0667	1.6333
	2	1	1	63	199	15	1	63	199	50	1	63	199	0.1000	1.5333
2	1	1	1	62	189	15	1	62	189	50	1	62	189	0.0667	1.6667
2	1	1	1	62	149	15	1	62	149	50	1	62	149	0.0667	1.4000
1	1	1	1	63	188	15	1	63	188	50	1	63	188	0.1000	1.5000
1	1	1	1	63	199	15	1	63	199	50	1	63	199	0.1000	1.5333
1	1	1	1	62	186	15	1	62	186	50	1	62	186	0.0667	1.5333
1	1	1	1	62	174	15	1	62	174	50	1	62	174	0.0667	1.6000
1	1	1	1	62	163	15	1	62	163	50	1	62	163	0.0667	1.6333
1	1	1	1	62	194	15	1	62	194	50	1	62	194	0.0667	1.5333
1	1	1	1	62	180	15	1	62	180	50	1	62	180	0.0667	1.5667
1	1	1	1	62	206	15	1	62	206	50	1	62	206	0.0667	1.8667
1	1	1	1	62	228	15	1	62	228	50	1	62	228	0.0667	1.8000
1	1	1	1	62	171	15	1	62	171	50	1	62	171	0.0667	1.6000
1	1	1	1	63	213	15	1	63	213	50	1	63	213	0.1000	1.5000
1	1	1	1	62	199	15	1	62	199	50	1	62	199	0.0667	1.6333
1	1	1	1	62	160	15	1	62	160	50	1	62	160	0.0667	1.6000
1	1	1	1	62	193	15	1	62	193	50	1	62	193	0.0667	1.5333
1	1	1	1	62	165	15	1	62	165	50	1	62	165	0.0667	1.6333
1	1	1	1	63	201	15	1	63	201	50	1	63	201	0.1000	1.5333
1	1	1	1	63	291	15	1	63	291	50	1	63	291	0.1000	1.2333
1	1	1	1	63	175	15	1	63	175	50	1	63	175	0.1000	1.1333
1	1	1	1	63	182	15	1	63	182	50	1	63	182	0.1000	1.1333
1	1	1	1	64	181	15	1	64	181	50	1	64	181	0.1333	0.9333
1	1	1	1	64	223	15	1	64	223	50	1	64	223	0.1333	1.1667
1	1	1	1	64	276	15	1	64	276	50	1	64	276	0.1333	1.0000
1	1	1	1	63	204	15	1	63	204	50	1	63	204	0.1000	1.2333
1	1	1	1	64	210	15	1	64	210	50	1	64	210	0.1333	1.1333
1	1	1	1	64	236	15	1	64	236	50	1	64	236	0.1333	1.0667
1	1	1	1	64	223	15	1	64	223	50	1	64	223	0.1333	1.0667
1	1	1	1	63	232	15	1	63	232	50	1	63	232	0.1000	1.3667
1	1	1	1	64	199	15	1	64	199	50	1	64	199	0.1333	0.9333
1	1	1	1	64	255	15	1	64	255	50	1	64	255	0.1333	1.0333
1	1	1	1	64	209	15	1	64	209	50	1	64	209	0.1333	1.1333
1	1	1	1	63	200	15	1	63	200	50	1	63	200	0.1000	1.2333
1	1	1	1	64	227	15	1	64	227	50	1	64	227	0.1333	1.0667
1	1	1	1	64	217	15	1	64	217	50	1	64	217	0.1333	1.0667
1	1	1	1	63	230	15	1	63	230	50	1	63	230	0.1000	1.3667
1	1	1	1	64	214	15	1	64	214	50	1	64	214	0.1333	1.1000
1	1	1	1	64	231	15	1	64	231	50	1	64	231	0.1333	1.0667
1	1	1	1	62	159	15	1	62	159	50	1	62	159	0.2000	6.1000
1	1	1	1	62	128	15	1	62	128	50	1	62	128	0.2000	4.8000
1	1	1	1	62	157	15	1	62	157	50	1	62	157	0.2000	6.0000
1	1	1	1	62	134	15	1	62	134	50	1	62	134	0.2000	5.0000
1	1	1	1	62	134	15	1	62	134	50	1	62	134	0.2000	5.0000
1	1	1	1	62	117	15	1	62	117	50	1	62	117	0.2000	4.1000
1	1	1	1	62	133	15	1	62	133	50	1	62	133	0.2000	4.9000
1	1	1	1	62	149	15	1	62	149	50	1	62	149	0.2000	5.4000
1	1	1	1	62	122	15	1	62	122	50	1	62	122	0.2000	4.7000
1	1	1	1	62	137	15	1	62	137	50	1	62	137	0.2000	5.0000
1	1	1	1	62	154	15	1	62	154	50	1	62	154	0.2000	6.1000
1	1	1	1	62	139	15	1	62	139	50	1	62	139	0.2000	5.5000
1	1	1	1	62	138	15	1	62	138	50	1	62	138	0.2000	5.0000
1	1	1	1	62	133	15	1	62	133	50	1	62	133	0.2000	4.9000
1	1	1	1	62	116	15	1	62	116	50	1	62	116	0.2000	4.1000
1	1	1	1	62	119	15	1	62	119	50	1	62	119	0.2000	4.2000
1	1	1	1	62	150	15	1	62	150	50	1	62	150	0.2000	6.1000
1	1	1	1	62	133	15	1	62	133	50	1	62	133	0.2000	5.0000
1	1	1	1	62	113	15	1	62	113	50	1	62	113	0.2000	4.0000
1	1	1	1	62	124	15	1	62	124	50	1	62	124	0.2000	4.7000
1	1	1	38	109	118	15	8	64	134	50	2	64	134	1.6333	0.0333
1	1	29	66	162	15	8	66	225	50	1	66	225	0.2000	0.1000	
1	1	1	2	581	15	1	2	581	50	1	2	581	1.9333	13.5667	
1	1	1	2	581	15	1	2	581	50	1	2	581	1.9333	14.2333	
2	1	1	2	581	15	1	2	581	50	1	2	581	1.9333	15.5333	
2	1	1	2	581	15	1	2	581	50	1	2	581	1.9333	14.3667	
2	1	18	75	101	15	7	69	135	50	1	69	135	0.5000	0.9333	
2	1	13	105	116	15	2	72	126	50	1	72	126	1.5000	0.4667	
2	1	1	2	581	15	1	2	581	50	1	2	581	1.9333	14.5333	
2	1	1	2	581	15	1	2	581	50	1	2	581	1.9333	15.5333	
2	1	1	2	581	15	1	2	581	50	1	2	581	1.9333	13.1000	
2	1	1	2	581	15	1	2	581	50	1	2	581	1.9333	15.3333	
2	1	1	2	581	15	1	2	581	50	1	2	581	1.9333	14.2000	

2	1	1	2	581	15	1	2	581	50	1	2	581	1.9333	12.6667
2	1	1	2	581	15	1	2	581	50	1	2	581	1.9333	14.8333
2	1	30	90	192	15	9	81	206	50	1	81	206	1.0000	0.0000
2	1	30	80	158	15	9	69	208	50	1	69	208	0.6667	0.3667
2	1	1	2	581	15	1	2	581	50	1	2	581	1.9333	14.7333
2	1	1	2	581	15	1	2	581	50	1	2	581	1.9333	13.8333
2	1	1	2	581	15	1	2	581	50	1	2	581	0.9667	7.1500
2	1	1	2	581	15	1	2	581	50	1	2	581	0.9667	4.8167
2	1	37	77	117	15	8	67	218	50	4	67	218	0.2833	1.3667
2	1	1	2	581	15	1	2	581	50	1	2	581	0.9667	5.2500
2	1	33	94	315	15	9	70	337	50	2	70	337	0.5667	0.1500
2	1	1	2	581	15	1	2	581	50	1	2	581	0.9667	6.4667
2	1	1	2	581	15	1	2	581	50	1	2	581	0.9667	5.7500
2	1	1	2	581	15	1	2	581	50	1	2	581	0.9667	7.3833
2	1	1	2	581	15	1	2	581	50	1	2	581	0.9667	7.0667
2	1	1	2	581	15	1	2	581	50	1	2	581	0.9667	6.7833
2	1	1	2	581	15	1	2	581	50	1	2	581	0.9667	7.3833
2	1	1	2	581	15	1	2	581	50	1	2	581	0.9667	7.1667
2	1	105	189	202	15	6	49	264	50	5	49	264	2.1500	0.7500
2	1	15	88	90	15	7	82	108	50	0	0	0	0.4667	1.1833
2	1	7	114	124	15	2	147	172	50	0	0	0	0.9000	1.3167
2	1	1	2	581	15	1	2	581	50	1	2	581	0.9667	6.2667
2	1	18	21	27	15	4	103	153	50	1	103	153	0.6500	2.3167
2	1	1	2	581	15	1	2	581	50	1	2	581	0.9667	6.9000
2	1	1	2	581	15	1	2	581	50	1	2	581	0.9667	7.1667
2	1	12	144	221	15	1	116	262	50	1	116	262	1.4000	1.0333
2	1	40	120	286	15	9	89	301	50	1	89	301	0.5000	0.1333
2	1	1	2	581	15	1	2	581	50	1	2	581	0.4833	2.7083
2	1	1	2	581	15	1	2	581	50	1	2	581	0.4833	1.1833
2	1	1	2	581	15	1	2	581	50	1	2	581	0.4833	2.3167
2	1	60	169	188	15	5	58	330	50	1	58	330	0.9083	1.6250
2	1	15	118	313	15	6	76	319	50	1	76	319	0.4833	0.1083
2	1	40	149	189	15	6	100	350	50	1	100	350	0.7417	1.5583
2	1	1	2	581	15	1	2	581	50	1	2	581	0.4833	1.9750
2	1	32	142	157	15	6	109	255	50	1	109	255	0.6833	0.5333
2	1	1	2	581	15	1	2	581	50	1	2	581	0.4833	1.0667
2	1	16	205	535	15	3	178	580	50	1	178	580	1.2083	4.4583
2	1	1	2	581	15	1	2	581	50	1	2	581	0.4833	1.8917
2	1	9	87	446	15	5	87	467	50	1	87	467	0.2250	0.1500
2	1	1	2	581	15	1	2	581	50	1	2	581	0.4833	0.9583
2	1	21	85	484	15	3	85	580	50	1	85	580	0.2083	0.4250
2	1	1	2	581	15	1	2	581	50	1	2	581	0.4833	1.1750
2	1	80	132	172	15	8	39	281	50	2	39	281	0.6000	0.9000
2	1	1	2	581	15	1	2	581	50	1	2	581	0.4833	0.9917
2	1	35	50	167	15	7	6	228	50	2	6	228	0.0833	0.6250
2	1	15	117	281	15	5	87	314	50	1	87	314	0.4750	0.3083
2	1	1	2	581	15	1	2	581	50	1	2	581	0.4833	1.5000
2	1	2	111	112	15	1	111	114	50	0	0	0	0.4250	0.9750
2	1	1	2	581	15	1	2	581	50	1	2	581	0.4833	1.3083
2	1	1	2	581	15	1	2	581	50	1	2	581	0.4833	2.8417
2	1	8	143	180	15	3	133	185	50	1	133	185	0.6917	0.6583
2	1	1	2	581	15	1	2	581	50	1	2	581	0.4833	1.1500
2	1	1	2	581	15	1	2	581	50	1	2	581	0.4833	1.8917
2	1	1	2	581	15	1	2	581	50	1	2	581	0.4833	2.0667
2	1	1	2	581	15	1	2	581	50	1	2	581	0.4833	1.7417
2	1	1	2	581	15	1	2	581	50	1	2	581	0.4833	0.6833
2	1	1	2	581	15	1	2	581	50	1	2	581	0.4833	0.4583
2	1	1	2	581	15	1	2	581	50	1	2	581	0.4833	0.7000
2	1	1	2	581	15	1	2	581	50	1	2	581	0.4833	0.5083
2	1	54	99	268	15	3	49	345	50	2	49	345	0.3250	0.0833
2	1	1	2	581	15	1	2	581	50	1	2	581	0.4833	3.0833
2	1	1	2	581	15	1	2	581	50	1	2	581	0.4833	0.5667
2	1	13	123	534	15	3	121	551	50	1	121	551	0.5250	0.5000
2	1	1	2	581	15	1	2	581	50	1	2	581	0.4833	2.2083
2	1	11	72	407	15	4	72	481	50	1	72	481	0.1000	0.0167
2	1	1	2	581	15	1	2	581	50	1	2	581	0.4833	1.5500
2	1	1	2	581	15	1	2	581	50	1	2	581	0.4833	0.0500
2	1	23	71	323	15	1	2	579	50	1	2	579	0.0917	0.1667
2	1	1	2	581	15	1	2	581	50	1	2	581	0.4833	0.1000
2	1	1	2	581	15	1	2	581	50	1	2	581	0.4833	2.3417
2	1	1	2	581	15	1	2	581	50	1	2	581	0.4833	2.3750
2	1	22	82	264	15	9	70	264	50	2	70	264	0.1833	0.0500
2	1	44	136	156	15	6	78	238	50	1	78	238	0.6333	0.7667
2	1	1	2	581	15	1	2	581	50	1	2	581	0.4833	2.5750
2	1	10	90	273	15	5	71	287	50	1	71	287	0.2500	0.0667
2	1	13	103	282	15	5	73	299	50	1	73	299	0.3583	0.1000
2	1	1	2	581	15	1	2	581	50	1	2	581	0.4833	1.7167
2	1	1	2	581	15	1	2	581	50	1	2	581	0.4833	0.4333

2	1	1	2	581	15	1	2	581	50	1	2	581	0.4833	1.4750
2	1	1	2	581	15	1	2	581	50	1	2	581	0.4833	2.8333
2	1	1	2	581	15	1	2	581	50	1	2	581	0.4833	2.4167
2	1	16	86	479	15	6	82	497	50	1	82	497	0.2167	0.2667
2	1	1	2	581	15	1	2	581	50	1	2	581	0.4833	2.4333
2	1	17	72	370	15	4	72	389	50	2	72	389	0.1000	0.0417
2	1	1	2	581	15	1	2	581	50	1	2	581	0.4833	1.4833
2	1	32	67	241	15	5	30	260	50	3	30	260	0.0583	0.2250
2	1	11	117	144	15	6	111	165	50	1	111	165	0.4750	1.8583
2	1	17	100	173	15	5	92	295	50	1	92	295	0.3333	1.1000
2	1	31	86	287	15	7	53	321	50	2	53	321	0.2167	0.2250
2	1	1	2	581	15	1	2	581	50	1	2	581	0.4833	1.6500
2	1	1	2	581	15	1	2	581	50	1	2	581	0.4833	2.3083
2	1	1	2	581	15	1	2	581	50	1	2	581	0.4833	2.7167
2	1	1	2	581	15	1	2	581	50	1	2	581	0.4833	2.1333
2	1	8	169	483	15	1	140	544	50	1	140	544	0.9083	0.4083
2	1	1	2	581	15	1	2	581	50	1	2	581	0.4833	2.1833
2	1	1	2	581	15	1	2	581	50	1	2	581	0.4833	1.5083
2	1	26	451	488	15	8	21	135	50	3	21	135	3.2583	2.3500
2	1	48	168	248	15	10	156	333	50	4	156	333	0.9000	0.7250
2	1	1	2	581	15	1	2	581	50	1	2	581	0.4833	0.9917
2	1	1	2	581	15	1	2	581	50	1	2	581	0.4833	1.6083
2	1	1	2	581	15	1	2	581	50	1	2	581	0.4833	1.9833
2	1	1	2	581	15	1	2	581	50	1	2	581	0.4833	1.1083
2	1	36	95	315	15	1	5	579	50	1	5	579	0.2917	0.1333
2	1	13	304	358	15	3	260	358	50	2	##	358	2.0333	0.3083
2	1	17	145	152	15	6	372	406	50	0	0	0	0.7083	2.0750
2	1	18	116	398	15	4	93	403	50	2	93	403	0.4667	0.1833
2	1	1	2	581	15	1	2	581	50	1	2	581	0.4833	1.6667
2	1	1	2	581	15	1	2	581	50	1	2	581	0.4833	2.6667
2	1	35	156	470	15	4	120	578	50	1	120	578	0.8000	0.3083
2	1	10	184	450	15	3	135	450	50	1	135	450	1.0333	0.5583
2	1	17	106	222	15	6	89	312	50	1	89	312	0.3833	0.4583
2	1	1	2	581	15	1	2	581	50	1	2	581	0.4833	2.6167
2	1	1	2	581	15	1	2	581	50	1	2	581	0.4833	2.3250
2	1	1	2	581	15	1	2	581	50	1	2	581	0.4833	1.4000
2	1	1	2	581	15	1	2	581	50	1	2	581	0.4833	3.0917
2	1	1	2	581	15	1	2	581	50	1	2	581	0.4833	2.3333
2	1	1	2	581	15	1	2	581	50	1	2	581	0.4833	1.9083
2	1	1	2	581	15	1	2	581	50	1	2	581	0.4833	1.8333
2	1	1	2	581	15	1	2	581	50	1	2	581	0.4833	2.4917
2	1	1	2	581	15	1	2	581	50	1	2	581	0.4833	2.0333
2	1	25	53	259	15	2	39	578	50	1	39	578	0.0583	0.1750
2	1	20	95	340	15	5	36	356	50	1	36	356	0.2917	0.1833
2	1	1	2	581	15	1	2	581	50	1	2	581	0.4833	0.5917
2	1	1	2	581	15	1	2	581	50	1	2	581	0.4833	2.7500
2	1	1	2	581	15	1	2	581	50	1	2	581	0.4833	2.2250
2	1	1	2	581	15	1	2	581	50	1	2	581	0.4833	2.1250
2	1	1	2	581	15	1	2	581	50	1	2	581	0.4833	1.3250
2	1	6	65	542	15	2	65	568	50	1	65	568	0.0417	1.0750
2	1	7	53	370	15	2	53	513	50	1	53	513	0.0583	0.2417
2	1	14	70	498	15	1	2	581	50	1	2	581	0.0833	0.1667
2	1	1	2	581	15	1	2	581	50	1	2	581	0.4833	1.5417
2	1	7	61	478	15	3	61	511	50	1	61	511	0.0083	1.2000
2	1	2	49	527	15	1	49	548	50	1	49	548	0.0917	1.3000
2	1	5	77	539	15	2	77	564	50	1	77	564	0.1417	0.7083
2	1	6	83	508	15	3	83	536	50	1	83	536	0.1917	0.0250
2	1	1	2	581	15	1	2	581	50	1	2	581	0.4833	2.0167
2	1	1	2	581	15	1	2	581	50	1	2	581	0.4833	1.5083
2	1	11	67	552	15	2	43	581	50	1	43	581	0.0583	1.5583
2	1	20	70	231	15	9	70	280	50	2	70	280	0.0833	0.2167
2	1	26	57	311	15	4	3	362	50	3	3	362	0.0250	0.7917
2	1	1	2	581	15	1	2	581	50	1	2	581	0.4833	1.0500
2	1	1	2	581	15	1	2	581	50	1	2	581	0.4833	0.7583
2	1	1	2	581	15	1	2	581	50	1	2	581	0.4833	2.0167
2	1	10	64	358	15	3	64	578	50	1	64	578	0.0333	0.3667
2	1	27	67	391	15	4	7	427	50	2	7	427	0.0583	1.0917
2	1	1	2	581	15	1	2	581	50	1	2	581	0.4833	2.7083
2	1	9	102	339	15	2	95	365	50	1	95	365	0.3500	0.1417
2	1	17	78	416	15	3	46	493	50	2	46	493	0.1500	0.2000
2	1	1	2	581	15	1	2	581	50	1	2	581	0.4833	1.5333
2	1	1	2	581	15	1	2	581	50	1	2	581	0.4833	2.0000
2	1	1	2	581	15	1	2	581	50	1	2	581	0.4833	1.0083
2	1	19	99	393	15	6	73	460	50	1	73	460	0.3250	0.1750
2	1	23	97	331	15	5	73	360	50	1	73	360	0.3083	0.1500
2	1	1	2	581	15	1	2	581	50	1	2	581	0.4833	2.1833
2	1	17	101	467	15	5	94	494	50	1	94	494	0.3417	0.2333
2	1	1	2	581	15	1	2	581	50	1	2	581	0.4833	1.5000

2	1	1	2	581	15	1	2	581	50	1	2	581	0.4833	1.0833
2	1	1	2	581	15	1	2	581	50	1	2	581	0.4833	1.3583
2	1	1	2	581	15	1	2	581	50	1	2	581	0.4833	2.0667
2	1	1	2	581	15	1	2	581	50	1	2	581	0.4833	1.4917
2	1	2	95	308	15	2	95	308	50	1	95	308	0.2917	0.1167
2	1	1	2	581	15	1	2	581	50	1	2	581	0.4833	2.4000
2	1	1	2	581	15	1	2	581	50	1	2	581	0.4833	0.4250
2	1	1	2	581	15	1	2	581	50	1	2	581	0.4833	0.3333
2	1	1	2	581	15	1	2	581	50	1	2	581	0.4833	1.5750
2	1	8	132	540	15	2	123	568	50	1	123	568	0.6000	0.4500

**Table B.5 Analysis Comparison (w/Threshold Detect): Sensor and Target Information**

S Info	S Rate	Pixel X	Pixel Y	Noise	Jitter	T Info	#	Lengt h	Widt h	Speed	Ibk	ITgt	O Noise	En I	En 2	Ex I	Ex 2
	120	30	30	0.01	0		4	9.08	2.59	16.357	4	0.2	0.9	60	127	280	347
	120	30	30	0.01	0		5	19.27	2.44	16.521	6	0.2	0.9	60	200	278	418
	120	30	30	0.01	0		5	19.27	2.44	20.501	9	0.2	0.9	60	173	236	349
	120	30	30	0	0		2	10.19	2.44	16.614	7	0.2	0.9	60	134	277	351
	120	30	30	0	0		2	10.19	2.44	18.783	9	0.2	0.9	60	125	252	317
	120	30	30	0	0		1	4.57	2.16	20.132	1	0.2	0.9	60	87	239	266
	120	30	30	0	0		5	19.27	2.44	19.082	1	0.2	0.9	60	181	249	370
	120	30	30	0	0		1	4.57	2.16	27.225	5	0.2	0.9	60	80	192	212
	120	30	30	0	0		4	9.08	2.59	14.254	2	0.2	0.9	60	136	313	389
	120	30	30	0	0		1	4.57	2.16	28.584	8	0.2	0.9	60	79	186	205
	120	30	30	0	0		5	19.27	2.44	21.713	2	0.2	0.9	60	166	226	332
	120	30	30	0	0		2	10.19	2.44	16.710	4	0.2	0.9	60	133	275	348
	120	30	30	0	0		5	19.27	2.44	16.378	3	0.2	0.9	60	201	280	421
	120	30	30	0	0		1	4.57	2.16	17.041	5	0.2	0.9	60	92	271	303
	120	30	30	0	0		2	10.19	2.44	22.369	0.2	0.9	60	115	221	276	
	120	30	30	0	0		1	4.57	2.16	21.706	2	0.2	0.9	60	85	226	251
	120	30	30	0	0		5	19.27	2.44	15.759	3	0.2	0.9	60	207	288	435
	120	30	30	0	0		4	9.08	2.59	17.420	6	0.2	0.9	60	123	267	330
	120	30	30	0	0		2	10.19	2.44	14.234	9	0.2	0.9	60	146	313	399
	120	30	30	0	0		1	4.57	2.16	21.810	2	0.2	0.9	60	116	225	281
	120	30	30	0.04	0		2	10.19	2.44	20.940	4	0.2	0.9	60	108	232	280
	120	30	30	0.04	0		6	8.32	2.43	18.386	3	0.2	0.9	60	186	256	382
	120	30	30	0.04	0		5	19.27	2.44	15.235	0.2	0.9	60	132	296	368	
	120	30	30	0.04	0		4	9.08	2.59	15.543	8	0.2	0.9	60	130	292	362
	120	30	30	0.04	0		4	9.08	2.59	11.749	1	0.2	0.9	60	153	366	459
	120	30	5	0.04	0		4	9.08	2.59	15.645	0.2	0.9	60	138	290	368	
	120	30	5	0.04	0		2	10.19	2.44	20.122	5	0.2	0.9	60	121	239	300
	120	30	5	0.04	0		2	10.19	2.44	15.552	7	0.2	0.9	60	130	291	361
	120	30	5	0.04	0		4	9.08	2.59	23.284	6	0.2	0.9	60	103	215	258
	120	30	5	0.04	0		6	8.32	2.43	18.955	1	0.2	0.9	60	117	250	307
	120	30	5	0.04	0		6	8.32	2.43	18.052	5	0.2	0.9	60	115	259	314
	120	30	5	0.04	0		2	10.19	2.44	24.508	2	0.2	0.9	60	110	207	257
	120	30	5	0.04	0		5	19.27	2.44	15.052	1	0.2	0.9	60	214	299	453
	120	30	5	0.04	0		1	4.57	2.16	26.334	5	0.2	0.9	60	81	197	218
	120	30	5	0.04	0		6	8.32	2.43	13.837	7	0.2	0.9	60	132	320	392
	120	30	5	0.04	0		4	9.08	2.59	15.643	5	0.2	0.9	60	130	290	360
	120	30	5	0.04	0		3	24.89	3.68	15.305	6	0.2	0.9	60	255	295	490
	120	30	5	0.04	0		2	10.19	2.44	18.564	2	0.2	0.9	60	126	254	320
	90	30	5	0.02	0		3	24.89	3.68	15.262	0.2	0.9	60	207	237	384	
	90	30	5	0.02	0		1	4.57	2.16	20.895	9	0.2	0.9	60	80	189	209
	90	30	5	0.02	0		3	24.89	3.68	15.983	9	0.2	0.9	60	200	229	369
	90	30	5	0.02	0		1	4.57	2.16	22.602	5	0.2	0.9	60	78	179	197
	90	30	5	0.02	0		1	4.57	2.16	20.752	3	0.2	0.9	60	80	190	210
	90	30	5	0.02	0		6	8.32	2.43	22.509	8	0.2	0.9	60	93	180	213

90	30	5	0.02	0	3	24.89	3.68	16.013	2	0.2	0.9	60	200	229	369					
90	30	5	0.02	0	2	10.19	2.44	15.448	5	0.2	0.9	60	119	235	294					
90	30	5	0.02	0	6	8.32	2.43	16.011	1	0.2	0.9	60	107	229	276					
90	30	5	0.02	0	3	24.89	3.68	10.565	2	0.2	0.9	60	272	316	528					
90	30	10	0.02	0	4	9.08	2.59	13.783	9	0.2	0.9	60	119	256	315					
90	30	10	0.02	0	3	24.89	3.68	18.380	7	0.2	0.9	60	182	207	329					
90	30	10	0.02	0	4	9.08	2.59	19.937	7	0.2	0.9	60	101	195	236					
90	30	10	0.02	0	3	24.89	3.68	14.683	7	0.2	0.9	60	214	244	398					
90	30	10	0.02	0	5	19.27	2.44	20.277	8	0.2	0.9	60	146	193	279					
90	30	10	0.02	0	6	8.32	2.43	20.509	5	0.2	0.9	60	97	192	229					
90	30	10	0.02	0	5	19.27	2.44	13.352	7	0.2	0.9	60	190	262	392					
90	30	10	0.02	0	6	8.32	2.43	19.858	4	0.2	0.9	60	98	196	234					
90	30	10	0.02	0	6	8.32	2.43	11.593	6	0.2	0.9	60	130	293	363					
90	30	10	0.02	0	4	9.08	2.59	12.806	8	0.2	0.9	60	124	271	335					
90	30	30	0.02	0	4	9.08	2.59	19.318	3	0.2	0.9	60	176	200	316					
90	30	30	0.02	0	3	24.89	3.68	18.449	2	0.2	0.9	60	101	206	247					
90	30	30	0.02	0	6	8.32	2.43	17.600	9	0.2	0.9	60	159	213	312					
90	30	30	0.02	0	5	19.27	2.44	12.661	2	0.2	0.9	60	237	273	450					
90	30	30	0.02	0	3	24.89	3.68	24.497	1	0.2	0.9	60	91	170	201					
90	30	30	0.02	0	6	8.32	2.43	11.789	7	0.2	0.9	60	250	289	479					
90	30	30	0.02	0	3	24.89	3.68	19.450	7	0.2	0.9	60	81	199	220					
90	30	30	0.02	0	1	4.57	2.16	19.727	7	0.2	0.9	60	148	197	285					
90	30	30	0.02	0	5	19.27	2.44	10.488	9	0.2	0.9	60	274	317	531					
90	30	30	0.02	0	1	4.57	2.16	18.959	0	0.2	0.9	60	82	202	224					

Table B.6 Analysis Comparison (w/ Threshold Detection): PolyFit and FermiFit Results

Threshold	N	$\gamma$	#T	FAR2	#T	En1	Ex2	Poly	En1	En2	Ex1	Ex2	Fermi	En1	En2	Ex1	Ex2	
3	1		51	30	1	87	328	62.9	131	289	345	62.9	138	270	345			
3	1		25	30	1	101	378	58.7	196	276	419	58.7	184	284	419			
3	1		24	30	1	73	336	49.9	172	239	352	49.9	160	242	352			
3	1		1	30	1	107	305	60.7	136	275	350	61	144	267	350			
3	1		1	30	1	101	277	60.1	127	250	317	60	136	242	317			
3	1		0	30	0	0	0	60.1	127	250	317	60	133	244	317			
3	1		1	30	1	100	331	60.8	173	254	369	61	177	252	369			
3	1		0	30	0	0	0	60.8	173	254	369	61	155	275	369			
3	1		1	30	1	111	339	56.4	141	307	393	56	157	292	393			
3	1		0	30	0	0	0	56.4	141	307	393	56	155	294	393			
3	1		1	30	1	95	298	60.6	158	230	331	61	162	225	331			
3	1		1	30	1	106	303	60.7	135	273	347	61	143	265	347			
3	1		1	30	1	107	375	61.6	191	286	419	62	196	284	419			
3	1		0	30	0	0	0	61.6	191	286	419	62	173	308	419			
3	1		1	30	1	95	242	60.1	117	219	276	60	123	213	276			
3	1		0	30	0	0	0	60.1	117	219	276	60	120	216	276			
3	1		1	30	1	109	387	61.6	197	295	433	62	201	292	433			
3	1		1	30	1	102	289	57.2	127	263	332	57	137	252	332			
3	1		1	30	1	114	346	61.5	148	311	397	62	154	300	397			
2	1		132	30	2	23	405	0.76	157	325	341	1	117	225	341			
2	1		140	30	0	0	0	0.76	157	325	341	1	242	341				
2	1		125	30	2	20	505	28.7	228	408	517	29	206	340	517			
2	1		127	30	0	0	0	28.7	228	408	517	29	183	363	517			
2	1		121	30	3	21	395	49.1	119	276	385	49	166	268	385			
2	1		53	30	1	22	477	30.4	211	292	493	30	185	345	493			
2	1		71	30	2	20	381	33.7	195	253	392	34	164	262	392			
2	1		84	30	1	23	408	31.6	178	330	416	32	169	288	416			
2	1		78	30	0	0	0	31.6	178	330	416	32	159	288	416			
2	1		90	30	2	21	420	33.3	132	278	425	33	162	296	425			

2	1	86	30	2	60	325	44.1	138	221	339	44	149	242	339
2	1	85	30	2	66	331	52.5	128	233	340	53	158	234	340
2	1	57	30	1	73	250	58.4	106	208	258	58	118	198	258
2	1	53	30	1	79	456	56.8	206	215	482	57	202	338	482
2	1	101	30	4	61	210	58.9	90.3	191	214	59	99.2	174	214
2	1	66	30	1	61	385	45.6	143	312	408	46	153	301	408
2	1	74	30	2	63	352	44.5	139	283	365	44	162	247	365
2	1	40	30	1	58	488	30.4	339	212	518	30	198	350	518
2	1	81	30	2	75	299	59.3	124	254	313	59	133	239	313
2	1	64	30	5	22	388	33.7	322	251	387	34	162	259	387
2	1	109	30	3	58	209	57.5	84.3	188	207	58	84.1	181	207
2	1	53	30	3	22	403	34.7	295	152	390	35	157	268	390
2	1	104	30	5	52	204	56.5	85.5	177	200	56	88.2	168	200
2	1	83	30	1	50	211	53.3	84.4	194	209	53	86.5	176	209
2	1	101	30	5	61	246	51.9	127	237	241	52	118	175	241
2	1	53	30	1	62	368	58.7	188	243	370	59	171	258	370
2	1	77	30	2	64	308	38.7	165	324	301	39	132	208	301
2	1	87	30	1	55	282	57	111	226	277	57	106	229	277
2	1	29	30	1	61	524	58.5	253	335	530	59	225	363	530
2	1	68	30	1	80	314	66.7	120	264	312	67	139	240	312
2	1	68	30	2	63	338	61.6	169	200	337	62	159	240	337
2	1	105	30	5	62	243	60.7	99.7	197	235	61	107	189	235
2	1	68	30	4	70	392	60.7	197	260	397	61	182	276	397
2	1	97	30	2	64	287	58.3	142	187	283	58	137	204	283
2	1	84	30	2	63	228	60.8	98.5	195	229	61	99.3	191	229
2	1	65	30	1	40	387	48.4	208	267	390	48	173	265	390
2	1	107	30	3	20	232	22.7	144	212	233	23	65.9	191	233
2	1	58	30	1	83	361	65.3	135	296	359	65	146	278	359
2	1	75	30	1	38	327	44.7	125	268	331	45	126	250	331
2	1	91	30	3	71	309	64	151	225	312	64	155	221	312
2	1	112	30	2	174	229	196	183	250	80.6	196	94.2	183	81
2	1	105	30	3	90	285	62.7	173	269	287	63	121	229	287
2	1	75	30	3	21	456	30.3	372	289	453	30	191	292	453
2	1	134	30	3	70	138	63.3	77.8	125	188	63	87.4	163	188
2	1	73	30	2	64	488	51.6	228	323	475	52	224	303	475
2	1	131	30	4	92	183	70.9	66.2	175	189	71	76.4	184	189
2	1	109	30	2	22	280	35.9	424	207	273	36	102	207	273
2	1	54	30	1	52	515	46.7	257	345	533	47	223	357	533
2	1	125	30	3	99	196	91.2	115	183	196	91	99.2	188	196

Table B.7 Analysis Comparison (w/ Duration Detect): Sensor and Target Information

S Info	S Rate	Pixel X	Pixel Y	Noise	Jitter	Targ	#	Length	Width	Speed	Ibk	ITgt	0 Noise	En1	En2	Ex1	Ex2
	120	30	30	0.01	0.05	4	9.08	2.59	19.2456	0.2	0.9		60	117	247	304	
	120	30	30	0.01	0.05	5	19.27	2.44	16.9973	0.2	0.9		60	196	272	408	
	120	30	30	0.01	0.05	2	10.19	2.44	24.8741	0.2	0.9		60	109	205	254	
	120	30	30	0.01	0.05	3	24.89	3.68	12.998	0.2	0.9		60	290	337	567	
	120	30	30	0.01	0.05	5	19.27	2.44	13.5824	0.2	0.9		60	230	325	495	
	120	30	30	0.01	0.05	5	19.27	2.44	17.0304	0.2	0.9		60	196	271	407	
	120	30	30	0.01	0.05	3	24.89	3.68	14.4398	0.2	0.9		60	267	309	516	
	120	30	30	0.01	0.05	5	19.27	2.44	22.7559	0.2	0.9		60	162	218	320	
	10	30	30	0.01	0.05	6	8.32	2.43	15.9028	0.2	0.9		60	65	79	84	
	10	30	30	0.01	0.05	1	4.57	2.16	20.2498	0.2	0.9		60	62	75	77	
	10	30	30	0.01	0.05	2	10.19	2.44	18.4967	0.2	0.9		60	66	76	82	
	10	30	30	0.01	0.05	1	4.57	2.16	17.6384	0.2	0.9		60	63	77	80	
	10	30	30	0.01	0.05	4	9.08	2.59	17.4494	0.2	0.9		60	65	77	82	
	10	30	30	0.01	0.05	4	9.08	2.59	16.282	0.2	0.9		60	66	78	84	
	10	30	30	0.01	0.05	5	19.27	2.44	14.4018	0.2	0.9		60	73	81	94	
	10	30	30	0.01	0.05	6	8.32	2.43	14.2904	0.2	0.9		60	66	81	87	
	10	30	30	0.01	0.05	6	8.32	2.43	18.2569	0.2	0.9		60	65	76	81	
	10	30	30	0.01	0.05	4	9.08	2.59	15.5979	0.2	0.9		60	66	79	85	
	30	30	30	0.01	0.05	4	9.08	2.59	12.1187	0.2	0.9		60	82	134	156	
	30	30	30	0.01	0.05	6	8.32	2.43	25.3133	0.2	0.9		60	70	96	106	
	30	30	30	0.01	0.05	2	10.19	2.44	15.3386	0.2	0.9		60	80	119	139	
	30	30	30	0.01	0.05	1	4.57	2.16	22.1056	0.2	0.9		60	66	101	107	
	30	30	30	0.01	0.05	6	8.32	2.43	25.3133	0.2	0.9		60	70	96	106	
	30	30	30	0.01	0.05	4	9.08	2.59	12.1187	0.2	0.9		60	82	134	156	
	30	30	30	0.01	0.05	6	8.32	2.43	25.3133	0.2	0.9		60	70	96	106	
	30	30	30	0.01	0.05	2	10.19	2.44	15.3386	0.2	0.9		60	80	119	139	
	30	30	30	0.01	0.05	1	4.57	2.16	22.1056	0.2	0.9		60	66	101	107	
	60	30	30	0.01	0.05	3	24.89	3.68	18.8432	0.2	0.9		60	139	156	235	
	60	30	30	0.01	0.05	4	9.08	2.59	19.5218	0.2	0.9		60	88	152	180	
	60	30	30	0.01	0.05	3	24.89	3.68	12.8738	0.2	0.9		60	176	200	316	
	60	30	30	0.01	0.05	4	9.08	2.59	16.5197	0.2	0.9		60	93	169	202	
	60	30	30	0.01	0.05	1	4.57	2.16	25.1346	0.2	0.9		60	71	132	143	
	60	30	30	0.01	0.05	3	24.89	3.68	15.0369	0.2	0.9		60	159	180	279	
	60	30	30	0.01	0.05	1	4.57	2.16	16.4862	0.2	0.9		60	77	169	186	
	60	30	30	0.01	0.05	5	19.27	2.44	24.562	0.2	0.9		60	107	133	180	
	60	30	30	0.01	0.05	4	9.08	2.59	14.4115	0.2	0.9		60	98	185	223	
	60	30	30	0.01	0.05	4	9.08	2.59	19.3816	0.2	0.9		60	88	153	181	
	60	30	30	0.01	0.05	1	4.57	2.16	18.2653	0.2	0.9		60	75	159	174	
	90	30	30	0.01	0.05	5	19.27	2.44	23.1095	0.2	0.9		60	110	138	188	
	60	30	30	0.01	0.05	3	24.89	3.68	16.3089	0.2	0.9		60	152	170	262	
	60	30	30	0.01	0.05	6	8.32	2.43	24.9397	0.2	0.9		60	80	132	152	
	60	30	30	0.01	0.05	6	8.32	2.43	21.3418	0.2	0.9		60	83	144	167	
	90	30	30	0.01	0.05	2	10.19	2.44	22.5002	0.2	0.9		60	101	180	221	
	90	30	30	0.01	0.05	2	10.19	2.44	16.9493	0.2	0.9		60	114	219	273	
	90	30	30	0.01	0.05	3	24.89	3.68	17.4372	0.2	0.9		60	188	215	343	
	90	30	30	0.01	0.05	6	8.32	2.43	15.2469	0.2	0.9		60	109	237	286	
	90	30	30	0.01	0.05	2	10.19	2.44	20.5342	0.2	0.9		60	105	191	236	
	90	30	30	0.01	0.05	1	4.57	2.16	25.5661	0.2	0.9		60	76	166	182	
	90	30	30	0.01	0.05	5	19.27	2.44	14.1915	0.2	0.9		60	182	250	372	
	90	30	30	0.01	0.05	5	19.27	2.44	23.63	0.2	0.9		60	133	174	247	
	90	30	30	0.01	0.05	4	9.08	2.59	17.1668	0.2	0.9		60	108	217	265	
	90	30	30	0.01	0.05	6	8.32	2.43	23.8287	0.2	0.9		60	91	173	204	

Table B.8 Analysis Comparison (w/ Duration Detect): PolyFit and FermiFit Results

Duration	N	#T	FAR2	#T	En1	Ex2	Poly	En1	En2	Ex1	Ex2	Fermi	En1	En2	Ex1	Ex2
	3	45	30	1	91	276		57.7	107	247	303		58	124	237	303
	3	21	30	1	130	344		70.6	193	300	400		71	191	280	400
	3	27	30	1	97	234		15.8	145	198	253		16	59.1	210	253
	3	22	30	1	137	492		71.1	266	351	558		71	249	380	558
	3	30	30	1	115	432		73.1	249	388	502		73	231	344	502
	3	26	30	1	132	340		54.7	226	286	403		55	179	279	403
	3	19	30	1	130	447		65.1	254	331	514		65	231	348	514
23	3	17	30	1	113	276		67.4	171	226	332		67	154	245	332
	3	5	30	0	0	0		67.4	171	226	332		67	148	245	332
	3	3	30	0	0	0		67.4	171	226	332		67	148	251	332
	3	5	0	1	63	77		57.8	65.1	78	82.1		60	67.4	77	82
	3	4	0	1	63	77		50.4	70.3	74.7	83.6		60	67	76.5	80
	3	4	0	1	65	81		61.1	65.2	78.4	81.4		60	67.5	76.5	82
	3	2	0	1	67	77		60.4	64.6	77.7	86.1		60	65.6	76.4	84
	3	1	0	1	68	84		58.9	73.5	100	92.8		60	69.2	84.8	94
	3	3	0	1	71	79		58.9	73.4	102	84.9		60	67.8	79.2	87
	3	3	0	1	66	73		59.8	66.6	74.6	82.1		60	65.9	75.1	81
3.3	3	3	0	1	65	82		58.8	67.8	79	85.5		60	68.4	76.6	85
	3	14	0	1	75	137		57	87.6	132	167		60	86.4	130	156
	3	11	0	1	68	105		60.2	76	89.3	116		60	69.6	96.4	106
	3	9	0	1	79	119		56.3	81.1	120	141		60	73.3	126	139
	3	5	0	1	65	97		58.6	78.4	110	113		60	68.5	98.5	107
	3	11	0	1	68	105		60.2	76	89.3	116		60	69.6	96.4	106
	3	14	0	1	75	137		57	87.6	132	167		60	86.4	130	156
	3	11	0	1	68	105		60.2	76	89.3	116		60	69.6	96.4	106
	3	9	0	1	79	119		56.3	81.1	120	141		60	73	126	139
9.75	3	5	0	1	65	97		58.6	78.4	110	113		60	68.5	98.5	107
	3	3	0	1	92	204		48.1	173	150	240		60	103	191	235
	3	20	0	1	80	164		55.8	89.4	140	187		60	86.7	143	180
	3	13	0	1	97	278		45.5	224	171	327		60	156	220	316
	3	24	0	5	66	204		53.5	92.9	168	207		60	100	162	202
	3	13	0	1	69	135		58.8	71.2	134	146		60	82.9	120	143
	3	6	0	1	95	242		50.4	182	146	295		60	125	214	279
	3	29	0	5	67	117		57.4	74.3	173	183		60	87.5	158	186
	3	10	0	1	90	151		53.9	121	100	180		60	87.4	153	180
	3	32	0	1	85	198		52.3	110	170	232		60	89.5	194	223
	3	27	0	1	72	168		57.6	90.7	142	190		60	88.5	153	181
	3	16	0	1	71	159		44.6	95.9	165	175		60	78.4	156	174
	3	10	0	1	82	172		54.3	114	268	225		60	97.7	150	188
	3	7	0	1	88	228		52.3	163	134	276		60	114	208	262
	3	15	0	1	68	145		54.5	87	135	155		60	89.8	122	152
15.733333333	3	11	0	1	80	143		45.4	86.6	139	172		60	91.7	135	167
	3	27	0	1	84	210		54.5	101	174	231		60	107	174	221
	3	30	0	1	79	240		48.1	117	198	290		60	121	212	273
	3	13	0	1	116	288		48.6	218	198	352		60	167	236	343
	3	29	0	2	170	241		51.5	117	230	298		60	131	215	286
	3	26	0	1	88	208		54.7	102	192	243		60	105	191	236
	3	16	0	1	69	169		46.3	90.9	165	191		60	86.3	156	182
	3	24	0	1	125	318		44.5	199	177	382		60	183	249	372
	3	12	0	1	105	205		47.3	191	159	256		60	106	201	247
	3	24	0	1	97	227		48.9	125	193	281		60	117	208	265
21.8	3	17	0	2	126	169		57.3	93.3	162	205		60	101	163	204

Table B.9 Analysis Comparison (w/ FAPI Detect): Sensor and Target Information

S Rate	Pixel X	Pixel Y	Noise	Jitter	Tar	#	Length	Width	Speed	Ibk	ITgt	EnI	En2	ExI	Ex2
120	30	30	0.02	0.25		4	9.08	2.59	10.7529	0.2	0.9	60	161	395	496
120	30	30	0.02	0.25		3	24.89	3.68	15.7323	0.2	0.9	60	250	289	479
120	30	30	0.02	0.25		6	8.32	2.43	22.21	0.2	0.9	60	105	222	267
120	30	30	0.02	0.25		4	9.08	2.59	18.131	0.2	0.9	60	120	259	319
120	30	30	0.02	0.25		4	9.08	2.59	16.5743	0.2	0.9	60	126	277	343
120	30	30	0.02	0.25		5	19.27	2.44	19.3292	0.2	0.9	60	180	246	366
120	30	30	0.02	0.25		6	8.32	2.43	20.0954	0.2	0.9	60	110	239	289
120	30	30	0.02	0.25		1	4.57	2.16	17.9799	0.2	0.9	60	91	260	291
120	30	30	0.02	0.25		4	9.08	2.59	14.5874	0.2	0.9	60	135	307	382

Table B.10 Analysis Comparison (w/ FAPI Detect): PolyFit and FermiFit Results

FAPI																
N	$\gamma$	#T	FAR2	#T	En1	Ex2	Poly	En1	En2	Ex1	Ex2	Fermi	En1	En2	Ex1	Ex2
3	1	5	30	1	85	470		55	155	396	507		55	172	327	507
3	1	1	30	1	98	441		68.9	243	172	489		69	225	323	489
3	1	2	30	1	101	248		78.6	119	229	280		79	149	223	280
3	1	0	30	0	0	0		78.6	119	229	280		79	134	225	280
3	1	12	30	1	107	299		51.1	132	290	315		51	130	297	315
3	1	2	30	1	85	339		55.1	195	252	364		55	137	222	364
3	1	10	30	2	91	186		73.4	94.6	208	234		73	119	210	234
3	1	0	30	0	0	0		73.4	94.6	208	234		73	107	200	234
3	1	0	30	0	0	0		73.4	94.6	208	234		73	107	200	234

Table B.11 Sample Rate Analysis Data from Analysis Comparison w/ Duration Detect

Pe1	Pe2	Pex1	Pex2	Fen1	Fen2	Fex1	Fex2		
10	0.316	2.353	3.464	5.141	0.140	1.862	3.545	5.03	2.818
30	0.163	0.208	0.258	0.246	0.000	0.106	0.104	0	0.219
60	0.126	0.204	0.314	0.131	0.000	0.242	0.250	0	0.194
90	0.109	0.170	0.195	0.111	0.000	0.126	0.126	0	0.146
120	0.103	0.151	0.165	0.046	0.102	0.172	0.166	0.045833333	0.116
	0.163	0.617	0.879	1.135		0.502	0.838		
		0.967	0.82			1.029	0.870		

Table B.12 Pixel Size Analysis Data from Analysis comparison w/ Threshold Detect

	Pe1	Pe2	Pex1	Pex2	Fen1	Fen2	Fex1	Fex2	
5	0.762	0.905	0.701	3.049	0.761	0.996	0.658	3.049	1.354
10	0.902	1.027	0.784	3.417	0.901	1.144	0.860	3.419	1.532
30	1.217	0.968	0.977	3.319	1.216	0.992	1.042	3.319	1.620
	0.960	0.967	0.820	3.262	0.959	1.044	0.854	3.262	

Table B.13 Noise Effects Results in Detection Testing

N	# F	Act Det	Th D	Pixel X		Pixel Y		Duration						FAPI					
				60		30		Threshold		Du FA	FAR D	FAR FA	Du D	FAR D	FAR FA	FPI D	FPI FA	FAR D	FAR FA
				30	30	30	30												
1	600	339	232	116	339	239	132	51	319	183	339	241	339	241	339	241	339	241	
	600	155	50	136	155	416	100	244	155	440	95	204	110	240	244	7	244	0	
	600	467	319	40	467	106	243	20	444	96	421	29	444	29	444	7	444	0	
	600	198	91	95	198	378	69	59	198	193	156	20	178	0	178	0	178	0	
	600	238	130	158	238	337	141	179	238	349	238	342	238	342	238	342	238	342	
	600	241	132	110	241	330	92	52	241	204	237	165	241	275	241	275	241	275	
	600	220	92	104	220	357	171	247	220	378	220	360	220	360	220	360	220	360	
	600	189	60	75	189	356	84	118	189	341	90	4	151	0	151	0	151	0	
	600	192	96	128	192	385	123	179	192	403	192	388	192	388	192	388	192	388	
	600	245	93	98	245	322	24	0	159	0	227	242	245	300	245	300	245	300	
	600	246	156	133	246	324	99	53	241	96	245	230	246	293	246	293	246	293	
	600	241	98	95	241	336	163	180	241	351	195	95	211	110	211	110	211	110	
	600	179	57	61	177	334	98	159	179	414	140	82	148	70	148	70	148	70	
	600	184	97	151	184	393	26	0	129	0	184	396	184	396	184	396	184	396	
	600	249	110	75	249	324	115	90	249	323	249	331	249	331	249	331	249	331	
	600	202	82	89	202	320	132	184	202	392	202	378	202	378	202	378	202	378	
	600	215	97	89	215	350	141	161	215	374	203	103	210	100	210	100	210	100	
	600	158	54	100	158	418	29	23	125	0	99	57	135	156	135	156	135	156	
	600	210	88	83	210	366	88	87	210	384	210	370	210	370	210	370	210	370	
	600	207	59	92	207	365	19	8	74	0	207	373	207	373	207	373	207	373	
	600	206	113	124	206	371	19	0	62	0	206	374	206	374	206	374	206	374	
	600	468	297	31	468	101	183	0	408	0	468	112	468	112	468	112	468	112	
	600	122	42	148	122	458	96	313	122	478	122	458	122	458	122	458	122	458	
	600	158	67	133	158	416	103	234	158	437	158	422	158	422	158	422	158	422	
	600	168	45	74	168	402	109	218	168	426	168	412	168	412	168	412	168	412	
	600	151	52	84	151	426	26	23	111	32	151	429	151	429	151	429	151	429	
	600	317	131	84	317	263	184	120	317	278	231	49	291	114	291	114	291	114	
	600	303	189	64	303	267	114	2	220	0	277	60	282	102	282	102	282	102	
	600	185	53	100	185	392	54	108	185	377	63	97	101	83	101	83	101	83	
	600	167	59	87	167	407	107	216	167	423	118	49	159	6	159	6	159	6	
	600	246	90	68	246	325	135	144	246	348	246	334	246	334	246	334	246	334	
	600	302	225	102	302	271	108	0	249	0	302	278	302	278	302	278	302	278	
	600	378	242	60	378	200	132	0	275	0	378	202	378	202	378	202	378	202	
	600	238	90	108	238	339	145	199	238	355	238	342	238	342	238	342	238	342	
	600	208	78	63	208	246	54	21	165	39	170	64	203	4	203	4	203	4	
	600	175	60	96	175	405	94	171	175	420	175	405	175	405	175	405	175	405	
	600	185	97	128	185	394	46	33	160	42	185	395	185	395	185	395	185	395	
	600	194	79	103	194	376	136	205	194	399	149	51	185	102	185	102	185	102	
	600	256	85	57	256	282	112	99	256	311	148	13	162	0	162	0	162	0	
	600	111	72	231	111	466	78	271	111	478	111	469	111	469	111	469	111	469	
	600	198	46	38	198	279	147	236	198	401	112	17	126	0	126	0	126	0	
	600	251	91	74	251	326	194	214	251	343	182	50	209	0	209	0	209	0	
	600	228	97	96	228	348	105	116	228	366	228	352	228	352	228	352	228	352	
	600	151	50	107	151	427	23	25	65	39	104	67	137	6	137	6	137	6	
	600	217	111	160	217	362	106	153	217	371	217	363	217	363	217	363	217	363	
	600	131	36	67	131	435	34	62	111	294	131	449	131	449	131	449	131	449	
	600	284	213	124	284	296	153	56	263	241	284	296	284	296	284	296	284	296	
	600	151	48	78	151	397	30	33	91	69	80	14	112	0	112	0	112	0	
	600	131	33	103	131	441	40	147	131	461	131	449	131	449	131	449	131	449	
	600	228	87	117	228	340	43	28	145	35	228	352	228	352	228	352	228	352	
1.5	600	148	44	100	144	397	7	7	0	0	51	59	90	141	90	141	90	141	
	600	239	44	25	207	186	33	0	42	0	159	37	199	0	199	0	199	0	
	600	226	54	31	226	141	4	0	0	0	226	354	226	354	226	354	226	354	
	600	296	187	78	296	270	94	0	233	0	296	284	296	284	296	284	296	284	
	600	237	84	48	237	294	84	50	237	196	237	343	237	343	237	343	237	343	
	600	117	26	39	117	333	45	129	117	451	117	463	117	463	117	463	117	463	
	600	209	50	16	197	86	159	216	209	385	209	371	209	371	209	371	209	371	
	600	268	58	23	263	181	140	111	268	323	268	312	268	312	268	312	268	312	
	600	405	206	17	400	95	127	0	322	0	405	175	405	175	405	175	405	175	
	600	319	93	29	319	237	50	0	140	0	235	57	284	110	284	110	284	110	
	600	158	29	40	158	281	106	250	158	434	158	422	158	422	158	422	158	422	
	600	150	46	95	150	394	101	264	150	445	150	430	150	430	150	430	150	430	
	600	138	20	20	104	88	29	64	104	193	138	442	138	442	138	442	138	442	
	600	210	42	23	198	42	124	194	210	383	210	370	210	370	210	370	210	370	
	600	381	176	25	381	168	108	0	226	0	381	199	381	199	381	199	381	199	
	600	280	112	52	280	293	89	23	248	18	280	300	280	300	280	300	280	300	
	600	295	156	59	295	282	82	0	209	0	295	285	295	285	295	285	295	285	
	600	239	75	49	239	329	118	112	239	348	239	341	239	341	239				

600	217	62	71	217	327	98	131	217	359	217	363	217	363
600	186	71	96	186	394	131	235	186	406	186	394	186	394
600	316	157	81	316	252	75	0	231	0	266	76	309	163
600	250	46	19	243	126	38	9	171	0	250	330	250	330
600	228	49	9	219	24	38	0	167	0	168	1	178	0
600	181	59	87	181	394	128	232	181	412	181	399	181	399
600	185	43	66	185	321	41	64	167	328	185	395	185	395
600	179	41	47	162	284	87	154	179	395	110	32	97	0
600	268	51	20	268	115	84	73	254	293	48	0	91	0
600	250	107	99	250	325	157	179	250	344	250	330	250	330
600	181	57	17	174	161	119	173	181	414	181	399	181	399
600	226	107	59	226	302	76	29	206	35	226	354	226	354
600	136	27	57	136	369	85	279	136	464	136	444	136	444
600	252	91	46	252	261	140	122	252	340	252	328	252	328
600	308	125	10	284	0	77	0	212	0	230	5	237	0
600	283	150	40	265	260	91	0	211	0	283	297	283	297
600	244	152	108	244	334	96	37	241	101	244	336	244	336
600	212	49	49	212	286	7	0	0	0	212	368	212	368
600	382	173	11	369	45	114	0	261	0	306	0	327	0
600	122	32	92	122	455	58	194	122	468	15	1	0	0
600	212	73	109	212	361	94	169	212	381	8	6	0	0
600	249	98	66	249	286	153	126	249	343	249	331	249	331
600	304	204	74	304	276	136	24	289	13	304	276	304	276
600	253	37	2	175	0	94	80	253	295	38	2	0	0
600	255	66	25	223	224	53	0	153	0	255	325	255	325
600	144	32	48	144	367	57	118	144	448	73	6	0	0
600	251	95	104	251	323	57	42	218	112	251	329	251	329
600	180	96	114	180	400	107	162	180	411	180	400	180	400
600	186	39	49	186	373	108	190	186	406	186	394	186	394
2	600	120	2	0	0	0	0	0	0	120	460	120	460
600	229	34	2	140	0	59	57	213	225	229	351	229	351
600	141	15	2	103	0	34	88	117	321	141	439	141	439
600	177	31	0	99	0	84	96	177	329	108	1	118	0
600	124	23	47	124	12	67	231	124	471	62	56	85	58
600	200	33	0	131	0	32	0	113	0	200	380	200	380
600	145	0	0	0	0	110	296	145	448	145	435	145	435
600	196	37	19	184	15	109	159	196	398	196	384	196	384
600	274	22	0	171	0	142	138	274	319	274	306	274	306
600	292	46	0	195	0	78	12	219	0	292	288	292	288
600	116	4	0	0	0	10	16	0	0	7	30	0	0
600	244	33	0	162	0	28	0	70	0	244	336	244	336
600	254	48	0	169	0	68	13	151	0	66	0	68	0
600	226	30	32	198	21	58	68	212	186	0	0	0	0
600	218	10	0	95	0	0	0	0	0	22	0	0	0
600	203	0	0	0	0	1	0	0	0	203	377	203	377
600	186	15	0	122	0	97	159	186	409	10	0	0	0
600	275	64	0	190	0	54	0	143	0	199	0	207	0
600	152	5	0	0	0	37	81	135	313	152	428	152	428
600	230	7	0	0	0	138	146	230	362	230	350	230	350
600	184	20	0	141	0	29	21	109	0	184	396	184	396
600	250	20	0	150	0	68	56	208	281	250	330	250	330
600	345	25	0	202	0	65	16	284	32	190	10	260	0
600	177	24	0	112	0	93	142	177	417	177	403	177	403
600	144	22	22	144	12	70	178	144	447	144	436	144	436
600	187	9	0	75	0	33	22	124	44	187	393	187	393
600	173	33	55	173	30	0	0	0	0	173	407	173	407
600	203	50	34	203	30	37	13	149	0	203	377	203	377
600	149	5	0	0	0	80	169	149	446	149	431	149	431
600	212	21	13	88	10	155	252	212	381	212	368	212	368
600	163	21	0	135	0	70	124	162	412	163	417	163	417
600	223	37	0	176	0	127	100	223	370	223	357	223	357
600	280	65	41	275	35	17	0	0	0	101	4	164	0
600	331	192	48	331	48	76	0	218	0	287	4	327	1
600	263	20	0	118	0	48	19	165	0	263	317	263	317
600	332	125	4	286	0	74	0	172	0	332	248	332	248
600	208	54	57	208	51	84	111	208	362	208	372	208	372
600	214	38	0	162	0	10	0	32	0	214	366	214	366
600	460	207	4	427	41	97	0	246	0	460	120	460	120
600	124	24	73	124	50	9	15	32	0	124	456	124	456
600	171	62	74	171	6-	107	191	171	419	171	409	171	409
600	325	59	19	317	8	19	0	0	0	269	26	307	0
600	228	10	0	61	0	1	0	0	0	228	352	228	352
600	138	13	0	97	0	11	0	56	0	138	442	138	442
600	263	91	6	234	31	77	0	198	0	263	317	263	317
600	284	77	0	214	0	73	0	168	0	284	296	284	296
600	345	117	0	268	0	89	0	222	0	345	235	345	235
600	240	52	32	240	28	44	29	187	93	240	340	240	340
600	374	150	0	349	0	84	0	251	0	322	7	323	0

	600	195	57	49	195	30	110	136	195	372	195	385	195	385
2.5	600	233	33	0	134	0	108	98	217	360	233	347	233	347
	600	146	0	0	0	0	32	79	114	269	146	434	146	434
	600	435	124	0	334	0	128	0	310	0	371	35	360	0
	600	237	26	0	118	0	104	97	230	318	114	0	120	0
	600	236	1	0	0	0	8	0	0	0	236	344	236	344
	600	239	6	0	0	0	113	128	239	340	239	341	239	341
	600	369	90	0	249	0	58	0	198	0	369	211	369	211
	600	258	7	0	35	0	64	40	233	172	62	0	0	0
	600	241	15	0	96	0	18	0	76	0	241	339	241	339
	600	183	4	0	0	0	45	51	183	207	47	9	70	0
	600	238	0	0	0	0	0	0	0	0	238	342	238	342
	600	162	8	0	87	0	0	0	0	0	162	418	162	418
	600	370	106	0	290	0	53	0	187	0	370	210	370	210
	600	196	6	0	52	0	117	184	196	396	7	0	0	0
	600	316	120	1	301	0	50	0	166	0	291	41	302	0
	600	373	97	0	267	0	26	0	94	0	293	0	295	0
	600	305	43	0	121	0	47	0	121	0	305	275	305	275
	600	170	0	0	0	0	44	82	148	358	170	410	170	410
	600	277	52	0	175	0	79	0	209	0	214	1	221	0
	600	138	9	0	76	0	62	157	138	435	138	442	138	442
	600	275	55	0	134	0	51	0	134	0	195	6	214	0
	600	286	46	3	157	41	169	147	286	308	286	294	286	294
	600	308	23	0	161	0	140	65	308	227	308	272	308	272
	600	392	68	0	252	0	55	0	172	0	291	0	282	0
	600	347	140	0	293	0	54	0	185	0	294	0	307	0
	600	380	104	0	308	0	58	0	217	0	380	200	380	200
	600	198	6	0	0	0	94	125	198	394	198	382	198	382
	600	191	0	0	0	0	26	34	141	121	191	389	191	389
	600	205	0	0	0	0	92	145	205	350	205	375	205	375
	600	142	0	0	0	0	0	0	0	0	0	0	0	0
	600	303	81	0	194	0	98	0	235	0	303	277	303	277
	600	311	51	0	243	0	99	43	294	159	181	0	206	0
	600	273	92	0	214	0	58	0	160	0	273	307	273	307
	600	137	0	0	0	0	6	0	0	0	10	8	0	0
	600	228	0	0	0	0	141	170	228	366	228	352	228	352
	600	268	28	0	180	0	132	120	268	327	57	0	65	0
	600	338	23	0	165	0	36	2	136	0	338	242	338	242
	600	131	0	0	0	0	63	241	131	463	131	449	131	449
	600	226	3	0	0	0	0	0	0	0	226	354	226	354
	600	403	138	0	318	0	71	0	172	0	403	177	403	177
	600	295	24	0	99	0	23	0	70	0	295	285	295	285
	600	162	15	0	84	0	97	189	162	433	162	418	162	418
	600	217	0	0	0	0	33	9	132	0	217	363	217	363
	600	200	11	0	73	0	21	0	74	0	136	6	153	0
	600	284	16	0	79	0	60	1	208	0	86	0	111	0
	600	367	127	0	289	0	56	0	173	0	305	0	307	0
	600	138	0	0	0	0	64	183	138	455	138	442	138	442
	600	237	18	0	131	0	59	41	223	0	237	343	237	343
	600	285	84	0	204	0	81	0	204	0	285	295	285	295
	600	204	0	0	0	0	105	144	204	387	151	25	186	0
3	600	270	35	0	131	0	29	0	131	0	213	12	224	0
	600	173	1	0	0	0	71	131	173	421	173	407	173	407
	600	197	0	0	0	0	1	0	0	0	0	0	0	0
	600	154	0	0	0	0	0	0	0	0	6	0	0	0
	600	307	52	0	192	0	64	0	207	0	177	0	196	0
	600	170	7	0	0	0	14	0	44	0	170	410	170	410
	600	218	0	0	0	0	20	0	82	0	218	362	218	362
	600	208	21	0	84	0	83	72	208	292	208	372	208	372
	600	328	0	0	0	0	96	50	295	249	328	252	328	252
	600	303	43	0	166	0	40	0	128	0	303	277	303	277
	600	224	38	0	156	0	67	21	224	25	224	356	224	356
	600	276	10	0	68	0	28	0	111	0	276	304	276	304
	600	168	0	0	0	0	46	81	168	354	168	412	168	412
	600	179	0	0	0	0	53	19	145	0	179	401	179	401
	600	216	8	0	57	0	91	120	216	366	216	364	216	364
	600	174	0	0	0	0	69	135	174	419	174	406	174	406
	600	447	111	0	309	0	166	0	316	0	275	0	301	0
	600	478	75	0	249	0	124	0	310	0	284	0	294	0
	600	250	1	0	0	0	136	147	250	344	250	330	250	330
	600	167	0	0	0	0	29	45	138	207	167	413	167	413
	600	316	46	0	211	0	50	0	211	0	316	264	316	264
	600	225	0	0	0	0	1	0	0	0	225	355	225	355
	600	194	0	0	0	0	63	94	194	346	0	0	0	0
	600	252	10	0	47	0	151	125	252	342	252	328	252	328
	600	188	0	0	0	0	90	124	184	396	0	0	0	0
	600	225	0	0	0	0	0	0	0	0	225	355	225	355
	600	210	0	0	0	0	19	0	96	0	210	370	210	370

600	122	0	0	0	0	61	223	122	470	122	458	122	458	
600	158	0	0	0	0	20	0	68	0	0	0	0	0	
600	140	0	0	0	0	55	155	140	455	1	0	0	0	
600	150	7	0	71	0	26	20	140	0	150	430	150	430	
600	108	0	0	0	0	64	263	108	484	0	0	0	0	
600	292	6	0	0	0	1	0	0	0	292	288	292	288	
600	244	0	0	0	0	17	0	0	0	6	0	0	0	
600	183	26	0	148	0	36	28	161	59	25	0	0	0	
600	197	0	0	0	0	46	14	131	0	197	383	197	383	
600	219	12	0	105	0	8	0	0	0	219	361	219	361	
600	440	91	0	278	0	59	0	196	0	440	140	440	140	
600	365	77	0	207	0	84	0	166	0	255	0	267	0	
600	165	0	0	0	0	39	20	108	37	165	415	165	415	
600	207	5	0	30	0	9	0	56	0	9	0	0	0	
600	249	7	0	56	0	59	11	197	0	249	331	249	331	
600	245	0	0	0	0	106	104	229	349	245	335	245	335	
600	149	0	0	0	0	78	190	149	446	149	431	149	431	
600	275	24	0	124	0	46	0	161	0	118	0	131	0	
600	153	7	0	81	0	0	0	0	0	153	427	153	427	
600	363	49	0	161	0	71	0	193	0	265	0	307	0	
600	117	0	0	0	0	9	18	0	0	117	463	117	463	
600	280	0	0	0	0	141	128	280	310	280	300	280	300	
600	455	125	0	329	0	68	0	240	0	455	125	455	125	
35	600	394	15	0	87	0	28	0	61	0	394	186	394	186
600	147	0	0	0	0	19	0	0	0	147	433	147	433	
600	128	0	0	0	0	54	154	128	458	128	452	128	452	
600	162	0	0	0	0	79	159	162	432	23	0	0	0	
600	276	0	0	0	0	11	0	0	0	276	304	276	304	
600	317	0	0	0	0	11	0	43	0	5	0	0	0	
600	277	0	0	0	0	22	0	95	0	101	0	108	0	
600	240	0	0	0	0	37	11	172	32	161	28	227	0	
600	178	4	0	0	0	0	0	0	0	178	402	178	402	
600	250	0	0	0	0	117	121	250	345	39	0	91	0	
600	109	0	0	0	0	38	159	109	485	109	471	109	471	
600	303	0	0	0	0	72	37	262	126	303	277	303	277	
600	289	0	0	0	0	106	77	287	270	38	0	0	0	
600	241	0	0	0	0	33	0	121	0	112	2	98	0	
600	166	0	0	0	0	74	151	166	413	166	414	166	414	
600	202	0	0	0	0	99	134	202	391	174	78	202	91	
600	308	31	0	131	0	64	0	201	0	308	272	308	272	
600	277	57	0	171	0	10	0	38	0	106	0	119	0	
600	245	3	0	0	0	11	0	30	0	49	0	75	0	
600	241	0	0	0	0	0	0	0	0	241	339	241	339	
600	178	0	0	0	0	46	48	162	247	178	402	178	402	
600	187	0	0	0	0	51	40	187	111	5	0	0	0	
600	338	47	0	148	0	49	0	148	0	161	0	164	0	
600	312	11	0	45	0	26	0	90	0	312	268	312	268	
600	259	0	0	0	0	0	0	0	0	259	321	259	321	
600	128	0	0	0	0	69	186	128	464	128	452	128	452	
600	212	0	0	0	0	10	0	0	0	0	0	0	0	
600	267	65	0	172	0	14	0	69	0	267	313	267	313	
600	302	0	0	0	0	40	0	205	0	302	278	302	278	
600	227	0	0	0	0	0	0	0	0	58	0	110	0	
600	159	0	0	0	0	12	0	0	0	159	421	159	421	
600	136	0	0	0	0	6	0	0	0	0	0	0	0	
600	144	0	0	0	0	0	0	0	0	144	436	144	436	
600	191	0	0	0	0	17	0	56	0	167	233	191	283	
600	167	0	0	0	0	5	0	0	0	1	0	0	0	
600	287	0	0	0	0	57	0	167	0	287	293	287	293	
600	158	0	0	0	0	53	105	158	381	158	422	158	422	
600	166	0	0	0	0	81	174	166	426	0	0	0	0	
600	175	0	0	0	0	23	0	105	0	175	405	175	405	
600	171	0	0	0	0	22	0	60	0	171	409	171	409	
600	209	0	0	0	0	20	1	91	0	209	371	209	371	
600	237	0	0	0	0	4	0	0	0	237	343	237	343	
600	249	0	0	0	0	21	0	108	0	249	331	249	331	
600	195	0	0	0	0	24	9	141	0	195	385	195	385	
600	272	0	0	0	0	98	76	272	281	5	0	0	0	
600	391	29	0	117	0	30	0	117	0	391	189	391	189	
600	242	0	0	0	0	66	28	240	47	46	0	62	0	
600	166	0	0	0	0	60	109	166	372	31	0	0	0	
600	284	0	0	0	0	95	39	257	140	284	296	284	296	
600	333	0	0	0	0	9	0	0	0	333	247	333	247	
4	600	217	0	0	0	0	0	0	0	217	363	217	363	
600	199	5	0	0	0	1	0	0	0	97	0	114	0	
600	185	0	0	0	0	10	0	30	0	152	43	175	0	
600	255	0	0	0	0	14	0	64	0	92	0	96	0	
600	352	6	0	30	0	17	0	46	0	276	1	305	0	

600	217	0	0	0	0	47	19	188	1	217	363	217	363	
600	166	0	0	0	0	0	0	0	0	166	414	166	414	
600	182	0	0	0	0	47	104	131	370	7	2	0	0	
600	127	0	0	0	0	62	188	127	466	127	453	127	453	
600	191	0	0	0	0	64	78	191	292	191	389	191	389	
600	152	0	0	0	0	68	127	152	434	0	0	0	0	
600	146	0	0	0	0	0	0	0	0	146	434	146	434	
600	221	13	0	95	0	72	15	189	7	221	359	221	359	
600	455	21	0	119	0	59	0	191	0	236	0	236	0	
600	110	0	0	0	0	0	0	0	0	110	470	110	470	
600	108	0	0	0	0	0	0	0	0	3	0	0	0	
600	178	0	0	0	0	38	20	154	16	178	402	178	402	
600	213	0	0	0	0	21	0	32	0	213	367	213	367	
600	146	0	0	0	0	0	0	0	0	0	0	0	0	
600	190	2	0	0	0	44	14	161	4	190	390	190	390	
600	466	24	0	135	0	16	0	69	0	466	114	466	114	
600	257	16	0	60	0	11	0	40	0	257	323	257	323	
600	303	43	0	129	0	17	0	82	0	303	277	303	277	
600	341	7	0	40	0	36	0	126	0	161	0	175	0	
600	253	0	0	0	0	1	0	0	0	253	327	253	327	
600	239	0	0	0	0	72	72	223	293	239	341	239	341	
600	152	0	0	0	0	25	26	118	4	49	17	104	0	
600	232	0	0	0	0	0	0	0	0	5	0	0	0	
600	261	0	0	0	0	44	0	113	0	63	0	110	0	
600	220	0	0	0	0	0	0	0	0	0	0	0	0	
600	177	2	0	0	0	1	0	0	0	177	403	177	403	
600	211	0	0	0	0	14	0	76	0	30	0	78	0	
600	146	0	0	0	0	1	0	0	0	0	0	0	0	
600	243	0	0	0	0	40	20	182	35	0	0	0	0	
600	215	0	0	0	0	0	0	0	0	1	0	0	0	
600	127	0	0	0	0	42	115	127	406	127	453	127	453	
600	224	0	0	0	0	10	0	0	0	224	356	224	356	
600	299	7	0	0	0	15	0	58	0	299	281	299	281	
600	173	0	0	0	0	0	0	0	0	173	407	173	407	
600	178	0	0	0	0	0	0	0	0	178	402	178	402	
600	306	0	0	0	0	0	0	0	0	306	274	306	274	
600	308	8	0	38	0	19	0	59	0	308	272	308	272	
600	205	0	0	0	0	47	56	176	143	205	375	205	375	
600	218	0	0	0	0	1	0	0	0	218	362	218	362	
600	336	0	0	0	0	1	0	0	0	336	244	336	244	
600	109	0	0	0	0	0	0	0	0	0	0	0	0	
600	149	0	0	0	0	1	0	0	0	149	431	149	431	
600	298	0	0	0	0	35	0	158	0	6	0	0	0	
600	176	0	0	0	0	1	0	0	0	0	0	0	0	
600	221	0	0	0	0	101	138	206	370	221	359	221	359	
2	600	172	17	0	62	0	12	0	40	0	172	408	172	408
600	181	26	1	126	0	87	162	181	405	20	0	0	0	
600	261	118	0	233	0	56	0	139	0	261	319	261	319	
600	181	2	0	0	0	46	61	164	218	8	0	0	0	
600	222	96	95	222	344	45	7	123	0	110	1	116	0	
600	250	17	0	155	0	83	56	250	138	250	330	250	330	
600	300	86	31	300	187	28	0	97	0	300	280	300	280	
600	148	29	23	131	113	16	0	33	0	148	432	148	432	
600	196	63	20	186	83	76	43	194	161	118	0	133	0	
600	254	135	9	235	0	60	0	163	0	195	0	200	0	
600	382	195	0	367	0	86	0	228	0	382	198	382	198	
600	197	69	51	197	326	114	149	197	395	197	383	197	383	
600	185	17	0	107	0	95	170	185	407	76	11	113	0	
600	423	212	5	384	0	98	0	260	0	423	157	423	157	
600	275	129	0	246	0	150	27	246	53	275	305	275	305	
600	169	12	8	93	0	109	239	169	426	169	411	169	411	
600	198	50	0	157	0	87	58	198	267	198	382	198	382	
600	254	101	0	195	0	135	25	229	52	254	326	254	326	
600	141	35	19	123	76	96	236	141	452	141	439	141	439	
600	206	51	31	188	222	18	0	0	105	2	143	0	0	
600	122	5	0	0	0	35	120	114	433	2	0	0	0	
600	152	51	65	152	407	112	215	152	442	152	428	152	428	
600	121	0	0	0	0	39	103	121	456	2	0	0	0	
600	166	28	0	125	0	79	112	166	413	166	414	166	414	
600	330	150	0	276	0	136	0	212	0	290	0	296	0	
600	148	21	0	96	0	50	63	133	230	55	0	57	0	
600	195	35	13	195	13	61	54	163	132	61	0	57	0	
600	230	1	0	0	0	69	70	218	294	230	350	230	350	
600	328	40	0	198	0	41	0	178	0	171	0	191	0	
600	191	23	0	153	0	104	158	191	401	191	389	191	389	
600	196	66	19	163	50	24	0	95	0	196	384	196	384	
600	285	134	0	263	0	57	0	116	0	251	28	264	23	

600	142	13	0	52	0	56	147	128	431	70	8	96	0	
600	173	37	30	147	247	114	224	173	420	25	0	0	0	
600	210	37	13	183	0	115	151	210	383	210	370	210	370	
600	489	263	3	458	28	181	0	351	0	453	0	468	0	
600	264	50	7	216	0	175	169	264	331	65	1	99	0	
600	217	25	0	151	0	71	70	217	278	21	0	0	0	
600	277	40	0	198	0	188	143	277	311	277	303	277	303	
600	175	29	16	157	132	117	211	175	419	175	405	175	405	
600	190	22	0	114	0	132	165	190	404	190	390	190	390	
600	261	29	0	156	0	53	2	228	0	261	319	261	319	
600	388	155	0	315	0	89	0	196	0	318	0	341	0	
600	188	59	21	188	147	52	0	128	0	188	392	188	392	
600	457	153	0	332	0	167	0	322	0	457	123	457	123	
600	163	19	0	92	0	97	178	163	430	163	417	163	417	
600	268	59	8	242	28	85	45	237	171	268	312	268	312	
600	305	53	0	211	0	46	0	152	0	253	10	281	13	
600	173	27	42	173	339	59	96	173	401	32	0	51	0	
0 03	600	181	55	3	159	0	21	0	46	0	181	399	181	399
600	174	56	45	147	282	51	27	147	107	126	0	132	0	
600	283	102	0	257	0	79	0	216	0	283	297	283	297	
600	255	147	0	200	0	99	0	180	0	255	325	255	325	
600	249	57	0	227	0	119	71	249	268	249	331	249	331	
600	182	54	0	131	0	88	19	167	0	182	398	182	398	
600	153	24	53	153	336	24	51	121	217	153	427	153	427	
600	185	55	31	185	273	85	70	185	267	185	395	185	395	
600	243	72	26	243	156	136	119	243	350	67	0	0	0	
600	154	20	11	119	61	92	190	154	439	154	426	154	426	
600	272	0	0	0	0	113	95	272	307	272	308	272	308	
600	144	14	0	93	0	83	185	144	450	144	436	144	436	
600	121	10	0	79	0	15	7	41	0	121	459	121	459	
600	203	56	0	148	0	52	0	140	0	199	31	203	40	
600	337	59	0	239	0	28	0	103	0	192	0	206	0	
600	196	28	0	112	0	84	129	196	397	28	0	0	0	
600	193	57	0	170	0	44	0	84	0	107	0	125	0	
600	265	181	42	265	251	97	0	163	0	216	0	215	0	
600	243	85	26	243	172	82	25	229	26	243	337	243	337	
600	217	27	0	145	0	44	0	131	0	217	363	217	363	
600	278	97	33	272	249	56	0	185	0	210	2	218	0	
600	337	48	0	244	0	114	23	322	98	184	0	263	0	
600	183	55	13	175	117	59	31	148	10	141	4	148	4	
600	199	69	25	198	96	17	0	58	0	199	381	199	381	
600	175	29	6	172	8	139	273	175	418	18	0	0	0	
600	290	73	29	290	209	51	0	159	0	290	290	290	290	
600	132	4	0	0	0	0	0	0	0	0	0	0	0	
600	210	85	57	210	358	18	0	96	0	135	0	145	0	
600	293	220	61	293	285	105	0	195	0	293	287	293	287	
600	466	265	0	410	0	193	0	305	0	466	114	466	114	
600	250	64	0	228	0	44	0	200	0	189	0	216	0	
600	201	75	6	171	0	51	0	117	0	201	379	201	379	
600	218	40	0	158	0	43	0	145	0	218	362	218	362	
600	336	75	16	302	163	168	92	336	259	149	0	199	0	
600	364	205	0	327	0	138	0	212	0	364	216	364	216	
600	325	172	0	263	0	126	0	229	0	325	255	325	255	
600	224	77	33	208	184	24	0	109	0	102	0	142	0	
600	212	26	0	141	0	42	0	147	0	93	0	131	0	
600	148	41	15	123	51	52	28	145	59	55	0	89	0	
600	228	101	89	228	349	8	0	0	0	228	352	228	352	
600	288	65	8	268	30	164	108	288	300	288	292	288	292	
600	226	29	0	159	0	100	66	226	302	182	2	185	2	
600	347	199	0	297	0	127	0	214	0	303	0	309	0	
600	199	77	49	183	254	66	33	181	123	199	381	199	381	
600	154	28	0	128	0	43	31	144	59	102	0	109	0	
600	280	124	37	280	221	105	22	276	3	280	300	280	300	
600	263	36	0	178	0	70	27	209	31	263	317	263	317	
600	108	39	104	108	467	37	97	102	443	108	472	108	472	
600	210	42	0	157	0	51	0	170	0	2	0	0	0	
600	210	46	3	192	20	41	0	157	0	2	0	0	0	
0 02	600	249	42	0	170	0	27	0	100	0	184	0	199	0
600	180	39	0	125	0	45	0	125	0	110	0	112	0	
600	253	59	0	196	0	108	60	250	263	198	0	205	0	
600	193	55	0	161	0	44	0	156	0	193	387	193	387	
600	447	334	0	419	0	262	0	348	0	350	0	350	0	
600	251	85	8	243	36	55	0	172	0	251	329	251	329	
600	284	119	0	227	0	124	0	239	0	204	0	205	0	
600	277	211	0	257	0	210	0	257	0	237	0	237	0	
600	173	28	0	137	0	69	88	173	377	173	407	173	407	
600	172	68	30	172	201	80	63	172	235	108	0	123	0	

600	135	37	36	125	313	35	20	107	0	91	4	97	0	
600	157	0	0	0	0	86	190	157	437	0	0	0	0	
600	220	77	0	156	0	59	0	125	0	160	0	170	0	
600	244	92	0	173	0	74	0	164	0	244	336	244	336	
600	186	85	58	186	340	31	0	129	0	111	0	114	0	
600	243	145	3	225	0	148	18	234	32	243	337	243	337	
600	303	218	0	266	0	229	21	274	60	303	277	303	277	
600	342	119	0	211	0	119	0	211	0	201	0	204	0	
600	288	131	0	233	0	99	0	194	0	288	292	288	292	
600	143	47	14	139	57	47	18	132	31	143	437	143	437	
600	122	21	0	100	0	62	148	122	463	0	0	0	0	
600	333	154	0	285	0	84	0	204	0	206	0	213	0	
600	238	58	0	184	0	44	0	169	0	28	0	0	0	
600	346	104	0	313	0	75	0	274	0	346	234	346	234	
600	157	60	119	157	419	111	229	157	434	4	0	0	0	
600	297	201	0	248	0	179	0	227	0	222	0	222	0	
600	213	53	0	175	0	70	15	185	0	213	367	213	367	
600	141	33	0	114	0	70	76	139	355	141	439	141	439	
600	201	43	11	194	61	27	0	150	0	201	379	201	379	
600	153	23	0	110	0	45	12	134	0	48	0	97	0	
600	228	27	0	168	0	20	0	41	0	168	0	178	0	
600	286	202	0	261	0	168	0	214	0	286	294	286	294	
600	179	42	0	148	0	71	31	171	121	111	0	132	0	
600	211	45	0	147	0	36	0	104	0	55	0	59	0	
600	138	0	0	0	0	35	47	138	146	138	442	138	442	
600	225	80	1	197	0	44	0	137	0	146	0	146	0	
600	327	210	0	287	0	170	0	235	0	327	253	327	253	
600	326	254	29	326	218	229	0	292	0	291	0	291	0	
600	207	66	0	123	0	86	0	133	0	207	373	207	373	
600	302	115	9	299	35	111	4	288	0	302	278	302	278	
600	204	134	45	204	270	99	0	144	0	150	0	152	0	
600	177	107	25	177	128	134	116	177	396	177	403	177	403	
600	175	75	44	158	344	91	84	175	335	175	405	175	405	
600	113	9	0	35	0	31	41	108	145	113	467	113	467	
600	215	53	0	163	0	46	0	153	0	128	0	150	0	
600	228	77	0	161	0	86	0	165	0	228	352	228	352	
600	186	54	0	162	0	85	45	167	169	77	0	95	0	
600	471	336	0	422	0	268	0	364	0	471	109	471	109	
600	303	123	0	244	0	108	0	196	0	303	277	303	277	
600	117	0	0	0	0	1	0	0	0	6	0	0	0	
0.01	600	185	130	0	151	0	155	47	185	164	144	0	144	0
600	183	64	0	124	0	88	0	149	0	111	0	111	0	
600	175	18	0	121	0	61	5	151	0	0	0	0	0	
600	186	86	0	151	0	156	100	186	379	121	0	121	0	
600	116	10	0	64	0	68	105	116	467	0	0	0	0	
600	189	64	0	137	0	102	0	166	0	189	391	189	391	
600	205	80	0	162	0	113	0	173	0	133	0	133	0	
600	177	49	0	147	0	84	64	165	238	177	403	177	403	
600	154	0	0	0	0	31	0	124	0	154	426	154	426	
600	360	284	0	315	0	268	0	304	0	303	0	303	0	
600	168	94	0	127	0	55	0	101	0	168	412	168	412	
600	179	47	0	126	0	102	0	150	0	179	401	179	401	
600	212	63	0	148	0	78	0	155	0	139	0	139	0	
600	218	146	0	177	0	154	0	181	0	218	362	218	362	
600	299	188	0	235	0	174	0	216	0	219	0	224	0	
600	149	66	0	108	0	86	0	130	0	149	431	149	431	
600	181	59	0	135	0	58	0	135	0	108	0	114	0	
600	152	74	0	134	0	47	0	110	0	152	428	152	428	
600	214	87	0	144	0	117	0	168	0	214	366	214	366	
600	348	189	0	300	0	96	0	243	0	348	232	348	232	
600	174	45	0	125	0	60	0	127	0	65	0	68	0	
600	265	215	0	235	0	200	0	226	0	232	0	232	0	
600	180	133	0	159	0	133	0	159	0	140	0	140	0	
600	306	254	0	281	0	227	0	257	0	306	274	306	274	
600	185	48	0	118	0	63	0	121	0	185	395	185	395	
600	266	219	0	243	0	203	0	226	0	266	314	266	314	
600	122	27	0	100	0	51	59	122	244	122	458	122	458	
600	202	48	0	135	0	64	0	141	0	130	0	130	0	
600	142	58	21	140	92	44	0	128	0	0	0	0	0	
600	152	73	0	123	0	58	0	115	0	152	428	152	428	
600	148	72	0	109	0	122	114	142	367	95	0	95	0	
600	196	15	0	102	0	73	14	184	6	196	384	196	384	
600	186	34	0	117	0	65	0	141	0	186	394	186	394	
600	258	93	0	198	0	145	0	224	0	258	322	258	322	
600	278	175	0	218	0	161	0	196	0	278	302	278	302	
600	203	116	0	168	0	99	0	168	0	142	0	142	0	
600	486	398	0	452	0	356	0	411	0	415	0	416	0	

600	369	284	0	319	0	277	0	313	0	300	0	300	0	
600	211	121	0	156	0	163	0	197	0	149	0	149	0	
600	203	131	0	165	0	117	0	139	0	203	377	203	377	
600	238	118	0	185	0	128	0	198	0	166	0	166	0	
600	270	216	0	230	0	208	0	229	0	270	310	270	310	
600	160	50	0	105	0	89	0	132	0	160	420	160	420	
600	122	7	0	65	0	50	0	112	0	122	458	122	458	
600	183	120	0	147	0	128	0	160	0	183	397	183	397	
600	367	303	0	325	0	269	0	301	0	307	0	307	0	
600	228	53	0	159	0	80	0	177	0	228	352	228	352	
600	201	131	0	170	0	163	60	191	283	144	0	146	0	
600	261	130	0	216	0	135	0	216	0	261	319	261	319	
600	339	222	0	269	0	206	0	253	0	227	0	227	0	
0	600	216	152	0	152	0	152	0	152	0	156	0	156	0
600	191	125	0	125	0	159	0	159	0	127	0	127	0	
600	297	195	0	195	0	247	0	247	0	198	0	198	0	
600	138	86	0	86	0	106	0	106	0	83	0	83	0	
600	180	128	0	128	0	128	0	128	0	129	0	129	0	
600	138	86	0	86	0	106	0	106	0	83	0	83	0	
600	214	138	0	138	0	172	0	172	0	140	0	140	0	
600	170	106	0	106	0	130	0	130	0	105	0	105	0	
600	194	124	0	124	0	156	0	156	0	126	0	126	0	
600	158	102	0	102	0	128	0	128	0	102	0	102	0	
600	319	263	0	263	0	255	0	255	0	266	0	266	0	
600	217	143	0	143	0	181	0	181	0	144	0	144	0	
600	208	130	0	130	0	160	0	160	0	131	0	131	0	
600	414	342	0	342	0	330	0	330	0	345	0	345	0	
600	178	126	0	126	0	126	0	126	0	129	0	129	0	
600	240	150	0	150	0	184	0	184	0	151	0	151	0	
600	230	150	0	150	0	192	0	192	0	153	0	153	0	
600	359	297	0	297	0	287	0	287	0	300	0	300	0	
600	219	143	0	143	0	181	0	181	0	145	0	145	0	
600	218	140	0	140	0	176	0	176	0	143	0	143	0	
600	148	92	0	92	0	112	0	112	0	91	0	91	0	
600	453	375	0	375	0	361	0	361	0	378	0	378	0	
600	234	166	0	166	0	166	0	166	0	169	0	169	0	
600	274	194	0	194	0	194	0	194	0	197	0	197	0	
600	312	258	0	258	0	248	0	248	0	260	0	260	0	
600	159	99	0	99	0	121	0	121	0	98	0	98	0	
600	186	116	0	116	0	142	0	142	0	117	0	117	0	
600	230	150	0	150	0	192	0	192	0	153	0	153	0	
600	209	131	0	131	0	161	0	161	0	132	0	132	0	
600	287	203	0	203	0	203	0	203	0	207	0	207	0	
600	300	212	0	212	0	212	0	212	0	216	0	216	0	
600	289	205	0	205	0	205	0	205	0	208	0	208	0	
600	205	131	0	131	0	165	0	165	0	134	0	134	0	
600	195	121	0	121	0	149	0	149	0	122	0	122	0	
600	148	96	0	96	0	120	0	120	0	96	0	96	0	
600	256	212	0	212	0	204	0	204	0	213	0	213	0	
600	175	109	0	109	0	133	0	133	0	108	0	108	0	
600	181	119	0	119	0	151	0	151	0	119	0	119	0	
600	146	94	0	94	0	118	0	118	0	94	0	94	0	
600	241	171	0	171	0	171	0	171	0	174	0	174	0	
600	175	109	0	109	0	133	0	133	0	108	0	108	0	
600	344	244	0	244	0	244	0	244	0	248	0	248	0	
600	238	156	0	156	0	198	0	198	0	158	0	158	0	
600	157	97	0	97	0	119	0	119	0	96	0	96	0	
600	237	155	0	155	0	197	0	197	0	157	0	157	0	
600	157	97	0	97	0	119	0	119	0	96	0	96	0	
600	265	173	0	173	0	221	0	221	0	177	0	177	0	
600	246	160	0	160	0	204	0	204	0	163	0	163	0	
600	343	283	0	283	0	273	0	273	0	286	0	286	0	
600	152	94	0	94	0	116	0	116	0	93	0	93	0	

Table B.14 Noise Effects Analysis

Tot D	Duration			Threshold			FAPI				
	Tot FA	FAD	FA FA	Tot D	Tot FA	FAD	FA FA	Tot D	Tot FA	FAD	FA FA
46.66%	26.10%	99.98%	91.00%	45.11%	29.29%	89.39%	65.46%	89.42%	62.56%	94.32%	63.65%
35.20%	13.89%	96.97%	67.10%	38.30%	24.86%	80.99%	57.84%	87.48%	69.89%	88.63%	70.46%
19.30%	3.36%	69.36%	2.45%	27.38%	16.77%	64.07%	41.76%	85.80%	72.51%	87.74%	72.09%
14.78%	0.02%	46.00%	0.24%	24.88%	15.02%	63.15%	39.92%	83.68%	61.00%	84.42%	60.24%
7.58%	0.00%	27.64%	0.00%	22.93%	12.84%	60.22%	34.99%	77.58%	63.91%	78.31%	63.85%
2.28%	0.00%	7.58%	0.00%	16.47%	9.82%	47.16%	29.29%	69.35%	56.59%	70.79%	56.76%
1.39%	0.00%	5.84%	0.00%	10.09%	5.24%	31.39%	14.99%	68.70%	55.25%	70.64%	54.92%
<b>Vary Noise, Keep N @ 2</b>											
19.30%	3.36%	66.94%	23.50%	27.02%	15.44%	63.50%	40.71%	86.24%	73.29%	87.73%	72.65%
26.96%	2.87%	76.18%	14.85%	36.70%	21.59%	77.13%	55.29%	78.65%	51.07%	80.44%	50.93%
31.58%	4.46%	83.40%	24.96%	31.78%	9.89%	72.91%	26.82%	78.96%	50.76%	80.97%	50.80%
41.17%	2.34%	81.32%	13.13%	40.19%	7.19%	76.98%	21.69%	78.52%	42.72%	79.88%	42.70%
52.11%	0.11%	77.98%	0.48%	56.89%	2.98%	82.31%	11.28%	83.23%	51.22%	83.38%	51.22%
69.48%	0.00%	69.48%	0.00%	77.87%	0.00%	77.87%	0.00%	70.14%	0.00%	70.14%	0.00%

Table B.15 Jitter Effect Results in Detection Testing

S Info	S Rate	Pixel X		Pixel Y													
		60		30		30		Duration (values - # frames)				FAPI (values - # frames)					
						Du	D	FAR	D	FAR	D	FPI	FPI	FAR	FAR		
# F	Act D	Th D	Th FA	FAR D	FAR FA	Du D	Du FA	FAR D	FAR FA	FPI D	FPI FA	FAR D	FAR FA				
0.25	600	269	221	71	269	305	239	103	269	315	269	311	269	311			
	600	182	70	69	182	367	172	184	182	412	85	0	143	0			
	600	223	191	86	223	348	212	173	223	369	195	1	195	12			
	600	193	165	85	193	386	169	99	193	379	173	16	173	30			
	600	245	181	69	219	306	205	108	245	308	245	335	245	335			
	600	341	312	57	341	233	311	54	340	229	341	239	341	239			
	600	225	115	46	225	238	202	134	225	366	225	355	225	355			
	600	281	227	68	281	287	245	87	281	272	243	8	252	3			
	600	168	122	65	168	375	139	133	168	388	168	412	168	412			
	600	358	325	51	358	216	335	64	358	190	358	222	358	222			
	600	191	161	121	191	378	178	175	191	401	191	389	191	389			
	600	242	145	34	242	217	227	149	242	353	242	338	242	338			
	600	224	169	42	224	291	216	173	224	370	224	356	224	356			
	600	254	220	56	254	307	217	39	241	152	254	326	254	326			
	600	202	169	104	202	372	193	169	202	385	173	0	177	0			
	600	254	200	63	254	325	222	106	248	326	254	326	254	326			
	600	203	163	73	203	371	184	145	203	377	158	0	161	0			
	600	374	350	66	374	205	324	34	365	133	357	70	357	89			
	600	274	251	61	274	296	250	58	274	229	256	11	256	15			
	600	189	143	54	189	369	162	113	189	361	155	0	161	0			
	600	121	74	146	121	457	105	170	121	463	53	0	0	0			
	600	235	155	50	224	292	202	125	235	359	235	345	235	345			
	600	323	277	67	323	252	282	77	323	251	323	257	323	257			
	600	162	129	84	162	375	139	108	162	357	123	0	123	0			
	600	206	160	42	206	228	180	108	206	350	178	0	178	0			
	600	285	227	36	284	211	263	108	285	305	285	295	285	295			
	600	195	144	89	195	356	156	118	180	356	155	0	155	0			
	600	184	160	101	184	391	171	184	184	410	184	396	184	396			
	600	180	150	118	180	392	147	105	180	381	180	400	180	400			
	600	314	286	65	314	263	281	61	314	262	290	8	290	0			
	600	190	167	82	190	386	169	102	190	386	165	1	166	1			
	600	208	181	110	208	372	178	103	208	386	208	372	208	372			
	600	209	167	82	209	360	198	186	209	384	173	0	173	0			
	600	218	178	55	218	300	191	95	218	346	218	362	218	362			
	600	119	40	54	117	327	62	138	119	457	52	0	0	0			
	600	330	251	52	316	226	99	13	252	0	330	250	330	250			
	600	123	43	88	123	426	115	188	123	471	123	457	123	457			
	600	336	307	84	336	238	242	7	309	3	309	29	309	41			
	600	256	224	51	256	195	229	63	242	295	256	324	256	324			
	600	260	176	37	260	259	33	0	151	0	203	0	205	0			
	600	183	152	109	183	385	164	147	183	404	183	397	183	397			
	600	151	45	72	151	397	138	171	151	444	76	0	56	0			
	600	427	372	39	427	148	393	47	427	163	386	2	386	0			
	600	199	156	76	199	338	169	109	199	261	166	2	166	0			
	600	155	136	132	155	420	138	152	155	433	155	425	155	425			
	600	290	261	80	290	286	279	114	290	300	290	290	290	290			
	600	176	68	59	176	351	101	98	168	393	113	0	124	0			
	600	313	249	47	313	233	281	91	313	277	313	267	313	267			
	600	325	264	59	325	252	92	5	277	0	325	255	325	255			
	600	163	120	71	163	348	154	185	163	431	133	0	133	0			
	600	420	206	0	267	0	330	15	390	3	420	160	420	160			
	600	138	40	7	130	69	114	118	138	425	36	0	0	0			
	600	281	232	21	257	105	230	18	257	105	281	299	281	299			
	600	187	116	4	167	40	160	55	184	188	135	0	135	0			
	600	191	26	0	119	0	163	87	191	353	191	389	191	389			
	600	159	72	11	124	113	133	88	159	366	159	421	159	421			
	600	128	22	16	128	83	53	115	128	377	128	452	128	452			
	600	204	160	53	196	301	179	111	204	357	138	0	138	0			
	600	145	17	0	119	0	66	108	145	368	0	0	0	0			
	600	230	116	22	201	128	178	88	230	300	230	350	230	350			
	600	281	124	9	257	33	217	58	281	209	281	299	281	299			
	600	264	206	16	248	97	244	90	264	306	264	316	264	316			
	600	193	19	0	153	0	140	122	193	397	193	387	193	387			
	600	200	65	7	181	4	179	126	200	352	117	0	119	0			
	600	252	205	21	242	102	222	78	242	227	252	328	252	328			
	600	121	32	42	121	338	52	100	121	381	121	459	121	459			
	600	159	68	14	149	46	125	83	159	246	95	0	95	0			
	600	359	285	17	342	67	289	22	342	72	359	221	359	221			
	600	170	21	0	97	0	145	132	170	371	24	0	0	0			
	600	299	199	37	299	220	242	69	299	262	299	281	299	281			
	600	279	66	7	245	0	253	103	279	297	279	301	279	301			

600	194	49	5	147	46	163	107	194	392	102	0	102	0
600	341	162	26	330	175	22	0	66	0	341	239	341	239
600	170	110	51	170	322	132	79	170	330	170	410	170	410
600	238	127	20	238	168	220	116	238	357	157	0	157	0
600	187	126	38	180	249	150	78	187	261	113	0	115	0
600	246	157	19	228	172	221	105	246	341	246	334	246	334
600	156	44	2	143	14	128	98	156	424	156	424	156	424
600	260	106	28	260	229	212	84	260	229	260	320	260	320
600	141	33	0	111	0	123	119	141	415	141	439	141	439
600	254	213	26	243	106	208	21	238	58	254	326	254	326
600	151	108	43	151	325	122	129	151	420	151	429	151	429
600	169	30	32	169	139	115	136	169	393	0	0	0	0
600	216	158	19	206	95	173	55	212	162	216	364	216	364
600	198	145	68	198	355	173	120	198	362	133	0	135	0
600	396	307	17	359	92	351	54	396	196	308	0	316	0
600	234	148	10	218	110	197	111	234	357	234	346	234	346
600	150	49	6	129	0	130	144	150	442	150	430	150	430
600	329	231	25	293	181	301	92	329	256	329	251	329	251
600	370	263	11	328	78	282	26	330	118	280	0	280	0
600	217	115	44	197	253	193	116	217	373	217	363	217	363
600	156	40	5	132	23	125	89	153	305	156	424	156	424
600	460	384	14	440	60	0	0	0	0	376	0	377	0
600	239	168	53	239	296	209	123	239	355	163	0	166	0
600	196	55	6	161	52	150	77	196	249	196	384	196	384
600	150	67	36	150	178	124	123	150	414	66	0	0	0
600	170	21	2	128	3	107	122	170	360	170	410	170	410
600	202	76	7	183	93	177	122	202	370	202	378	202	378
600	186	89	15	178	69	154	108	185	380	186	394	186	394
600	367	280	20	322	152	303	32	342	94	367	213	367	213
600	325	238	10	294	51	246	10	294	51	325	255	325	255
600	307	232	5	284	0	241	7	284	0	243	0	243	0
600	172	3	0	0	0	140	83	172	398	172	408	172	408
600	197	16	0	106	0	143	53	184	210	197	383	197	383
600	148	14	0	90	0	108	86	141	402	0	0	0	0
600	451	280	0	359	0	351	13	410	41	320	0	321	0
600	308	174	0	266	0	223	26	282	37	308	272	308	272
600	108	6	0	35	0	63	156	108	412	108	472	108	472
600	153	3	0	0	0	75	109	153	398	0	0	0	0
600	299	154	0	235	0	209	37	246	130	299	281	299	281
600	253	181	7	224	37	183	7	224	15	253	327	253	327
600	147	33	0	108	0	110	71	147	363	147	433	147	433
600	186	98	0	134	0	147	31	174	3	110	0	112	0
600	241	126	1	176	0	186	50	225	171	131	0	131	0
600	196	96	1	128	0	162	51	196	88	196	384	196	384
600	303	171	3	229	0	231	39	285	156	178	0	178	0
600	348	150	0	224	0	257	38	348	193	348	232	348	232
600	387	261	4	341	24	320	36	369	147	387	193	387	193
600	250	170	3	219	0	193	13	231	57	182	0	182	0
600	261	12	0	76	0	204	47	256	187	261	319	261	319
600	222	42	0	168	0	190	100	222	367	222	358	222	358
600	181	26	2	129	0	140	114	181	397	181	399	181	399
600	191	23	0	132	0	159	103	191	399	191	389	191	389
600	469	276	0	347	0	358	10	406	57	469	111	469	111
600	197	19	0	110	0	170	109	197	375	0	0	0	0
600	187	16	0	55	0	132	48	178	211	187	393	187	393
600	249	11	0	85	0	177	36	240	96	0	0	0	0
600	131	0	0	0	0	63	128	131	370	0	0	0	0
600	203	1	0	0	0	159	62	203	293	0	0	0	0
600	187	0	0	0	0	139	57	181	232	187	393	187	393
600	307	221	7	277	55	221	7	270	0	207	0	207	0
600	285	19	0	130	0	40	0	200	0	285	295	285	295
600	352	243	3	295	0	294	38	332	142	238	0	238	0
600	449	277	0	381	0	336	9	410	50	449	131	449	131
600	260	147	1	199	0	187	30	223	84	260	320	260	320
600	341	137	0	193	0	247	40	321	153	341	239	341	239
600	140	9	0	0	0	101	84	140	328	140	440	140	440
600	181	13	0	92	0	135	72	181	325	181	399	181	399
600	207	19	0	100	0	150	62	205	214	207	373	207	373
600	288	192	5	245	33	223	19	263	43	288	292	288	292
600	216	48	0	171	0	155	51	206	206	216	364	216	364
600	330	231	4	298	38	277	23	326	80	239	0	239	0
600	298	208	1	253	0	223	9	264	35	219	0	224	0
600	159	38	0	119	0	114	60	146	267	159	421	159	421
600	257	170	4	226	28	184	12	235	46	257	323	257	323
600	179	87	0	134	0	135	46	171	124	179	401	179	401
600	328	8	0	77	0	36	0	194	0	328	252	328	252
600	143	23	0	89	0	120	119	143	393	143	437	143	437
600	184	10	0	72	0	139	91	184	315	184	396	184	396

600	177	83	0	143	0	134	46	176	133	86	0	89	0
600	198	8	0	85	0	93	29	175	67	0	0	0	0
600	219	0	0	0	0	143	38	204	66	219	361	219	361
600	333	105	0	170	0	214	8	260	0	126	0	126	0
600	316	199	2	249	0	211	3	252	0	184	0	190	0
600	183	0	0	0	0	55	58	171	199	183	397	183	397
600	171	13	0	69	0	74	33	165	110	171	409	171	409
600	146	26	0	96	0	112	81	142	246	146	434	146	434
600	157	0	0	0	0	75	48	156	106	157	423	157	423
600	222	4	0	0	0	176	67	222	248	222	358	222	358
600	193	6	0	35	0	145	82	193	303	0	0	0	0
600	272	160	0	198	0	179	5	178	0	272	308	272	308
600	148	0	0	0	0	64	23	136	36	148	432	148	432
600	152	0	0	0	0	52	69	152	324	0	0	0	0
600	284	126	0	192	0	181	16	255	98	284	296	284	296
600	181	49	0	76	0	136	57	169	244	181	399	181	399
600	232	0	0	0	0	126	46	215	99	0	0	0	0
600	187	0	0	0	0	61	79	187	310	0	0	0	0
600	261	155	0	193	0	174	2	196	0	261	319	261	319
600	173	0	0	0	0	86	38	173	79	173	407	173	407
600	147	0	0	0	0	103	27	133	32	0	0	0	0
600	217	0	0	0	0	162	86	194	308	217	363	217	363
600	179	0	0	0	0	88	40	171	94	0	0	0	0
600	187	0	0	0	0	120	32	187	49	0	0	0	0
600	109	0	0	0	0	36	95	109	436	109	471	109	471
600	215	0	0	0	0	105	37	159	124	0	0	0	0
600	285	180	0	219	0	190	0	226	0	285	295	285	295
600	261	0	0	0	0	148	51	243	159	261	319	261	319
600	341	51	0	142	0	235	14	302	42	341	239	341	239
600	117	0	0	0	0	39	87	117	370	0	0	0	0
600	139	0	0	0	0	65	28	133	129	0	0	0	0
600	331	104	0	172	0	236	20	319	48	331	249	331	249
600	229	0	0	0	0	173	77	229	298	229	351	229	351
600	369	245	7	299	48	292	22	338	51	369	211	369	211
600	213	0	0	0	0	140	27	200	157	0	0	0	0
600	219	0	0	0	0	109	36	206	86	219	361	219	361
600	164	0	0	0	0	88	51	164	153	0	0	0	0
600	200	0	0	0	0	116	25	178	62	0	0	0	0
600	274	63	0	114	0	186	19	257	67	274	306	274	306
600	115	0	0	0	0	45	89	101	382	115	465	115	465
600	177	59	0	93	0	120	10	159	49	75	0	75	0
600	174	0	0	0	0	108	16	170	8	0	0	0	0
600	113	0	0	0	0	29	42	104	0	113	467	113	467
600	185	83	0	117	0	142	34	179	93	185	395	185	395
600	445	199	0	252	0	293	7	363	0	260	0	260	0
600	206	40	0	72	0	140	21	182	64	206	374	206	374
600	187	0	0	0	0	145	75	187	277	0	0	0	0
600	259	96	0	147	0	163	10	221	73	259	321	259	321
600	162	8	0	53	0	78	43	143	170	162	418	162	418
600	112	0	0	0	0	25	54	110	216	112	468	112	468
600	170	0	0	0	0	58	65	170	207	0	0	0	0
600	228	0	0	0	0	76	11	196	0	228	352	228	352
600	183	69	0	108	0	105	4	152	0	8	0	0	0
600	163	0	0	0	0	79	5	152	0	0	0	0	0
600	167	0	0	0	0	53	49	167	153	167	413	167	413
600	213	20	0	79	0	129	3	183	0	55	0	55	0
600	250	0	0	0	0	179	29	230	74	0	0	0	0
600	193	0	0	0	0	135	60	193	192	0	0	0	0
600	297	162	0	204	0	182	0	214	0	297	283	297	283
600	312	168	0	208	0	186	0	214	0	312	268	312	268
600	185	0	0	0	0	141	39	181	22	0	0	0	0
600	317	13	0	83	0	184	13	271	49	46	0	65	0
600	150	0	0	0	0	85	40	150	103	0	0	0	0
600	281	168	1	195	0	192	5	237	37	281	299	281	299
600	239	0	0	0	0	173	60	220	263	0	0	0	0
600	301	147	0	186	0	194	1	237	0	301	279	301	279
600	450	233	0	268	0	309	9	390	46	247	0	248	0
600	204	0	0	0	0	68	12	159	0	204	376	204	376
600	121	0	0	0	0	27	59	112	266	121	459	121	459
600	324	0	0	0	0	0	0	0	0	0	0	0	0
600	112	0	0	0	0	25	54	78	157	112	468	112	468
600	114	0	0	0	0	31	59	92	246	114	466	114	466
600	144	0	0	0	0	23	6	102	0	0	0	0	0
600	148	0	0	0	0	99	40	130	60	0	0	0	0
600	208	0	0	0	0	70	10	187	31	208	372	208	372
600	334	0	0	0	0	0	0	0	0	334	246	334	246
600	146	0	0	0	0	56	9	107	33	146	434	146	434
600	317	188	0	243	0	189	0	243	0	169	0	169	0

600	342	0	0	0	0	0	0	0	0	0	0	0	0
600	185	0	0	0	0	101	42	181	76	0	0	0	0
600	308	59	0	120	0	181	4	276	1	0	0	0	0
600	256	0	0	0	0	172	37	229	173	0	0	0	0
600	206	0	0	0	0	49	47	192	112	206	374	206	374
600	301	0	0	0	0	102	12	273	0	0	0	0	0
600	221	0	0	0	0	86	19	189	0	221	359	221	359
600	279	141	0	188	0	172	0	219	0	279	301	279	301
600	114	0	0	0	0	21	13	95	1	0	0	0	0
600	267	0	0	0	0	183	40	235	107	267	313	267	313
600	159	0	0	0	0	52	57	159	242	0	0	0	0
600	194	0	0	0	0	69	9	186	4	194	386	194	386
600	403	182	0	210	0	231	0	282	0	403	177	403	177
600	298	0	0	0	0	185	4	255	0	298	282	298	282
600	176	10	0	59	0	113	4	145	0	0	0	0	0
600	206	24	0	70	0	119	2	178	0	0	0	0	0
600	232	0	0	0	0	143	4	197	0	0	0	0	0
600	325	159	0	201	0	209	1	247	0	169	0	169	0
600	425	183	0	230	0	303	4	357	0	425	155	425	155
600	128	0	0	0	0	34	57	113	200	0	0	0	0
600	318	135	0	159	0	195	0	213	0	170	0	170	0
600	195	0	0	0	0	85	6	157	0	195	385	195	385
600	346	0	0	0	0	0	0	0	0	0	0	0	0
600	181	0	0	0	0	45	3	133	0	181	399	181	399
600	195	0	0	0	0	94	0	134	0	195	385	195	385
600	226	0	0	0	0	118	0	169	0	226	354	226	354
600	203	0	0	0	0	48	21	182	55	203	377	203	377
600	147	0	0	0	0	32	5	103	0	147	433	147	433
600	281	110	0	120	0	152	0	179	0	126	0	126	0
600	369	169	0	199	0	243	0	302	0	369	211	369	211
600	328	101	0	142	0	187	0	231	0	141	0	141	0
600	268	0	0	0	0	59	1	211	0	0	0	0	0
600	280	0	0	0	0	128	0	194	0	280	300	280	300
600	223	0	0	0	0	116	0	165	0	223	357	223	357
600	162	0	0	0	0	33	4	124	0	162	418	162	418
600	410	142	0	156	0	259	1	308	0	172	0	172	0
600	396	121	0	146	0	216	0	255	0	396	184	396	184
600	166	0	0	0	0	65	33	152	95	166	414	166	414
600	249	0	0	0	0	136	15	196	0	249	331	249	331
600	264	0	0	0	0	55	2	185	0	0	0	0	0
600	249	0	0	0	0	132	1	177	0	249	331	249	331
600	159	0	0	0	0	41	32	139	83	159	421	159	421
600	193	0	0	0	0	41	0	151	0	193	387	193	387
600	175	0	0	0	0	72	27	158	60	175	405	175	405
600	378	157	0	203	0	205	0	245	0	153	0	153	0
600	213	0	0	0	0	50	6	157	38	213	367	213	367
600	258	0	0	0	0	59	1	191	0	0	0	0	0
600	166	0	0	0	0	90	42	166	48	0	0	0	0
600	227	0	0	0	0	0	0	0	0	227	353	227	353
600	261	75	0	88	0	147	0	171	0	261	319	261	319
600	122	0	0	0	0	27	20	100	0	0	0	0	0
600	146	0	0	0	0	29	33	135	134	146	434	146	434
600	250	79	0	94	0	143	0	184	0	250	330	250	330
600	157	0	0	0	0	58	37	147	135	0	0	0	0
600	257	0	0	0	0	55	0	185	0	0	0	0	0
600	290	120	0	155	0	154	0	202	0	131	0	131	0
600	143	0	0	0	0	29	17	113	30	143	437	143	437
600	300	12	0	0	0	148	0	196	0	0	0	0	0
600	120	0	0	0	0	24	32	76	45	0	0	0	0
600	387	121	0	156	0	206	0	235	0	387	193	387	193
600	148	0	0	0	0	43	6	109	0	0	0	0	0
600	217	0	0	0	0	54	0	164	0	217	363	217	363
600	144	0	0	0	0	30	32	96	77	0	0	0	0
600	225	0	0	0	0	87	17	211	46	0	0	0	0
600	162	0	0	0	0	67	20	142	0	162	418	162	418
600	189	0	0	0	0	44	1	162	0	0	0	0	0
600	336	0	0	0	0	0	0	0	0	0	0	0	0
600	281	0	0	0	0	0	0	0	0	0	0	0	0
600	123	0	0	0	0	27	33	89	68	123	457	123	457
600	193	0	0	0	0	43	0	162	0	193	387	193	387
600	171	0	0	0	0	86	17	139	84	0	0	0	0
600	334	0	0	0	0	165	0	216	0	334	246	334	246
600	120	0	0	0	0	16	18	83	41	120	460	120	460
600	143	0	0	0	0	26	0	88	0	143	437	143	437
600	301	0	0	0	0	111	0	174	0	0	0	0	0
600	267	0	0	0	0	41	0	177	0	0	0	0	0
600	139	0	0	0	0	15	0	31	0	0	0	0	0
600	385	155	0	190	0	219	0	278	0	128	0	128	0

600	182	0	0	0	0	32	6	130	2	182	398	182	398	
600	211	0	0	0	0	29	10	44	9	0	0	0	0	
600	346	0	0	0	0	0	0	0	0	346	234	346	234	
600	476	78	0	121	0	208	0	260	0	476	104	476	104	
600	255	76	0	99	0	111	0	120	0	255	325	255	325	
600	200	0	0	0	0	39	0	122	0	200	380	200	380	
600	179	0	0	0	0	72	0	114	0	179	401	179	401	
600	198	0	0	0	0	32	0	135	0	0	0	0	0	
600	128	0	0	0	0	1	0	0	0	128	452	128	452	
600	262	101	0	113	0	120	0	144	0	93	0	93	0	
600	268	84	0	109	0	121	0	160	0	268	312	268	312	
600	208	0	0	0	0	35	0	133	0	208	372	208	372	
600	340	120	0	147	0	149	0	188	0	340	240	340	240	
600	176	0	0	0	0	20	1	36	0	176	404	176	404	
600	151	0	0	0	0	19	0	55	0	0	0	0	0	
600	469	70	0	86	0	0	0	0	0	469	111	469	111	
600	153	0	0	0	0	21	0	77	0	153	427	153	427	
600	229	0	0	0	0	100	0	147	0	229	351	229	351	
600	415	42	0	69	0	187	0	235	0	106	0	106	0	
600	181	0	0	0	0	57	2	137	0	0	0	0	0	
600	283	9	0	0	0	137	0	148	0	91	0	91	0	
600	185	0	0	0	0	1	0	0	0	185	395	185	395	
600	229	0	0	0	0	33	0	141	0	0	0	0	0	
600	205	0	0	0	0	24	2	113	0	205	375	205	375	
600	204	0	0	0	0	28	5	153	0	204	376	204	376	
600	132	0	0	0	0	15	5	52	0	132	448	132	448	
600	274	61	0	80	0	122	0	150	0	110	0	110	0	
600	252	0	0	0	0	41	0	137	0	0	0	0	0	
600	185	0	0	0	0	24	7	63	0	185	395	185	395	
600	132	0	0	0	0	17	8	53	0	132	448	132	448	
600	302	0	0	0	0	117	0	179	0	302	278	302	278	
600	247	0	0	0	0	90	0	136	0	247	333	247	333	
600	350	65	0	92	0	163	0	191	0	350	230	350	230	
600	184	0	0	0	0	0	0	0	0	184	396	184	396	
600	178	0	0	0	0	48	12	138	0	178	402	178	402	
600	154	0	0	0	0	30	0	108	0	154	426	154	426	
600	185	0	0	0	0	70	0	121	0	0	0	0	0	
600	155	0	0	0	0	41	5	135	8	155	425	155	425	
600	429	104	0	127	0	227	0	271	0	190	0	190	0	
600	482	85	0	132	0	50	0	90	0	111	0	111	0	
600	185	0	0	0	0	77	0	124	0	185	395	185	395	
600	239	0	0	0	0	32	0	131	0	239	341	239	341	
600	206	0	0	0	0	91	0	134	0	0	0	0	0	
600	234	0	0	0	0	34	0	148	0	0	0	0	0	
600	288	33	0	66	0	128	0	167	0	288	292	288	292	
0	600	183	111	0	111	0	141	0	141	0	111	0	111	0
600	185	0	0	0	0	149	0	149	0	0	0	0	0	
600	146	0	0	0	0	108	0	108	0	0	0	0	0	
600	264	0	0	0	0	212	0	212	0	0	0	0	0	
600	214	130	0	130	0	164	0	164	0	130	0	130	0	
600	176	92	0	92	0	130	0	130	0	80	0	80	0	
600	179	109	0	109	0	137	0	137	0	108	0	108	0	
600	247	133	0	133	0	189	0	189	0	0	0	0	0	
600	128	0	0	0	0	94	0	94	0	0	0	0	0	
600	321	195	0	195	0	247	0	247	0	195	0	195	0	
600	244	148	0	148	0	188	0	188	0	148	0	148	0	
600	168	0	0	0	0	136	0	136	0	0	0	0	0	
600	174	0	0	0	0	128	0	128	0	0	0	0	0	
600	219	115	0	115	0	163	0	163	0	104	0	104	0	
600	262	0	0	0	0	210	0	210	0	0	0	0	0	
600	288	220	0	220	0	208	0	208	0	220	0	220	0	
600	201	123	0	123	0	155	0	155	0	122	0	122	0	
600	339	207	0	207	0	261	0	261	0	205	0	205	0	
600	155	0	0	0	0	115	0	115	0	0	0	0	0	
600	467	359	0	359	0	339	0	339	0	357	0	357	0	
600	198	106	0	106	0	152	0	152	0	0	0	0	0	
600	238	124	0	124	0	176	0	176	0	114	0	114	0	
600	241	147	0	147	0	185	0	185	0	145	0	145	0	
600	220	118	0	118	0	168	0	168	0	0	0	0	0	
600	189	0	0	0	0	151	0	151	0	0	0	0	0	
600	192	116	0	116	0	148	0	148	0	116	0	116	0	
600	245	0	0	0	0	197	0	197	0	0	0	0	0	
600	246	150	0	150	0	190	0	190	0	148	0	148	0	
600	241	125	0	125	0	177	0	177	0	115	0	115	0	
600	179	97	0	97	0	137	0	137	0	0	0	0	0	
600	184	112	0	112	0	142	0	142	0	111	0	111	0	
600	249	129	0	129	0	183	0	183	0	120	0	120	0	
600	202	122	0	122	0	154	0	154	0	122	0	122	0	

600	215	131	0	131	0	165	0	165	0	129	0	129	0	
600	158	82	0	82	0	116	0	116	0	69	0	69	0	
600	210	128	0	128	0	162	0	162	0	127	0	127	0	
600	207	0	0	0	0	153	0	153	0	0	0	0	0	
600	206	126	0	126	0	158	0	158	0	125	0	125	0	
600	468	358	0	358	0	338	0	338	0	358	0	358	0	
600	122	0	0	0	0	90	0	90	0	0	0	0	0	
600	158	0	0	0	0	126	0	126	0	0	0	0	0	
600	168	88	0	88	0	124	0	124	0	76	0	76	0	
600	151	79	0	79	0	111	0	111	0	65	0	65	0	
600	317	171	0	171	0	245	0	245	0	0	0	0	0	
600	303	231	0	231	0	219	0	219	0	231	0	231	0	
600	185	0	0	0	0	137	0	137	0	0	0	0	0	
600	167	0	0	0	0	135	0	135	0	0	0	0	0	
600	246	128	0	128	0	182	0	182	0	118	0	118	0	
600	302	232	0	232	0	218	0	218	0	231	0	231	0	
600	378	290	0	290	0	274	0	274	0	289	0	289	0	
0.1	600	238	15	0	32	0	164	0	185	0	238	342	238	342
600	208	121	0	139	0	162	0	178	0	118	0	118	0	
600	175	11	0	66	0	123	0	139	0	0	0	0	0	
600	185	116	0	117	0	142	0	153	0	106	0	106	0	
600	194	28	0	104	0	158	1	174	0	194	386	194	386	
600	256	116	0	163	0	206	0	226	0	3	0	0	0	
600	111	0	0	0	0	26	0	94	0	0	0	0	0	
600	198	2	0	0	0	136	0	148	0	0	0	0	0	
600	251	51	0	148	0	169	0	187	0	0	0	0	0	
600	228	6	0	0	0	163	0	176	0	228	352	228	352	
600	151	46	0	91	0	124	0	136	0	37	0	0	0	
600	217	28	0	108	0	151	0	173	0	0	0	0	0	
600	131	0	0	0	0	41	0	105	0	0	0	0	0	
600	284	214	0	230	0	208	0	216	0	217	0	217	0	
600	151	0	0	0	0	108	0	120	0	0	0	0	0	
600	131	0	0	0	0	44	0	103	0	0	0	0	0	
600	228	38	0	127	0	188	2	207	0	0	0	0	0	
600	446	308	0	321	0	327	0	341	0	446	134	446	134	
600	207	42	0	110	0	171	2	176	0	207	373	207	373	
600	150	1	0	0	0	107	0	118	0	150	430	150	430	
600	310	236	0	249	0	224	0	238	0	310	270	310	270	
600	169	0	0	0	0	46	0	142	0	0	0	0	0	
600	262	58	0	146	0	212	0	238	0	0	0	0	0	
600	207	42	0	108	0	172	0	189	0	1	0	0	0	
600	209	26	0	104	0	144	0	155	0	1	0	0	0	
600	211	127	0	132	0	157	0	163	0	211	369	211	369	
600	148	0	0	0	0	37	0	114	0	148	432	148	432	
600	239	48	0	128	0	195	0	210	0	3	0	0	0	
600	226	45	0	136	0	183	2	198	0	0	0	0	0	
600	296	224	0	235	0	211	0	217	0	296	284	296	284	
600	237	140	0	157	0	176	0	189	0	139	0	139	0	
600	117	0	0	0	0	26	0	95	0	117	463	117	463	
600	209	52	0	120	0	159	1	185	0	209	371	209	371	
600	268	20	0	0	0	193	0	217	0	268	312	268	312	
600	405	276	0	300	0	302	0	317	0	405	175	405	175	
600	319	177	0	198	0	238	0	261	0	175	0	175	0	
600	158	0	0	0	0	36	0	112	0	158	422	158	422	
600	150	4	0	0	0	100	0	108	0	150	430	150	430	
600	138	4	0	0	0	104	0	111	0	0	0	0	0	
600	210	1	0	0	0	141	0	160	0	0	0	0	0	
600	381	287	0	297	0	276	0	286	0	381	199	381	199	
600	280	153	0	168	0	219	0	243	0	280	300	280	300	
600	295	225	0	245	0	212	0	213	0	295	285	295	285	
600	239	139	0	157	0	194	1	215	0	239	341	239	341	
600	146	31	0	80	0	114	1	120	0	2	0	0	0	
600	205	0	0	0	0	147	0	160	0	0	0	0	0	
600	272	173	0	184	0	201	0	223	0	156	0	156	0	
600	217	37	0	121	0	151	0	158	0	217	363	217	363	
600	186	0	0	0	0	136	0	153	0	186	394	186	394	
600	316	200	0	222	0	240	0	264	0	316	264	316	264	
0.2	600	250	16	0	72	0	194	69	250	295	0	0	0	
600	228	115	0	154	0	167	10	203	72	228	352	228	352	
600	181	0	0	0	0	141	33	171	72	0	0	0	0	
600	185	39	0	120	0	139	58	164	107	0	0	0	0	
600	179	2	0	0	0	144	64	172	135	179	401	179	401	
600	268	10	0	0	0	199	34	241	76	0	0	0	0	
600	250	0	0	0	0	1	0	0	0	0	0	0	0	
600	181	85	0	121	0	129	13	149	61	181	399	181	399	
600	226	101	0	141	0	179	24	210	70	226	354	226	354	
600	136	8	0	0	0	112	64	136	271	136	444	136	444	
600	252	125	0	155	0	180	12	219	42	133	0	137	0	

600	308	209	0	226	0	229	4	240	0	225	0	225	0	
600	283	209	4	229	0	211	4	242	0	207	0	207	0	
600	244	141	0	163	0	184	25	230	87	131	0	131	0	
600	212	41	0	138	0	163	46	207	132	6	0	0	0	
600	382	252	0	282	0	292	6	341	30	275	0	275	0	
600	122	0	0	0	0	74	138	122	458	122	458	122	458	
600	212	0	0	0	0	70	52	209	181	0	0	0	0	
600	249	145	0	176	0	173	9	224	3	142	0	143	0	
600	304	213	0	247	0	223	2	247	0	304	276	304	276	
600	253	42	0	120	0	188	29	223	65	253	327	253	327	
600	255	119	0	160	0	193	8	237	11	255	325	255	325	
600	144	0	0	0	0	119	73	144	341	144	436	144	436	
600	251	20	0	76	0	194	35	240	110	251	329	251	329	
600	180	80	0	99	0	136	12	156	0	99	0	99	0	
600	186	0	0	0	0	150	48	186	235	186	394	186	394	
600	120	6	0	0	0	62	97	120	405	0	0	0	0	
600	229	28	0	84	0	165	30	216	86	229	351	229	351	
600	141	5	0	0	0	114	68	141	267	141	439	141	439	
600	177	84	0	116	0	131	12	160	72	177	403	177	403	
600	124	0	0	0	0	36	59	120	240	124	456	124	456	
600	200	121	0	150	0	148	19	192	82	119	0	121	0	
600	145	0	0	0	0	34	66	138	202	0	0	0	0	
600	196	23	0	109	0	155	31	192	50	196	384	196	384	
600	274	21	0	67	0	202	31	274	105	274	306	274	306	
600	292	123	0	167	0	224	25	274	96	165	0	165	0	
600	116	0	0	0	0	52	81	113	281	116	464	116	464	
600	244	153	0	187	0	175	3	226	0	244	336	244	336	
600	254	131	0	175	0	202	22	238	82	132	0	132	0	
600	226	34	0	133	0	167	44	215	226	226	354	226	354	
600	218	5	0	0	0	170	48	218	113	0	0	0	0	
600	203	0	0	0	0	30	1	108	0	0	0	0	0	
600	186	10	0	0	0	151	54	186	274	0	0	0	0	
600	275	213	14	219	73	227	22	258	95	206	0	206	0	
600	152	4	0	0	0	120	63	148	209	0	0	0	0	
600	230	5	0	0	0	183	49	230	158	0	0	0	0	
600	184	21	0	79	0	138	27	169	37	0	0	0	0	
600	250	17	0	37	0	184	31	238	68	250	330	250	330	
600	345	0	0	0	0	271	47	336	168	345	235	345	235	
600	177	80	0	104	0	125	8	147	0	93	0	93	0	
0 3	600	144	17	0	52	0	119	140	136	421	144	436	144	436
600	187	37	9	129	0	154	117	187	383	187	393	187	393	
600	173	0	0	0	0	64	90	173	351	173	407	173	407	
600	203	92	24	197	12	164	88	203	291	203	377	203	377	
600	149	5	0	0	0	103	78	149	351	0	0	0	0	
600	212	0	0	0	0	55	52	196	180	212	368	212	368	
600	163	17	0	70	0	114	59	157	153	163	417	163	417	
600	223	107	2	185	0	172	66	203	248	107	0	107	0	
600	280	11	0	0	0	226	81	280	280	280	300	280	300	
600	331	219	7	277	31	283	51	321	171	331	249	331	249	
600	263	2	0	0	0	31	1	114	0	0	0	0	0	
600	332	233	16	292	62	254	24	316	95	332	248	332	248	
600	208	39	3	156	0	171	102	208	368	208	372	208	372	
600	214	122	7	197	1	155	44	205	106	214	366	214	366	
600	460	261	0	319	0	348	18	420	76	460	120	460	120	
600	124	0	0	0	0	50	141	124	448	0	0	0	0	
600	171	42	3	122	0	150	133	171	391	171	409	171	409	
600	325	5	0	0	0	36	0	154	0	0	0	0	0	
600	228	49	6	159	0	174	95	228	334	0	0	0	0	
600	138	0	0	0	0	86	90	136	362	0	0	0	0	
600	263	211	41	263	103	226	60	263	273	263	317	263	317	
600	284	212	20	250	109	230	54	273	196	223	0	225	0	
600	345	272	22	339	109	297	40	339	134	252	0	252	0	
600	240	8	0	40	0	143	81	230	277	0	0	0	0	
600	374	275	15	349	7	316	47	365	138	254	0	254	0	
600	195	29	0	127	0	147	97	195	379	195	385	195	385	
600	233	122	7	201	1	194	101	233	313	233	347	233	347	
600	146	0	0	0	0	61	111	146	409	0	0	0	0	
600	435	284	7	354	0	340	16	415	88	303	0	309	0	
600	237	54	0	102	0	190	80	237	306	237	343	237	343	
600	236	67	0	123	0	174	52	236	234	128	0	128	0	
600	239	14	0	49	0	168	64	239	260	239	341	239	341	
600	369	266	14	330	43	310	41	350	114	369	211	369	211	
600	258	41	2	131	0	206	92	258	316	0	0	0	0	
600	241	116	0	185	0	175	40	241	175	241	339	241	339	
600	183	16	0	43	0	149	117	183	412	183	397	183	397	
600	238	60	16	170	0	185	100	224	336	0	0	0	0	
600	162	29	1	117	0	129	102	155	405	0	0	0	0	
600	370	259	14	324	56	272	20	332	91	267	0	270	0	

	600	196	18	6	57	0	165	112	196	379	196	384	196	384
	600	316	205	6	244	0	231	17	294	54	224	0	224	0
	600	373	201	0	260	0	289	24	338	53	373	207	373	207
	600	305	204	6	279	18	226	13	279	30	305	275	305	275
	600	170	0	0	0	0	68	105	170	405	170	410	170	410
	600	277	208	21	259	59	216	30	260	98	203	0	203	0
	600	138	9	0	0	0	109	125	138	428	138	442	138	442
	600	275	193	10	240	43	209	20	247	84	275	305	275	305
	600	286	83	21	263	59	37	0	153	0	0	0	0	0
	600	308	137	2	223	0	240	50	293	231	308	272	308	272
	600	392	225	2	293	0	307	39	372	141	392	188	392	188
0.4	600	347	209	16	294	62	289	62	347	218	257	0	273	0
	600	380	213	16	297	38	168	4	189	0	272	0	272	0
	600	198	23	10	97	0	139	106	184	387	198	382	198	382
	600	191	8	7	0	0	66	112	180	393	0	0	0	0
	600	205	23	8	92	0	169	141	205	356	205	375	205	375
	600	142	0	0	0	0	50	113	142	349	0	0	0	0
	600	303	161	8	235	19	220	39	286	164	303	277	303	277
	600	311	103	12	226	0	258	102	311	279	107	0	107	0
	600	273	169	12	229	22	213	39	273	181	192	0	194	0
	600	137	21	24	28	106	44	98	137	334	137	443	137	443
	600	228	30	8	106	0	182	100	228	350	0	0	0	0
	600	268	36	10	165	2	61	25	166	88	268	312	268	312
	600	338	2	0	0	0	66	20	263	34	338	242	338	242
	600	131	6	7	0	0	61	147	131	460	131	449	131	449
	600	226	16	1	56	0	187	127	226	338	226	354	226	354
	600	403	245	12	352	75	338	42	393	176	262	0	268	0
	600	295	142	22	225	99	234	90	295	273	295	285	295	285
	600	162	0	0	0	0	127	134	162	429	162	418	162	418
	600	217	2	0	0	0	152	109	217	360	217	363	217	363
	600	200	81	11	165	21	155	104	200	390	200	380	200	380
	600	284	55	2	181	0	235	87	284	296	136	0	143	0
	600	367	214	10	323	12	292	46	367	180	367	213	367	213
	600	138	10	17	6	53	71	169	138	456	138	442	138	442
	600	237	6	0	0	0	185	108	237	358	0	0	0	0
	600	285	213	30	284	97	242	81	285	249	285	295	285	295
	600	204	1	0	0	0	137	106	204	350	204	376	204	376
	600	270	144	9	181	0	203	44	264	209	178	0	185	0
	600	173	0	0	0	0	140	150	173	421	0	0	0	0
	600	197	20	6	65	0	161	129	197	395	197	383	197	383
	600	154	0	0	0	0	120	129	154	410	154	426	154	426
	600	307	194	18	277	44	262	76	307	247	307	273	307	273
	600	170	4	0	0	0	120	108	170	381	0	0	0	0
	600	218	23	8	86	0	39	29	148	15	0	0	0	0
	600	208	89	18	162	53	171	103	208	341	87	0	87	0
	600	328	0	0	0	0	74	34	246	150	328	252	328	252
	600	303	244	66	303	255	256	75	303	260	303	277	303	277
	600	224	88	18	182	50	174	100	224	365	224	356	224	356
	600	276	215	53	276	199	235	78	276	239	276	304	276	304
	600	168	22	25	64	0	147	162	168	422	0	0	0	0
	600	179	63	7	92	14	133	83	179	386	179	401	179	401
	600	216	1	0	0	0	156	105	216	378	0	0	0	0
	600	174	21	4	105	0	143	120	174	418	174	406	174	406
	600	447	247	10	364	48	1	0	0	0	447	133	447	133
	600	478	212	1	303	0	1	0	0	0	319	0	319	0
	600	250	13	0	0	0	203	99	250	337	250	330	250	330
	600	167	9	2	0	0	85	119	167	407	167	413	167	413
	600	316	119	13	218	0	250	78	316	260	316	264	316	264
	600	225	45	24	178	80	187	125	225	316	225	355	225	355
	600	194	0	0	0	0	51	78	155	370	194	386	194	386
	600	252	50	24	184	78	193	115	252	262	252	328	252	328
0.5	600	188	20	19	0	0	68	99	188	361	188	392	188	392
	600	225	9	7	0	0	38	42	121	77	0	0	0	0
	600	210	49	52	180	222	155	132	210	383	32	0	0	0
	600	122	0	0	0	0	49	147	122	454	0	0	0	0
	600	158	16	13	57	1	78	141	158	429	158	422	158	422
	600	140	0	0	0	0	54	135	140	452	140	440	140	440
	600	150	0	0	0	0	72	126	132	398	150	430	150	430
	600	108	10	7	45	0	42	143	108	411	0	0	0	0
	600	292	41	10	132	45	217	97	288	288	55	0	76	0
	600	244	77	67	244	233	181	120	244	335	13	0	0	0
	600	183	35	20	167	34	154	141	183	409	183	397	183	397
	600	197	39	9	112	0	140	87	197	301	88	0	93	0
	600	219	100	45	219	160	185	131	219	376	92	0	101	0
	600	440	182	8	310	6	35	0	82	0	440	140	440	140
	600	365	117	5	236	0	286	68	365	226	240	0	251	0
	600	165	2	1	0	0	129	150	165	407	0	0	0	0
	600	207	58	11	179	0	155	124	207	366	207	373	207	373

600	249	105	44	186	142	193	100	249	296	249	331	249	331
600	245	2	0	0	0	205	139	245	350	0	0	0	0
600	149	16	18	68	43	77	143	149	437	149	431	149	431
600	275	29	14	149	37	218	114	275	308	275	305	275	305
600	153	16	18	88	44	68	116	153	421	0	0	0	0
600	363	116	6	217	2	271	59	363	195	363	217	363	217
600	117	28	40	115	152	56	121	117	433	0	0	0	0
600	280	16	3	0	0	182	103	280	306	280	300	280	300
600	455	64	1	126	0	26	0	90	0	455	125	455	125
600	394	78	5	135	0	315	52	393	139	212	0	214	0
600	147	41	73	120	307	109	168	147	448	147	433	147	433
600	128	7	12	0	0	48	146	128	461	128	452	128	452
600	162	3	6	0	0	85	134	162	429	162	418	162	418
600	276	41	18	166	44	213	109	276	317	0	0	0	0
600	317	32	5	99	0	245	106	317	274	317	263	317	263
600	277	68	19	207	73	232	113	277	314	277	303	277	303
600	240	21	8	68	0	154	123	240	351	240	340	240	340
600	178	42	38	133	122	138	150	178	398	0	0	0	0
600	250	3	4	0	0	138	113	250	340	0	0	0	0
600	109	0	0	0	0	41	156	109	482	109	471	109	471
600	303	3	0	0	0	71	52	269	137	303	277	303	277
600	289	52	34	212	165	237	103	289	305	289	291	289	291
600	241	56	35	200	92	176	105	241	340	241	339	241	339
600	166	32	61	120	283	105	150	166	406	3	0	0	0
600	202	20	20	4	34	130	133	202	390	202	378	202	378
600	308	185	32	297	120	233	56	308	190	190	0	201	0
600	277	159	56	277	214	222	112	277	302	277	303	277	303
600	245	19	9	71	0	200	119	245	321	245	335	245	335
600	241	0	0	0	0	137	101	241	318	0	0	0	0
600	178	16	7	42	0	130	157	178	417	178	402	178	402
600	187	20	19	103	30	146	149	187	404	0	0	0	0
600	338	191	23	297	41	289	89	338	247	197	0	214	0
600	312	166	20	271	73	243	72	291	266	206	0	213	0

Table B.16 Jitter Effects Analysis

Duration				Threshold				FAPI			
Tot D	Tot FA	FAD	FA FA	Tot D	Tot FA	FAD	FA FA	Tot D	Tot FA	FAD	FA FA
78.61%	19.58%	99.54%	85.68%	83.16%	29.98%	97.20%	85.61%	91.65%	48.43%	91.39%	48.66%
54.00%	5.12%	90.09%	%	76.11%	23.51%	92.04%	77.30%	86.31%	62.06%	85.36%	62.06%
40.65%	0.35%	65.23%	1.51%	72.38%	14.43%	92.79%	52.06%	82.74%	62.76%	82.83%	62.76%
18.80%	0.05%	28.90%	0.25%	60.16%	10.38%	90.75%	34.61%	65.05%	54.52%	65.11%	54.52%
17.20%	0.01%	23.45%	0.00%	48.35%	5.21%	74.89%	14.70%	51.54%	41.34%	51.64%	41.34%
10.55%	0.00%	12.75%	0.00%	38.09%	2.57%	69.25%	5.60%	61.81%	56.42%	61.81%	56.42%
8.91%	0.00%	11.77%	0.00%	28.00%	0.35%	49.90%	0.11%	65.01%	61.12%	65.01%	61.12%
Vary Noise, N=2				23.50							
40.65%	0.35%	61.00%	%	69.86%	14.00%	92.12%	48.56%	80.63%	63.14%	80.76%	63.14%
45.62%	0.00%	45.62%	0.00%	73.48%	0.00%	73.48%	0.00%	39.27%	0.00%	39.27%	0.00%
34.64%	0.00%	46.96%	0.00%	70.43%	0.05%	80.69%	0.00%	59.18%	40.83%	58.76%	40.83%
27.84%	0.09%	39.21%	0.38%	69.70%	9.47%	89.47%	32.27%	61.23%	44.73%	61.24%	44.73%
40.25%	1.78%	61.61%	4.10%	70.71%	19.09%	93.05%	67.68%	72.60%	55.35%	72.68%	55.35%
30.83%	3.11%	51.77%	8.09%	63.46%	25.23%	87.53%	81.86%	76.65%	61.77%	76.96%	61.77%

Table B.17 Velocity and Length Testing Results

S	Rate	Pixel X	Pixel Y	Noise	T	Info#	N	FARI	FAR2	Analysis	C L	Length	Speed	Actual	length	%Diff L	C V	%Diff V
120	30	30	0.01	1	2.6	14	50	T/P	4.54	30.73	29.06	4.57	0.0066	0.0575				
120	30	30	0.01	1	2.8	10	50	T/P	4.59	24.25	23.88		0.0044	0.0155				
120	30	30	0.01	1	2.8	10	50	T/P	5.08	26.38	24.06		0.1116	0.0964				
120	30	30	0.01	1	2.4	10	50	T/P	4.45	24.97	22.41		0.0263	0.1142				
120	30	30	0.01	1	2	8	50	T/P	5.2	24.66	22.41		0.1379	0.1004				
120	30	30	0.01	1	2.9	10	10	T/P	4.71	18.16	16.86		0.0306	0.0771				
120	30	30	0.01	1	1.5	15	50	D/P	4.27	19.76	18.12		0.0656	0.0905				
120	30	30	0.01	1	2.5	25	50	T/P	4.78	17.23	15.86		0.0460	0.0864				
120	30	30	0.01	1	2.5	20	50	T/P	4.44	19.67	18.01		0.0284	0.0922				
120	30	30	0.01	1	2.3	15	30	T/P	4.73	25.51	23.58		0.0350	0.0818				
120	30	30	0.01	1	2.5	20	50	T/P	4.06	29.81	28.16		0.1116	L Avg	0.0586			
120	30	30	0.01	1	2.7	9	50	T/P	5.18	23.02	21.23		0.1335	4.6862	0.0843			
120	30	30	0.01	1	2.6	15	50	T/P	4.89	26.03	24.01		0.0700	0.0254	0.0841	0.0799		
120	30	30	0.02	1	2	5	80	T/P	3.69	18.62	18.01		0.1926	% error	0.0339			
120	30	30	0.02	1	3	10	80	T/P	4.44	18.76	20.35		0.0284	0.0781				
120	30	30	0.02	1	3	10	50	T/P	4.86	16.99	16.86		0.0635	0.0077				
120	30	30	0.02	1	2.1	40	80	D/F	4.77	21.83	22.5		0.0438	0.0298				
120	30	30	0.02	1	2.5	8	50	T/P	4.44	18.76	18.01		0.0284	0.0416				
120	30	30	0.02	1	2.9	6	50	T/P	4.71	26.47	23.15		0.0306	L Avg	0.1434			
120	30	30	0.02	1	2.5	6	50	T/P	4.48	25.33	23.15		0.0197	4.4013	0.0942			
120	30	30	0.02	1	3	20	50	T/P	3.82	28.21	23.9		0.1641	0.0369	0.1803	0.0761		
120	30	30	0.03	1	1.1	15	80	D/F	4.68	25.53	26.24		0.0241	% error	0.0271			
120	30	30	0.03	1	4.7	30	80	D/F	4.45	27.17	26.24		0.0263	0.0354				
120	30	30	0.03	1	2.6	20	140	T/F	5.21	29.06	28.92		0.1400	0.0048				
120	30	30	0.03	1	2.5	35	80	D/P	5.53	16.28	17		0.2101	0.0424				
120	30	30	0.03	1	6	35	80	D/P	4.81	25.54	23.54		0.0525	0.0850				
120	30	30	0.03	1	7	60	80	D/P	4.45	20.9	14.77		0.0263	0.4150				
120	30	30	0.03	1	2.7	20	100	D/P	4.74	22.49	32.3		0.0372	L Avg	0.3037			
120	30	30	0.03	1	4	30	80	T/P	5.12	13.49	14.77	avg v	0.1204	4.9456	0.0867			
60	30	30	0.03	1	2.8	25	10	T/P	4.69	5.52	36.58	28.26	1.219	0.2079	0.0822	0.2944	0.1438	
60	30	30	0.03	2	3.2	15	150	T/P	10.55	22.28	25.03	10.19	0.0353	% error	0.1099			
60	30	30	0.03	2	4.5	15	80	D/F	10.91	26.68	25.48		0.0707	0.0471				
60	30	30	0.03	2	2.5	40	150	T/P	11.25	14.59	14.45		0.1040	0.0097				
60	30	30	0.03	2	1.5	25	80	D/F	11.45	20.38	19.08		0.1237	0.0681				
60	30	30	0.03	2	4.2	33	80	T/P	8.91	18.18	19.08		0.1256	0.0472				
60	30	30	0.03	2	3.3	20	40	T/P	9.91	21.74	21.51		0.0275	0.0107				
60	30	30	0.03	2	2.6	33	150	T/F	11.61	17.65	18		0.1394	0.0194				
60	30	30	0.03	2	4.5	50	150	T/F	11.24	22.1	22.22		0.1030	L Avg	0.0054			
60	30	30	0.03	2	4.5	10	150	T/F	9.92	17.29	16.78		0.0265	10.6290	0.0304			
60	30	30	0.03	2	3.3	10	80	T/F	10.54	22.31	22.22		0.0343	0.0431	0.0041	0.0352		
60	30	30	0.02	2	3.3	15	55	T/F	10.81	21.29	22.22		0.0608	% error	0.0419			
60	30	30	0.02	2	1	22	55	D/P	9.63	14.86	15.38		0.0550	0.0338				
60	30	30	0.02	2	1	5	10	D/P	10.34	14.77	15.38		0.0147	0.0397				
60	30	30	0.02	2	1.3	15	55	D/F	10.04	17.16	19.95		0.0147	0.1398				
60	30	30	0.02	2	1.3	15	55	D/F	10.87	17.39	16.86		0.0667	0.0314				

60	30	30	0.02	2	1.3	15	55	D/F	10.06	17.35	16.86	0.0128	0.0291
60	30	30	0.02	2	2.4	15	55	D/P	10.14	17.04	15.82	0.0049	0.0771
60	30	30	0.02	2	4	25	0	T/P	11.07	18.9	15.82	0.0864	0.1947
60	30	30	0.02	2	3.5	15	15	T/F	10.72	25.99	25.03	0.0520	0.0384
60	30	30	0.02	2	1	15	55	D/F	9.87	22.15	22.79	0.0314	L Avg 0.0281
60	30	30	0.02	2	3	15	55	D/F	10.31	20.67	19.25	0.0118	10.3325 0.0738
60	30	30	0.02	2	1.5	15	55	D/F	10.13	20.31	20.69	0.0059	0.0140 0.0184 0.0622
60	30	30	0.01	2	1	15	55	D/F	10.52	22.51	20.69	0.0324	% error 0.0880
60	30	30	0.01	2	2.3	10	30	T/P	9.77	13.84	13.41	0.0412	0.0321
60	30	30	0.01	2	2.5	30	0	D/P	9.93	25.37	22.83	0.0255	0.1113
60	30	30	0.01	2	1.5	11	55	D/F	10.14	15.54	15.66	0.0049	0.0077
60	30	30	0.01	2	2.1	22	55	T/P	9.89	21.46	22.78	0.0294	0.0579
60	30	30	0.01	2	3	30	0	D/P	9.52	25.16	22.78	0.0658	0.1045
60	30	30	0.01	2	1	15	0	D/P	10.41	14.41	14.45	0.0216	0.0028
60	30	30	0.01	2	1.5	11	55	D/F	10.41	15.35	15.26	0.0216	0.0059
60	30	30	0.01	2	2.6	11	55	T/F	10.4	20.2	21.51	0.0206	0.0609
60	30	30	0.01	2	2.4	11	55	T/F	10.15	16.17	17.78	0.0039	0.0906 0.0561
120	30	30	0.01	2	3	30	15	T/P	10.72	16.21	15.54	0.0520	0.0431
120	30	30	0.01	2	3	10	0	T/P	9.65	25.84	24.28	0.0530	L Avg 0.0643
120	30	30	0.01	2	2.1	5	55	T/P	9.46	23.53	23.88	avg v 0.0716	10.0179 0.0147
120	30	30	0.01	2	3	30	0	D/P	10.3	9.28	15.24	14.46	0.186 0.0893 0.0169 0.0539 0.0527
60	30	30	0.03	3	5	15	15	T/P	16.12	19.91	20.12	24.89	0.3524 % error 0.0104
120	30	30	0.03	3	4	30	15	T/P	17	20.45	20.12	0.3170	0.0164
60	45	30	0.03	3	4	30	15	T/P	26.19	20.94	20.12	0.0522	L Avg 0.0408
60	45	30	0.03	3	4	30	15	T/P	24.29	11	10.92	0.0241	21.2460 0.0073
60	45	30	0.03	3	4	15	30	T/P	22.63	14.57	13.42	0.0908	0.1464 0.0857 0.0321
60	45	30	0.02	3	3	15	15	T/P	23.15	10.66	10.21	0.0699	% error 0.0441
60	45	30	0.02	3	3	15	15	T/P	27.58	23.3	19.85	0.1081	0.1738
60	45	30	0.02	3	3	15	30	T/P	21.85	11.45	11.12	0.1221	0.0297
60	45	30	0.02	3	3	15	0	T/P	23.07	15.26	13.79	0.0731	0.1066
60	45	30	0.02	3	3	15	55	T/P	20.65	18.67	20.12	0.1703	0.0721
60	45	30	0.02	3	4	10	50	T/P	20.96	12.7	12.13	0.1579	0.0470
60	45	30	0.02	3	4	10	0	T/P	27.82	13.14	12.57	0.1177	0.0453
60	45	30	0.02	3	3	8	55	T/P	25.26	13.66	12.57	0.0149	0.0867
60	45	30	0.02	3	3	8	55	T/P	23.78	12.83	12.78	0.0446	L Avg 0.0039
60	45	30	0.02	3	3	8	55	T/P	23.66	19.87	12.78	0.0494	23.4645 0.5548
60	45	30	0.02	3	3	15	50	T/P	20.33	20.75	19.18	0.1832	0.0573 0.0819 0.1133
60	45	30	0.01	3	2	10	80	T/P	21.58	20.93	19.18	0.1330	% error 0.0912
60	45	30	0.01	3	1	1	20	T/P	22.23	11.5	11	0.1069	0.0455
60	45	30	0.01	3	1.3	1	20	T/P	22.01	20.87	18.63	0.1157	0.1202
60	45	30	0.01	3	3	10	50	T/P	26.85	17.63	16.49	0.0787	0.0691
60	45	30	0.01	3	1.8	15	40	D/P	23.5	19.47	18.95	0.0558	0.0274
60	45	30	0.01	3	3	10	55	T/P	23.91	10.13	10.12	0.0394	0.0010
60	45	30	0.01	3	3	15	0	T/P	22.32	10.53	10.12	0.1033	0.0405
60	45	30	0.01	3	3	15	0	T/P	23.88	20.9	18.55	0.0406	0.1267
60	45	30	0.01	3	3	15	0	T/P	21.3	11.94	11.5	0.1442	L Avg 0.0383
60	45	30	0.01	3	3	15	0	T/P	24.09	17.53	15.85	avg v 0.0321	23.1027 0.1060
60	45	30	0.01	3	1.5	10	50	D/P	22.9	22.46	17.7	18.63	1.017 0.0976 0.0718 0.0499 0.0651
									19.81	19.0500			% error
Average delta for HUMMWV					0.1180	m	1.219	m/s	2.7306	miles/hour			
Average delta for HEMTT					0.1025	m	0.186	m/s	0.4169	miles/hour			
Average delta for M1070					1.9837	m	1.017	m/s	2.2790	miles/hour			
Total delta					0.7347	m	0.808	m/s	1.8088	miles/hour			

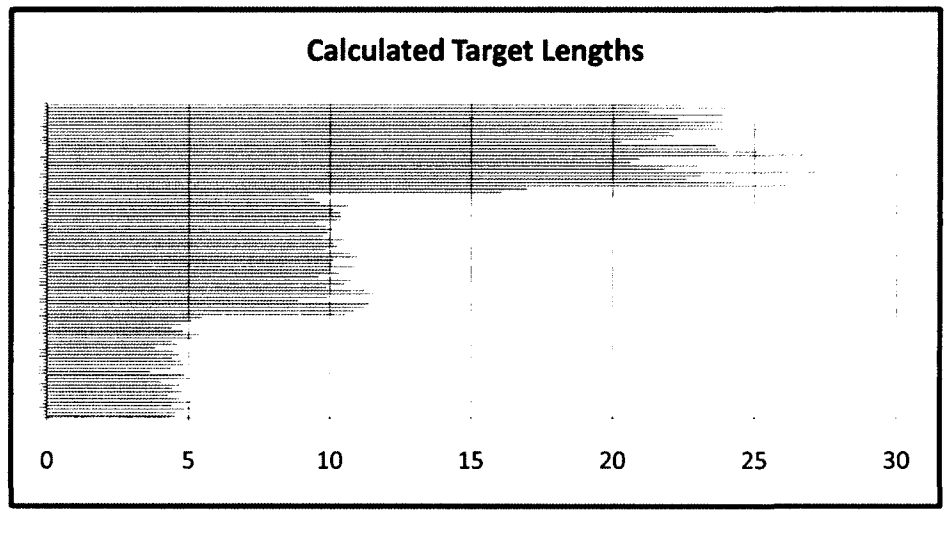


**Table B.18 Sensor Data Threshold Detection**

Run Information	Threshold	N	$\gamma$	#T	En1	Ex2	FAR1	#T	En1	Ex2	FAR2	#T	En1	Ex2
SumPixel(Multi05_1(3:3,3:5,:),1,1);		2	1	3	85	105	3	3	85	105	5	1	85	105
Multi05_1(3,4,:)		2	1	13	91	100	3	13	91	100	5	1	91	100
SumPixel(Multi05_1(3:3,3:4,:),1,1);		2	1	4	85	100	3	4	85	100	5	1	85	100
EnlargePixel(Multi05_1,3,4,5,5);		2	1	4	85	103	3	4	85	103	5	1	85	103
TwoPix05_1(1,2,:);		2	1	2	83	96	3	2	83	96	5	1	83	96
SumPixel(TwoPix05_1,1,1);		2	1	4	83	95	3	4	83	95	5	1	83	95
OnePix05_2;		2	1	3	83	111	3	3	83	111	5	1	83	111
EnlargePixel(Multi05_1,3,4,5,1);		2	1	12	92	100	3	12	92	100	5	1	92	100
EnlargePixel(Multi05_1,3,4,1,5);		2	1	5	85	105	3	5	85	105	5	1	85	105
OnePix96_2;		2	1	8	159	179	3	8	159	179	5	1	155	185

**Table B.19 Sensor Data Duration Detection**

Run Information	Duration	N	#T	En1	Ex2	FAR1	#T	En1	Ex2	FAR2	#T	En1	Ex2
SumPixel(Multi05_1(3:3,3:5,:),1,1);		1	17	85	106	3	17	85	106	2	17	85	106
Multi05_1(3,4,:)		1	1	92	100	3	1	92	100	2	1	92	100
SumPixel(Multi05_1(3:3,3:4,:),1,1);		1	1	85	100	3	1	85	100	2	1	85	100
EnlargePixel(Multi05_1,3,4,5,5);		1	3	86	91	3	2	93	100	2	2	93	100
TwoPix05_1(1,2,:);		1	1	83	95	3	1	83	95	2	1	83	95
SumPixel(TwoPix05_1,1,1);		1	6	83	95	3	6	83	95	2	5	83	95
OnePix05_2;		1	16	83	111	3	16	83	111	2	8	83	111
EnlargePixel(Multi05_1,3,4,5,1);		1	7	92	100	3	7	92	100	2	1	92	100
EnlargePixel(Multi05_1,3,4,1,5);		1	8	85	105	3	8	85	105	2	4	85	105
OnePix96_2;		1	2	160	178	3	2	160	178	10	1	160	178

**Table B.20 Sensor Data FAPI Detection**

Run Information	FAPI	N	$\gamma$	#T	En1	Ex2	FAR1	#T	En1	Ex2	FAR2	#T	En1	Ex2
SumPixel(Multi05_1(3:3,3:5,:),1,1);		2	1	0	0	0	1	0	0	0	5	0	0	0
Multi05_1(3,4,:)		2	1	1	99	100	1	1	99	100	5	0	0	0
SumPixel(Multi05_1(3:3,3:4,:),1,1);		2	1	1	2	210	1	1	2	210	5	1	2	210
EnlargePixel(Multi05_1,3,4,5,5);		2	1	1	2	210	1	1	2	210	5	1	2	210
TwoPix05_1(1,2,:);		2	1	1	90	99	1	1	90	99	5	1	90	99
SumPixel(TwoPix05_1,1,1);		2	1	1	2	210	1	1	2	210	5	1	2	210
OnePix05_2;		2	1	1	2	210	1	1	2	210	5	1	2	210
EnlargePixel(Multi05_1,3,4,5,1);		2	1	1	2	210	1	1	2	210	5	1	2	210
EnlargePixel(Multi05_1,3,4,1,5);		2	1	0	0	0	1	0	0	0	5	0	0	0
OnePix96_2;		2	1	1	2	486	1	1	2	486	5	1	2	486

**Table B.21 Sensor Data PolyFit and FermiFit Analysis Data**

Run Information	Poly	En1	En2	Ex1	Ex2	Fermi	En1	En2	Ex1	Ex2	Real	En1	En2	Ex1	Ex2
SumPixel(Multi05_1(3:3,3:5,:),1,1);	84.4	86.8	103	105		85	91.3	98.7	105		83	86	103	107	
Multi05_1(3,4,:)	85.5	47.8	108	107		91	93.1	97.9	100		84	87	97		
SumPixel(Multi05_1(3:3,3:4,:),1,1);	72.7	67.7	136	113		85	91.3	98.7	105		84	87	103	108	
EnlargePixel(Multi05_1,3,4,5,5);	84.7	87.3	101	104		85	89.7	102	108		84	87	103		
TwoPix05_1(1,2,:);	73.2	68.4	2964	116		83	87.1	91.9	96		81	86	93	96	
SumPixel(TwoPix05_1,1,1);	68.9	63.9	-324	142		83	86.7	91.3	95		61	71	93	96	
OnePix05_1;	61.0	66.4	73.6	83.0		62	70.0	77.0	85		62	67	80	85	
OnePix05_2;	76.4	85.8	109	114		80	85.3	106	111		81	86	109	115	
EnlargePixel(Multi05_1,3,4,5,1);	86.5	60.5	118	111		92	93.9	98.1	100		87	94	97	101	
EnlargePixel(Multi05_1,3,4,1,5);	85.4	91.8	85.9	102		85	89.9	100	105		84	87	103	108	
OnePix96_2;	157	165	171	183		155	167	173	185		156	162	175	180	

## REFERENCES

- [1] Kostka, D., "Moving Toward a Joint Acquisition Process to Support ISR," *Joint Force Quarterly* National Defense University Press, 2009 [Online] Available: <http://www.ndu.edu/press/lib/images/jfq-55/11.pdf>.
- [2] "Fundamentals of Remote Sensing Satellites and Sensors," *Natural Resources Canada*, Nov. 17, 2009 [Online] Available: Sep. 28, 2010, [www.ccrs.nrcan.gc.ca/resource/tutor/fundam/chapter2/02\\_e.php](http://www.ccrs.nrcan.gc.ca/resource/tutor/fundam/chapter2/02_e.php).
- [3] "Border Patrol Overview," *US Customs and Border Protection* [Online]. Available: [http://www.cbp.gov/xp/cgov/border\\_security/border\\_patrol/border\\_patrol\\_ohs/overview.xml](http://www.cbp.gov/xp/cgov/border_security/border_patrol/border_patrol_ohs/overview.xml).
- [4] "Transit Zone Interdiction Operations," *Office of National Drug Control Policy*, Oct. 16, 2009 [Online] Available: [http://www.whitehousedrugpolicy.gov/publications/international/factsht/transit\\_zone\\_interdic\\_op.html](http://www.whitehousedrugpolicy.gov/publications/international/factsht/transit_zone_interdic_op.html).
- [5] Maher, H., "Analysts Say U.S. Intelligence System Overloaded, Out of Data," *Radio Free Europe*, 2010, [Online] Available: [http://www.rferl.org/content/Analysts\\_Say\\_US\\_Intelligence\\_System\\_Overloaded\\_Out\\_Of\\_Date/1930418.html](http://www.rferl.org/content/Analysts_Say_US_Intelligence_System_Overloaded_Out_Of_Date/1930418.html).
- [6] Shachtman, N., "Robert Gates: Overhaul the Pentagon," *Wired News*, Sep. 21, 2009, [Online] Available: [http://www.wired.com/techbiz/people/magazine/17-10/ff\\_smartlist\\_gates?currentPage=all](http://www.wired.com/techbiz/people/magazine/17-10/ff_smartlist_gates?currentPage=all).
- [7] Zhang, F., Li, C. and Shi, L., "Detecting and Tracking Dim Moving Point Target in IR Image Sequence," *Infrared Phys Tech*, vol. 46, pp. 323-328, Jul. 2004.
- [8] Barniv, Y and Kella, O, "Dynamic Programming Solution for Detecting Dim Moving Targets PART II: Analysis," *IEEE T Aero Elec Sys*, vol. 6, pp. 776-788, Nov. 1987.
- [9] Blostein, S. D. and Huang, T. S., "Detecting Small, Moving Objects in Image Sequences Using Sequential Hypothesis Testing," *IEEE T on Signal Process*, vol. 19, no. 7, pp. 1611-1629, 1991.
- [10] Wei, W. and Jiaxiong, P., "Detection of Moving Small Targets in Infrared Image Sequences Containing Clour Clutter," *Intl J Pattern Recogn and AI*, vol. 18, no. 2, pp. 247-260, 2004.

- [11] Sun, Y. Q., Tian, J. W. and Liu, J., "Background Suppression Based on Wavelet Transformation to Detect Infrared Target," *Proc Fourth Int Conf Mach Learning Cyb*, pp. 4611-4615, Aug 2005.
- [12] Mei, X., Zhou, S. and Wu, H., "Integrated Detection, Tracking and Recognition for IR Video-Based Vehicle Classification," *IEEE ICASSP*, pp. 745-748, 2006.
- [13] Simonson, K. and Ma, T., *Robust Real-Time Change Detection in High Jitter*, Albuquerque: Sandia National Laboratories, 2009.
- [14] Badeau, R., David, B. and Richard, G., "Fast Approximated Power Iteration Subspace Tracking," *IEEE T on Sig Process*, vol. 53, no. 8, pp. 2931-2946, Aug 2005.
- [15] Caefer, C. E., Mooney, J. M. and Silverman, J., "Point Target Detection in Consecutive Frame IR Imagery With Evolving Cloud Clutter," *Proc SPIE*, vol. 2561, pp. 14-24, 1995.
- [16] Tzannes, A. P. and Mooney, J. M., *Point Target Detection in IR Image Sequences Using Spatio-Temporal Hypothesis Testing*, Hanscom AFB, MA: Air Force Research Laboratory, February 1999.
- [17] Liu, D., Zhang, J. and Dong, W., "Temporal Profile Based Small Moving Target Detection Algorithm in Infrared Image Sequences," *Int J Infrared Milli*, vol. 28, pp. 272-281, Mar. 2007.
- [18] Lim, E. T., Shue, L. and Venkateswarlu, R., "Adaptive Mean and Variance Filter for Detection of Dim Point-Like Targets," *Proc SPIE: Signal and Data Proc of Small Targets*, vol. 4728, pp. 492-502, 2002.
- [19] Tzannes, A. P. and Brooks, D. H., "Detecting Small Moving Objects Using Temporal Hypothesis Testing," *IEEE T Aero Elec Sys* vol. 38, pp. 570-585, Apr. 2002.
- [20] Tursun, D., Guiying, X. and Hamdulla, A., "A Particle Filter Based Algorithm for State Estimation of Dim Moving Point Target in IR Image Sequence," *Intel Info Tech App*, vol. 2, pp. 127-131, Dec. 2008.
- [21] Zaveri, M. A., Merchant, S. N. and Desai, U. B., "Wavelet-Based Detection and Its Application to Tracking in an IR Sequence," *IEEE T Sys Man Cyb*, vol. 37, no. 6, pp. 1269-1286, Nov. 2007.
- [22] Zhang, X. and Ding, X., "A Note on Continuous Wavelet Transform," *J Guangxi Acad Sc*, vol. 23, pp. 4-6, 2007.
- [23] Gao, T. and Liu, L., "Moving Video Object Segmentation Based on Redundant Wavelet Transform," *IEEE IC Info Auto*, pp. 156-160, Jun. 2008.

- [24] "Army Wheeled Vehicles," *US Army Factfiles* [Online] Available: <http://www.army.mi/factfiles/equipment/wheeled>.
- [25] Simonson, K M and Ma, T J, *Robuts Real-Time Change Detection in High Jitter*, Albuquerque: Sandia National Laboratories, 2009.
- [26] Ran, Q., Chi, Y. and Wang, Z., "Property and Removal of Jitter in Beijing-1 Small Satellite," *Int Arch Photo Remote Sens Spat Info*, vol. 37, no. B1, pp. 929-934, 2008.
- [27] Reed, I. S., "Optical Moving Target Detection with 3D Matched Filtering," *IEEE T Signal Process* vol. 24, pp. 327-336, 1998.
- [28] Brain, Y., "Dynamic Programming Solution for Detection of Dim Moving Targets," *IEEE T Aero Elec Sys*. vol. 21, pp. 144-156, 1985.
- [29] Radke, R., et al., "Image Change Detection Algorithms: A Systematic Survey," *IEEE T Image Process*, vol. 14, no. 3, pp. 294-307, Mar 2005.
- [30] Rosin, P., "Thresholding for Change Detection," *Comp Vis Image Und*, vol. 86, no. 2, pp. 79-95, May 2002.
- [31] Rosin, P. and Ioannidis, E., "Evaluation of Global Image Thresholding for Change Detection," *Pattern Recogn Lett*, vol. 24, no. 14, pp. 2345-2356, Oct 2003.
- [32] Poor, H., *An Introduction to Signal Detection and Estimation*, New York : Springer-Verlag, 2000.
- [33] Forstner, W., "A Framework for Low Level Feature Extraction," *Lecture Notes in Computer Science*, Stockholm: Springer-Verlag, 1994, vol. 801, pp. 383-394.
- [34] Haag, M. and Nagel, H., "Combination of Edge Element and Optical Flow Estimates for 3D Model Based Vehicle Tracking in Traffic Sequences," *Int J Comput Vision*, vol. 35, no. 3, pp. 295-319, 1999.
- [35] Hinz, S., "Integrating Local and Global Features for Vehicle Detection in High Resolution Aerial Imagery," *Int Arch Photo Remote Sens Spat Info*, vol. 34, pp. 119-124, 2003.
- [36] Hinz, S. and Baumgartner, A., "Vehicle Detection in Aerial Images Using Generic Features Grouping and Context," *Lecture Notes on Computer Science*, Munich : Springer Berlin / Heidelberg, 2001, vol. 2191, pp. 45-52.
- [37] Meer, P., Jolion, J. and Rosenfeld, A., "A Fast Parallel Algorithm for blind Estimation of Noise Variance," *IEEE T Pattern Anal.* vol. 12, no. 2, pp. 216-223, 1990.
- [38] Yang, B., "Projection Approximation Subspace Tracking," *IEEE T Signal Process*, vol. 44, no. 1, pp. 95-107, Jan 1995.

- [39] Abed-Meraim, K., Chkeif, A. and Hua, Y., "Fast Orthonormal PAST Algorithm," *IEEE T Signal Process*, vol. 7, no. 3, pp. 60-62, Mar 2000.
- [40] Miao, Y. and Hua, Y, "Fast Subspace Tracking and Neural Network Learning By a Novel Information Criterion," *IEEE T Signal Process*, vol. 46, no. 7, pp. 1967-1979, Jul 1998.
- [41] Cavallaro, A. and Ebrahimi, T., "Video Object Extraction Based on Adaptive Background and Statistical Change Detection," *Proc SPIE Vis Image Process*. pp. 465-475, Jan 2001.
- [42] Huwer, S. and Niemann, H., "Adaptive Change Detection for Real-Time Surveillance Applications," *Proc Visual Surv*, pp. 75-91, 2000.
- [43] Kanade, T. and Collins, R., "Advances in Cooperative Multi-Sensor Video Surveillance," *Proc DARPA Image Understanding Workshop*, vol. 1, pp. 3-24, Nov 1998.
- [44] Zelen, M and Severo, N, "Probability Functions ,," *Hanbook of Mathematical Functions with Formulas, Graphs, and Mathematical Tables*, New York: National Bureau of Standards, 1964, pp. 936-964.
- [45] "R2010b Documentation Matlab Hist," *MathWorks*, [Online] Available: <http://www.mathworks.com/help/techdoc/ref/hist.html>.
- [46] Badeau, R, David, B and Richard, G, Fast Approximated Power Iteration Subspace Tracking, *IEEE T Signal Process*, 2005, vol. 53, 6.
- [47] Choi, W. C., et al., "Automatic Tracking System with Target Classification," *Proc SPIE*, vol. 7335, pp. 73350T1-73350T8, 2009.
- [48] Nair, D. and Aggarwal, J. K., "Robust Automatic Target Recognition in Second Generation FLIR Images," *IEEE T Signal Process*, pp. 194-201, 1996.
- [49] Manikandan, J., Venkataramani, B. and Jayachandran, M., "Evaluation of Edge Detection Techniques Towards Implementation of Automatic Target Recognition," *Int Conf on Comp Intel Multimedia Apps.* , pp. 441-445, 2007.
- [50] Clarkson, T., "Automatic Target Recognition Using Neural Networks," *Neural Network World*, pp. 1-9, 1995.
- [51] Gupte, S., et al., "Detection and Classification of Vehicles," *IEEE T Intel Trans Sys.* vol. 3, pp. 37-47, Mar. 2002.
- [52] Hoffman, J D, "Polynomial Approximation and Interpolation," *Numerical Methods for Engineers and Scientists*, New York: Marcel Dekker, 2001, pp. 228-231.
- [53] Robinson, G., "Test Data," *RP Flight Systems*, Jul. 9, 2010 [Online] Available: <ftp://ftp.rpflightsystems.com/>.

- [54] Melgaard, D and Larson, K, *Practical Considerations for a Velocity Matched Filter Applies to Dim Target Detection*, s.l.: Sandia National Lab Report, 2010.
- [55] Boult, T., "Into the Woods: Visual Surveillance of Non-Cooperative and Camouflaged Targets in Complex Outdoor Settings.", *Proc IEEE*, vol. 89, pp. 1382-1402, Oct 2001.
- [56] Bhuiyan, S. M., Alam, M. S. and Alkanhal, M., "New Two-Stage Correlation-Based Approach for Target Detection and Tracking in Forward-Looking Infrared Imagery Using Filters Based on Extended Maximum Average Correlation Height and Polynomial Distance Classifier Correlation," *Opt Eng*, vol. 46, no. 8, pp. 864011-8640114, Aug. 2007.
- [57] Hinz, S. and Still, U., "Car Detection in Aerial Thermal Images by Local and Global Evidence Accumulation," *Pattern Recogn Lett*, vol. 27, pp. 308-315, 2006.
- [58] Xue, M., Zhou, S. and Hao, W., "Integrated Detection, Tracking and Recognition for IR Video-Based Vehicle Classification," *IEEE T Acoust Speech*. vol. 5, pp. 745-748, Apr 2006.
- [59] Gordon, N. J., Salmond, D. J. and Smith, A. F., "Novel Approach to Nonlinear/Non-Gaussian Bayesian State Estimation." *IEEE Proc*, vol. 140, no. 2, pp. 107-113, 1993.
- [60] Doucet, A., Godsill, S. and Andrieu, C., "On Sequential Monte Carlo Sampling Methods for Bayesian filtering," *Stat Comp*, vol. 10, no. 3, pp. 197-208, 2000.
- [61] Ling, J., Liu, E. Q. and Yang, J., "Approach of Infrared Small Target Motion Prediction and Tracking Based on H Filter," *J Infrared Milli*, vol. 24, no. 5, pp. 366-369, 2005.
- [62] Caefer, C. E., Silverman, J. and Mooney, J. M., "Optimization of Point Target Tracking Filters," *IEEE T Aero Elec Sys*, vol. 36, no. 1, pp. 496-507, 15-25, 2000.
- [63] Caefer, C. E., Mooney, J. M. and Silverman, J., "Point Target Detection in Consecutive Frame IR Imagery with Evolving Cloud Clutter," *Proc SPIE*, vol. 2561, pp. 14-24, 1995.